POWER TRANSFER OPTIMISED AUTOMATIC MATCHING NETWORKS

REINHARD JÖRG GLÖCKNER
(REINHARD JOERG GLOECKNER)

A thesis submitted in partial fulfilment
of the requirements of the
University of Northumbria at Newcastle
for the degree of
Doctor of Philosophy

Research undertaken in the School
of Computing, Engineering and
Information Sciences

July 2008

Abstract

Matching networks are widely used to enhance active power transfer when radio frequency generators drive complex loads. The tuning of the network for varying loads typically involves searching for optimum matching conditions.

However, improving the matching condition of the network does not necessarily indicate an increase in active power transfer. As an example, a π network with three adjustable elements may achieve comparable matches for a variety of elements' settings, each matching triple exhibiting a different transferred active power.

Furthermore, the influence of the transmission lines used to connect the matching network to its source and load is rarely taken into account.

The purpose of the work is to optimise the power gain of a narrowband matching system in the frequency range of $1.8 - 30\,\mathrm{MHz}$. The system consists of a source, a matching network, a load and two interconnecting lines whose characteristic impedance is complex. The optimisation process involves optimum choice of the transmission lines' lengths and development of a matching strategy. Its objective is to ensure automatic and continuous adjustment of the matching network for optimum active power transfer to its load while matching the network's input impedance to a resistive source.

The network topologies employed are limited to the most common π and T networks consisting of two variable capacitors and one central inductor. Losses are assumed to be mainly caused by the inductor. An appropriate simple and synthetic model of the losses is proposed — which is suitable for active power transfer optimisation. The model is validated against losses of inductors derived by different works.

After choosing a proper network parametrisation and exact inclusion of the losses during network design, the losses of a network terminated by a resistance and designed to match (exactly) a source resistance at its input are derived. Then its power gain is optimised by a proper choice of the network's parameter and the impact of changing the purely resistive termination to impedances exhibiting capacitive or inductive imaginary parts is considered. An explicit solution is calculated for networks with a constant Q factor central inductor, its differences from the approximate solution (network elements designed as if the network would be lossless) are considered. Example diagrams are given illustrating those differences and power gain contour Smith charts are drawn for typical ranges of the L, π, and T networks' elements. Combining the results of the different approaches yields an optimum matching strategy.

The losses of transmission lines connecting source and network of load and network are determined, where the lines' complex characteristic impedance is taken into account. Those losses are included in a power gain optimisation of the complete matching system.

Finally, an experimental setup is designed under which the matching strategy of the network is tested and validated.

Contents

Tables

Figures

Definitions

Notations

$\underline{\ }$	Complex variable (or constant), e. g. $\underline{V}$ is the complex amplitude of a voltage
$'$	Per-unit-length variable (or constant), e. g. R' is the per-unit-length resistance of a transmission line
*	Complex conjugate, e. g. $\underline{Z}^*$ is the complex conjugate of $\underline{Z}$
$\lvert\ldots\rvert$	Absolute value of ...
Im{...}	Imaginary part of ...
Max{...}	Maximum of ...
Min{...}	Minimum of ...
Re{...}	Real part of ...
φ...	Phase of ...
$(\#.\#)$	The right hand side of the equation was derived by applying Equation (#.#)

Indices

0	If used with an impedance/resistance/reactance/admittance/conductance/susceptance, it denotes a characteristic value of a transmission line, if used with a voltage/current, it denotes the (complex) amplitude of an ideal voltage/current source
1	If used with an impedance/reflection coefficient/active power, it denotes a value at the input of a transmission line or a network as first index or the line number as second index
2	If used with an impedance/reflection coefficient/active power, it denotes a value at the load of a transmission line or a network as first index or the line number as second index
act	Active power (index used only in conjunction with a power)
ax	Axial
A	Arnold
C	Coil
i	If used with an impedance/resistance/reactance/admittance/conductance/susceptance/reflection coefficient, it denotes a value of a source impedance, if used with a voltage/current, it denotes an incident value in a transmission line
$_{i,\ell}$	Either index i or ℓ is used in all variables with index $_{i,\ell}$ throughout an equation
$_{i,\ell,0}$	Either index i, ℓ, or 0 is used in all variables with index $_{i,\ell,0}$ throughout an equation
inma	network (exactly) matched at its input
ℓ	Load
ll	Lossless
llcapdes	Network designed as if all capacitors were lossless
lldes	Network designed as if all elements were lossless
L	Transmission line
M	Medhurst
MB	Matchbox (matching network)
outma	network (exactly) matched at its output
p	Parallel
r	Reflected

rad	Radial
s	Series
t	T network (the lower case letter was chosen to avoid confusion of g_t (power gain of a T network), with g_T (transducer power gain))
tp	Two-port
T	Transducer
T	Turn
$\underline{\widetilde{Z}}_0$	Reference impedance of a reflection coefficient, e. g. $\underline{\widetilde{Z}}_0$
π	π network

Latin letters

arctan()	Arc tangens function
arsinh()	Inverse hyperbolic sine function
B	Susceptance, imaginary part of admittance $\underline{Y}$
c_0	Speed of light in a vacuum
cos()	Cosine function
cosh()	Hyperbolic cosine function
C	Capacitance
e	Exponential constant (base of natural logarithms)
$e^{(\cdots)}$	Exponential function of ...
f	Frequency
g	Power gain (named as usual, although it's a ratio of active powers (an active power gain))
g_T	Transducer power gain
G	Conductance, real part of admittance $\underline{Y}$
G_p	Parallel conductance
$\underline{I}$	Complex amplitude of a current
j	Imaginary unit $\sqrt{-1}$
l	Length of a transmission line
lg()	Logarithm function to base 10
ln()	Natural logarithm function
L	Inductance
$\mathbb{R}$	Set of real numbers
$\mathbb{R}_0^+$	Set of real numbers greater or equal than zero
R	Resistance, real part of impedance $\underline{Z}$
R_s	Series resistance
sin()	Sine function
sinh()	Hyperbolic sine function
tanh()	Hyperbolic tangens function
$\underline{V}$	Complex amplitude of a voltage
X	Reactance, imaginary part of impedance $\underline{Z}$
$\underline{Y}$	Admittance ($\underline{Y} = \frac{1}{\underline{Z}}$)
$\mathbb{Z}$	Set of whole numbers (integers)
$\underline{Z}$	Impedance

Greek letters

α	Attenuation constant of a transmission line
β	Phase constant of a transmission line
$\underline{\gamma}$	Propagation constant of a transmission line
μ	Permeability
μ_0	Permeability constant (in a vacuum), often approximated as $4\pi\ 10^{-7}\,\frac{\mathrm{H}}{\mathrm{m}}$

π	Number pi
ϱ	Resistivity
ω	Angular frequency ($\omega = 2\pi f$)

Abbreviations

(1.#)	Equation number of an equation in a chapter, e. g. equation number # in Chapter 1
(A.#)	Equation number of an equation in a chapter of the appendix, e. g. equation number # in Appendix A
[#]	Citation number #
AC	Alternating current
DC	Direct current
MMIC	Monolithic microwave integrated circuit

Acknowledgements

It is my pleasure to thank Professor Dr. J. Kel Fidler, my principal supervisor, for his interest in my thesis. His continuous support and constructive advice contributed to the successful accomplishment of this work.

I am also very grateful to Dr. Krishna Busawon, my second supervisor, for his steady support regarding mathematical questions, his assistance in solving surprising problems, and his advice in administrative matters.

I express my sincere thanks to both supervisors for granting the necessary freedom in conducting my work.

Furthermore, I like to thank Peter Schwarzmann, retired from the Institut für Physikalische Elektronik, University of Stuttgart, 70569 Stuttgart, Germany, for his comments, suggestions, proofreading, and support during the early stage of the work.

I am obliged to Jürgen Hartmann, Armin Vogt, and Alexander Balz from Imaging Development Systems GmbH, 74182 Obersulm, Germany, my employer, for their understanding and generous support, in particular during the final stage of my thesis.

I am particularly grateful to my parents, whose continuous support was essential to conduct my thesis work in addition to my professional duties.

Declaration

I declare that the work contained in this thesis has not been submitted for any other award and that it is all my own work.

Name: Reinhard Jörg Glöckner (Reinhard Joerg Gloeckner)

Signature:

Date: July 29th, 2008

Chapter 1

Introduction

1.1 Introduction

Matching networks are widely used to enhance active power transfer when radio frequency generators drive complex loads. The tuning of the network for varying loads typically involves searching for optimum matching conditions. A number of interesting algorithm and techniques were developed to search for optimum matching condition (see e. g. [1], [2], [3] for continuously variable elements or [4], [5], [6], [7], and [8] for binary switchable elements).

However, improving the matching condition of the network does not necessarily indicate an increase in active power transfer. As an example, a π network with three adjustable elements may achieve comparable matches for a variety of elements' settings while each matching triple exhibits a different transferred active power.

Another important aspect in developing an optimum matching strategy is a proper choice of the network's parametrisation. In effect, during the last decades, a couple of π and T network parametrisations were developed for lossless networks suiting different needs. A more filter theoretical approach involving hyperbolic functions was summarised in [9c] and examined in more detail in [10]. The so called Q-based design was used in [11], [12] and further developed in [13], [14], [15], [16], [17], and [18]. The problem of exact loss inclusion in network design was introduced by [3]. However, the authors in the previous mentioned works assumed that the losses are low enough so that the same element values are used as in the lossless case whenever deriving analytical solutions. This obviously is not valid for the entire parameter range or for badly chosen element values. Additionally, although realistic loads are often complex loads, the element values were calculated for resistive loads only. In [13] and [18], absorption and resonance methods are used for complex load matching, but both works do not systematically describe the impact of complex loads on the chosen parametrisation. However, [19], [20], and [21] graphically visualise the complex load range for a given tunable range of the network's components. In addition, the required minimum π network component values' range to acquire a match for a given magnitude of the load reflection coefficient is calculated in [21], assuming a lossless network and using no explicit parametrisation (it's done implicitly by variation of the components in their tunable range).

Furthermore, in all the above work the losses are described by a constant Q factor only.

On the other hand, it is important to realise that in practice, the source and the load are connected to the matching network via transmission lines which also have some influence on active power transfer. However, the influence of the transmission lines used to connect the matching network is rarely taken into account in various research works.

The purpose of the work is to optimise the power gain of a matching system in the frequency range of $1.8-30\,\mathrm{MHz}$. The system consists of a source, a matching network, a load and two interconnecting lines whose characteristic impedance is complex. The optimisation process involves optimum choice of the transmission lines' lengths and development of a matching strategy. Its objective is to ensure automatic and continuous adjustment of the matching network for optimum active power transfer to its load while matching the network's input impedance to a resistive source.

Its application is restricted to carrier based applications, thus only narrowband matching is considered. The overall system can be applied to radio broadcast, ham radio, and industrial applications (as plasma deposition systems).

The network topology is limited to the most common π and T networks consisting of two variable capacitors and one central inductor, including the four possible L networks derived by omitting one of the capacitors.

In the desired frequency range the total loss of such networks is mainly determined by the losses of the inductor while the capacitors' losses can be neglected. Thus, a simple and synthetic model for the losses of the inductor is proposed. One of the main features of the proposed model is that it describes the general case of non constant Q and includes the case of constant Q as well as a special case. It applies to different variable inductor realisations, compared to losses derived in different works (examples for a solenoidal variable air-core inductor are [22] and [23] for a low number of turns, [24] for a high number of turns, and [25] for any number of turns).

Next, the losses due to the inductor are included exactly in the network's parametrisation.

The choice of a proper parametrisation suiting the needs of active power transfer optimisation is especially important, because it determines the characteristic behaviour of the system. This in turn simplifies considerably the analysis of the system.

Within this work, the initial parametrisation of [13] (based on the graphical design method of [11]) is employed. Its extension to exact loss inclusion by [3] is used for π and T network design and the influence of complex loads on the parametrisation and the transferred active power is derived systematically.

Furthermore, additional losses of the feedlines between generator, matching network, and load are taken into account using the lines' complex characteristic impedance, which results in a system description enabling active power transfer optimisation of the complete system.

Finally, the optimum matching strategy of the network is tested and validated experimentally by designing a prototype system.

1.2 The aims of the thesis

The main aims of the thesis are:

- To develop a narrowband matching strategy which is suited for automatic and continuous adjustment of L, π, and T matching networks for optimum active power transfer to their load while matching the network's input impedance to a resistive source applicable in a frequency range of $1.8-30\,\mathrm{MHz}$.
- To investigate the influence of the transmission lines' lengths (which connect the matching network to source and load) on power gain of the matching system and derive optimum line lengths, where the transmission lines' characteristic impedance is complex.
- To design a prototype system to test and validate the matching strategy of the network experimentally.

1.3 The objectives of the thesis

The main objectives of the proposed research work are:

- To propose a simple model for the losses in the central inductor of π and T networks in the given frequency range and validate it by comparison to existing loss models for different types of variable inductors used in matching networks.
- To choose a proper network parametrisation suitable for the needs of power gain opimisation.
- To derive optimum network settings with exact inclusion of the network's central inductor's losses for matching of a purely resistive load to a purely resistive source.
- To extend the method to complex loads.
- To solve explicitly for the central inductor's loss resistance in case of a constant Q factor inductor.
- To apply optimum network settings using the general loss model and appropriate results of the constant Q factor inductor calculations to develop an optimum matching strategy for the network.
- To optimise the load impedance of a transmission line whose characteristic impedance is complex for optimum power gain and the according source impedance for maximum active power input.

- To examine the impact of common sub-optimal source impedance choices/matching network input impedance design on the power gain of the matching system for low-loss coaxial transmission lines.

- To investigate the influence of common sub-optimal source impedance choices on optimum matching strategy for low-loss coaxial transmission lines.

- To derive optimum line lengths in a matching system for lossless and lossy matching networks, thus optimising the power gain of the complete matching system.

- To test and validate the matching strategy of the network experimentally.

1.4 Scope of the thesis

The majority of research work in narrowband π and T matching network design focus on constant Q factor central network inductors and apply Q based design to parametrise those networks. Exceptionally, the work in [3] exactly includes the variable inductor's losses. On the other hand, whenever analytical solutions are given and parameter's limits are derived, the networks are assumed to be designed as if all elements were lossless. Moreover, the impact of complex loads on the chosen parametrisation is usually not systematically described. In particular, the possibility that the resulting load related element of the equivalent circuit is an inductor instead of a capacitor is usually not considered.

Additionally, when losses in the connecting transmission lines are taken into account, their complex characteristic impedance is approximated by a real characteristic impedance, despite the fact that its complex propagation constant is used.

The present work uses a general loss model that is applicable to different types of variable inductors. The chosen parametrisation is particularly suited for power gain optimisation of π and T matching networks because, unlike Q based design, the power gain's derivative with respect to the parameter exhibits a unique sign over the entire parameter range for purely resistive and capacitive complex loads if the general loss model is applied. The losses of the central inductor are exactly included in network design and the design formulae are systematically extended to complex loads. Analytical solutions and parameter limits are given for π and T matching networks with a constant Q factor central inductor and any types of complex loads. The results obtained from the general loss model and those from the constant Q factor inductor are combined to derive a general optimum matching strategy for L, π, and T networks.

The losses in the connecting transmission lines are taken into account by their complex characteristic impedance and attenuation.

1.5 Contributions

The contributions resulting from this work are as follows:

- A simple and synthetic general loss model applicable to different types of variable inductors used in matching networks is derived.
- Applying the loss model to L, π, and T networks, an analytically proven matching strategy which optimises the networks' power gain if purely resistive or capacitive complex loads are matched to a purely resistive source is given. In addition, an adaptation to match purely resistive/capacitive complex sources to purely resistive loads is presented.
- An analytical solution for the L, π, and T networks' central inductor's loss resistance as a function of the chosen parametrisation and the appropriate parameter's limits if the inductor's Q factor is constant is provided.
- An optimum matching strategy suitable for automatic and continuous adjustment of L, π, and T matching networks obtained by combining general loss model and constant Q factor results is derived.
- An optimisation of the complete matching system including optimum splitting of the connecting lines' total length is achieved.
- Finally, an experimental setup is designed under which the matching strategy of the network is tested and validated.

1.6 Thesis structure

The thesis is broken down in seven chapters. Chapter 1 gives a brief introduction to matching network system design, the scope of the thesis, and summaries of each chapter.

Chapter 2 describes basic transmission line properties and gives a motivation as to why the complex characteristic impedance of coaxial transmission lines has to be considered although its imaginary part is much lower than its real part. Furthermore, it includes definitions, basic equations used in subsequent chapters, and a derivation of the complete matching system's power gain.

Chapter 3 considers the losses in π and T matching networks, proposes a simple loss model suitable for different types of the networks' central inductor, and validates the model by comparing to existing loss models for different types of variable inductors. A proper network parametrisation is chosen suiting the needs of power gain optimisation. Application of the general loss model to π and T networks designed including the losses exactly yields the optimum parameter's (and load resistance's) value for maximum active power transfer in case of resistive sources and loads.

Since realistic loads are usually complex, Chapter 4 extends the method presented in Chapter 3 to complex loads, thereby obtaining the first part of the optimum

matching strategy which applies to purely resistive or capacitive complex loads. To implement a matching strategy for inductive complex loads, an explicit solution is calculated for networks with a constant Q factor central inductor, its differences from the approximate solution (network elements designed as if the network would be lossless) are considered. Example diagrams are given illustrating those differences and power gain contour Smith charts are drawn for typical ranges of the L, π, and T networks' elements. Combining the results of the different approaches yields an optimum matching strategy for L, π, and T matching networks suitable for any types of loads.

Chapter 5 determines the losses of transmission lines connecting source and network or load and network. The impact of the complex characteristic impedance on both lines is considered. Splitting of the total line length is optimised for highest power gain, and a power gain optimisation of the complete matching system is derived.

Chapter 6 describes the experimental setup designed to test the network's matching strategy. The performed measurements are explained and results are given validating the matching strategy for optimum power gain of the network.

Chapter 7 presents final conclusions, discusses optimum matching strategies, and suggests possible directions for further work.

Note: In order to facilitate the readability of Chapters 2 – 5, lengthy calculations or proofs were moved towards the appropriate appendices.

Chapter 2

RF Basics

2.1 Introduction

In this chapter, we derive all the neccesary equations that describe the active power transfer in a system consisting of a matching network embedded in two lossy transmission lines — described by their attenuation and complex characteristic impedance — between source and load.

In effect, the calculation and optimisation of active power transfer in matching systems using matching networks involves lossy transmission lines. This is due to the fact that generally the matching network is embedded in two lines connecting it to source and load. Both lines introduce impedance transformation and losses. Although lossy transmission lines are usually described by their attenuation and an approximately real characteristic impedance, the small imaginary part of the characteristic impedance of the mismatched line between matching network and load needs to be taken into account.

We start by recalling some basic definitions and notations that are used throughout the thesis.

2.2 Definitions/notations

From this chapter on, the following definitions/notations will be used:

Latin letters

a	Attenuation of a transmission line
$a_{\mathrm{dB/100\,m}}$	Attenuation of a transmission line in dB/100 m
C'	Per-unit-length capacitance of a transmission line
g_{tot}	Power gain of the complete matching system
g_{tp}	Power gain of a two-port
$g_{\mathrm{tp}}(\underline{r}_{\ell\mathrm{tp}}, \underline{z}_{0\mathrm{tp}2})$	Power gain of a two-port as a function of reflection coefficient $\underline{r}_{\ell\mathrm{tp}}, \underline{z}_{0\mathrm{tp}2}$
g_{L}	Power gain of a transmission line
$g_{\mathrm{L}1}$	Power gain of a transmission line 1
$g_{\mathrm{L}1}(\underline{r}_{1\mathrm{tp}}, \underline{z}_{01})$	Power gain of a transmission line 1 as a function of reflection coefficient $\underline{r}_{1\mathrm{tp}}, \underline{z}_{01}$

g_{L2}	Power gain of a transmission line 2
$g_{L2}(\underline{r}_{\ell,\underline{Z}_{02}})$	Power gain of a transmission line 2 as a function of reflection coefficient $\underline{r}_{\ell,\underline{Z}_{02}}$
$g_{T,L}$	Transducer power gain of a transmission line
$g_{T,L1}$	Transducer power gain of a transmission line 1
$g_{T,L1}(\underline{r}_{i,\underline{Z}_{01}},\underline{r}_{1tp,\underline{Z}_{01}})$	Transducer power gain of a transmission line 1 as a function of the reflection coefficients $\underline{r}_{i,\underline{Z}_{01}}$ and $\underline{r}_{1tp,\underline{Z}_{01}}$
g_{Ttot}	Transducer power gain of the complete matching system
l_1	Length of transmission line 1
l_2	Length of transmission line 2
P_{act1}	Active power transferred to the input of a transmission line
P_{act2}	Active power transferred to the load of a transmission line
P_{act11}	Active power transferred to the input of transmission line 1
P_{act12}	Active power transferred to the input of transmission line 2
P_{act1tp}	Active power transferred to the input of a two-port
P_{act21}	Active power transferred to the load of transmission line 1
P_{act22}	Active power transferred to the load of transmission line 2
$P_{act\ell}$	Active power transferred to the load impedance $\underline{Z}_\ell$
$P_{act\ell1}$	Active power transferred to the load of transmission line 1
$P_{act\ell2}$	Active power transferred to the load of transmission line 2
$P_{act\ell tp}$	Active power transferred to the load of a two-port
$P_{actmaxi}$	Available power of source with source impedance $\underline{Z}_i$
$\underline{r}$	(Complex) reflection coefficient (without reference index referred to $\underline{Z}_0$)
$\underline{r}(\tilde{r})$	Reflection coefficient as a function of reflection coefficient $\tilde{r}$ (both reflection coefficients referred to $\underline{Z}_0$)
$\underline{r}(\underline{Z})$	Reflection coefficient of $\underline{Z}$ (without reference index referred to $\underline{Z}_0$)
$\underline{r}_1$	Reflection coefficient at the beginning of a transmission line (at its input, referred to $\underline{Z}_0$)
$\underline{r}_{11,\underline{Z}_{01}}$	Reflection coefficient at the beginning of transmission line 1 (at its input) referred to $\underline{Z}_{01}$
$\underline{r}_{12,\underline{Z}_{02}}$	Reflection coefficient at the beginning of transmission line 2 (at its input) referred to $\underline{Z}_{02}$
$\underline{r}_{1tp,\underline{Z}_{0tp1}}$	Reflection coefficient at the input of a two-port referred to $\underline{Z}_{0tp1}$
$\underline{r}_{1tp,\underline{Z}_{0tp1}}(\underline{r}_{\ell tp,\underline{Z}_{0tp2}})$	Reflection coefficient $\underline{r}_{1tp,\underline{Z}_{0tp1}}$ as a function of reflection coefficient $\underline{r}_{\ell tp,\underline{Z}_{0tp2}}$
$\underline{r}_2$	Reflection coefficient at the end of a transmission line (of its load, referred to $\underline{Z}_0$)
$\underline{r}_{21,\underline{Z}_{01}}$	Reflection coefficient at the end of transmission line 1 (of its load) referred to $\underline{Z}_{01}$
$\underline{r}_{22,\underline{Z}_{02}}$	Reflection coefficient at the end of transmission line 2 (of its load) referred to $\underline{Z}_{02}$
$\underline{r}_i$	Reflection coefficient of source impedance $\underline{Z}_i$ (referred to $\underline{Z}_0$)
$\underline{r}_{i,\underline{Z}_{01}}$	Reflection coefficient of source impedance $\underline{Z}_i$ referred to $\underline{Z}_{01}$
$\underline{r}_{i1,\underline{Z}_{01}}$	Reflection coefficient of the source impedance of transmission line 1 referred to $\underline{Z}_{01}$
$\underline{r}_{itp,\underline{Z}_{01}}$	Reflection coefficient of the source impedance of a two-port referred to $\underline{Z}_{01}$
$\underline{r}_{itp,\underline{Z}_{0tp1}}$	Reflection coefficient of the source impedance of a two-port referred to $\underline{Z}_{0tp1}$
$\underline{r}_\ell$	Reflection coefficient of load impedance $\underline{Z}_\ell$ (referred to $\underline{Z}_0$)
$\underline{r}_{\ell,\underline{Z}_{02}}$	Reflection coefficient of the load impedance of $\underline{Z}_\ell$ referred to $\underline{Z}_{02}$
$\underline{r}_{\ell tp,\underline{Z}_{02}}$	Reflection coefficient of the load impedance of a two-port referred to $\underline{Z}_{02}$
$\underline{r}_{\ell tp,\underline{Z}_{0tp2}}$	Reflection coefficient of the load impedance of a two-port referred to $\underline{Z}_{0tp2}$
$\underline{r}_{\tilde{\underline{Z}}_0}$	(Complex) reflection coefficient (reference index indicates that it's referred to $\tilde{\underline{Z}}_0$)
$\underline{r}_{\tilde{\underline{Z}}_0}(\underline{Z})$	Reflection coefficient of $\underline{Z}$ referred to $\tilde{\underline{Z}}_0$
R'	Per-unit-length resistance of a transmission line
R_0	Real part of $\underline{Z}_0$, the complex characteristic impedance of a transmission line
R_{01}	Real part of $\underline{Z}_{01}$, the complex characteristic impedance of transmission line 1
R_{02}	Real part of $\underline{Z}_{02}$, the complex characteristic impedance of transmission line 2
$\underline{V}_0$	Complex amplitude of an ideal voltage source
X_0	Imaginary part of $\underline{Z}_0$, the complex characteristic impedance of a transmission line
X_{01}	Imaginary part of $\underline{Z}_{01}$, the complex characteristic impedance of transmission line 1
X_{02}	Imaginary part of $\underline{Z}_{02}$, the complex characteristic impedance of transmission line 2

$\underline{Z}_0$	Complex characteristic impedance of a transmission line
$\underline{Z}_{01}$	Complex characteristic impedance of transmission line 1
$\underline{Z}_{02}$	Complex characteristic impedance of transmission line 2
Z_{0ll}	Real characteristic impedance of a lossless transmission line, nominal (real) characteristic impedance of a transmission line
$\underline{Z}_{0tp1}$	Reference impedance of the reflection coefficients at a two-port's input
$\underline{Z}_{0tp2}$	Reference impedance of the reflection coefficients at a two-port's output
$\underline{Z}_i$	Source impedance
$\underline{Z}_\ell$	Load impedance

Greek letters

α_1	Attenuation constant of transmission line 1
α_2	Attenuation constant of transmission line 2
β_1	Phase constant of transmission line 1
β_2	Phase constant of transmission line 2

2.3 Basic definitions

- The active power transferred to an impedance is the real part of the product of the voltage at the impedance times the complex conjugate of the current flowing through the impedance.
- As usual, a power gain is the ratio of active powers, although "active power gain" would be a more precise terminology.
- The Q factor of an impedance is the ratio of its reactance to its resistance.

2.4 Properties of lossy (coaxial) transmission lines

In the system under consideration, lossy coaxial transmission lines connect the source and the load to the matching network. These lines exhibit a nominal characteristic impedance of

$$Z_{0ll} = 50\,\Omega, \tag{2.1}$$

a per-unit-length capacitance C' and an attenuation a at the frequency of interest, usually specified as $a_{\mathrm{dB/100\,m}}$ in dB/100 m.

In this work, matching network and connecting lines will be operated within the short wave frequency range of about 1.8 – 30 MHz. It is well known that the coaxial line's losses in this frequency range are dominated by its series resistance characterised by the per-unit-length resistance R' ([26a], [26h], [27a], [27b], and [27c]). Thus certain approximations apply, in particular for the calculation of the attenuation constant α [†], the phase constant β [†], and the line's characteristic impedance $\underline{Z}_0$

[†]Despite their names, α, β, and thus $\underline{\gamma}$ are not constant, but depend on the operating frequency.

([26h], [26b], [26c] or [27a]). Additionally the ratio of attenuation to phase constant may be assumed to be much less than unity, $\frac{\alpha}{\beta} \ll 1$, and α is approximately proportional to the square root of the operating frequency f or angular frequency $\omega = 2\pi f$, respectively; i. e. $\alpha \sim \sqrt{\omega}$.

More specifically,

$$\alpha = \frac{1}{2} \frac{\frac{1}{10} \frac{a_{\mathrm{dB/100\,m}}}{\mathrm{dB/100\,m}} \ln 10}{100\,\mathrm{m}} \left[\approx \frac{R'}{2Z_{0\mathrm{II}}} \right], \tag{2.2}$$

$$\beta \approx \omega Z_{0\mathrm{II}} C', \tag{2.3}$$

$$\underline{Z}_0 \approx Z_{0\mathrm{II}} \left(1 - \mathrm{j}\frac{\alpha}{\beta}\right) \overset{(2.3)}{\approx} Z_{0\mathrm{II}} - \mathrm{j}\frac{\alpha}{\omega C'}. \tag{2.4}$$

Since $\frac{\alpha}{\beta} \ll 1$, the worse approximation

$$\underline{Z}_0 \approx Z_{0\mathrm{II}} \tag{2.5}$$

is usually employed.

The error introduced by this approximation is low for transmission lines terminated by its characteristic impedance. Conversely, it may be quite high for terminations strongly deviating from its characteristic impedance. This issue is discussed in Section 5.4.1 in detail.

Thus in the following sections all formulae will be derived for a complex characteristic impedance. To use the real characteristic impedance instead, we just have to put $X_0 = \mathrm{Im}\{\underline{Z}_0\} = 0$.

As usual, the transmission line's propagation constant[†]

$$\underline{\gamma} = \alpha + \mathrm{j}\beta \tag{2.6}$$

is always assumed to be complex.

2.5 Rewriting of some circuit parameters as functions of their reflection coefficients

All equations derived in the following sections will depend solely on reflection coefficients, S-parameters, and power gains. Thus, as a first step, some of the original circuit parameters have to be rewritten as functions of their reflection coefficients; namely, the real and imaginary part of the impedance or admittance, the change of the reference characteristic impedance of a reflection coefficient, and the reflection coefficient of the conjugate complex impedance.

In this section, the "reflection coefficient" is used as a conformal mapping with parameter $\underline{Z}_0$. Its physical relevance for transmission lines is delayed to Section 2.6.

The "reflection coefficient" $\underline{r}$ of a complex impedance

$$\underline{Z} := R + \mathrm{j}X \tag{2.7}$$

referred to a reference impedance

$$\underline{Z}_0 := R_0 + \mathrm{j}X_0, \tag{2.8}$$

is defined by [26e]:

$$\underline{r} := \frac{\underline{Z} - \underline{Z}_0}{\underline{Z} + \underline{Z}_0}. \tag{2.9}$$

Conversely, the complex impedance $\underline{Z}$ may be calculated as a function of $\underline{r}$ as

$$\underline{Z} = \underline{Z}_0 \frac{1 + \underline{r}}{1 - \underline{r}}. \tag{2.10}$$

Solving for the real part R of the impedance yields

$$R = \mathrm{Re}\left\{\underline{Z}_0 \frac{1 + \underline{r}}{1 - \underline{r}}\right\} = \frac{1}{2}\left(\underline{Z}_0 \frac{1 + \underline{r}}{1 - \underline{r}} + \underline{Z}_0^* \frac{1 + \underline{r}^*}{1 - \underline{r}^*}\right),$$

or equivalently,

$$R = \frac{1}{2} \frac{\underline{Z}_0 (1 + \underline{r} - \underline{r}^* - |\underline{r}|^2) + \underline{Z}_0^* (1 - \underline{r} + \underline{r}^* - |\underline{r}|^2)}{|1 - \underline{r}|^2}.$$

By applying (2.8), it can be shown that

$$R = \frac{R_0 (1 - |\underline{r}|^2) - 2X_0 \,\mathrm{Im}\{\underline{r}\}}{1 - 2\,\mathrm{Re}\{\underline{r}\} + |\underline{r}|^2} = \mathrm{Re}\{\underline{Z}\}. \tag{2.11}$$

Similar derivation of the imaginary part X of the impedance gives

$$X = \mathrm{Im}\left\{\underline{Z}_0 \frac{1 + \underline{r}}{1 - \underline{r}}\right\} = \frac{1}{2\mathrm{j}}\left(\underline{Z}_0 \frac{1 + \underline{r}}{1 - \underline{r}} - \underline{Z}_0^* \frac{1 + \underline{r}^*}{1 - \underline{r}^*}\right)$$

or

$$X = \frac{2R_0 \,\mathrm{Im}\{\underline{r}\} + X_0 (1 - |\underline{r}|^2)}{1 - 2\,\mathrm{Re}\{\underline{r}\} + |\underline{r}|^2} = \mathrm{Im}\{\underline{Z}\}. \tag{2.12}$$

In some cases we will use the admittance

$$\underline{Y} := \frac{1}{\underline{Z}} = G + \mathrm{j}B \tag{2.13}$$

rather than the impedance $\underline{Z}$.

Rearranging (2.9) as $-\underline{r} = (\frac{1}{\underline{Z}} - \frac{1}{\underline{Z}_0})/(\frac{1}{\underline{Z}} + \frac{1}{\underline{Z}_0})$ and applying $(-\underline{r})^* = -\underline{r}^*$, one can solve, in a similar fashion as above, for the real part G and the imaginary part B of the admittance:

$$G = \frac{R_0 (1 - |\underline{r}|^2) - 2X_0 \,\mathrm{Im}\{\underline{r}\}}{|\underline{Z}_0|^2 (1 + 2\,\mathrm{Re}\{\underline{r}\} + |\underline{r}|^2)} = \mathrm{Re}\left\{\frac{1}{\underline{Z}}\right\}, \tag{2.14}$$

$$B = -\frac{2R_0 \,\mathrm{Im}\{\underline{r}\} + X_0 (1 - |\underline{r}|^2)}{|\underline{Z}_0|^2 (1 + 2\,\mathrm{Re}\{\underline{r}\} + |\underline{r}|^2)} = \mathrm{Im}\left\{\frac{1}{\underline{Z}}\right\}. \tag{2.15}$$

Sometimes we may need to change the reference characteristic impedance from a given reflection coefficient $\underline{r}$ referred to $\underline{Z}_0$ to a reflection coefficient $\underline{r}_{\widetilde{\underline{Z}}_0}$ referred to $\widetilde{\underline{Z}}_0$, which is equivalent to a transformation of the coordinates from parameter $\underline{Z}_0$ to parameter $\widetilde{\underline{Z}}_0$.

Both reflection coefficients describe the same impedance, hence combining of (2.9) and (2.10) yields

$$\underline{r}_{\widetilde{\underline{Z}}_0} = \frac{(1+\underline{r})\,\underline{Z}_0 - (1-\underline{r})\,\widetilde{\underline{Z}}_0}{(1+\underline{r})\,\underline{Z}_0 + (1-\underline{r})\,\widetilde{\underline{Z}}_0} = \frac{\underline{r} - \underline{r}_{\underline{Z}_0}(\widetilde{\underline{Z}}_0)}{1 - \underline{r}\,\underline{r}_{\underline{Z}_0}(\widetilde{\underline{Z}}_0)} = \frac{\underline{r} + \underline{r}_{\widetilde{\underline{Z}}_0}(\underline{Z}_0)}{1 + \underline{r}\,\underline{r}_{\widetilde{\underline{Z}}_0}(\underline{Z}_0)} \tag{2.16}$$

$$\text{where} \quad \underline{r}_{\underline{Z}_0}(\widetilde{\underline{Z}}_0) = \frac{\widetilde{\underline{Z}}_0 - \underline{Z}_0}{\widetilde{\underline{Z}}_0 + \underline{Z}_0} = -\frac{\underline{Z}_0 - \widetilde{\underline{Z}}_0}{\underline{Z}_0 + \widetilde{\underline{Z}}_0} = -\underline{r}_{\widetilde{\underline{Z}}_0}(\underline{Z}_0). \tag{2.17}$$

In what follows the reflection coefficient $\underline{r}(\underline{Z}^*)$ of the impedance's $\underline{Z}$ conjugate complex $\underline{Z}^*$ will be derived.

Starting from the reflection coefficient's definition in (2.9)

$$\underline{r}(\underline{Z}^*) = \frac{\underline{Z}^* - \underline{Z}_0}{\underline{Z}^* + \underline{Z}_0}$$

and applying (2.10) yields

$$\underline{r}(\underline{Z}^*) = \frac{\underline{Z}_0^* \frac{1+\underline{r}^*}{1-\underline{r}^*} - \underline{Z}_0}{\underline{Z}_0^* \frac{1+\underline{r}^*}{1-\underline{r}^*} + \underline{Z}_0} = \frac{\underline{Z}_0^*(1+\underline{r}^*) - \underline{Z}_0(1-\underline{r}^*)}{\underline{Z}_0^*(1+\underline{r}^*) + \underline{Z}_0(1-\underline{r}^*)}$$

In other words:

$$\begin{aligned} \underline{r}(\underline{Z}^*) &= \frac{(\underline{Z}_0 + \underline{Z}_0^*)\,\underline{r}^* - (\underline{Z}_0 - \underline{Z}_0^*)}{\underline{Z}_0 + \underline{Z}_0^* - (\underline{Z}_0 - \underline{Z}_0^*)\,\underline{r}^*} \\ &= \frac{R_0\,\underline{r}^* - \mathrm{j}X_0}{R_0 - \mathrm{j}X_0\,\underline{r}^*}. \end{aligned} \tag{2.18}$$

We may conclude from (2.18) that $\underline{r}(\underline{Z}^*)$ equals $\underline{r}^*$ for any $\underline{r}$ for a real characteristic impedance ($X_0 = 0$) only[‡].

If $\underline{Z} = \underline{Z}_0$, thus $\underline{Z}^* = \underline{Z}_0^*$, (2.18) becomes

$$\underline{r}(\underline{Z}_0^*) = -\mathrm{j}\,\frac{X_0}{R_0}. \tag{2.19}$$

[‡]However, two $\underline{r}(\underline{Z})$ exist where $\underline{r}(\underline{Z}^*) = \underline{r}(\underline{Z}) = \underline{r}^*(\underline{Z})$, in particular $\underline{r}(\underline{Z}) = \pm 1$. They describe an impedance of $\underline{Z} \to \infty$ and $\underline{Z} = 0$, respectively, which are idealised impedance limits.

2.6 Active power in a transmission line and its transducer and power gain

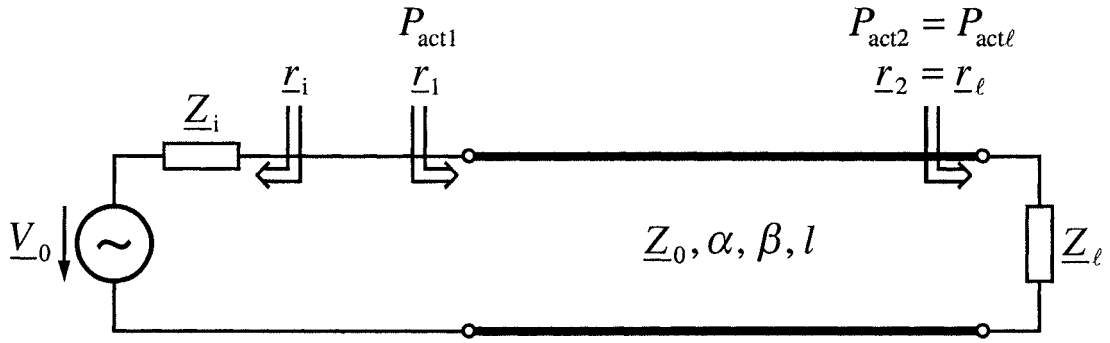

Figure 2.1: Basic transmission line with source and load

In Figure 2.1, a transmission line with input reflection coefficient $\underline{r}_1$ connected to a source $\underline{V}_0$ and load with impedance $\underline{Z}_\ell$ is depicted.

In what follows we are going to derive the transmission line's power gain g_L.

All the necessary formulae that are given below are presented in detail in Appendix A.2 and Appendix A.3.

From (A.3), the reflection coefficient $\underline{r}_1$ at the input of the line is obtained as

$$\underline{r}_1 = \underline{r}_\ell \, e^{-2\alpha l} \, e^{-j2\beta l}. \tag{2.20}$$

The transducer power gain $g_{T,L}$ of the line is given in (A.10) by

$$g_{T,L} := \frac{P_{act\ell}}{P_{actmaxi}} = e^{-2\alpha l} \, \frac{[R_0 (1-|\underline{r}_i|^2)-2X_0 \, \mathrm{Im}\{\underline{r}_i\}]\,[R_0 (1-|\underline{r}_\ell|^2)-2X_0 \, \mathrm{Im}\{\underline{r}_\ell\}]}{|\underline{Z}_0|^2 \, |1-\underline{r}_i \underline{r}_\ell \, e^{-2\alpha l} \, e^{-j2\beta l}|^2}, \tag{2.21}$$

where $P_{actmaxi}$ is the available power, defined in (A.1) as

$$P_{actmaxi} = \frac{|\underline{V}_0|^2}{8 \, \mathrm{Re}\{\underline{Z}_i\}}. \tag{2.22}$$

The power gain g_L of the line is described in (A.12) as

$$g_L := \frac{P_{act\ell}}{P_{act1}} = e^{-2\alpha l} \, \frac{R_0 (1 - |\underline{r}_\ell|^2) - 2X_0 \, \mathrm{Im}\{\underline{r}_\ell\}}{R_0 (1 - e^{-4\alpha l} \, |\underline{r}_\ell|^2) - 2X_0 \, e^{-2\alpha l} \, \mathrm{Im}\{\underline{r}_\ell \, e^{-j2\beta l}\}}. \tag{2.23}$$

A similar formula is derived in [28] and [29].

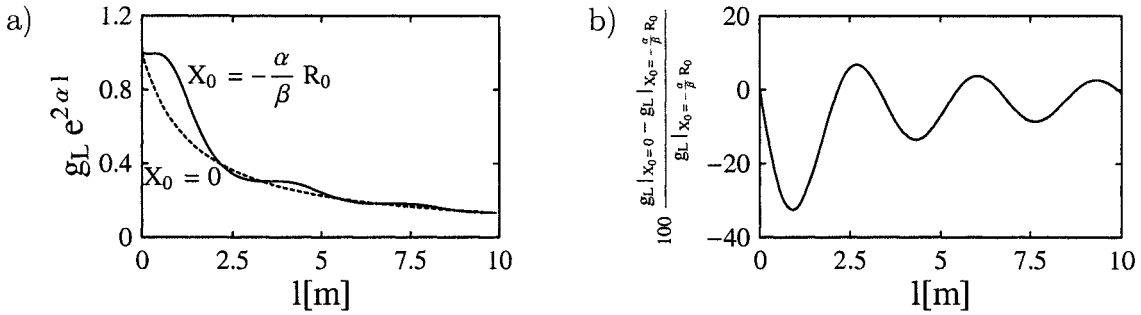

Figure 2.2: a) Power gain g_L of the line and b) percentage error for a RG-213/U coaxial transmission line at 30 MHz

To illustrate the magnitude of the error in mismatched transmission lines, an example for (2.23) was calculated in Figure 2.2. Numerical values employed are: $Z_{0ll} = 50\,\Omega$, $C' = 101\,\frac{\text{pF}}{\text{m}}$, $a_{\text{dB/100 m}} = 3.7\,\frac{\text{dB}}{100\,\text{m}}$, $\alpha = 0.004260\,\frac{1}{\text{m}}$, $\beta = 0.9519\,\frac{1}{\text{m}}$, $R_0 = \text{Re}\{\underline{Z}_0\}$, $X_0 = \text{Im}\{\underline{Z}_0\}$, and the line's length l. The transmission line was terminated by $5\,\Omega$ in series to $1.06\,\mu\text{H}$ (equal to $5\,\Omega + \text{j}\,200\,\Omega$).

Although $\frac{\alpha}{\beta} = 0.004475 \ll 1$, using (2.5) instead of (2.4) causes a deviation of up to 33 % for the line's power gain!

Despite the impressive result, we should keep in mind that the error depends on line length and termination impedance. Additionally, even the "more accurate" calculation using (2.4) relies on cable data which might be erroneous due to changes of its characteristic impedance caused by bending, connectors, etc.

However, regarding the system under consideration, we might conclude that calculations should always be done using the complex characteristic impedance (2.4), enabling calculation of its influence on the optimisation's results and estimation of the errors introduced by using (2.5).

2.7 Transferred active power in a source, line 1, two-port, line 2, and load system

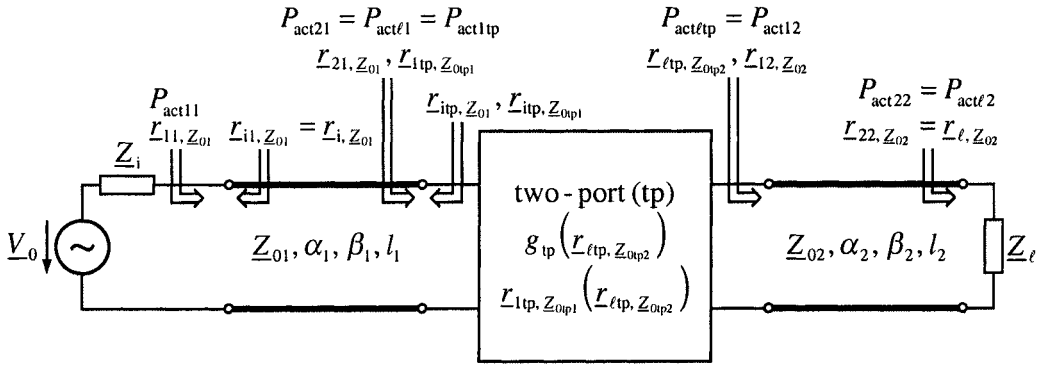

Figure 2.3: Definitions and setup of a system consisting of a source, transmission line 1, two-port tp, transmission line 2, and load

As shown in Figure 2.3, the input of a two-port (tp) is connected to a source (source impedance $\underline{Z}_\mathrm{i}$) using transmission line 1 of length l_1. Its output is connected to a load $\underline{Z}_\ell$ using transmission line 2 of length l_2. The complex characteristic impedances of the lines are $\underline{Z}_{01,2}$, their attenuation constants $\alpha_{1,2}$, and their phase constants $\beta_{1,2}$.

The two-port will be characterised by its power gain

$$g_\mathrm{tp} = \frac{P_\mathrm{act\ell tp}}{P_\mathrm{act1tp}} \tag{2.24}$$

and its input impedance, which depend on its load impedance.

However, for our purpose it's more convenient to replace the two-port's input impedance with its reflection coefficient $\underline{r}_{1\mathrm{tp},\underline{Z}_{0\mathrm{tp1}}}$, which is referred to $\underline{Z}_{0\mathrm{tp1}}$, and the two-ports load with its reflection coefficient $\underline{r}_{\ell\mathrm{tp},\underline{Z}_{0\mathrm{tp2}}}$, which is referred to $\underline{Z}_{0\mathrm{tp2}}$.

Choosing $\underline{Z}_{0\mathrm{tp1}} = \underline{Z}_{01}$ and $\underline{Z}_{0\mathrm{tp2}} = \underline{Z}_{02}$ simplifies calculations, but such choice might be impossible if measured values are used. For example, the network analyser measurement results will typically be referred to $\underline{Z}_{0\mathrm{tp1}} = \underline{Z}_{0\mathrm{tp2}} = 50\,\Omega$. However, $\underline{Z}_{01,2}$ might be complex.

If $\underline{Z}_{0\mathrm{tp1}} \neq \underline{Z}_{01}$ or $\underline{Z}_{0\mathrm{tp2}} \neq \underline{Z}_{02}$, then $\underline{r}_{1\mathrm{tp},\underline{Z}_{0\mathrm{tp1}}}$ has to be rewritten in $\underline{r}_{1\mathrm{tp},\underline{Z}_{01}} = \underline{r}_{21,\underline{Z}_{01}}$ or $\underline{r}_{\ell\mathrm{tp},\underline{Z}_{02}} = \underline{r}_{12,\underline{Z}_{02}} = \underline{r}_{\ell,\underline{Z}_{02}}\,\mathrm{e}^{-2\alpha_2 l_2}\,\mathrm{e}^{-\mathrm{j}2\beta_2 l_2}$ in $\underline{r}_{\ell\mathrm{tp},\underline{Z}_{0\mathrm{tp2}}}$ by changing the reflection coefficient's reference characteristic impedance using (2.16).

Finally, the active power delivered to the load $\underline{Z}_\ell$ in the system of Figure 2.3 is given by

$$P_\mathrm{act\ell} = P_\mathrm{actmaxi}\, g_\mathrm{Ttot}, \tag{2.25}$$

where g_Ttot is the transducer power gain of the complete system.

The system's transducer power gain g_Ttot might be computed using (2.21) and (2.23):

$$g_\mathrm{Ttot} := \frac{P_\mathrm{act\ell}}{P_\mathrm{actmaxi}} = g_{\mathrm{T,L1}}(\underline{r}_{\mathrm{i},\underline{Z}_{01}}, \underline{r}_{1\mathrm{tp},\underline{Z}_{01}})\, g_\mathrm{tp}(\underline{r}_{\ell\mathrm{tp},\underline{Z}_{0\mathrm{tp2}}})\, g_\mathrm{L2}(\underline{r}_{\ell,\underline{Z}_{02}}),$$

which after simplification yields:

$$g_{\mathrm{Ttot}} = \mathrm{e}^{-2(\alpha_1 l_1+\alpha_2 l_2)} \frac{[R_{01}\,\mathrm{Im}\{\underline{r}_{\mathrm{i},\underline{Z}_{01}}\}]\,[R_{01}\,(1-|\underline{r}_{1\mathrm{tp},\underline{Z}_{01}}|^2)-2X_{01}\,\mathrm{Im}\{\underline{r}_{1\mathrm{tp},\underline{Z}_{01}}\}]}{|\underline{Z}_{01}|^2\,|1-\underline{r}_{\mathrm{i},\underline{Z}_{01}}\,\underline{r}_{1\mathrm{tp},\underline{Z}_{01}}\,\mathrm{e}^{-2\alpha_1 l_1}\,\mathrm{e}^{-\mathrm{j}2\beta_1 l_1}|^2}$$
$$\cdot\, g_{\mathrm{tp}}(\underline{r}_{\ell\mathrm{tp},\underline{Z}_{0\mathrm{tp}2}})\,\frac{R_{02}\,(1-|\underline{r}_{\ell,\underline{Z}_{02}}|^2)-2X_{02}\,\mathrm{Im}\{\underline{r}_{\ell,\underline{Z}_{02}}\}}{R_{02}\,(1-\mathrm{e}^{-4\alpha_2 l_2}\,|\underline{r}_{\ell,\underline{Z}_{02}}|^2)-2X_{02}\,\mathrm{e}^{-2\alpha_2 l_2}\,\mathrm{Im}\{\underline{r}_{\ell,\underline{Z}_{02}}\,\mathrm{e}^{-\mathrm{j}2\beta_2 l_2}\}}. \tag{2.26}$$

To minimise the losses of the complete system, its power gain g_{tot} is used instead, which is given by

$$g_{\mathrm{tot}} := \frac{P_{\mathrm{act}\ell}}{P_{\mathrm{act}11}} = g_{\mathrm{L}1}(\underline{r}_{1\mathrm{tp},\underline{Z}_{01}})\,g_{\mathrm{tp}}(\underline{r}_{\ell\mathrm{tp},\underline{Z}_{0\mathrm{tp}2}})\,g_{\mathrm{L}2}(\underline{r}_{\ell,\underline{Z}_{02}}),$$

which after simplification yields:

$$g_{\mathrm{tot}} = \mathrm{e}^{-2(\alpha_1 l_1+\alpha_2 l_2)} \frac{R_{01}\,(1-|\underline{r}_{1\mathrm{tp},\underline{Z}_{01}}|^2)-2X_{01}\,\mathrm{Im}\{\underline{r}_{1\mathrm{tp},\underline{Z}_{01}}\}}{R_{01}\,(1-\mathrm{e}^{-4\alpha_1 l_1}\,|\underline{r}_{1\mathrm{tp},\underline{Z}_{01}}|^2)-2X_{01}\,\mathrm{e}^{-2\alpha_1 l_1}\,\mathrm{Im}\{\underline{r}_{1\mathrm{tp},\underline{Z}_{01}}\,\mathrm{e}^{-\mathrm{j}2\beta_1 l_1}\}}$$
$$\cdot\, g_{\mathrm{tp}}(\underline{r}_{\ell\mathrm{tp},\underline{Z}_{0\mathrm{tp}2}})\,\frac{R_{02}\,(1-|\underline{r}_{\ell,\underline{Z}_{02}}|^2)-2X_{02}\,\mathrm{Im}\{\underline{r}_{\ell,\underline{Z}_{02}}\}}{R_{02}\,(1-\mathrm{e}^{-4\alpha_2 l_2}\,|\underline{r}_{\ell,\underline{Z}_{02}}|^2)-2X_{02}\,\mathrm{e}^{-2\alpha_2 l_2}\,\mathrm{Im}\{\underline{r}_{\ell,\underline{Z}_{02}}\,\mathrm{e}^{-\mathrm{j}2\beta_2 l_2}\}}. \tag{2.27}$$

2.8 Summary

In this chapter we have recalled some definitions and shown how different variables can be written in terms of reflection coefficients. The power gain of a single transmission line and of the complete matching system is given. Several notations used throughout this work are also presented.

Chapter 3

Lossy L, π, and T Matching Networks

3.1 Introduction

The following chapter addresses the losses in L, π, and T matching networks. Firstly, we propose a simple and synthetical loss model, which will be validated using the results of [22], [24], and [25]. Next, after chosing a proper parametrisation, we consider the networks' behaviour if source and load are purely resistive. Application of the model yields the optimum parameter's (and load resistance's) value for maximum active power transfer.

3.2 Definitions/notations

From this chapter on, the following definitions/notations will be used:

Latin letters

a	Real coefficient of the series loss model
$a_{0\mathrm{ldd}\Phi_\mathrm{M}}$	Constant linearisation coefficient of $\frac{i_\mathrm{C}}{d_\mathrm{C}}\,\Phi_\mathrm{M}$
$a_{0\mathrm{r}}$	Constant linearisation coefficient of r'_PS
$a_{0\mathrm{L}}$	Constant linearisation coefficient of series inductance L_s
$a_{0\mathrm{N}\Phi_\mathrm{A}}$	Constant linearisation coefficient of $N_\mathrm{T}\,\Phi_\mathrm{A}$
$a_{0\mathrm{R}}$	Constant linearisation coefficient of series resistance R_s
$a_{0\Phi_\mathrm{A}}$	Constant linearisation coefficient of Φ_A
$a_{0\Phi_\mathrm{M}}$	Constant linearisation coefficient of Φ_M
$a_{1\mathrm{ldd}\Phi_\mathrm{M}}$	Linear linearisation coefficient of $\frac{i_\mathrm{C}}{d_\mathrm{C}}\,\Phi_\mathrm{M}$
$a_{1\mathrm{r}}$	Linear linearisation coefficient of r'_PS
$a_{1\mathrm{L}}$	Linear linearisation coefficient of series inductance L_s
$a_{1\mathrm{N}\Phi_\mathrm{A}}$	Linear linearisation coefficient of $N_\mathrm{T}\,\Phi_\mathrm{A}$
$a_{1\mathrm{R}}$	Linear linearisation coefficient of series resistance R_s
$a_{1\Phi_\mathrm{A}}$	Linear linearisation coefficient of Φ_A
$a_{1\Phi_\mathrm{M}}$	Linear linearisation coefficient of Φ_M
$a_{2\mathrm{R}}$	Quadratic linearisation coefficient of series resistance R_s

a_n	n-th real coefficient of the series loss model
$\tilde{a}_n$	n-th real coefficient of the parallel loss model
b	Real exponent of the series loss model
b_n	n-th real exponent of the series loss model (sorted in ascending order with increasing n)
$\tilde{b}_n$	n-th real exponent of the parallel loss model
b_N	Real exponent of the series loss model with the highest index, thus the highest real exponent of the model
C_{m1}	Capacitance calculated from imaginary part of parallel-to-series transformed G_i and C_1 in a π network
C_{m1}	Capacitance calculated from imaginary part of series-to-parallel transformed R_i and C_1 in a T network
C_{m2}	Capacitance calculated from imaginary part of parallel-to-series transformed G_ℓ and C_2 in a π network
C_{m2}	Capacitance calculated from imaginary part of series-to-parallel transformed R_ℓ and C_2 in a T network
C_p	Parallel capacitance
C_s	Series capacitance
d	Diameter of round wire used to make the windings of a solenoidal coil
d_C	Mean diameter of a solenoidal coil
D	Distance of wire centres (winding centres) in a solenoidal coil (pitch)
g_t	Power gain of a T network
$g_{\mathrm{t,inma}}$	Power gain of a T network which is (exactly) matched at its input
g_π	Power gain of a π network
$g_{\pi,\mathrm{inma}}$	Power gain of a π network which is (exactly) matched at its input
G_i	Source conductance
G_ℓ	Load conductance — "special" definition in matching networks: in case of a π network, load conductance (real part of load admittance) of that network, in case of a T network, $G_\ell = \frac{1}{R_\ell}$, where R_ℓ is the load resistance (real part of load impedance)
G_m	"Virtual" conductance, the parameter describing the degree of freedom in a T network
G_{m1}	Real part of series-to-parallel transformed R_i and C_1 in a T network
G_{m2}	Real part of series-to-parallel transformed R_ℓ and C_2 in a T network
G_{mlim}	Limit of G_m derived by solving (3.34) — may yield several solutions — without additional index the highest valid solution of (3.34) (T network exactly matched at its input) or (B.16) (T network exactly matched at its output)
G_p	Parallel conductance of parallel inductance L_p
G_{p0}	Constant conductance term of the parallel loss model
G_{p0}	Constant parallel conductance of constant parallel inductance L_{p0}
$\underline{I}_0$	Complex amplitude of an ideal current source
K	(Tabulated) factor to derive the inductance of an air core single-layer solenoidal coil
$K(\ldots)$	(Tabulated) factor to derive the inductance of an air core single-layer solenoidal coil as a function of ...
l_{ax}	Axial length of rectangular wire used to make the windings of a solenoidal coil
l_{rad}	Radial length of rectangular wire used to make the windings of a solenoidal coil
l_C	Mean length of a solenoidal coil
L_p	Parallel inductance
L_{p0}	Constant parallel inductance
L_{p1}	Parallel inductance of the left L network if a T network is separated in two L networks
L_{p2}	Parallel inductance of the right L network if a T network is separated in two L networks
L_s	Series inductance
L_{s0}	Constant series inductance
L_{s1}	Series inductance of the left L network if a π network is separated in two L networks
L_{s2}	Series inductance of the right L network if a π network is separated in two L networks
$L_{\mathrm{s}n_\mathrm{C}}$	One series inductance of switchable series connected inductors (sorted in ascending order of inductances)
$L_{\mathrm{s}N_\mathrm{C}}$	Last series inductance of switchable series connected inductors (highest inductance)
n	Natural number

n_{C}	Number of one switchable series connected inductor
n_{T}	Partial number of turns
N	Natural number
N_{C}	Total number of switchable series connected inductors
N_{T}	Total number of turns
P_{actp}	Active power transferred to the parallel conductance G_{p}
P_{acts}	Active power transferred to the series resistance R_{s}
Q	Q factor of the central inductor of a π or T network
r'_{PS}	Ratio of the per-unit-length resistance including proximity effect to the per-unit-length-resistance calculated for a pure skin effect
$r'_{\mathrm{PS}}(\ldots,\ldots)$	Ratio of the per-unit-length resistance including proximity effect to the per-unit-length-resistance calculated for a pure skin effect as a function of ... and ...
R_{i}	Source resistance
R_ℓ	Load resistance — "special" definition in matching networks: in case of a T network, load resistance (real part of load impedance) of that network, in case of a π network, $R_\ell = \frac{1}{G_\ell}$, where G_ℓ is the load conductance (real part of load admittance)
R_{m}	"Virtual" resistance, the parameter describing the degree of freedom in a π network
R_{m1}	Real part of parallel-to-series transformed G_{i} and C_{i} in a π network
R_{m2}	Real part of parallel-to-series transformed G_ℓ and C_2 in a π network
R_{mlim}	Limit of R_{m} derived by solving (3.21) — may yield several solutions — without additional index the highest valid solution of (3.21) (π network exactly matched at its input) or (B.7) (π network exactly matched at its output)
R_{s}	Series resistance of series inductance L_{s}
R_{s0}	Constant resistance term of the series loss model
R_{s0}	Constant series resistance of constant series inductance L_{s0}
$R_{\mathrm{s}n_{\mathrm{C}}}$	Series resistance of one of the series inductances of switchable series connected inductors
$R_{\mathrm{s}N_{\mathrm{C}}}$	Series resistance of the last series inductance of switchable series connected inductors
$\mathrm{S}_{n_{\mathrm{C}}}$	Switch shorting one of the series inductances of switchable series connected inductors
$\mathrm{S}_{N_{\mathrm{C}}}$	Switch shorting the last series inductance of switchable series connected inductors
S_{t}	Abbreviation for a sum in Section 3.5.3.2
S_π	Abbreviation for a sum in Section 3.5.2.2
$\underline{Y}_{1\mathrm{i}}$	Admittance of source and first L network as defined in Figure 3.15
$\underline{Y}_{2\mathrm{i}}$	Admittance of source, first L network, and parallel conductance as defined in Figure 3.15
$\underline{Y}_{1\ell}$	Admittance of load, second L network, and parallel conductance as defined in Figure 3.15
$\underline{Y}_{2\ell}$	Admittance of load and second L network as defined in Figure 3.15
$\underline{Z}_{1\mathrm{i}}$	Impedance of source and first L network as defined in Figure 3.14
$\underline{Z}_{1\ell}$	Impedance of load, second L network, and series resistance as defined in Figure 3.14
$\underline{Z}_{2\mathrm{i}}$	Impedance of source, first L network, and series resistance as defined in Figure 3.14
$\underline{Z}_{2\ell}$	Impedance of load and second L network as defined in Figure 3.14

Greek letters

Λ	An abbreviation for the reactance of the parallel-to-series transformed lossy inductor of a T network $\left(\Lambda = \frac{\frac{1}{\omega L_{\mathrm{p}}}}{G_{\mathrm{p}}^2 + \frac{1}{\omega^2 L_{\mathrm{p}}^2}}\right)$
Φ_{A}	Ratio of an inductor's AC resistance to a straight wire's AC resistance at $\omega \to \infty$ derived by [25] (straight wire is uncoiled windings' wire)
$\Phi_{\mathrm{A}}(\ldots,\ldots,\ldots)$	Ratio of an inductor's AC resistance to a straight wire's AC resistance at $\omega \to \infty$ derived by [25] as a function of ..., ..., and ... (straight wire is uncoiled windings' wire)
Φ_{M}	Ratio of an inductor's AC resistance to a straight wire's AC resistance at $\omega \to \infty$ derived by [24] (straight wire is uncoiled windings' wire)
$\Phi_{\mathrm{M}}(\ldots,\ldots)$	Ratio of an inductor's AC resistance to a straight wire's AC resistance at $\omega \to \infty$ derived by [24] as a function of ... and ... (straight wire is uncoiled windings' wire)
ψ_{t}	Implicit function of parallel conductance G_{p} in a T network
ψ_π	Implicit function of series resistance R_{s} in a π network

3.3 Considered types of networks, losses involved

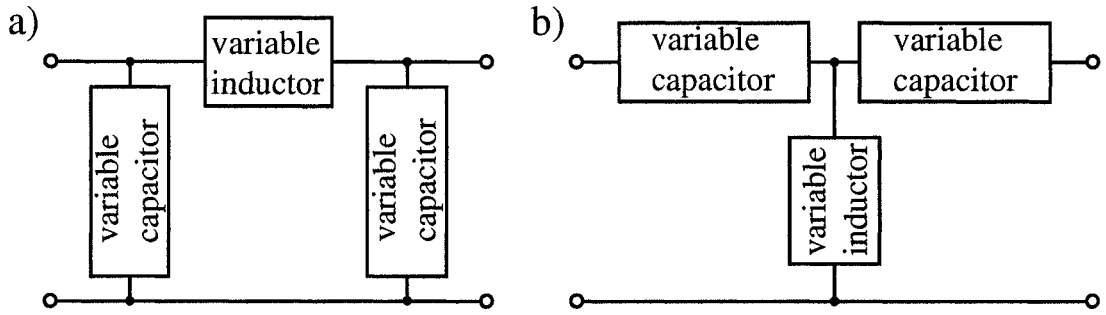

Figure 3.1: Considered types of network, a) π, and b) T network

If a matching network is used where radio frequency generators drive complex loads, it is usually a L, π, or T network with a "central" inductor as indicated in Figure 3.1. The four possible L networks are just limits of π or T networks if one of the two variable capacitances is set to zero or tends to infinity, respectively.

Thus consideration of π and T networks includes all networks we are interested in.

Variable capacitors and inductors used in those networks are not ideal. They exhibit a couple of parasitic elements as indicated in [30b] or [9b], for example. This is also true for any connection made between them. However, some parasitics may be neglected.

In the frequency range of $1.8-30\,\mathrm{MHz}$ variable capacitors are usually high-Q air or vacuum variable types, especially in high power applications. Both exhibit very low (dielectric) losses which are small and negligible compared to the losses of the variable inductor. Additionally (high power) variable capacitors are usually employed for connections of high cross-sectional area. Thus parasitic inductances and resistances of those connections may also be neglected.

These assumptions hold even for switchable automatic antenna matching units, developed in [4], [5], [6], [7], and [8]. Their tuning procedure is enhanced in [1] and "quiet" tuning is considered in [31], [2]. Useful element values are proposed in [32], [3]. For example, a realisation is given in [33] for a frequency range of $1.8-30\,\mathrm{MHz}$. Such automatic antenna matching units use switchable capacitors, whose dielectric losses are higher than those of air or vacuum variable capacitors, but still low compared to the losses of the switchable inductors due to the relatively low frequency. However, care has to be taken because the nonzero minimum inductance and capacitance steps may prevent exact matching.

Compared to variable capacitors, the variable inductor involves relatively high losses of different origins (which are indicated in detail in the following section). Thus the number of variable inductors is usually reduced to a minimum — as in the networks of Figure 3.1 which use only one.

The losses of the inductor may be described by a series resistance, but variable inductors additionally have a parasitic parallel capacitance which may be estimated according to [34b], [35], [36], [37], and [38]. An approach more focused on air core single-layer solenoidal coils is given in [24], [39], and [40]. It limits the useful frequency range of the coil. However, for a useful variable inductor the parallel capacitance should be negligible in the frequency range it's used.

Parasitic inductances and resistances of the variable inductor's connections may simply be added to its inductance and loss resistance.

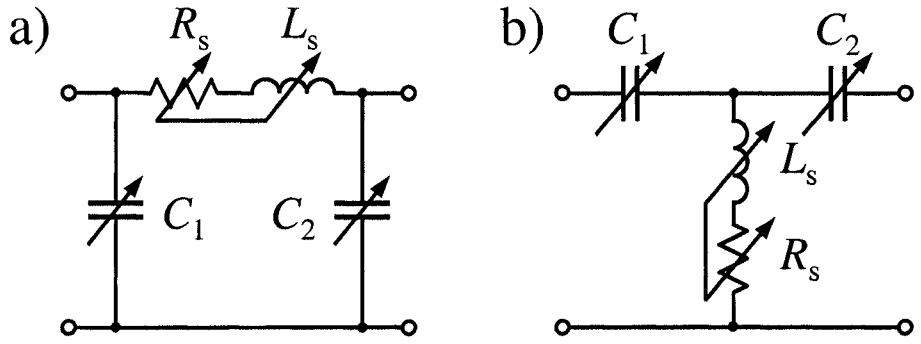

Figure 3.2: Simplified equivalent circuit of a) a π and b) a T network

Combining all preceding considerations yield the π and T network's simplified equivalent circuits of Figure 3.2, which are quite common in literature (see e. g. [9c] and [18]).

3.4 Losses of a variable inductor

3.4.1 Modeling losses of a variable inductor

Losses in inductors have different origins (refer to [30c] for a thorough review[1]). Losses are introduced by finite conductance of the wire, skin effect, proximity effect, or core losses (whenever a core is used); all of which may be described by series resistors, and a parallel resistor describing losses by finite resistance of the wire's insulation. The latter may be neglected for variable inductors used in matching networks, because usually there is a certain gap between adjacent wires to ensure a low parasitic parallel capacitance.

In our application the bandwidth of the generated signal is low compared to its mean frequency and we are interested in narrow band matching only — we simply intend to match at some given angular frequency ω. We therefore need to know the

[1]However, all formulae used in [30c] cannot be applied unless their references are checked to be valid within the frequency range of interest. For example, the formula describing eddy current losses assumes that the current flows through the complete cross-section of the wire, which would require much lower frequencies than those in our application or moderately lower frequencies and the use of litz wire.

losses' dependence on the number of turns, hence on the inductance, rather than its dependence on frequency. Due to the fixed matching frequency, we also may use the inductor's reactance ωL_s instead of its inductance L_s.

The equivalent resistance of all types of losses indicated above is entirely positive and increases with an increasing number of turns. Thus the simplest model would consist of a sum of functions of the type $a\,(\omega L_\mathrm{s})^b$ where $a > 0$ (positive losses) and $b > 0$ (increase with increasing number of turns or inductance). Each term (or a sum of several terms) would then describe the different types of losses.

Then the total equivalent series resistance is given by

$$R_\mathrm{s} = R_\mathrm{s0} + \sum_{n=1}^{N} a_n\,(\omega L_\mathrm{s})^{b_n}, \quad \text{where} \quad R_\mathrm{s0}, a_n \geq 0,\ b_N > b_{N-1} > \ldots > b_1 > 0. \tag{3.1}$$

R_s0, a_n, and b_n are real and may all be frequency dependent.

Theoretically the model given by (3.1) is mainly restricted by the assumption $R_\mathrm{s0}, a_n \geq 0$, in particular if we describe the losses by several terms of a Taylor series (however, since real coefficients b_n are used (3.1), it generally differs from a Taylor series employing integer exponents). Although R_s has to be entirely positive in the range of ωL_s the series applies, R_s0 or some a_n could be negative provided the sum of all terms is still positive. However, the proofs in the following sections require $R_\mathrm{s0}, a_n \geq 0$, and at least we may use real $b_n > 0$ to further improve the series approximation.

Of course the restriction to $R_\mathrm{s0}, a_n \geq 0$ is only useful if the losses of the inductor may be described by the model, which will be proved in the following sections for different types of inductors used in matching networks.

The model also allows piecewise description of the losses, provided each line segment can be described by (3.1) and R_s exhibits no steps at the segments' limits (Section 4.6 addresses the impact of such steps).

3.4.2 Application and validation of the proposed model to different types of inductors used in matching networks

3.4.2.1 Variable air inductors

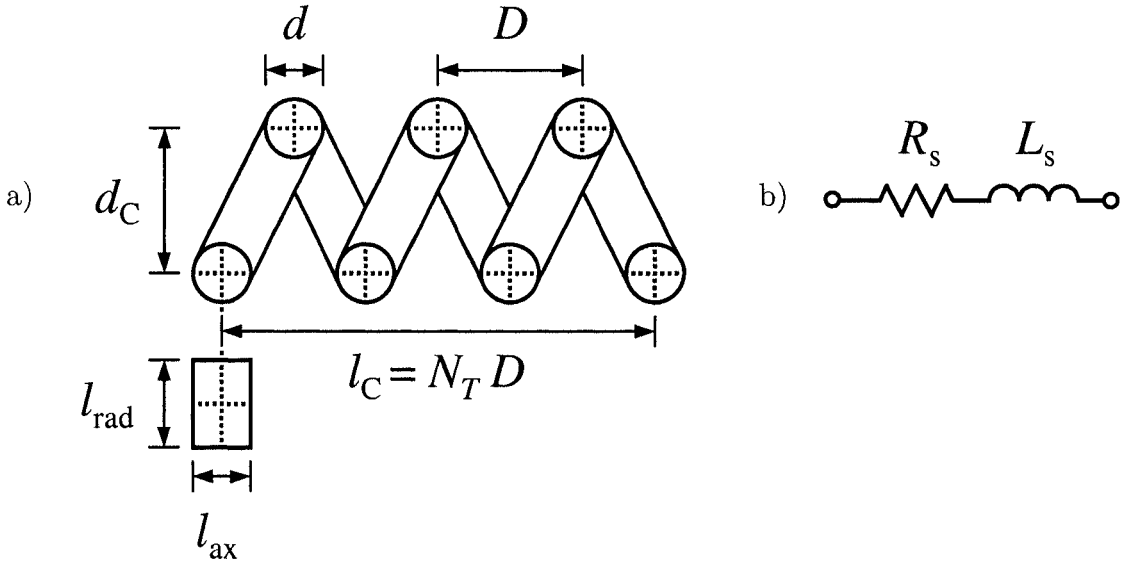

Figure 3.3: a) Air core single-layer solenoidal coil of round wire b) Simplified equivalent circuit of the inductor according to Section 3.3

In Figure 3.3 a), an air core single-layer solenoidal coil is shown. Its windings consist of round wire whose diameter is d, or of rectangular wire, whose radial length is l_{rad} and axial length is l_{ax}. As an example, the figure is drawn for a number of turns $N_T = 3$. D denotes the distance between centres of adjacent wires, d_C the mean diameter of the coil, and $l_C = N_T D$[†] the mean length of the coil.

Variable air core inductors usually look like a single-layer solenoid as illustrated in Figure 3.3. Additionally, they have a rotating contact which slides along the windings and provides a tap for the required amount of inductance.

As indicated in the previous section, we need to derive the coils's series loss resistance R_s as a function of its inductance L_s or its reactance ωL_s. However, R_s is usually calculated as a function of N_T, the number of coil's turns. Thus at first we have to derive the coil's inductance as a function of its number of turns.

[†]Care has to be taken regarding the definition of the coil's mean length, because it might differ if inductance or loss resistance are calculated. As in [41c], the inductance is usually calculated using $l_C = N_T D$. However, to calculate its series loss resistance, the helical coil is often approximated by parallel circular rings 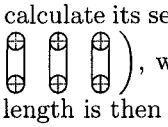 , whose dimensions are similar to those of Figure 3.3 (except l_C), but the coil's mean length is then defined by $(N_T - 1)\,D$.
Fortunately we do not have to distinguish between both definitions in the following sections, because [23] and [25] use the number of turns (and never its length) in all calculations and [24] defines the coil's length similar to Figure 3.3, although it examines coils of many windings, where $N_T \approx N_T - 1$ would hold.

The inductance of air core single-layer solenoidal coils is given by [41b]

$$L_s = \mu_0 \frac{\pi}{4} d_C \left(\frac{d_C}{D}\right)^2 \frac{l_C}{d_C} K\left(\frac{l_C}{d_C}\right), \tag{3.2}$$

where $\mu_0 \approx 4\pi\, 10^{-7}\, \frac{H}{m}$ and $l_C = N_T D$. The factor K is a function of the shape ratio $\frac{l_C}{d_C}$. Note that an estimate of K is given in [30a] as $K \approx \frac{1}{1+0{,}45\,\frac{d_C}{l_C}}$ for $\frac{l_C}{d_C} \geq \frac{1}{3}$ with a $< 1\,\%$ error[2].

In order to cater for different wire topologies, such as wires of circular or rectangular cross-section, some correction in (3.2) has to be made (see [41d], [41e], and [41c]). However, those corrections are usually small. Additionally, [41f] introduces a frequency correction, but it's also small and negligible.

Hence, using the basic inductance value of (3.2) provides sufficient accuracy. To gain insight in the inductance's dependence on the number of windings, we simply have to draw $\frac{l_C}{d_C} K\left(\frac{l_C}{d_C}\right)$ as a function of $\frac{l_C}{d_C}$ because all other factors do not depend on the number of turns and $\frac{l_C}{d_C} \sim N_T$.

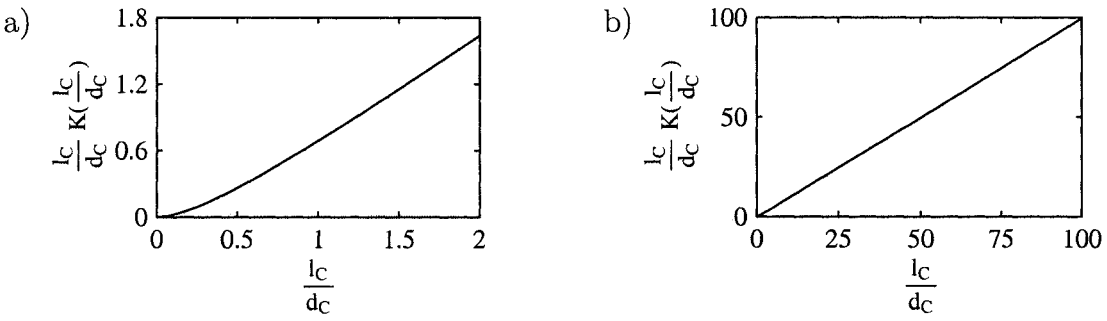

Figure 3.4: $\frac{l_C}{d_C} K\left(\frac{l_C}{d_C}\right)$ as a function of $\frac{l_C}{d_C}$ if a) $\frac{l_C}{d_C} \in [0, 2]$ or b) $\frac{l_C}{d_C} \in [0, 100]$

Inspection of Figure 3.4 reveals a linear function if $\frac{l_C}{d_C} \gg 1$, but a nonlinear function if $\frac{l_C}{d_C} \ll 1$.

Depending on dimensions and maximum number of turns of the used variable air core inductor we may assume a linear function in the range of interest, provided its accuracy suffices. If the approximation's accuracy is too poor, it's better to perform a piecewise linearisation which also may include all correcting terms mentioned above.

Performing the linearisation yields a functional description of the inductance L_s depending on the inductor's number of turns N_T,

$$L_s \approx a_{0L} + a_{1L} N_T, \tag{3.3}$$

from which we obtain by solving for the number of turns

$$N_T \approx \frac{L_s - a_{0L}}{a_{1L}}. \tag{3.4}$$

[2] [30a] indicates $\frac{l_C}{d_C} \geq \frac{1}{5}$, but compares the approximation to an inductance formula given in a different reference instead of comparing it to the tabulated values of [41b].

By analysing Figure 3.4 it can easily be observed that $a_{0L} \leq 0$ and $a_{1L} \geq 0$.

In the next step we calculate the loss itself.

In air-core inductors several different types of losses occur. As indicated in [34a], the current in the wire causes a current crowding in that wire towards its surface. This is the skin effect and is also observed in straight wires. The currents in adjacent wires lead to additional current crowding — the proximity effect. Both effects raise the inductor's AC resistance above its DC resistance.

Although losses caused by a pure skin effect may be calculated quite easily, description of the combined losses including the proximity effect is quite complicated and may be performed for round wires only.

Besides early approaches in [42] and [43] (corrected in [44]), the basis of the most common loss formulae are given in [45], [46], [47], and [48] — which derive the series loss resistance for short coils ($l_C \ll d_C$) or coils with a large number of turns. These works are summarised in [49] and [9a]. In addition, [24] checks the formula for coils with a large number of turns by measuring the losses of solenoidal air-core inductors of 30 – 50 turns and uses the results to correct that formula empirically. In [25], the formulae for short coils and coils of many turns given in [47] are combined and verified. The resulting (unrestricted) single formula is compared to several measurements of different works including [24]. In [39] a summary of all different existing formulae is given and the limiting conditions for their applicability is indicated. Note that in particular [47] does not state those limits explicitly. Furthermore, [39] confirms the results of [25] by additional measurements (in the range of 10 kHz to 23 MHz, all measurements are included in [50]) and derives a transmission line model of the coil incorporating parasitic capacitances. Finally, in [40] the preceding results are used to design optimum Q factor coils, which is described a little bit more detailed in [51a].

Additionally, [22] and [23] derive the series loss resistance of short coils using a different method involving fourier series, apply the results to multiturn loop antennas and check them by appropriate measurements. However, [22] and [23] assume the skin depth to be much lower than the wire's radius, but this assumption also holds for typical wire diameters of several millimeters used in solenoidal air-core inductors if the frequency is in the range of 1.8 – 30 MHz.

Regarding the publication dates of the preceding citations it should be noted that they apparently quite completely solve the problem of deriving losses of air-core inductors. "Modern" authors seem to focus on objectives applicable to integrated circuits (in particular losses of spiral inductors in MMICs, e. g. described in [52], [53], and [54]) or to coils in switching power supplies, e. g. considered in [55], [56], [57] — compared in [58] — and [59]. The former is not applicable due to the different shape of the inductor, the latter due to the assumption that the entire magnetic field is parallel to the coil's axis. Although there are also new techniques to calculate parasitic capacitances as those derived in [60], this work assumes that adjacent wires touch, but this winding style is not used for solenoidal air-core inductors to keep parasitic capacitances low and to ensure a high self resonance frequency.

Now the main question is:
If we compute all applicable loss formulae indicated above, can R_s be described by (3.1) *including all proposed restrictions?*

First, we consider short single-layer solenoidal air-core inductors. In [23], r'_{PS}, the ratio of the per-unit-length resistance including proximity effect to the per-unit-length-resistance calculated for a pure skin effect, is defined. Assuming $d < D$, $d \ll d_C$, $\frac{d}{2}\sqrt{\frac{\omega\mu}{2\varrho}} \gg 1$ (hence $\frac{1}{\frac{1}{9}\left(\frac{d}{2}\sqrt{\frac{\omega\mu}{2\varrho}}\right)^2-1} \ll 1$), $N_T^2 D^2 \ll d_C^2$ (which in our application limits the maximum number of turns the following formula applies to), and $N_T \frac{\omega}{c_0} \frac{d_C}{2} \ll 1$, where c_0 is the speed of light in vacuum. Then the series loss resistance R_s is obtained in [23] as

$$R_s = \frac{d_C}{d}\sqrt{\frac{\omega\mu\varrho}{2}}\, N_T \left(1 + r'_{PS}\left(N_T, \frac{D}{d}\right)\right). \tag{3.5}$$

r'_{PS} is tabulated in [22] as a function of N_T and $\frac{D}{d}$ for $N_T \in \{2, \ldots, 8\}$ and $\frac{D}{d} \in [1, 4]$.

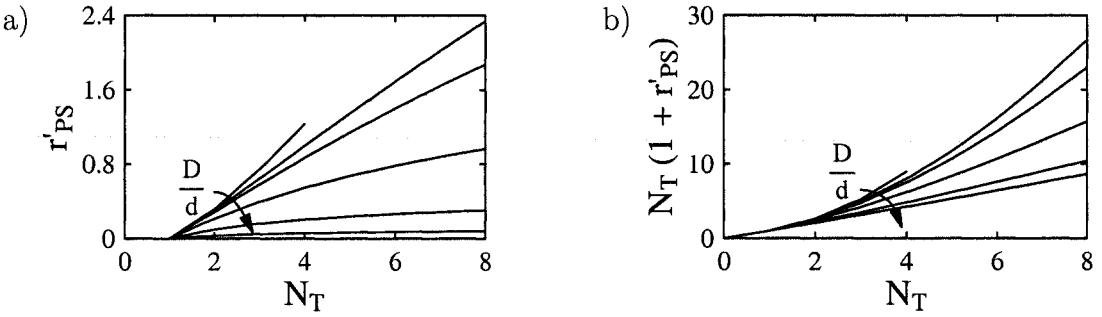

Figure 3.5: a) r'_{PS} and b) $N_T(1 + r'_{PS})$ as functions of N_T for $\frac{D}{d} \in \{1.05, 1.1, 1.15, 1.4, 2.2, 4\}$.

The resulting r'_{PS} is shown in Figure 3.5 a). $r'_{PS} = 0$ was added for $N_T \in [0, 1]$ (approximately assuming a pure skin effect). It's interesting to note that the deviation from the formula for short coils given in [47] is $< 5\,\%$ in its applicable range ($\frac{d}{D} \leq 0.6$ or $\frac{D}{d} \geq 1.7$).

Performing a piecewise linearisation of r'_{PS},

$$r'_{PS} \approx a_{0r} + a_{1r}\, N_T, \tag{3.6}$$

we obtain by combining with (3.5)

$$R_s \approx \frac{d_C}{d}\sqrt{\frac{\omega\mu\varrho}{2}}\,((1 + a_{0r})\, N_T + a_{1r}\, N_T^2). \tag{3.7}$$

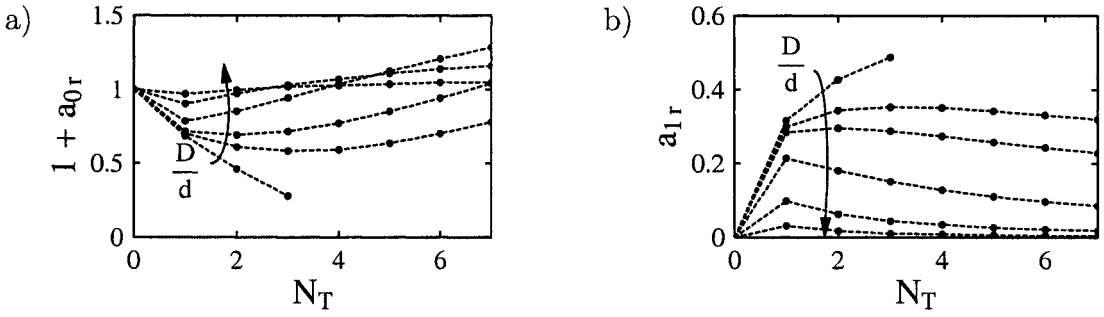

Figure 3.6: a) $1 + a_{0\mathrm{r}}$ and b) $a_{1\mathrm{r}}$ for $\frac{D}{d} \in \{1.05, 1.1, 1.15, 1.4, 2.2, 4\}$. (Dots at $N_\mathrm{T} = 0, 1, \ldots, 7$ are calculated values of a piecewise linearisation within the interval $[N_\mathrm{T}, N_\mathrm{T}+1)$. Dashed lines illustrate the tendency of values.)

Inspection of Figure 3.6 yields $1+a_{0\mathrm{r}} > 0$ and $a_{1\mathrm{r}} \geq 0$ if $\frac{D}{d} \geq 1.1$. Taking into account the tendency of the linearisation coefficients, we would expect those relations to hold if $N_\mathrm{T} \geq 8$. However, we cannot predict the behaviour for $1 \leq \frac{D}{d} < 1.1$ due to lack of data, but $\frac{D}{d}$ of useful single-layer solenoidal air-core inductors are never within this range because it would involve high parasitic capacitances.

Next, we consider single-layer solenoidal air-core inductors with a large number of turns.

In [24], Φ_M is defined as the ratio of the inductor's AC resistance to a straight wire's AC resistance at $\omega \to \infty$, where the straight wire's length equals the length of the coiled wire. Assuming $\frac{d}{2}\sqrt{\frac{\omega\mu}{\varrho}} \gg 1$, the series loss resistance R_s is obtained in [24] as

$$R_\mathrm{s} = \frac{d_\mathrm{C}}{d}\sqrt{\frac{\omega\mu\varrho}{2}}\, N_\mathrm{T}\, \Phi_\mathrm{M}\left(\frac{N_\mathrm{T} D}{d_\mathrm{C}}, \frac{d}{D}\right) = \frac{d_\mathrm{C}}{d}\sqrt{\frac{\omega\mu\varrho}{2}}\, \frac{d_\mathrm{C}}{D}\, \frac{l_\mathrm{C}}{d_\mathrm{C}}\, \Phi_\mathrm{M}\left(\frac{l_\mathrm{C}}{d_\mathrm{C}}, \frac{d}{D}\right). \quad (3.8)$$

In [24], Φ_M is tabulated as a function of $\frac{l_\mathrm{C}}{d_\mathrm{C}}$ and $\frac{d}{D}$ for $\frac{l_\mathrm{C}}{d_\mathrm{C}} \in [0, \infty)$ and $\frac{d}{D} \in [0.1, 1]$. An indication for the range of $\frac{d}{D}$ and $\frac{l_\mathrm{C}}{d_\mathrm{C}}$ the formula is valid in is given in [39].

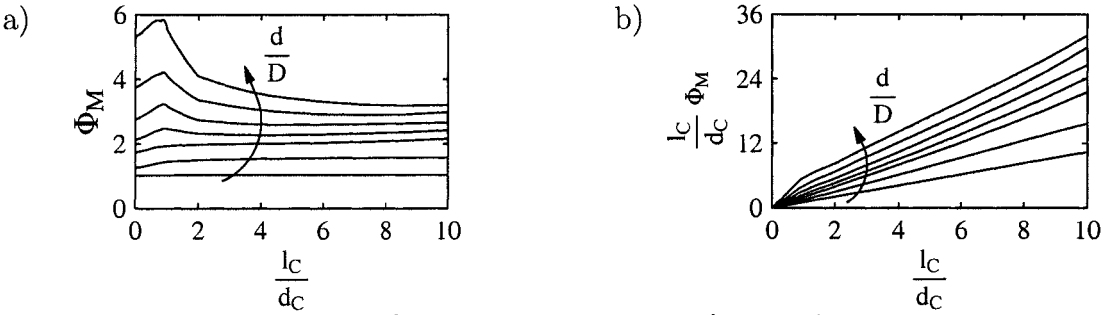

Figure 3.7: a) Φ_M and b) $\frac{l_\mathrm{C}}{d_\mathrm{C}}\,\Phi_\mathrm{M}$ as functions of $\frac{l_\mathrm{C}}{d_\mathrm{C}}$ for $\frac{d}{D} \in \{0.1, 0.4, 0.6, 0.7, 0.8, 0.9, 1\}$.

If we perform a piecewise linearisation of R_s as follows:

$$R_s \approx \begin{cases} \frac{d_C}{d}\sqrt{\frac{\omega\mu\varrho}{2}}\,\frac{d_C}{D}\,\frac{l_C}{d_C}\left(a_{0\Phi_M} + a_{1\Phi_M}\,\frac{l_C}{d_C}\right) & \text{if } \frac{d\Phi_M}{d\left(\frac{l_C}{d_C}\right)} \geq 0 \\ \frac{d_C}{d}\sqrt{\frac{\omega\mu\varrho}{2}}\,\frac{d_C}{D}\left(a_{0\mathrm{ldd}\Phi_M} + a_{1\mathrm{ldd}\Phi_M}\,\frac{l_C}{d_C}\right) & \text{if } \frac{d\Phi_M}{d\left(\frac{l_C}{d_C}\right)} < 0 \end{cases}, \tag{3.9}$$

we obtain $a_{0\Phi_M}$, $a_{1\Phi_M}$, $a_{0\mathrm{ldd}\Phi_M}$, $a_{1\mathrm{ldd}\Phi_M} \geq 0$ (as indicated in Table 3.1 and Table 3.2). If $\frac{l_C}{d_C} \geq 10$, the first type of linearisation applies, because Φ_M moderately increases in this case (check [24]). It's interesting to note that the practically relevant case $\frac{d}{D} \leq 0.6$ also involves only the first type of linearisation.

Applying $l_C = N_T D$ yields the required functional desription. (In [24], an additional frequency correction would be performed, but usually the skin depth is much lower than the wire's diameter in variable single-layer solenoidal air-core inductors in our frequency range of interest, thus it's small and negligible.)

Table 3.1: Calculated values of $a_{0\Phi_M}$ or $\boldsymbol{a_{0\mathrm{ldd}\Phi_M}}$ (in boldface) as a function of $\frac{l_C}{d_C}$ with parameter $\frac{d}{D}$ after a piecewise linearisation as given in (3.9). The values of each column are valid between $\frac{l_C}{d_C}$ of that column and $\frac{l_C}{d_C}$ of the next column to the right.

$a_{0\Phi_M}$, $\boldsymbol{a_{0\mathrm{ldd}\Phi_M}}$		$\frac{l_C}{d_C}$										
		0	0.2	0.4	0.6	0.8	1	2	4	6	8	10
$\frac{d}{D}$	1.0	5.31	5.25	5.35	5.80	**1.00**	**2.90**	**2.24**	**2.76**	**2.64**	3.08	(na)
	0.9	3.73	3.69	3.75	3.93	**0.28**	**1.48**	**1.24**	**1.56**	**0.48**	2.78	(na)
	0.8	2.74	2.69	2.71	2.80	**0.12**	**0.86**	**0.56**	2.60	2.54	2.50	(na)
	0.7	2.12	2.12	2.08	2.20	2.32	**0.30**	**0.20**	2.23	2.14	2.22	(na)
	0.6	1.74	1.71	1.71	1.80	1.84	1.90	1.95	1.97	1.88	2.00	(na)
	0.5	1.44	1.42	1.42	1.48	1.52	1.60	1.70	1.74	1.77	1.73	(na)
	0.4	1.26	1.25	1.23	1.26	1.30	1.40	1.46	1.50	1.53	1.53	(na)
	0.3	1.16	1.17	1.19	1.19	1.19	1.20	1.24	1.28	1.34	1.30	(na)
	0.2	1.07	1.08	1.04	1.10	1.10	1.07	1.11	1.13	1.16	1.12	(na)
	0.1	1.02	1.01	1.03	1.03	1.03	1.02	1.04	1.04	1.04	1.04	(na)

Table 3.2: Calculated values of $a_{1\Phi_M}$ or $\boldsymbol{a_{1lddd\Phi_M}}$ (in boldface) as a function of $\frac{l_C}{d_C}$ with parameter $\frac{d}{D}$ after a piecewise linearisation as given in (3.9). The values of each column are valid between $\frac{l_C}{d_C}$ of that column and $\frac{l_C}{d_C}$ of the next column to the right.

$a_{1\Phi_M}$, $a_{1lddd\Phi_M}$		$\frac{l_C}{d_C}$										
		0	0.2	0.4	0.6	0.8	1	2	4	6	8	10
$\frac{d}{D}$	1.0	0.70	1.00	0.75	0.00	**4.55**	**2.65**	**2.980**	**2.850**	**2.870**	0.015	(na)
	0.9	0.55	0.75	0.60	0.30	**3.82**	**2.62**	**2.740**	**2.660**	**2.840**	0.015	(na)
	0.8	0.45	0.70	0.65	0.50	**3.05**	**2.31**	**2.460**	0.000	0.010	0.015	(na)
	0.7	0.40	0.40	0.50	0.30	0.15	**2.17**	**2.220**	0.010	0.025	0.015	(na)
	0.6	0.15	0.30	0.30	0.15	0.10	0.04	0.015	0.010	0.025	0.010	(na)
	0.5	0.20	0.30	0.30	0.20	0.15	0.07	0.020	0.010	0.005	0.010	(na)
	0.4	0.15	0.20	0.25	0.20	0.15	0.05	0.020	0.010	0.005	0.005	(na)
	0.3	0.15	0.10	0.05	0.05	0.05	0.04	0.020	0.010	0.000	0.005	(na)
	0.2	0.05	0.00	0.10	0.00	0.00	0.03	0.010	0.005	0.000	0.005	(na)
	0.1	0.00	0.05	0.00	0.00	0.00	0.01	0.000	0.000	0.000	0.000	(na)

Finally, we consider single-layer solenoidal air-core inductors with any number of turns.

In [25], an (unrestricted) formula was derived based on [47] and a large amount of measurements including those of [24].

The resulting formula describes the ratio of the inductor's AC resistance to a straight wire's AC resistance, where the straight wire's length equals the length of the coiled wire. The formula depends on $\frac{d}{2}\sqrt{\frac{\omega\mu}{\varrho}}$, $\frac{D}{d_C}$, $\frac{d}{D}$, and N_T.

To reduce the number of parameters, we define the funcion Φ_A as the limit of the formula from [25] mentioned above for $\omega \to \infty$. In order to keep the values of Φ_A close to the formula's values in our frequency range of interest, $d \geq 2\,\text{mm}$ has to hold (ensuring the value of the function ϕ defined in [25] is less than 5 % lower compared to its value for $\omega \to \infty$ which is used with powers up to two in the formula, hence the error is estimated to stay within 10 %.) which is likely to be satisfied by the "high power" inductors under consideration. Then the losses are given by

$$R_s = \frac{d_C}{d}\sqrt{\frac{\omega\mu\varrho}{2}}\, N_T\, \Phi_A\left(\frac{D}{d_C}, \frac{d}{D}, N_T\right). \tag{3.10}$$

Compared to the previous loss descriptions, the resulting $\Phi_A\left(\frac{D}{d_C}, \frac{d}{D}, N_T\right)$ still involves one additional parameter, N_T. Thus its diagrams cannot be drawn as simple as those of the previous loss descriptions and the parameters have to be limited to useful ranges.

Firstly, typical variable "high power" inductors do not have more than 30 – 40 turns. Thus $N_T \leq 50$ is assumed. Secondly, $0.1 \leq \frac{d}{D} \leq 1$ is considered as [24] did (although it's typically close to 0.5). Finally, the diameter of typical variable "high power" inductors does not exceed 200 mm. Since $d \geq 2\,\text{mm}$ and $\frac{d}{D} \leq 1$ was assumed,

$0.01 \leq \frac{D}{d_C} \leq 0.5$ is chosen — at the lower limit, $d_C = 200\,\text{mm}$ if $d = 2\,\text{mm}$ and $\frac{d}{D} = 1$, the upper limit is introduced by one of the parameters' limits in the tables of [25] (in our notation, [25] defines ζ as $\frac{2D}{d_C}$, whose range is $0 \leq \zeta \leq 1$ in the tables).

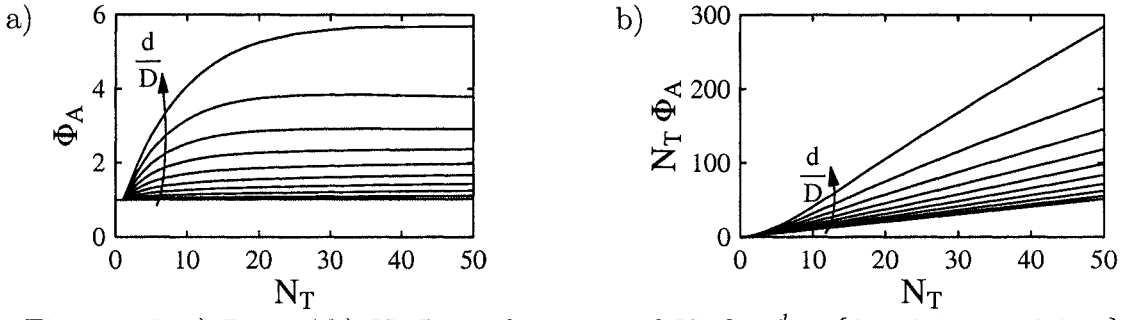

Figure 3.8: a) Φ_A and b) $N_T\,\Phi_A$ as functions of N_T for $\frac{d}{D} \in \{0.1, 0.2, \ldots, 0.9, 1\}$ and $\frac{D}{d_C} = \frac{1}{20}$.

An example for the obtained Φ_A is shown in Figure 3.8 a) for $\frac{D}{d_C} = \frac{1}{20}$ (a variable inductor with $d = 2\,\text{mm}$ and $\frac{d}{D} = 0.5$ would have a $d_C = 80\,\text{mm}$). $\Phi_A = 1$ was added for $N_T \in [0, 1]$ (approximately assuming a pure skin effect).

If we perform a piecewise linearisation as follows:

$$R_s \approx \begin{cases} \frac{d_C}{d}\sqrt{\frac{\omega\mu\varrho}{2}}\,N_T\,(a_{0\Phi_A} + a_{1\Phi_A}\,N_T) & \text{if} \quad \frac{d\Phi_A}{dN_T} \geq 0 \\ \frac{d_C}{d}\sqrt{\frac{\omega\mu\varrho}{2}}\,(a_{0N\Phi_A} + a_{1N\Phi_A}\,N_T) & \text{if} \quad \frac{d\Phi_A}{dN_T} < 0 \end{cases}, \tag{3.11}$$

we obtain $a_{0\Phi_A}$, $a_{1\Phi_A}$, $a_{0N\Phi_A}$, $a_{1N\Phi_A} \geq 0$ within the limits given above[3].

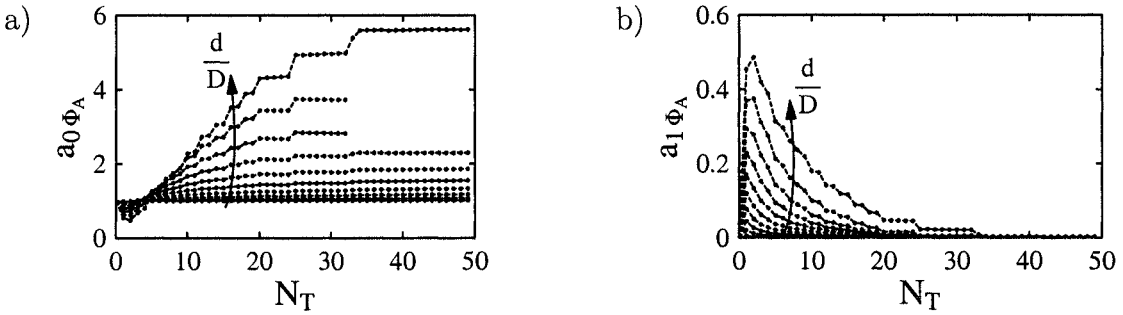

Figure 3.9: a) $a_{0\Phi_A}$ and b) $a_{1\Phi_A}$ as functions of N_T for $\frac{d}{D} \in \{0.1, 0.2, \ldots, 0.9, 1\}$ and $\frac{D}{d_C} = \frac{1}{20}$. (Dots at $N_T = 0, 1, \ldots, 49$ are calculated values of a piecewise linearisation within the interval $[N_T, N_T + 1)$. Dashed lines illustrate the tendency of values.)

[3]Calculations were performed with $\frac{D}{d_C} \in \{\frac{1}{2}, \frac{1}{3}, \ldots, \frac{1}{9}, \frac{1}{10}, \frac{1}{20}, \frac{1}{30}, \ldots, \frac{1}{90}, \frac{1}{100}\}$. Since Φ_A may be quite flat in some regions, care has to be taken if it is intended to get "smooth" linearisation coefficients, involving usage of the tabulated values of u_1 and u_2 instead of the approximate formulae, calculation of additional u_n, v_n, and w_n from the formulae given in [47], and application of the interpolation proposed in [47] for u_n, v_n, and w_n. Furthermore, u_2 may be computed directly as a function and it seems advantageous to interpolate u_1 uniformly against $\frac{1}{N_T}$. (u_1, u_2, u_n, v_n, and w_n are defined in [25].)

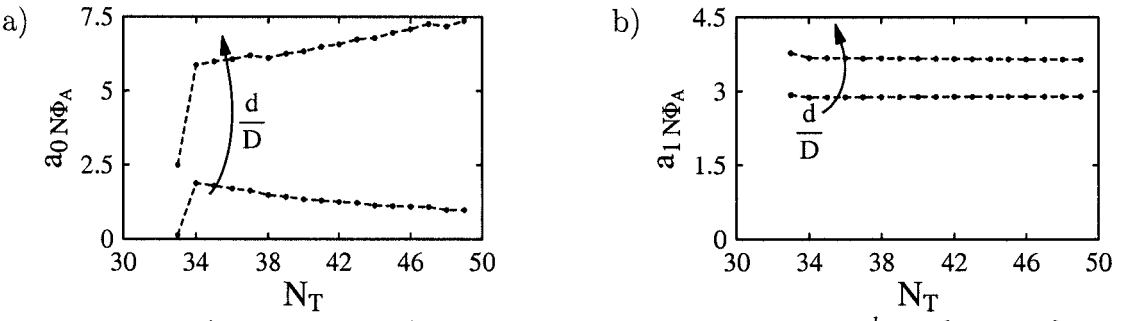

Figure 3.10: a) $a_{0N\Phi_A}$ and b) $a_{1N\Phi_A}$ as functions of N_T for $\frac{d}{D} \in \{0.8, 0.9\}$ and $\frac{D}{d_C} = \frac{1}{20}$. (Dashed lines illustrate the tendency of values.)

Figure 3.9 and Figure 3.10 are examples for such a linearisation performed for Φ_A of Figure 3.8 a). Dots at $N_T = 0, 1, \ldots, 49$ are calculated values of a piecewise linearisation within the interval $[N_T, N_T + 1)$. The type of linearisation changes for $N_T \geq 33$ in case $\frac{d}{D} \in \{0.8, 0.9\}$, which is clearly visible in Figure 3.9 a).

Summarising all preceding calculations, we may conclude that performing a piecewise linearisation of single-layer solenoidal air-core inductors' series loss resistance R_s, which was computed according to [22] for a small number of turns, [24] for a large number of turns, or [25] for any number of turns, yielded functions of the kind

$$R_s \approx a_{0R} + a_{1R}\, N_T + a_{2R}\, N_T^2, \tag{3.12}$$

where $a_{0R}, a_{1R}, a_{2R} \geq 0$.

Applying (3.4) gives

$$R_s \approx a_{0R} + \frac{-a_{0L}}{a_{1L}}\left(a_{1R} + \frac{-a_{0L}}{a_{1L}}\, a_{2R}\right) + \frac{1}{a_{1L}}\left(a_{1R} + 2\,\frac{-a_{0L}}{a_{1L}}\, a_{2R}\right) L_s + \frac{a_{2R}}{a_{1L}^2}\, L_s^2,$$

or, using new abbreviations,

$$R_s \approx R_{s0} + a_1\, \omega L_s + a_2\, (\omega L_s)^2, \tag{3.13}$$

$$\text{where} \quad R_{s0} = a_{0R} + \frac{-a_{0L}}{a_{1L}}\left(a_{1R} + \frac{-a_{0L}}{a_{1L}}\, a_{2R}\right),$$

$$a_1 = \frac{1}{\omega a_{1L}}\left(a_{1R} + 2\,\frac{-a_{0L}}{a_{1L}}\, a_{2R}\right),$$

$$a_2 = \frac{a_{2R}}{\omega^2 a_{1L}^2}.$$

As indicated above, $R_{s0}, a_1, a_2 \geq 0$, hence (3.1) is a valid model for the (piecewise linearised) series loss resistance of (variable) single-layer solenoidal air-core inductors.

Alternatively we may perform a series expansion of R_s as a function of ωL_s (without the temporary use of N_T), which also may be piecewise linearised.

3.4.2.2 Switchable inductors

Modern automatic antenna matching units (developed in [4], [5], [6], [7], and [8], a realisation given in [33] for a frequency range of 1.8 – 30 MHz) use switchable inductors (and capacitors).

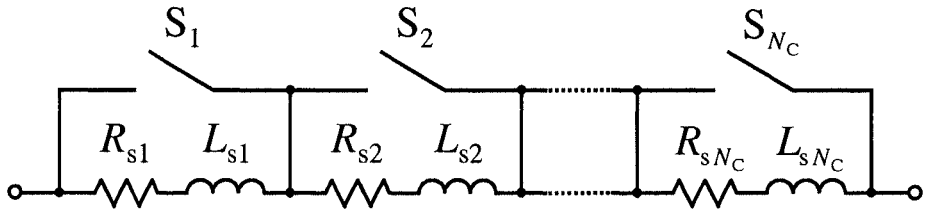

Figure 3.11: Simplified equivalent circuit of series connected switchable inductors

Switchable inductors in such matching networks are built as illustratated in Figure 3.11, wherein the inductances are sorted in ascending order. The first inductor ($n_C = 1$) has the lowest inductance L_{s1} and the N_C-th inductor (the last one, $n_C = N_C$) has the highest inductance L_{sN_C}. Unused inductors are shorted by closing the appropriate switches.

Usually the inductances increase by powers of two, hence the inductance of the n_C-th inductor may be computed from the first (and lowest) inductance as

$$L_{sn_C} = L_{s1}\, 2^{n_C - 1}.$$

Then the total inductance is changeable in inductance steps of L_{s1} and stays constant (likewise the losses) between two adjacent values — inductance and series loss resistance are piecewise constant,

$$L_s = \sum_{\text{all } n_C \text{ used}} L_{sn_C} = L_{s0}, \tag{3.14}$$

$$R_s = \sum_{\text{all } n_C \text{ used}} R_{sn_C} = R_{s0}. \tag{3.15}$$

The resulting piecewise constant series loss resistance can be described by (3.1) (application to T networks is similar to those described at the end of Section 3.4.2.3), but it involves steps at the line segments' limits (Section 4.6 addresses the impact of such steps).

Due to nonzero minimum inductance and capacitance step size we usually cannot tune the network for exact input matching. Then the transferred active power has to be computed using different formulae than those given in Sections 3.5.2.1 and 3.5.3.1. However, if the minimum inductance and capacitance step is sufficiently small, we may approximately use the inductance and capacitances required for exact input matching and the series loss resistance of the closest (switchable) inductance value.

3.4.2.3 Inductor in series/parallel to a variable capacitor

Another possible realisation of a variable inductor is a variable capacitor in series to a (fixed) inductor for usage in a π network or a variable capacitor in parallel to a (fixed) inductor for usage in a T network.

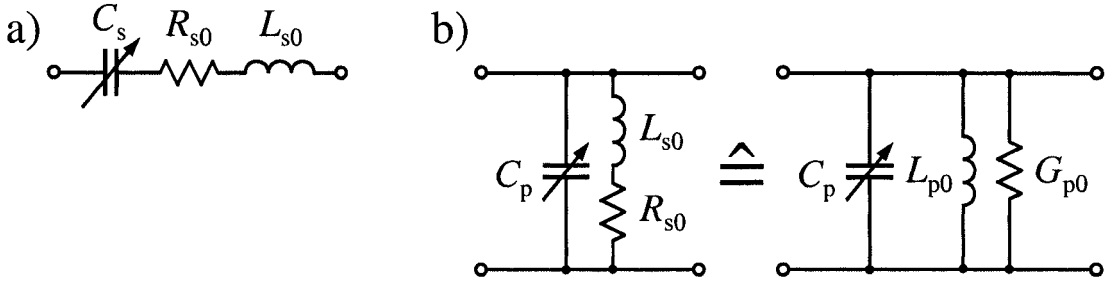

Figure 3.12: Simplified equivalent circuit of a) a variable capacitor and a serial (fixed) inductor (for use in a π network) and b) a variable capacitor and a parallel (fixed) inductor (for use in a T network).

Inspection of its simplified equivalent circuit in Figure 3.12 reveals its advantage — if the elements' values are chosen properly, the total inductance at matching frequency may be reduced to zero in a) or increased to infinity in b), which is difficult to achieve by "real" variable inductors if the matching frequency is high — and disadvantage — the series loss resistance in a) and the parallel loss conductance in b) are constant for any total inductance. Thus even low total inductances involve the "high" losses of the maximum inductance value. However, the losses may be reduced by using a switchable tapped inductor as proposed in [3].

The series loss resistance in a) is just a constant loss resistance R_{s0}, hence included in (3.1). The constant loss conductance in parallel to a variable inductance in b) is fortunately one of the exceptions mentioned in Footnote [7] (at the end of Section 3.5.3.1), where π and T network are exactly equivalent (this issue is also addressed in Section 3.5.3.4). Thus all relations derived in the following sections for π networks whose central inductor's series loss resistance is constant apply to T networks whose central inductor's parallel loss conductance is constant. Hence the model proposed in (3.1) is suitable to describe an inductor in series/parallel to a variable capacitor used as central variable inductor of a π or T network, respectively.

3.5 Matching of a resistive load to a resistive source (matching at the network's input)

3.5.1 Definition of the objectives and suitable parametrisations for π and T networks

The basic objective of the following sections is to match a (real) load resistance $R_\ell = \frac{1}{G_\ell} > 0$ to a (real) source resistance $R_i = \frac{1}{G_i} > 0$ at a given frequency using a π or T network as indicated in Figure 3.13.

The T network contains an inductance L_p in parallel to a conductance G_p to simplify its parametrisation and the matched network's element values' equations. The element values of the "original" network, L_s and R_s, are then computed by applying a parallel-to-series transformation according to (A.20) and (A.19).

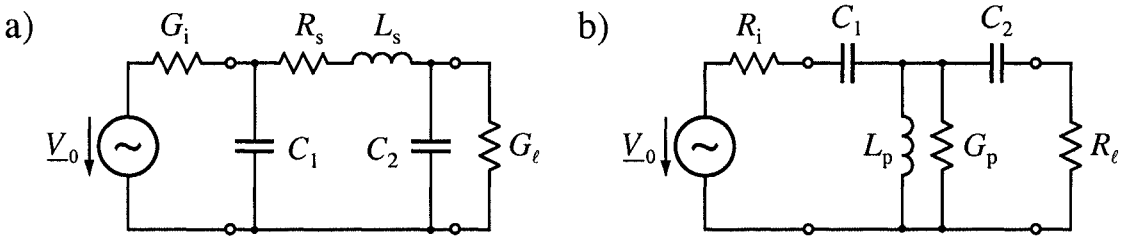

Figure 3.13: Considered lossy a) π and b) T network matching a (real) load resistance $R_\ell = \frac{1}{G_\ell}$ to a (real) source resistance $R_i = \frac{1}{G_i}$.

π and T networks consist of three (independent) elements, which have to be tuned to transform the load resistance to the source resistance, hence achieving a (conjugate complex) match of the load to the source at the network's input. Conjugate complex matching involves two independent equations to be solved, one for the real part and one for the imaginary part of the network's input impedance, yielding two conditions for the network's element settings. Since three independently adjustable elements are available, one may be chosen arbitrarily.

However, if a lossless L network is considered, two conditions yield unique settings of its elements, because it consists just of two independently adjustable elements. In a lossy L network, there may exist more than one distinct settings depending on the loss model applied (for example consider the capacitive solution in the right half of Figure 4.8 b)), although usually only one solution remains valid, in particular if network elements' limits are taken into account.

The degree of freedom in π and T networks is described by a parameter of those networks. To simplify calculations and optimisation proofs, it's especially important to choose a proper parametrisation suiting the needs of active power transfer optimisation.

During the last decades, a couple of π and T network parametrisations were developed for lossless networks suiting different needs. A more filter theoretical approach involving hyperbolic functions was summarised in [9c] and examined in more detail in [10]. Q-based design was used in [11], [12] and further developed in [13], [14], [15] (corrected/extended in [16]), [17], and [18].

Common to all preceding parametrisations is the difficulty to include the series loss resistance. Thus calculations of the losses of the inductor are usually performed using lossless network elements' values (assuming those values are not changed significantly by low losses), e. g. in [9c] or [18]. Then the power losses involved may be computed exactly, but the network's input is never matched to the source — the higher the losses, the worser the match.

It's interesting to note the loss calculation method of [61] using Tellegen's theorem [62] — it includes the losses of all network elements, but considers constant Q factors

only, assumes elements of the same type having similar Q factors, and designs the network using lossless network elements' values.

However, the parametrisation derived in [11] and [13] is extendable to exact loss inclusion (introduced by [3]), e. g. if the π network's equations for $C_{1,2}$ and L_s are rewritten in resistances and the loss resistance is taken into account when choosing the parameters of the two L networks the π network was split in. For a single L network, the exact loss inclusion is given in [3] (and rewritten for Q-based design).

Then the network's input is exactly matched within the entire parameter range. After deriving the network's power gain, it's optimised by applying (3.1) and the implicit function theorem.

To gain more insight in the network's behaviour, its power gain is derived in a little bit more complicated manner. The method described in [51b] is simpler and especially useful if the losses of the capacitors have to be included, too. It's used in Appendix B.3 where design and power gain of π and T networks are considered including losses of **all** network's elements.

3.5.2 π network

3.5.2.1 Elements' values and losses involved

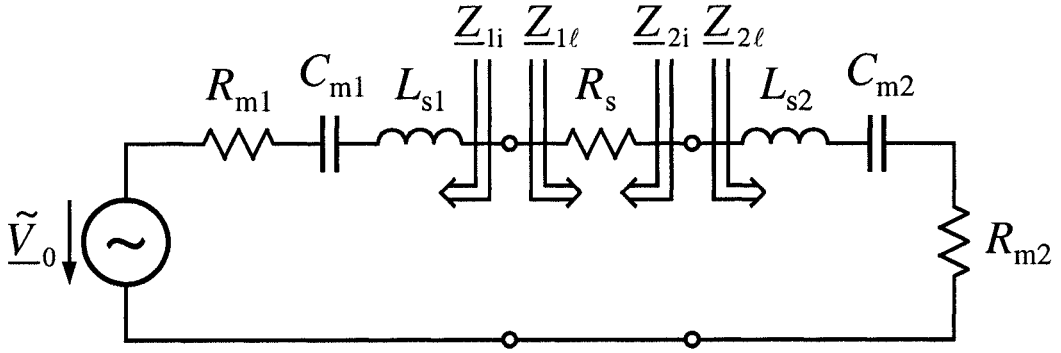

Figure 3.14: Resulting (transformed) π network's equivalent circuit for matching of a (real) load conductance $G_\ell = \frac{1}{R_\ell}$ to a (real) source conductance $G_i = \frac{1}{R_i}$

To derive the elements' values for matching of a (real) load conductance $G_\ell > 0$ to a (real) source conductance $G_i > 0$ if a π network with a lossy "central" inductor L_s is used as shown in Figure 3.13 a), we initially split L_s in two parts, L_{s1} and L_{s2}. We then may consider the π network to be composed of two lossless L networks (C_1, L_{s1} or C_2, L_{s2}, respectively), and R_s, which takes the (total) losses into account.

Applying Thevenin's theorem [63] to the voltage source of (complex) amplitude $\underline{V}_0$ and (real) source resistance $R_i = \frac{1}{G_i}$ in parallel to the capacitance C_1 yields

a Thevenin equivalent voltage source of (complex) amplitude $\underline{\widetilde{V}}_0$ and a (complex) source impedance consisting of a resistor $R_{\mathrm{m}1}$ in series to a capacitor $C_{\mathrm{m}1}$.

Finally $G_\ell = \frac{1}{R_\ell}$ in parallel to C_2 is parallel-to-series transformed in $R_{\mathrm{m}2}$ in series to $C_{\mathrm{m}2}$ using (A.19) and (A.20).

We then obtain Figure 3.14 from Figure 3.13, where

$$\underline{\widetilde{V}}_0 = \underline{V}_0 \frac{\frac{1}{\mathrm{j}\omega C_1}}{\frac{1}{G_\mathrm{i}} + \frac{1}{\mathrm{j}\omega C_1}} = \underline{V}_0 \frac{G_\mathrm{i}}{G_\mathrm{i} + \mathrm{j}\omega C_1} = \frac{\underline{V}_0}{1 + \mathrm{j}\omega R_\mathrm{i} C_1}. \tag{3.16}$$

(The formulae obtained for $R_{\mathrm{m}1,2}$ and $C_{\mathrm{m}1,2}$ will not be needed later on and thus are not shown here.)

Which conditions will cause matching in the circuit of Figure 3.14*?*

Firstly, capacitive and inductive reactances have to cancel at the matching frequency. If an approach similar to [13] (derivation for a lossless π network) is used, reactive cancellation applies to each of the two L networks — $C_{\mathrm{m}1}$ cancels $L_{\mathrm{s}1}$ and $C_{\mathrm{m}2}$ cancels $L_{\mathrm{s}2}$ at the matching frequency.

Secondly, the remaining resistances have to be equal. For a lossless inductor, choosing of $R_{\mathrm{m}1} = R_{\mathrm{m}2} = R_\mathrm{m}$ would yield $\underline{Z}_{1\mathrm{i}} = \underline{Z}_{1\ell} = \underline{Z}_{2\mathrm{i}} = \underline{Z}_{2\ell} = R_\mathrm{m}$ at the matching frequency (R_m is the independent parameter referred to in Section 3.5.1, denoted by "virtual resistance" R in [13]), thus providing a (conjugate complex) match of the source resistance to the load resistance and vice versa.

However, a lossy inductor involves an "asymmetry" R_s, which urges us to decide whether we want to match the load to the source or the source to the load. In the first case, we may choose $R_{\mathrm{m}2} = R_\mathrm{m}$ (as before, R_m is the independent parameter). At matching frequency, $\underline{Z}_{2\ell} = R_\mathrm{m}$ holds and thus $\underline{Z}_{1\ell} = \underline{Z}_{2\ell} + R_\mathrm{s} = R_\mathrm{m} + R_\mathrm{s}$. To achieve a (conjugate complex) match of the load to the source, $\underline{Z}_{1\ell}$ must be equal to $R_{\mathrm{m}1}$, hence $R_{\mathrm{m}1} = R_\mathrm{m} + R_\mathrm{s}$ (for a L network, where $C_1 = 0$ and thus $R_{\mathrm{m}1} = R_\mathrm{i}$, this condition was given in [3]). Conversely, $\underline{Z}_{1\mathrm{i}} = R_{\mathrm{m}1} = R_\mathrm{m} + R_\mathrm{s}$ and $\underline{Z}_{2\mathrm{i}} = \underline{Z}_{1\mathrm{i}} + R_\mathrm{s} = R_\mathrm{m} + 2R_\mathrm{s}$ at matching frequency, which is not equal to $R_{\mathrm{m}2} = R_\mathrm{m}$ as it would be for a conjugate complex match of the source to the load.

Different choices of $R_{\mathrm{m}1,2}$ are also possible, but those shown above are ideally suited for the extension to complex loads.

For our purpose, matching of the load to the source is needed. However, matching of the source to the load is quite similar and derived in Appendix B.4.1.

Using the preceding choice for $R_{\mathrm{m}1,2}$, we would obtain $C_{1,2}$ (and $C_{\mathrm{m}1,2}$) from parallel-to-series transformation equations for $R_{\mathrm{m}1,2}$. Applying reactive cancellation would then yield $L_{\mathrm{s}1,2}$ (and L_s). The calculations are not shown here because we alternatively may use the formulae from [13] if they are rewritten in our resistance notation and if we use $R_{\mathrm{m}1} = R_\mathrm{m} + R_\mathrm{s}$ for the left L network and $R_{\mathrm{m}2} = R_\mathrm{m}$ for the right L network ([13] derives the lossless case, where $R_{\mathrm{m}1} = R_{\mathrm{m}2} = R_\mathrm{m}$).

Since $R_{\mathrm{m}1,2}$ was obtained from parallel-to-series transformation of passive components (source resistance $R_\mathrm{i} > 0$ and load resistance $R_\ell > 0$), $R_{\mathrm{m}1,2} \geq 0$ holds. Then

the calculations described above yield the capacitances $C_{1,2}$ and the inductance L_s of the **original** π network in Figure 3.13 a), where

$$C_1 = \overset{+}{(-)}\frac{1}{\omega R_i}\sqrt{\frac{R_i - R_m - R_s}{R_m + R_s}}, \quad (3.17) \qquad C_2 = \overset{+}{[-]}\frac{1}{\omega R_\ell}\sqrt{\frac{R_\ell - R_m}{R_m}}, \quad (3.18)$$

$$L_s = \frac{\overset{+}{(-)}\sqrt{(R_m + R_s)(R_i - R_m - R_s)}\ \overset{+}{[-]}\sqrt{R_m(R_\ell - R_m)}}{\omega}. \quad (3.19)$$

(The negative signs in parentheses/square brackets would apply if we would use (lossless) variable inductors $L_{1,2} = -\frac{1}{\omega^2 C_{1,2}}$. Then a negative L_s might occur, which would be just equal to a variable capacitor $C_s = -\frac{1}{\omega^2 L_s}$. As indicated by using parentheses/square brackets, reactive cancellation causes a negative sign of the first square root in L_s, if L_1 is used instead of C_1, or a negative sign of the second square root in L_s, if L_2 is used instead of C_2, respectively. We will need these changes during the extension to inductive loads.)

In order to get valid solutions, all square roots must be real (if not, the π network of Figure 3.13 a) wouldn't be able to match). Thus, certain restrictions to the parameter R_m must apply. Since $R_\ell > 0$, only $0 \le R_m \le R_\ell$ yields $R_m(R_\ell - R_m) \ge 0$. Similarily, $R_s \ge 0$ and $R_i > 0$ imply $0 \le R_m + R_s \le R_i$.

Hence, for valid R_m the designability conditions are

$$0 \le R_m \le R_\ell \text{ and } 0 \le R_m + R_s \le R_i. \quad (3.20)$$

As $R_s \ge R_{s0}$ (from (3.1)), we immediately obtain that R_{s0} is limited by $R_{s0} \le R_i$. If R_{s0} would be higher, the π network would not be able to match any load.

However, both inequalities mainly describe the upper limit of the parameter R_m. This issue is best understood if we initially compute its limit for the lossless case ($R_s = 0$). Since both inequalities apply, the upper limit of R_m is given by R_ℓ if $R_\ell \le R_i$ or by R_i if $R_\ell > R_i$, respectively. The change in the upper limit occurs at $R_\ell = R_i$, where a match would not need any additional components ($L_s = 0$ and $C_{1,2} = 0$ would match).

The lossy network behaves quite similarily. The upper limit of R_m is given by R_ℓ if $R_\ell \le R_i - R_{s0}$ or by R_{mlim} if $R_\ell > R_i - R_{s0}$, respectively. R_{mlim} is the highest parameter R_m which solves

$$R_{mlim} = R_i - R_s(R_{mlim}) \quad (3.21)$$

for $0 \le R_{mlim} < R_\ell$ and involves valid network elements. The change in the upper limit occurs at $R_\ell = R_i - R_{s0}$, where, as before, a match would not need any additional components ($L_s = 0$ and $C_{1,2} = 0$ would match). It's interesting to note that (for a resistive load) there is no other solution where $L_s = 0$[‡].

[‡]Theoretically $L_s = 0$ might additionally occur for $R_m = 0$ if $R_s(R_m = 0) = 0$, which would be possible for $R_{s0} = 0$. However, since $L_s = 0$, the load resistor would not be transformed. Hence matching would be impossible unless $R_\ell = R_i - R_{s0} = R_i = R_m = 0$ — this solution is already described by (a limit of) R_{mlim}.

Depending on the particular R_s used (given as a function of ωL_s or R_m), additional restrictions to R_m might apply, limiting R_m even further or involving intervals within the limits derived above where matching is impossible. However, (3.20) holds throughout the valid range of R_m.

Additionally, the upper limits in (3.20) separate π and L networks — $C_1 = 0$ if $R_m = R_{mlim}$ or $C_2 = 0$ if $R_m = R_\ell$, respectively.

After designing the π network's input impedance to match the source resistance R_i, we compute the active power $P_{act\ell}$ delivered to its load resistance R_ℓ. Since the capacitive and inductive reactances in Figure 3.14 cancel at matching frequency, we obtain

$$\begin{aligned} P_{act\ell} &= \frac{1}{2} R_{m2} \frac{|\widetilde{V}_0|^2}{(R_{m1} + R_s + R_{m2})^2} \overset{(3.16)}{=} \frac{1}{2} R_m \frac{\frac{|V_0|^2}{1+\omega^2 R_i^2 C_1^2}}{4\,(R_m + R_s)^2} \\ P_{act\ell} &\overset{(3.17)}{=} \frac{|V_0|^2}{8\,R_i} \frac{R_m}{R_m + R_s} \overset{(2.22)}{=} P_{actmaxi} \frac{1}{1 + \frac{R_s}{R_m}}. \end{aligned} \tag{3.22}$$

Conversely, due to input matching the active power P_{acts} delivered to the loss resistance R_s is given by

$$P_{acts} = P_{actmaxi} - P_{act\ell} \overset{(3.22)}{=} P_{actmaxi} \frac{1}{1 + \frac{R_m}{R_s}}. \tag{3.23}$$

For optimisation, we will need the power gain $g_{\pi,inma}$ of the matched π network. Since its input impedance is matched to R_i, the active power delivered to the network's input is $P_{act1} = P_{actmaxi}$ (refer to Figure A.4). Thus we obtain

$$g_{\pi,inma} = \frac{P_{act\ell}}{P_{act1}} = \frac{P_{act\ell}}{P_{actmaxi}} \overset{(3.22)}{=} \frac{R_m}{R_m + R_s} = \frac{1}{1 + \frac{R_s}{R_m}}. \tag{3.24}$$

(Alternatively we could derive $g_{\pi,inma}$ from (A.15) if we put $C_{2tot} = C_2$. However, we gain more insight in the circuit's behaviour if it is computed as shown above.)

3.5.2.2 Optimum value of parameter R_m for maximum power gain

Minimising "losses of the π network" is achieved by transferring the highest portion of the active power delivered to the network's input to its load $R_\ell = \frac{1}{G_\ell}$. Thus neither P_{acts} has to be minimised nor $P_{act\ell}$ to be maximised, but we have to maximise $g_{\pi,inma}$. However, $P_{actmaxi}$ is independent of R_m and $P_{act\ell} = g_{\pi,inma} P_{actmaxi}$ holds (input matching), hence the highest $g_{\pi,inma}$ occurs for maximum $P_{act\ell}$.

To derive the value of R_m for maximum $g_{\pi,inma}$, we compute its derivative with respect to R_m.

Using (3.24) yields

$$\frac{dg_{\pi,inma}}{dR_m} = \frac{R_m}{(R_m + R_s)^2} \left(\frac{R_s}{R_m} - \frac{dR_s}{dR_m} \right). \tag{3.25}$$

Since R_m, $R_\mathrm{s} \geq 0$, the first term is always ≥ 0. Thus we need to check the sign of the second term only.

As R_s is a function of L_s, which itself is a function of R_m and implicitly[4] of R_s according to (3.19), we define the implicit function $\psi_\pi \equiv 0$ from (3.1),

$$\psi_\pi := R_{\mathrm{s}0} + \left(\sum_{n=1}^{N} a_n \left(\omega L_\mathrm{s}\right)^{b_n} \right) - R_\mathrm{s} \equiv 0.$$

Then we compute the implicit function's partial derivatives with respect to R_m and R_s,

$$\begin{aligned} \frac{\partial \psi_\pi}{\partial R_\mathrm{m}} &= \sum_{n=1}^{N} a_n b_n \left(\omega L_\mathrm{s}\right)^{b_n - 1} \frac{\partial(\omega L_\mathrm{s})}{\partial R_\mathrm{m}}, \\ \frac{\partial \psi_\pi}{\partial R_\mathrm{s}} &= \left(\sum_{n=1}^{N} a_n b_n \left(\omega L_\mathrm{s}\right)^{b_n - 1} \frac{\partial(\omega L_\mathrm{s})}{\partial R_\mathrm{s}} \right) - 1. \end{aligned}$$

Applying the implicit function theorem [64] gives

$$\frac{\mathrm{d}R_\mathrm{s}}{\mathrm{d}R_\mathrm{m}} = -\frac{\frac{\partial \psi_\pi}{\partial R_\mathrm{m}}}{\frac{\partial \psi_\pi}{\partial R_\mathrm{s}}} = \frac{\sum\limits_{n=1}^{N} a_n b_n \left(\omega L_\mathrm{s}\right)^{b_n - 1} \frac{\partial(\omega L_\mathrm{s})}{\partial R_\mathrm{m}}}{1 - \sum\limits_{n=1}^{N} a_n b_n \left(\omega L_\mathrm{s}\right)^{b_n - 1} \frac{\partial(\omega L_\mathrm{s})}{\partial R_\mathrm{s}}}.$$

If we multiply numerator and denominator by ωL_s, put the result in the second term of (3.25), and rearrange it, we obtain

$$\frac{R_\mathrm{s}}{R_\mathrm{m}} - \frac{\mathrm{d}R_\mathrm{s}}{\mathrm{d}R_\mathrm{m}} = \frac{R_\mathrm{s}\,\omega L_\mathrm{s} - \sum\limits_{n=1}^{N} a_n b_n \left(\omega L_\mathrm{s}\right)^{b_n} \left(R_\mathrm{s} \frac{\partial(\omega L_\mathrm{s})}{\partial R_\mathrm{s}} + R_\mathrm{m} \frac{\partial(\omega L_\mathrm{s})}{\partial R_\mathrm{m}} \right)}{R_\mathrm{m} \left(\omega L_\mathrm{s} - \sum\limits_{n=1}^{N} a_n b_n \left(\omega L_\mathrm{s}\right)^{b_n} \frac{\partial(\omega L_\mathrm{s})}{\partial R_\mathrm{s}} \right)}. \tag{3.26}$$

Replacing of ωL_s with (3.19) yields the missing partial derivatives,

$$\frac{\partial(\omega L_\mathrm{s})}{\partial R_\mathrm{m}} = \frac{R_\mathrm{i} - 2\left(R_\mathrm{m} + R_\mathrm{s}\right)}{2\sqrt{\left(R_\mathrm{m} + R_\mathrm{s}\right)\left(R_\mathrm{i} - R_\mathrm{m} - R_\mathrm{s}\right)}} + \frac{R_\ell - 2\,R_\mathrm{m}}{2\sqrt{R_\mathrm{m}\left(R_\ell - R_\mathrm{m}\right)}}, \tag{3.27}$$

$$\frac{\partial(\omega L_\mathrm{s})}{\partial R_\mathrm{s}} = \frac{R_\mathrm{i} - 2\left(R_\mathrm{m} + R_\mathrm{s}\right)}{2\sqrt{\left(R_\mathrm{m} + R_\mathrm{s}\right)\left(R_\mathrm{i} - R_\mathrm{m} - R_\mathrm{s}\right)}}. \tag{3.28}$$

To check which value of R_m yields the highest $g_{\pi,\,\mathrm{inma}}$, we need to know the sign of $\frac{R_\mathrm{s}}{R_\mathrm{m}} - \frac{\mathrm{d}R_\mathrm{s}}{\mathrm{d}R_\mathrm{m}}$, the second term in (3.26), throughout the valid range of R_m given by (3.20).

[4] In particular, R_s and L_s are both functions of R_m only. However, we usually may not be able to solve for R_s explicitly after applying (3.19) to (3.1).

For ease of understanding, an overview of the following proof is given below. The proof itself is quite lengthy and thus performed in Appendix B.2.1.1.

The idea is that $\frac{R_\mathrm{s}}{R_\mathrm{m}} - \frac{\mathrm{d}R_\mathrm{s}}{\mathrm{d}R_\mathrm{m}}$ remains ≥ 0 for all valid R_m. Then the highest possible value of R_m would yield the highest $g_{\pi,\,\mathrm{inma}}$.

To prove it, we will derive the highest b_N which still yields a numerator ≥ 0 and simultaneously a denominator ≥ 0. This approach involves more restrictions than necessary, because the ratio of a negative numerator to a negative denominator would also be positive, but the proof is then quite "easy" and straightforward. However, we should keep in mind that due to the additional restrictions $\frac{R_\mathrm{s}}{R_\mathrm{m}} - \frac{\mathrm{d}R_\mathrm{s}}{\mathrm{d}R_\mathrm{m}}$ might remain positive even for a higher b_N than those derived.

If we abbreviate $S_\pi = \sum_{n=1}^{N} a_n b_n \left(\omega L_\mathrm{s}\right)^{b_n}$, we obtain from (3.26)

$$\frac{R_\mathrm{s}}{R_\mathrm{m}} - \frac{\mathrm{d}R_\mathrm{s}}{\mathrm{d}R_\mathrm{m}} = \frac{R_\mathrm{s}\,\omega L_\mathrm{s} - S_\pi \left(R_\mathrm{s} \frac{\partial(\omega L_\mathrm{s})}{\partial R_\mathrm{s}} + R_\mathrm{m} \frac{\partial(\omega L_\mathrm{s})}{\partial R_\mathrm{m}}\right)}{R_\mathrm{m}\left(\omega L_\mathrm{s} - S_\pi \frac{\partial(\omega L_\mathrm{s})}{\partial R_\mathrm{s}}\right)}.$$

To prove that numerator and denominator are ≥ 0 for certain b_N, we firstly assume $S_\pi = 0$ or $R_\mathrm{s} = R_{\mathrm{s}0}$ and calculate $\frac{R_\mathrm{s}}{R_\mathrm{m}} - \frac{\mathrm{d}R_\mathrm{s}}{\mathrm{d}R_\mathrm{m}}$, which will be ≥ 0 throughout the valid range of R_m.

Secondly, we assume $S_\pi \neq 0$, hence $S_\pi > 0$ (according to (3.1)), and check numerator and denominator separately:

1. Since ωL_s, R_m, R_s are ≥ 0, and $S_\pi > 0$, the numerator will always be ≥ 0 for $R_\mathrm{s} \frac{\partial(\omega L_\mathrm{s})}{\partial R_\mathrm{s}} + R_\mathrm{m} \frac{\partial(\omega L_\mathrm{s})}{\partial R_\mathrm{m}} \leq 0$. Conversely, if $R_\mathrm{s} \frac{\partial(\omega L_\mathrm{s})}{\partial R_\mathrm{s}} + R_\mathrm{m} \frac{\partial(\omega L_\mathrm{s})}{\partial R_\mathrm{m}} > 0$, we have to use certain inequalities to prove that (at least) for $b_N \leq 2$ the numerator will be ≥ 0.

2. Since ωL_s, $R_\mathrm{m} \geq 0$, and $S_\pi > 0$, the denominator will always be ≥ 0 for $\frac{\partial(\omega L_\mathrm{s})}{\partial R_\mathrm{s}} \leq 0$. Conversely, if $\frac{\partial(\omega L_\mathrm{s})}{\partial R_\mathrm{s}} > 0$, we will have to use certain inequalities to prove that (at least) for $b_N \leq 2$ the denominator will be ≥ 0.

We then know that for all possible values of $R_{\mathrm{s}0}$, a_n, and b_n according to (3.1), $\frac{\mathrm{d}g_{\pi,\,\mathrm{inma}}}{\mathrm{d}R_\mathrm{m}} \geq 0$ if (at least) $b_N \leq 2$.

Hence the highest $g_{\pi,\,\mathrm{inma}}$ is obtained for the highest valid value of R_m, which is R_ℓ if $R_\ell \leq R_\mathrm{i} - R_{\mathrm{s}0}$ or R_{mlim} defined in (3.21) if $R_\ell > R_\mathrm{i} - R_{\mathrm{s}0}$, respectively. If we choose R_m accordingly, the particular type of network involved is one of the two L networks where $C_2 = 0$ or $C_1 = 0$.

However, we should keep in mind that the restriction $0 < b_N \leq 2$ aroused after applying inequalities to get upper estimates for certain terms. If $b_N > 2$, the method used in the preceding proof gives no indication of the network's behaviour[5].

[5]It's not obvious that by using the method applied within the proof $0 < b_N \leq 2$ is the utmost obtainable range for b_N. However, it can be achieved by performing it in a slightly different manner. Unfortunately the proof is then much more complicated and harder to understand.

It's interesting to note that usually the highest $g_{\pi,\mathrm{inma}}$ does not coincide with the lowest R_s (or, according to (3.1), the lowest L_s). This issue may be illustrated by comparison of Figure 4.11 to Figure 4.15.

3.5.2.3 Optimum value of load resistance R_ℓ for maximum power gain

In Section 3.5.2.2 we derived which value of R_m maximises $g_{\pi,\mathrm{inma}}$. However, the highest $g_{\pi,\mathrm{inma}}$ still depends on R_ℓ (R_i is fixed in our application of matching the load to the source).

Thus further investigations are required to determine which R_ℓ yields the highest $g_{\pi,\mathrm{inma}}$ if the parameter R_m was chosen for maximum $g_{\pi,\mathrm{inma}}$ according to Section 3.5.2.2.

R_ℓ is variable because the connecting line between matching network and load transforms the load depending on the line's length. As transformation usually involves additional susceptances even for a purely resistive load, optimisation of $g_{\pi,\mathrm{inma}}$ with respect to R_ℓ is only part of the solution, "complete" optimisation needs application of Sections 4.3.1.1 and 4.3.2.1, too.

The derivation of the optimum value of R_ℓ is quite similar to Section 3.5.2.2, but lengthy and thus performed in Appendix B.2.1.2.

Summarising Appendix B.2.1.2, we may conclude that if $0 < b_N \leq 2$ and R_m is chosen according to Section 3.5.2.2, $R_\ell = R_\mathrm{i} - R_\mathrm{s0}$ would yield the highest $g_{\pi,\mathrm{inma}}$. $g_{\pi,\mathrm{inma}}$ decreases for higher or lower R_ℓ with exception of the constant R_s case (all $a_n = 0$, hence $R_\mathrm{s} = R_\mathrm{s0}$), where $g_{\pi,\mathrm{inma}}$ stays constant for higher R_ℓ.

Unfortunately the optimisation gives no indication for which of the two load resistors $R_{\ell 1} > R_\mathrm{i} - R_\mathrm{s0}$, $R_{\ell 2} = \frac{(R_\mathrm{i}-R_\mathrm{s0})^2}{R_{\ell 1}} < R_\mathrm{i} - R_\mathrm{s0}$, exhibiting similar reflection coefficients referred to $R_\mathrm{i} - R_\mathrm{s0}$, we would achieve the higher $g_{\pi,\mathrm{inma}}$ (reference $R_\mathrm{i} - R_\mathrm{s0}$ is not related to the interconnecting transmission lines' characteristic impedances, but was used to obtain equal "transformation distances" from optimum value $R_\mathrm{i} - R_\mathrm{s0}$).

As mentioned before, "complete" optimisation involves taking into account of Sections 4.3.1.1 and 4.3.2.1. However, at least we may conclude that minimising losses of the matching network will always require consideration (and optimisation) of the length of the transmission line connecting it to the load.

3.5.3 T network

3.5.3.1 Elements' values and losses involved

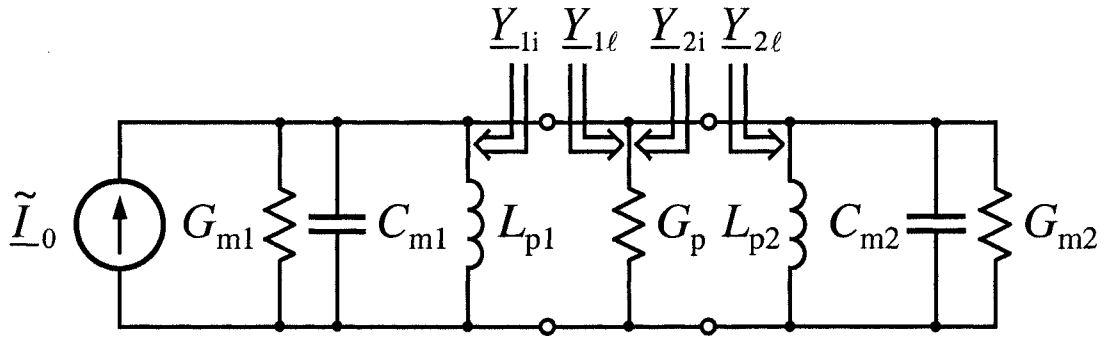

Figure 3.15: Resulting (transformed) T network's equivalent circuit for matching of a (real) load resistance $R_\ell = \frac{1}{G_\ell}$ to a (real) source resistance $R_i = \frac{1}{G_i}$

To derive the elements' values for matching of a (real) load resistance $R_\ell > 0$ to a (real) source resistance $R_i > 0$ if a T network with a lossy "central" inductor L_p is used as shown in Figure 3.13 b), we initially split $\frac{1}{L_p}$ in two parts, $\frac{1}{L_{p1}}$ and $\frac{1}{L_{p2}}$. We then may consider the T network to be composed of two lossless L networks (C_1, L_{p1} or C_2, L_{p2}, respectively), and G_p, which takes the (total) losses into account.

Applying Norton's theorem [63] to the voltage source of (complex) amplitude $\underline{V}_0$ and (real) source resistance $R_i = \frac{1}{G_i}$ in series to the capacitance C_1 yields a Norton equivalent current source of (complex) amplitude $\underline{\tilde{I}}_0$ and a (complex) source admittance consisting of a conductor G_{m1} in parallel to a capacitor C_{m1}.

Finally $R_\ell = \frac{1}{G_\ell}$ in series to C_2 is series-to-parallel transformed in G_{m2} in parallel to C_{m2} using (A.16) and (A.17) (or [34c]).

We then obtain Figure 3.15 from Figure 3.13, where

$$\underline{\tilde{I}}_0 = \frac{\underline{V}_0}{R_i + \frac{1}{j\omega C_1}} = \underline{V}_0 \frac{j\omega C_1}{1 + j\omega R_i C_1} = \underline{V}_0 \frac{j\omega G_i C_1}{G_i + j\omega C_1}. \tag{3.29}$$

(The formulae obtained for $R_{m1,2}$ and $C_{m1,2}$ will not be needed later on and thus are not shown here.)

Which conditions will cause matching in the circuit of Figure 3.15*?*

Firstly, capacitive and inductive susceptances have to cancel at the matching frequency. If an approach similar to [13] (derivation for a lossless T network) is used, susceptive cancellation applies to each of the two L networks — C_{m1} cancels L_{p1} and C_{m2} cancels L_{p2} at the matching frequency.

Secondly, the remaining conductances have to be equal. For a lossless inductor, choosing of $G_{m1} = G_{m2} = G_m$ would yield $\underline{Y}_{1i} = \underline{Y}_{1\ell} = \underline{Y}_{2i} = \underline{Y}_{2\ell} = G_m$ at the matching frequency (G_m is the independent parameter referred to in Section 3.5.1, which would be equivalent to a "virtual conductance" G — however, [13] uses a "virtual resistance" instead), thus providing a (conjugate complex) match of the source resistance to the load resistance and vice versa.

However, a lossy inductor involves an "asymmetry" G_p, which urges us to decide whether we want to match the load to the source or the source to the load. In the first case, we may choose $G_{m2} = G_m$ (as before, G_m is the independent parameter). At matching frequency, $\underline{Y}_{2\ell} = G_m$ holds and thus $\underline{Y}_{1\ell} = \underline{Y}_{2\ell} + G_p = G_m + G_p$. To achieve a (conjugate complex) match of the load to the source, $\underline{Y}_{1\ell}$ must be equal to G_{m1}, hence $G_{m1} = G_m + G_p$. Conversely, $\underline{Y}_{1i} = G_{m1} = G_m + G_p$ and $\underline{Y}_{2i} = \underline{Y}_{1i} + G_p = G_m + 2G_p$ at matching frequency, which is not equal to $G_{m2} = G_m$ as it would be for a conjugate complex match of the source to the load.

Different choices of $G_{m1,2}$ are also possible, but those shown above are ideally suited for the extension to complex loads.

For our purpose, matching of the load to the source is needed. However, matching of the source to the load is quite similar and derived in Appendix B.4.2.

Using the preceding choice for $G_{m1,2}$, we would obtain $C_{1,2}$ (and $C_{m1,2}$) from series-to-parallel transformation equations for $G_{m1,2}$. Applying susceptive cancellation would then yield $L_{p1,2}$ (and L_p). The calculations are not shown here because we alternatively may use the formulae from [13] if they are rewritten in our conductance notation and if we use $G_{m1} = G_m + G_p$ for the left L network and $G_{m2} = G_m$ for the right L network ([13] derives the lossless case in resistive notation, where $G_{m1} = G_{m2} = G_m$ and $\frac{1}{G_m}$ is denoted by R).

Since $G_{m1,2}$ was obtained from series-to-parallel transformation of passive components (source conductance $G_i > 0$ and load conductance $G_\ell > 0$), $G_{m1,2} \geq 0$ holds. Then the calculations described above yield the capacitances $C_{1,2}$ and the inductance L_p of the **original** T network in Figure 3.13 b), where

$$C_1 = \overset{+}{(-)} \frac{G_i}{\omega} \sqrt{\frac{G_m + G_p}{G_i - G_m - G_p}}, \quad (3.30) \qquad C_2 = \overset{+}{[-]} \frac{G_\ell}{\omega} \sqrt{\frac{G_m}{G_\ell - G_m}}, \quad (3.31)$$

$$L_p = \frac{1}{\omega \left(\overset{+}{(-)} \sqrt{(G_m + G_p)(G_i - G_m - G_p)} \overset{+}{[-]} \sqrt{G_m (G_\ell - G_m)} \right)}. \quad (3.32)$$

(The negative signs in parentheses/square brackets would apply if we would use (lossless) variable inductors $L_{1,2} = -\frac{1}{\omega^2 C_{1,2}}$. Then a negative L_p might occur, which would be just equal to a variable capacitor $C_p = -\frac{1}{\omega^2 L_p}$. As indicated by using parentheses/square brackets, susceptive cancellation causes a negative sign of the first square root in L_p, if L_1 is used instead of C_1, or a negative sign of the second

square root in L_p, if L_2 is used instead of C_2, respectively. We will need these changes during the extension to inductive loads.)

In order to get valid solutions, all square roots must be real (if not, the T network of Figure 3.13 b) wouldn't be able to match). Thus, certain restrictions to the parameter G_m must apply. Since $G_\ell > 0$, only $0 \leq G_m \leq G_\ell$ yields $G_m\,(G_\ell - G_m) \geq 0$. Similarily, $G_p \geq 0$ and $G_i > 0$ imply $0 \leq G_m + G_p \leq G_i$.

Hence, for valid G_m the designability conditions are

$$0 \leq G_m \leq G_\ell \text{ and } 0 \leq G_m + G_p \leq G_i. \tag{3.33}$$

Both inequalities mainly describe the upper limit of the parameter G_m. This issue is best understood if we initially compute its limit for the lossless case ($R_s = 0$ and thus $G_p = 0$). Since both inequalities apply, the upper limit of G_m is given by G_ℓ if $G_\ell \leq G_i$ or by G_i if $G_\ell > G_i$, respectively[6]. The change in the upper limit occurs at $G_\ell = G_i$, where a match would not need any additional components ($L_s \to \infty$, hence $L_p \to \infty$ (from (A.18)), and $C_{1,2} \to \infty$ would match).

The lossy network behaves quite similarily. The upper limit of G_m is given by G_ℓ if $G_\ell \leq G_i$ or by G_{mlim} if $G_\ell > G_i$, respectively. G_{mlim} is the highest parameter G_m which solves

$$G_{mlim} = G_i - G_p(G_{mlim}) \tag{3.34}$$

for $0 \leq G_{mlim} < G_\ell$ and involves valid network elements. The change in the upper limit occurs at $G_\ell = G_i$, where, as before, a match would not need any additional components ($L_s \to \infty$, hence $L_p \to \infty$, and $C_{1,2} \to \infty$ would match). It's interesting to note that (for a resistive load) there is no other solution where $L_{s,p} \to \infty$ or $\frac{1}{L_p} = 0$ [††].

[6]Usually there is no restriction to R_{s0} similar to those in Section 3.5.2.1. The reason is that G_p is usually not equal to $\frac{1}{R_{s0}} + \ldots$ due to series-to-parallel transformation of R_s and L_s, where R_s is given by (3.1). This issue is also addressed by the last two paragraphs of this section dealing with the differences of T and π network and by the exceptions mentioned in Footnotes [††] and [7].

[††] Theoretically $\frac{1}{L_p} = 0$ might additionally occur for $G_m = 0$ if $G_p(G_m = 0) = 0$. However, since $L_{s,p} \to \infty$ ($\frac{1}{L_p} = 0$ and $G_p = 0$ is case (ii) in (A.18)), the load conductor would not be transformed. Hence matching would be impossible unless $G_\ell = G_i = G_m = 0$ — this solution is already described by (a limit of) G_{mlim}.
Unique to the T network, case (i) b) in (A.18) describes a second point where $\frac{1}{L_p} = 0$ or $L_p \to \infty$, but $L_s = 0$, if $G_i \geq \frac{1}{R_{s0}}$ for $R_{s0} > 0$ and $G_m = G_{mlim} = G_i - \frac{1}{R_{s0}} = G_\ell$, hence $G_p = \frac{1}{R_{s0}}$ and $C_{1,2} \to \infty$. Compared to $L_s \to \infty$, which was lossless, $L_s = 0$ involves losses in R_{s0}.

Depending on the particular R_s used, hence the particular G_p used (given as a function of ωL_p or G_m), additional restrictions to G_m might apply, limiting G_m even further or involving intervals within the limits derived above where matching is impossible. However, (3.33) holds throughout the valid range of G_m.

Additionally, the upper limits in (3.33) separate T and L networks — $C_1 \to \infty$ if $G_m = G_{mlim}$ or $C_2 \to \infty$ if $G_m = G_\ell$, respectively.

After designing the T network's input impedance to match the source conductance G_i, we compute the active power $P_{act\ell}$ delivered to its load conductance G_ℓ. Since the capacitive and inductive susceptances in Figure 3.15 cancel at matching frequency, we obtain

$$\begin{aligned} P_{act\ell} &= \frac{1}{2} G_{m2} \frac{|\widetilde{I}_0|^2}{(G_{m1} + G_p + G_{m2})^2} \overset{(3.29)}{=} \frac{1}{2} G_m \frac{|\underline{V}_0|^2 \frac{\omega^2 G_i^2 C_1^2}{G_i^2 + \omega^2 C_1^2}}{4\,(G_m + G_p)^2} \\ P_{act\ell} &\overset{(3.30)}{=} \frac{|\underline{V}_0|^2}{8\,R_i} \frac{G_m}{G_m + G_p} \overset{(2.22)}{=} P_{actmaxi} \frac{1}{1 + \frac{G_p}{G_m}}. \end{aligned} \tag{3.35}$$

Conversely, due to input matching the active power P_{actp} delivered to the loss conductance G_p is given by

$$P_{actp} = P_{actmaxi} - P_{act\ell} \overset{(3.35)}{=} P_{actmaxi} \frac{1}{1 + \frac{G_m}{G_p}}. \tag{3.36}$$

For optimisation, we will need the power gain $g_{t,\,inma}$ of the matched T network. Since its input impedance is matched to G_i, the active power delivered to the network's input is $P_{act1} = P_{actmaxi}$ (refer to Figure A.6). Thus we obtain

$$g_{t,\,inma} = \frac{P_{act\ell}}{P_{act1}} = \frac{P_{act\ell}}{P_{actmaxi}} \overset{(3.35)}{=} \frac{G_m}{G_m + G_p} = \frac{1}{1 + \frac{G_p}{G_m}}. \tag{3.37}$$

(Alternatively we could derive $g_{t,\,inma}$ from (A.23) if we put $C_{2tot} = C_2$. However, we gain more insight in the circuit's behaviour if it is computed as shown above.)

Comparing the preceding formulae to those derived for the π network, we may conclude that π and T network would be equivalent if we would use an inductor L_p with a parallel loss conductance G_p which could be described as a function of $\frac{1}{\omega L_p}$ similar to the series loss resistance's R_s function of ωL_s for the π network.

Unfortunately, the same inductor is used in both networks, thus exhibiting the same R_s as a function of ωL_s. If it is rewritten in G_p as a function of $\frac{1}{\omega L_p}$, its functional description usually changes[7].

Thus the properties of lossy π and T networks with a lossy "central" inductor are usually not equivalent. Hence the following derivation of the optimum value of the parameter G_m or G_ℓ, respectively, differ from those for the π network, involving additional restrictions within the proofs.

3.5.3.2 Optimum value of parameter G_m for maximum power gain

Minimising "losses of the T network" is achieved by transferring the highest portion of the active power delivered to the network's input to its load $G_\ell = \frac{1}{R_\ell}$. Thus neither P_{actp} has to be minimised nor $P_{act\ell}$ to be maximised, but we have to maximise $g_{t,inma}$. However, $P_{actmaxi}$ is independent of G_m and $P_{act\ell} = g_{t,inma} P_{actmaxi}$ holds (input matching), hence the highest $g_{t,inma}$ occurs for maximum $P_{act\ell}$.

To derive the value of G_m for maximum $g_{t,inma}$, we compute its derivative with respect to G_m.

Using (3.37) yields

$$\frac{dg_{t,inma}}{dG_m} = \frac{G_m}{(G_m + G_p)^2}\left(\frac{G_p}{G_m} - \frac{dG_p}{dG_m}\right). \tag{3.38}$$

Since G_m, $G_p \geq 0$, the first term is always ≥ 0. Thus we need to check the sign of the second term only.

As R_s is a function of L_s, and both are functions of G_p and L_p according to (A.19), (A.20), and G_m according to (3.32), where G_p itself is a function of G_m and implicitly[8] of G_p, we define the implicit function $\psi_t \equiv 0$ from (3.1), (A.19), and (A.20),

$$\psi_t := R_{s0} + \left(\sum_{n=1}^{N} a_n \Lambda^{b_n}\right) - \frac{G_p}{G_p^2 + \frac{1}{\omega^2 L_p^2}} \equiv 0, \text{ where } \Lambda = \frac{\frac{1}{\omega L_p}}{G_p^2 + \frac{1}{\omega^2 L_p^2}}.$$

---

[7] One exception is the case of a coil with a constant Q factor, where $R_s = \frac{1}{Q}\omega L_s$ can be rewritten in $G_p = \frac{1}{Q}\frac{1}{\omega L_p}$.
There is another equivalence if the "variable inductor" consists of a fixed inductor $L_{s0} = \text{const.}$ in series to a variable capacitance for the π network or in parallel to a variable capacitance for the T network. Neglecting the losses in the variable capacitor yields $R_s = R_{s0}$ for the π network and $G_p = \frac{R_{s0}}{R_{s0}^2 + (\omega L_{s0})^2} = G_{p0}$ for the T network. Similar to the π network in Section 3.5.2.1, matching in the T network requires $G_{p0} \leq G_i$.

[8] In particular, R_s, L_s, G_p, and L_p are all functions of G_m only. However, we usually may not be able to solve for G_p explicitly after applying (A.19), (A.20), and (3.32) to (3.1).

Then we compute the implicit function's partial derivatives with respect to G_m and G_p,

$$\frac{\partial \psi_\mathrm{t}}{\partial G_\mathrm{m}} = \frac{\left(2\,G_\mathrm{p}\,\frac{1}{\omega L_\mathrm{p}} - \left(\frac{1}{\omega^2 L_\mathrm{p}^2} - G_\mathrm{p}^2\right)\sum_{n=1}^{N} a_n b_n\,\Lambda^{b_n-1}\right)\frac{\partial(\frac{1}{\omega L_\mathrm{p}})}{\partial G_\mathrm{m}}}{\left(G_\mathrm{p}^2 + \frac{1}{\omega^2 L_\mathrm{p}^2}\right)^2},$$

$$\frac{\partial \psi_\mathrm{t}}{\partial G_\mathrm{p}} = -\frac{\frac{1}{\omega^2 L_\mathrm{p}^2} - G_\mathrm{p}^2 + 2\,G_\mathrm{p}\,\frac{1}{\omega L_\mathrm{p}}\left(\sum_{n=1}^{N} a_n b_n\,\Lambda^{b_n-1}\right) - \left(2\,G_\mathrm{p}\,\frac{1}{\omega L_\mathrm{p}} - \left(\frac{1}{\omega^2 L_\mathrm{p}^2} - G_\mathrm{p}^2\right)\sum_{n=1}^{N} a_n b_n\,\Lambda^{b_n-1}\right)\frac{\partial(\frac{1}{\omega L_\mathrm{p}})}{\partial G_\mathrm{p}}}{\left(G_\mathrm{p}^2 + \frac{1}{\omega^2 L_\mathrm{p}^2}\right)^2}.$$

Applying the implicit function theorem [64] gives

$$\frac{\mathrm{d}G_\mathrm{p}}{\mathrm{d}G_\mathrm{m}} = -\frac{\frac{\partial \psi_\mathrm{t}}{\partial G_\mathrm{m}}}{\frac{\partial \psi_\mathrm{t}}{\partial G_\mathrm{p}}} = \frac{\left(2\,G_\mathrm{p}\,\frac{1}{\omega L_\mathrm{p}} - \left(\frac{1}{\omega^2 L_\mathrm{p}^2} - G_\mathrm{p}^2\right)\sum_{n=1}^{N} a_n b_n\,\Lambda^{b_n-1}\right)\frac{\partial(\frac{1}{\omega L_\mathrm{p}})}{\partial G_\mathrm{m}}}{\frac{1}{\omega^2 L_\mathrm{p}^2} - G_\mathrm{p}^2 + 2\,G_\mathrm{p}\,\frac{1}{\omega L_\mathrm{p}}\left(\sum_{n=1}^{N} a_n b_n\,\Lambda^{b_n-1}\right) - \left(2\,G_\mathrm{p}\,\frac{1}{\omega L_\mathrm{p}} - \left(\frac{1}{\omega^2 L_\mathrm{p}^2} - G_\mathrm{p}^2\right)\sum_{n=1}^{N} a_n b_n\,\Lambda^{b_n-1}\right)\frac{\partial(\frac{1}{\omega L_\mathrm{p}})}{\partial G_\mathrm{p}}}.$$

Then we obtain for the second term in (3.38)

$$\frac{G_\mathrm{p}}{G_\mathrm{m}} - \frac{\mathrm{d}G_\mathrm{p}}{\mathrm{d}G_\mathrm{m}} = \frac{G_\mathrm{p}\left(\frac{1}{\omega^2 L_\mathrm{p}^2} - G_\mathrm{p}^2 + 2\,G_\mathrm{p}\,\frac{1}{\omega L_\mathrm{p}}\sum_{n=1}^{N} a_n b_n\,\Lambda^{b_n-1}\right) - \left(2\,G_\mathrm{p}\,\frac{1}{\omega L_\mathrm{p}} - \left(\frac{1}{\omega^2 L_\mathrm{p}^2} - G_\mathrm{p}^2\right)\sum_{n=1}^{N} a_n b_n\,\Lambda^{b_n-1}\right)\left(G_\mathrm{p}\,\frac{\partial(\frac{1}{\omega L_\mathrm{p}})}{\partial G_\mathrm{p}} + G_\mathrm{m}\,\frac{\partial(\frac{1}{\omega L_\mathrm{p}})}{\partial G_\mathrm{m}}\right)}{G_\mathrm{m}\left(\frac{1}{\omega^2 L_\mathrm{p}^2} - G_\mathrm{p}^2 + 2\,G_\mathrm{p}\,\frac{1}{\omega L_\mathrm{p}}\left(\sum_{n=1}^{N} a_n b_n\,\Lambda^{b_n-1}\right) - \left(2\,G_\mathrm{p}\,\frac{1}{\omega L_\mathrm{p}} - \left(\frac{1}{\omega^2 L_\mathrm{p}^2} - G_\mathrm{p}^2\right)\sum_{n=1}^{N} a_n b_n\,\Lambda^{b_n-1}\right)\frac{\partial(\frac{1}{\omega L_\mathrm{p}})}{\partial G_\mathrm{p}}\right)}, \text{ where } \Lambda = \frac{\frac{1}{\omega L_\mathrm{p}}}{G_\mathrm{p}^2 + \frac{1}{\omega^2 L_\mathrm{p}^2}}. \quad (3.39)$$

Replacing of $\frac{1}{\omega L_\mathrm{p}}$ with (3.32) yields the missing partial derivatives,

$$\frac{\partial(\frac{1}{\omega L_\mathrm{p}})}{\partial G_\mathrm{m}} = \frac{G_\mathrm{i} - 2\,(G_\mathrm{m} + G_\mathrm{p})}{2\sqrt{(G_\mathrm{m} + G_\mathrm{p})\,(G_\mathrm{i} - G_\mathrm{m} - G_\mathrm{p})}} + \frac{G_\ell - 2\,G_\mathrm{m}}{2\sqrt{G_\mathrm{m}\,(G_\ell - G_\mathrm{m})}}, \tag{3.40}$$

$$\frac{\partial(\frac{1}{\omega L_\mathrm{p}})}{\partial G_\mathrm{p}} = \frac{G_\mathrm{i} - 2\,(G_\mathrm{m} + G_\mathrm{p})}{2\sqrt{(G_\mathrm{m} + G_\mathrm{p})\,(G_\mathrm{i} - G_\mathrm{m} - G_\mathrm{p})}}. \tag{3.41}$$

To check which value of G_m yields the highest $g_{\mathrm{t,\,inma}}$, we need to know the sign of $\frac{G_\mathrm{p}}{G_\mathrm{m}} - \frac{\mathrm{d}G_\mathrm{p}}{\mathrm{d}G_\mathrm{m}}$, the second term in (3.39), throughout the valid range of G_m given by (3.33).

For ease of understanding, an overview of the following proof is given below. The proof itself is quite lengthy and thus performed in Appendix B.2.2.1.

The idea is that $\frac{G_\mathrm{p}}{G_\mathrm{m}} - \frac{\mathrm{d}G_\mathrm{p}}{\mathrm{d}G_\mathrm{m}}$ remains ≥ 0 for all valid G_m. Then the highest possible value of G_m would yield the highest $g_{\mathrm{t,\,inma}}$.

To prove it, we will derive the highest b_N which still yields a numerator ≥ 0 and simultaneously a denominator ≥ 0. This approach involves more restrictions than necessary, because the ratio of a negative numerator to a negative denominator would also be positive, but the proof is then quite "easy" and straightforward. During the proof, we will limit the inductor's Q factor to $Q \geq 1$, which just indicates that $\omega L_\mathrm{s} \geq R_\mathrm{s}$ or $\frac{1}{\omega L_\mathrm{p}} \geq G_\mathrm{p}$ and is likely to assume for useful variable inductors. However, we should keep in mind that due to the additional restrictions $\frac{G_\mathrm{p}}{G_\mathrm{m}} - \frac{\mathrm{d}G_\mathrm{p}}{\mathrm{d}G_\mathrm{m}}$ might remain positive even for a higher b_N or lower Q than those derived.

If we abbreviate $S_\mathrm{t} = \sum_{n=1}^{N} a_n b_n \Lambda^{b_n - 1}$, we obtain from (3.39)

$$\frac{G_\mathrm{p}}{G_\mathrm{m}} - \frac{\mathrm{d}G_\mathrm{p}}{\mathrm{d}G_\mathrm{m}} = \frac{G_\mathrm{p}\left(\frac{1}{\omega^2 L_\mathrm{p}^2} - G_\mathrm{p}^2 + 2\,G_\mathrm{p}\,\frac{1}{\omega L_\mathrm{p}}\,S_\mathrm{t}\right) - \left(2\,G_\mathrm{p}\,\frac{1}{\omega L_\mathrm{p}} - \left(\frac{1}{\omega^2 L_\mathrm{p}^2} - G_\mathrm{p}^2\right) S_\mathrm{t}\right)\left(G_\mathrm{p}\,\frac{\partial(\frac{1}{\omega L_\mathrm{p}})}{\partial G_\mathrm{p}} + G_\mathrm{m}\,\frac{\partial(\frac{1}{\omega L_\mathrm{p}})}{\partial G_\mathrm{m}}\right)}{G_\mathrm{m}\left(\frac{1}{\omega^2 L_\mathrm{p}^2} - G_\mathrm{p}^2 + 2\,G_\mathrm{p}\,\frac{1}{\omega L_\mathrm{p}}\,S_\mathrm{t} - \left(2\,G_\mathrm{p}\,\frac{1}{\omega L_\mathrm{p}} - \left(\frac{1}{\omega^2 L_\mathrm{p}^2} - G_\mathrm{p}^2\right) S_\mathrm{t}\right)\frac{\partial(\frac{1}{\omega L_\mathrm{p}})}{\partial G_\mathrm{p}}\right)}.$$

To prove that numerator and denominator are ≥ 0 for certain b_N and Q, we firstly assume $S_\mathrm{t} = 0$ or $R_\mathrm{s} = R_\mathrm{s0}$ and calculate $\frac{G_\mathrm{p}}{G_\mathrm{m}} - \frac{\mathrm{d}G_\mathrm{p}}{\mathrm{d}G_\mathrm{m}}$, which will be ≥ 0 throughout the valid range of G_m.

Secondly, we assume $S_\mathrm{t} \neq 0$, hence $S_\mathrm{t} > 0$ (according to (3.1)). We then prove that $2\,G_\mathrm{p}\,\frac{1}{\omega L_\mathrm{p}} - \left(\frac{1}{\omega^2 L_\mathrm{p}^2} - G_\mathrm{p}^2\right) S_\mathrm{t} \geq 0$ if $0 < b_N \leq 2$. If we further limit the variable inductor's Q factor to $Q \geq 1$, hence $\frac{1}{\omega L_\mathrm{p}} \geq G_\mathrm{p}$, it is obvious that $\frac{1}{\omega^2 L_\mathrm{p}^2} - G_\mathrm{p}^2 \geq 0$, thus $2\,G_\mathrm{p}\,\frac{1}{\omega L_\mathrm{p}} \geq 2\,G_\mathrm{p}\,\frac{1}{\omega L_\mathrm{p}} - \left(\frac{1}{\omega^2 L_\mathrm{p}^2} - G_\mathrm{p}^2\right) S_\mathrm{t} \geq 0$ and $\frac{1}{\omega^2 L_\mathrm{p}^2} - G_\mathrm{p}^2 + 2\,G_\mathrm{p}\,\frac{1}{\omega L_\mathrm{p}} S_\mathrm{t} \geq 0$. We then check numerator and denominator separately:

1. Since ωL_p, G_m, G_p are ≥ 0, $S_\mathrm{t} > 0$, and the preceding estimates apply, the numerator will always be ≥ 0 for $G_\mathrm{p}\,\frac{\partial(\frac{1}{\omega L_\mathrm{p}})}{\partial G_\mathrm{p}} + G_\mathrm{m}\,\frac{\partial(\frac{1}{\omega L_\mathrm{p}})}{\partial G_\mathrm{m}} \leq 0$. Conversely, if

$G_\mathrm{p} \frac{\partial(\frac{1}{\omega L_\mathrm{p}})}{\partial G_\mathrm{p}} + G_\mathrm{m} \frac{\partial(\frac{1}{\omega L_\mathrm{p}})}{\partial G_\mathrm{m}} > 0$, we have to use the preceding estimates and certain inequalities to prove that then the numerator will be ≥ 0.

2. Since ωL_p, G_m, G_p are ≥ 0, $S_\mathrm{t} > 0$, and the preceding estimates apply, the denominator will always be ≥ 0 for $\frac{\partial(\frac{1}{\omega L_\mathrm{p}})}{\partial G_\mathrm{p}} \leq 0$. Conversely, if $\frac{\partial(\frac{1}{\omega L_\mathrm{p}})}{\partial G_\mathrm{p}} > 0$, we will have to use the preceding estimates and certain inequalities to prove that then the denominator will be ≥ 0.

We then know that for all possible values of $R_{\mathrm{s}0}$, a_n, and b_n according to (3.1), $\frac{\mathrm{d}g_{\mathrm{t,\,inma}}}{\mathrm{d}G_\mathrm{m}} \geq 0$ if (at least) $b_N \leq 2$ and $Q \geq 1$ (hence $\omega L_\mathrm{s} \geq R_\mathrm{s}$ or $\frac{1}{\omega L_\mathrm{p}} \geq G_\mathrm{p}$).

Hence the highest $g_{\mathrm{t,\,inma}}$ is obtained for the highest valid value of G_m, which is G_ℓ if $G_\ell \leq G_\mathrm{i}$ or G_{mlim} defined in (3.34) if $G_\ell > G_\mathrm{i}$, respectively. If we choose G_m accordingly, the particular type of network involved is one of the two L networks where $C_2 \to \infty$ or $C_1 \to \infty$.

However, we should keep in mind that the restrictions $0 < b_N \leq 2$ and $Q \geq 1$ (hence $\omega L_\mathrm{s} \geq R_\mathrm{s}$ or $\frac{1}{\omega L_\mathrm{p}} \geq G_\mathrm{p}$) aroused after applying inequalities to get upper estimates for certain terms. If $b_N > 2$ or $0 \leq Q < 1$, the method used in the preceding proof gives no indication of the network's behaviour. To illustrate this, it should be noted that if all $a_n = 0$, hence $R_\mathrm{s} = R_{\mathrm{s}0}$, the proof involved no restrictions to the Q factor of the variable inductor[9].

It's interesting to note that usually the highest $g_{\mathrm{t,\,inma}}$ does not coincide with the lowest R_s (or, according to (3.1), the lowest L_s), where R_s, L_s are the elements yielded by parallel-to-series transformation of G_p and L_p.

3.5.3.3 Optimum value of load conductance G_ℓ for maximum power gain

In Section 3.5.3.2 we derived which value of G_m maximises $g_{\mathrm{t,\,inma}}$. However, the highest $g_{\mathrm{t,\,inma}}$ still depends on G_ℓ (G_i is fixed in our application of matching the load to the source).

Thus further investigations are required to determine which G_ℓ yields the highest $g_{\mathrm{t,\,inma}}$ if the parameter G_m was chosen for maximum $g_{\mathrm{t,\,inma}}$ according to Section 3.5.3.2.

G_ℓ is variable because the connecting line between matching network and load transforms the load depending on the line's length. As transformation usually involves additional reactances even for a purely resistive load, optimisation of $g_{\mathrm{t,\,inma}}$ with

[9]Similar proofs without any restrictions to the Q factor of the variable inductor could also be performed for different single loss terms, e. g. $R_\mathrm{s} = a_1 (\omega L_\mathrm{s})^{\frac{1}{2}}$, $R_\mathrm{s} = \frac{1}{Q} \omega L_\mathrm{s}$, and $R_\mathrm{s} = a_2 (\omega L_\mathrm{s})^2$, which also holds for the two cases equivalent to the π network, $G_\mathrm{p} = G_{\mathrm{p}0}$ and $G_\mathrm{p} = \frac{1}{Q} \frac{1}{\omega L_\mathrm{p}}$ (described in Footnote [7]). However, each term generates a different solution for G_p, and usually the sum of the single loss terms does not generate a G_p equal to the sum of the single terms' G_p. Thus these proofs do not help to extend the proof for (3.1).

respect to G_ℓ is only part of the solution, "complete" optimisation needs application of Sections 4.3.1.2 and 4.3.2.2, too.

The derivation of the optimum value of G_ℓ is quite similar to Section 3.5.3.2, but lengthy and thus performed in Appendix B.2.2.2.

Summarising Appendix B.2.2.2, we may conclude that if $0 < b_N \leq 2$, $Q \geq 1$ (hence $\omega L_\mathrm{s} \geq R_\mathrm{s}$ or $\frac{1}{\omega L_\mathrm{p}} \geq G_\mathrm{p}$), and G_m is chosen according to Section 3.5.3.2, $G_\ell = G_\mathrm{i}$ would yield the highest $g_{\mathrm{t,\,inma}}$. $g_{\mathrm{t,\,inma}}$ decreases for higher or lower G_ℓ.

Unfortunately the optimisation gives no indication for which of the two load conductors $G_{\ell 1} > G_\mathrm{i}$, $G_{\ell 2} = \frac{G_\mathrm{i}^2}{G_{\ell 1}} < G_\mathrm{i}$, exhibiting similar reflection coefficients referred to $R_\mathrm{i} = \frac{1}{G_\mathrm{i}}$, we would achieve the higher $g_{\mathrm{t,\,inma}}$ (reference $R_\mathrm{i} = \frac{1}{G_\mathrm{i}}$ is not related to the interconnecting transmission lines' characteristic impedances, but was used to obtain equal "transformation distances" from optimum value $R_\mathrm{i} = \frac{1}{G_\mathrm{i}}$).

As mentioned before, "complete" optimisation involves taking into account of Sections 4.3.1.2 and 4.3.2.2. However, at least we may conclude that minimising losses of the matching network will always require consideration (and optimisation) of the length of the transmission line connecting it to the load.

3.5.3.4 Approximate equivalence of π and T network for a high-Q central inductor L_s

Usually the T network behaves different than the π network because the losses of the inductor are of a serial type in both cases (some remarks at the end of Section 3.5.3.1 already addressed this issue). Thus, if we perform a series to parallel transformation of L_s and R_s in L_p and G_p as shown in Figure 3.13 b), we may rewrite (3.1), the functional description of the losses, using (A.19) and (A.20), obtaining

$$\frac{G_\mathrm{p}}{G_\mathrm{p}^2 + \left(\frac{1}{\omega L_\mathrm{p}}\right)^2} = R_{\mathrm{s0}} + \sum_{n=1}^{N} a_n \Lambda^{b_n},$$

or, slightly rearranged,

$$G_\mathrm{p} = R_{\mathrm{s0}} \left(G_\mathrm{p}^2 + \left(\frac{1}{\omega L_\mathrm{p}}\right)^2 \right) + \sum_{n=1}^{N} a_n \frac{\left(\frac{1}{\omega L_\mathrm{p}}\right)^{b_n}}{\left(G_\mathrm{p}^2 + \left(\frac{1}{\omega L_\mathrm{p}}\right)^2 \right)^{b_n - 1}},$$

which, if solved for G_p, is usually not equal to $G_\mathrm{p} = G_{\mathrm{p0}} + \sum_{n=0}^{N} \tilde{a}_n \left(\frac{1}{\omega L_\mathrm{p}}\right)^{\tilde{b}_n}$ (with some exceptions indicated in Footnote [7]).

Although the proofs for the T network did not need any approximation, we might get some hint why they also involved a constraint of $b_N \leq 2$ if we consider an inductor

with $\omega L_\mathrm{s} \gg R_\mathrm{s}$ (or $Q \gg 1$). Hence $\frac{1}{\omega L_\mathrm{p}} \gg G_\mathrm{p}$ holds, allowing us to approximate

$$G_\mathrm{p} \approx R_{\mathrm{s}0} \left(\frac{1}{\omega L_\mathrm{p}}\right)^2 + \sum_{n=1}^{N} a_n \left(\frac{1}{\omega L_\mathrm{p}}\right)^{2-b_n}.$$

Assuming $0 < b_N \leq 2$, the powers are simply "mirrored" at $b_n = 1$. If we define $\tilde{a}_n := a_n$, $\tilde{b}_n := 2 - b_n$, we get an equation in G_p and $\frac{1}{\omega L_\mathrm{p}}$ similar to those in R_s and ωL_s. If $b_N = 2$ for the R_s used, a $G_{\mathrm{p}0} = a_N$ would occur, involving additional restrictions similar to those involved by $R_{\mathrm{s}0}$ for the π network.

Thus, if $Q \gg 1$ for the central inductor L_s, the T network is (approximately) equivalent to the π network.

Chapter 4

Extension of the Method to Complex Loads

4.1 Introduction

In the previous chapter, the optimum parameter's (and load resistance's) value for maximum active power transfer was derived for resistive sources and loads.

Since realistic loads are usually complex, the method presented in the previous chapter is extended to complex loads in the following chapter. Then exact analytical solutions for a constant Q factor central inductor are derived. Thereby the power gain of different types of networks may be compared and its increase introduced by a suitable matching strategy may be estimated. Important characteristics of the exact solution help to derive an optimum matching strategy for any types of loads. Finally its applicability to switchable matching networks is considered.

4.2 Definitions/notations

From this chapter on, the following definitions/notations will be used:

Latin letters

$B_{2\mathrm{tot}}$	Total load susceptance (including C_2 of the network and the load's (equivalent) inductance)
$C_{2\mathrm{tot}}$	Total load capacitance (including C_2 of the network and the load's (equivalent) capacitance or inductance)
$C_{\ell\mathrm{p}}$	Load capacitance in parallel to load conductance G_ℓ
$C_{\ell\mathrm{s}}$	Load capacitance in series to load resistance R_ℓ
$g_{\mathrm{t,inma,maxind+}}$	Maximum $g_{\mathrm{t,inma}}$ (of solution $G_{\mathrm{pind+}}$ if $G_\ell < G_\mathrm{i}$)
$g_{\pi\mathrm{,inma,maxind+}}$	Maximum $g_{\pi\mathrm{,inma}}$ (of solution $R_{\mathrm{sind+}}$ if $R_\ell < R_\mathrm{i}$)
$g_{\pi\mathrm{,lldes}}$	Power gain of a π network designed as if it would be lossless
$G_{\ell\mathrm{limofGmlim}}$	Load conductance for which the maximum of C_1 tends to infinity (solution $G_{\mathrm{pcap+}}$)
$G_{\mathrm{m}1/L_\mathrm{p}0}$	G_m which yields $\frac{1}{L_\mathrm{p}} = 0$ in the case of an inductively loaded T network (equal sqare roots in L_p formula)
$G_{\mathrm{m}C_{\ell\mathrm{s}}}$	G_m which yields $C_{2\mathrm{tot}} = C_{\ell\mathrm{s}}$

$G_{\mathrm{mgmaxind+}}$	G_m which yields the maximum $g_{\mathrm{t,inma}}$ (solution $G_{\mathrm{pind+}}$)
G_{mlim1}	Lower pole of C_1 (solution $G_{\mathrm{pcap+}}$)
G_{mlim2}	Upper pole of C_1 (solution $G_{\mathrm{pcap+}}$)
$G_{\mathrm{m}L_{\ell\mathrm{s}}}$	G_m which yields $L_{2\mathrm{tot}} = L_{\ell\mathrm{s}}$
G_{mu01}	Lower zero of u_t
G_{mu02}	Upper zero of u_t
G_{mv01}	Lower zero of v_t
G_{mv02}	Upper zero of v_t
$G_{\mathrm{pcap}\mp}$	Exact solutions of G_p for a constant Q factor central inductor and capacitive/resistive/(over-)compensated inductive loads, distinguished by the sign in front of $\sqrt{u_\mathrm{t}}$
$G_{\mathrm{pind}\mp}$	Exact solutions of G_p for a constant Q factor central inductor and undercompensated inductive loads, distinguished by the sign in front of $\sqrt{v_\mathrm{t}}$
$L_{2\mathrm{tot}}$	Total load inductance (including C_2 of the network and the load's (equivalent) inductance)
$L_{\ell\mathrm{p}}$	Load inductance in parallel to load conductance G_ℓ
$L_{\ell\mathrm{s}}$	Load inductance in series to load resistance R_ℓ (T network)
$L_{\mathrm{pind+}}$	Parallel inductance derived from the exact solution $G_{\mathrm{pind+}}$ for a constant Q factor central inductor and undercompensated inductive loads
$L_{\mathrm{sind+}}$	Series inductance derived from the exact solution $R_{\mathrm{sind+}}$ for a constant Q factor central inductor and undercompensated inductive loads (π network)
$L_{\mathrm{sind+}}$	Series inductance yielded by parallel-to-series transformation of $G_{\mathrm{pind+}}$ and $L_{\mathrm{pind+}}$ (T network)
$R_{\ell\mathrm{limofRmlim}}$	Load resistance for which the minimum of C_1 equals zero (solution $R_{\mathrm{scap+}}$)
$R_{\mathrm{m}C_{\ell\mathrm{p}}}$	R_m which yields $C_{2\mathrm{tot}} = C_{\ell\mathrm{p}}$
R_{mgmaxind}	R_m which yields the maximum $g_{\pi,\mathrm{llde s}}$ (constant Q factor central inductor and undercompensated inductive load)
$R_{\mathrm{mgmaxind+}}$	R_m which yields the maximum $g_{\pi,\mathrm{inma}}$ (solution $R_{\mathrm{sind+}}$)
R_{mlim1}	Lower zero of C_1 (solution $R_{\mathrm{scap+}}$)
R_{mlim2}	Upper zero of C_1 (solution $R_{\mathrm{scap+}}$)
$R_{\mathrm{m}L_{\ell\mathrm{p}}}$	R_m which yields $L_{2\mathrm{tot}} = L_{\ell\mathrm{p}}$
$R_{\mathrm{m}L_\mathrm{s}0}$	R_m which yields $L_\mathrm{s} = 0$ in the case of an inductively loaded T network (equal sqare roots in L_s formula)
R_{mu01}	Lower zero of u_π
R_{mu02}	Upper zero of u_π
R_{mv01}	Lower zero of v_π
R_{mv02}	Upper zero of v_π
$R_{\mathrm{scap}\mp}$	Exact solutions of R_s for a constant Q factor central inductor and capacitive/ resistive/(over-)compensated inductive loads, distinguished by the sign in front of $\sqrt{u_\pi}$
$R_{\mathrm{sind}\mp}$	Exact solutions of R_s for a constant Q factor central inductor and undercompensated inductive loads, distinguished by the sign in front of $\sqrt{v_\pi}$
u_t	Argument of "large" square root in $G_{\mathrm{pcap}\mp}$
u_π	Argument of "large" square root in $R_{\mathrm{scap}\mp}$
v_t	Argument of "large" square root in $G_{\mathrm{pind}\mp}$
v_π	Argument of "large" square root in $R_{\mathrm{sind}\mp}$
$X_{2\mathrm{tot}}$	Total load reactance (including C_2 of the network and the load's (equivalent) inductance)

Greek letters

ΔG_m	Step in G_m accompanied by a resistance step due to switching to next inductor value in a T network with switchable elements
ΔR_m	Step in R_m accompanied by a resistance step due to switching to next inductor value in a π network with switchable elements

4.3 Matching of a complex load to a resistive source (matching at the network's input)

4.3.1 Complex load exhibiting a capacitive imaginary part

4.3.1.1 π network

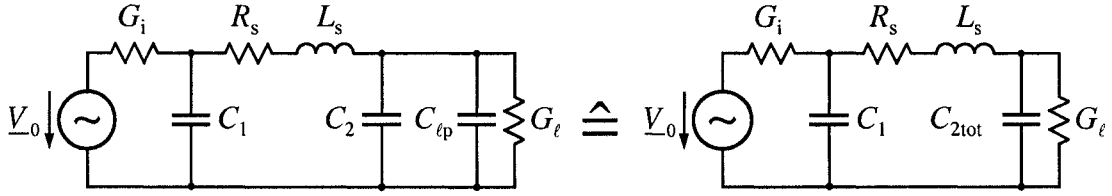

Figure 4.1: Resulting π network's equivalent circuit for matching of a (complex) load admittance consisting of a conductance G_ℓ in parallel to a capacitance $C_{\ell\mathrm{p}}$ to a (real) source conductance G_i

If the load impedance $\underline{Z}_\ell$, hence the load admittance $\frac{1}{\underline{Z}_\ell}$, exhibits a capacitive imaginary part, thus $\mathrm{Im}\{\underline{Z}_\ell\} < 0$ and $\mathrm{Im}\left\{\frac{1}{\underline{Z}_\ell}\right\} > 0$, we may describe the load admittance at matching frequency by a conductance G_ℓ in parallel to a capacitance $C_{\ell\mathrm{p}}$, where

$$G_\ell = \mathrm{Re}\left\{\frac{1}{\underline{Z}_\ell}\right\}, \quad (4.1) \qquad\qquad C_{\ell\mathrm{p}} = \frac{1}{\omega}\,\mathrm{Im}\left\{\frac{1}{\underline{Z}_\ell}\right\}. \quad (4.2)$$

If we combine the π network's capacitance C_2 and the load capacitance $C_{\ell\mathrm{p}}$ (refer to Figure 4.1), and denote the total capacitance by $C_{2\mathrm{tot}}$, we obtain

$$C_{2\mathrm{tot}} = C_2 + C_{\ell\mathrm{p}}.$$

The resulting equivalent circuit's components are similar to those of the π network in Section 3.5.2.1. Thus all results obtained in Sections 3.5.2.1 and 3.5.2.2 are applicable if we put $R_\mathrm{i} = \frac{1}{G_\mathrm{i}}$, $R_\ell = \frac{1}{G_\ell}$, and replace C_2 with $C_{2\mathrm{tot}}$ in all formulae derived[1], in particular in (3.18). Then the remaining capacitance C_2 of the π network is given by

$$C_2 = C_{2\mathrm{tot}} - C_{\ell\mathrm{p}} = \frac{1}{\omega R_\ell}\sqrt{\frac{R_\ell - R_\mathrm{m}}{R_\mathrm{m}}} - C_{\ell\mathrm{p}}. \quad (4.3)$$

However, C_2 is a variable capacitance, thus the lowest value of $C_{2\mathrm{tot}}$ is $C_{\ell\mathrm{p}}$, which differs from the case of a resistive load, where the minimum value was (theoretically) zero (but a "real world" variable capacitor's minimum value wouldn't be zero).

To illustrate the impact of the preceding restriction to the minimum $C_{2\mathrm{tot}}$, we compute the derivative of $C_{2\mathrm{tot}}$ with respect to R_m from (3.18), $\frac{\mathrm{d}C_{2\mathrm{tot}}}{\mathrm{d}R_\mathrm{m}} =$

[1]We should note that there is a slight inconsistency in the definition of R_ℓ because $R_\ell \neq \mathrm{Re}\left\{\frac{1}{G_\ell + \mathrm{j}\omega C_{\ell\mathrm{p}}}\right\}$ as we would expect it to be according to the definitions in (2.7) and (2.13).

$-\frac{1}{2\omega R_\mathrm{m}\sqrt{R_\mathrm{m}(R_\ell - R_\mathrm{m})}}$, which is < 0 for the (utmost) valid range of R_m indicated in (3.20). Thus R_m has to be lower than or equal to

$$R_{\mathrm{m}C_{\ell\mathrm{p}}} = \frac{R_\ell}{1+(\omega R_\ell C_{\ell\mathrm{p}})^2} \left(= \frac{\mathrm{Re}\left\{\frac{1}{\underline{Z}_\ell}\right\}}{\left|\frac{1}{\underline{Z}_\ell}\right|^2} = \mathrm{Re}\{\underline{Z}_\ell\} \right), \tag{4.4}$$

ensuring $C_{2\mathrm{tot}} \geq C_{\ell\mathrm{p}}$. For AC excitation $\omega > 0$, hence $R_{\mathrm{m}C_{\ell\mathrm{p}}} < R_\ell$ holds (which is easy to understand because $C_{2\mathrm{tot}} = 0$ if $R_\mathrm{m} = R_\ell$, but $C_{2\mathrm{tot}} \geq C_{\ell\mathrm{p}} > 0$ due to $C_{\ell\mathrm{p}} > 0$ for a complex load exhibiting a capacitive imaginary part).

Differing from a purely resistive load, the (utmost) limits of the parameter R_m are given by $0 \leq R_\mathrm{m} \leq R_{\mathrm{m}C_{\ell\mathrm{p}}}$ if $R_\ell \leq R_\mathrm{i} - R_{\mathrm{s}0}$ or by $0 \leq R_\mathrm{m} \leq \mathrm{Min}\{R_{\mathrm{m}C_{\ell\mathrm{p}}}, R_{\mathrm{m}\mathrm{lim}}\}$ if $R_\ell > R_\mathrm{i} - R_{\mathrm{s}0}$.

Similar to Section 3.5.2.2, $g_{\pi,\mathrm{inma}}$ increases (or stays constant) with increasing R_m. Thus the highest valid R_m yields the maximum $g_{\pi,\mathrm{inma}}$, hence $R_\mathrm{m} = R_{\mathrm{m}C_{\ell\mathrm{p}}}$ if $R_\ell \leq R_\mathrm{i} - R_{\mathrm{s}0}$ or $R_\mathrm{m} = \mathrm{Min}\{R_{\mathrm{m}C_{\ell\mathrm{p}}}, R_{\mathrm{m}\mathrm{lim}}\}$ if $R_\ell > R_\mathrm{i} - R_{\mathrm{s}0}$, respectively. In both cases, the resulting matching network is a L network, because $C_{2\mathrm{tot}} = C_{\ell\mathrm{p}}$ and $C_2 = 0$ for $R_\mathrm{m} = R_{\mathrm{m}C_{\ell\mathrm{p}}}$, or $C_1 = 0$ for $R_\mathrm{m} = R_{\mathrm{m}\mathrm{lim}}$. In particular, for $R_\mathrm{m} = R_{\mathrm{m}C_{\ell\mathrm{p}}}$ the resulting circuit is a π network, but the type of the **external** matching network is a L network[2].

4.3.1.2 T network

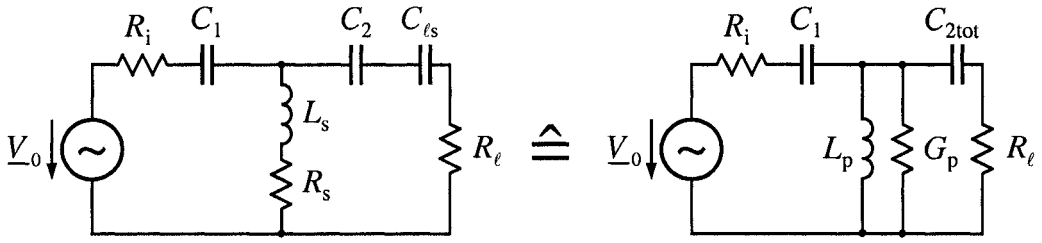

Figure 4.2: Resulting T network's equivalent circuit for matching of a (complex) load reactance consisting of a resistance R_ℓ in series to a capacitance $C_{\ell\mathrm{s}}$ to a (real) source resistance R_i

If the load impedance $\underline{Z}_\ell$ exhibits a capacitive imaginary part, thus $\mathrm{Im}\{\underline{Z}_\ell\} < 0$, we may describe the load impedance at matching frequency by a resistance R_ℓ in series to a capacitance $C_{\ell\mathrm{s}}$, where

$$R_\ell = \mathrm{Re}\{\underline{Z}_\ell\}, \tag{4.5}$$

$$C_{\ell\mathrm{s}} = -\frac{1}{\omega\,\mathrm{Im}\{\underline{Z}_\ell\}}. \tag{4.6}$$

[2] However, due to parasitic capacitances, a "real world" matching network would always be a π network and could not be set to $R_\mathrm{m} = R_{\mathrm{m}\mathrm{lim}}$, although these parasitic capacitances might be remarkably small, e. g. for switchable capacitors in a network similar to [33]. But within this section we investigate the networks' principal behaviour, the impact of minimum and maximum values of C_1, L_s, and C_2 will be considered in Section 4.5.1.

If we combine the T network's capacitance C_2 and the load capacitance $C_{\ell s}$ (refer to Figure 4.2), and denote the total capacitance by $C_{2\text{tot}}$, we obtain

$$C_{2\text{tot}} = \frac{1}{\frac{1}{C_2} + \frac{1}{C_{\ell s}}}.$$

The resulting equivalent circuit's components are similar to those of the T network in Section 3.5.3.1. Thus all results obtained in Sections 3.5.3.1 and 3.5.3.2 are applicable if we put $G_{\text{i}} = \frac{1}{R_{\text{i}}}$, $G_\ell = \frac{1}{R_\ell}$, and replace C_2 with $C_{2\text{tot}}$ in all formulae derived[3], in particular in (3.31). Then the remaining capacitance C_2 of the T network is given by

$$C_2 = \frac{1}{\frac{1}{C_{2\text{tot}}} - \frac{1}{C_{\ell s}}} = \frac{1}{\frac{\omega}{G_\ell}\sqrt{\frac{G_\ell - G_{\text{m}}}{G_{\text{m}}}} - \frac{1}{C_{\ell s}}}. \tag{4.7}$$

However, C_2 is a variable capacitance, thus the highest value of $C_{2\text{tot}}$ is $C_{\ell s}$, which differs from the case of a resistive load, where the maximum value tended (theoretically) to infinity (but a "real world" variable capacitor's maximum value would be finite).

To illustrate the impact of the preceding restriction to the maximum $C_{2\text{tot}}$, we compute the derivative of $C_{2\text{tot}}$ with respect to G_{m} from (3.31), $\frac{\text{d}C_{2\text{tot}}}{\text{d}G_{\text{m}}} = \frac{G_\ell^2}{2\omega(G_\ell - G_{\text{m}})\sqrt{G_{\text{m}}(G_\ell - G_{\text{m}})}}$, which is > 0 for the (utmost) valid range of G_{m} indicated in (3.33). Thus G_{m} has to be lower than or equal to

$$G_{\text{m}C_{\ell s}} = \frac{G_\ell}{1 + \left(\frac{G_\ell}{\omega C_{\ell s}}\right)^2} \left(= \frac{\text{Re}\{\underline{Z}_\ell\}}{|\underline{Z}_\ell|^2} = \text{Re}\left\{\frac{1}{\underline{Z}_\ell}\right\}\right), \tag{4.8}$$

ensuring $C_{2\text{tot}} \leq C_{\ell s}$. For AC excitation $\omega > 0$, hence $G_{\text{m}C_{\ell s}} < G_\ell$ holds (which is easy to understand because $C_{2\text{tot}} \to \infty$ if $G_{\text{m}} = R_\ell$, but since $C_{\ell s} \in (0, \infty)$ and $0 < C_{2\text{tot}} \leq C_{\ell s}$, $C_{2\text{tot}} \in (0, \infty)$ holds).

Differing from a purely resistive load, the (utmost) limits of the parameter G_{m} are given by $0 \leq G_{\text{m}} \leq G_{\text{m}C_{\ell s}}$ if $G_\ell \leq G_{\text{i}}$ or by $0 \leq G_{\text{m}} \leq \text{Min}\{G_{\text{m}C_{\ell s}}, G_{\text{mlim}}\}$ if $G_\ell > G_{\text{i}}$.

Similar to Section 3.5.3.2, $g_{\text{t, inma}}$ increases (or might stay constant) with increasing G_{m}. Thus the highest valid G_{m} yields the maximum $g_{\text{t, inma}}$, hence $G_{\text{m}} = G_{\text{m}C_{\ell s}}$ if $G_\ell \leq G_{\text{i}}$ or $G_{\text{m}} = \text{Min}\{G_{\text{m}C_{\ell s}}, G_{\text{mlim}}\}$ if $G_\ell > G_{\text{i}}$, respectively. In both cases, the resulting matching network is a L network, because $C_{2\text{tot}} = C_{\ell s}$ and $C_2 \to \infty$ for $G_{\text{m}} = G_{\text{m}C_{\ell s}}$, or $C_1 \to \infty$ for $G_{\text{m}} = G_{\text{mlim}}$. In particular, for $G_{\text{m}} = G_{\text{m}C_{\ell s}}$ the resulting circuit is a T network, but the type of the **external** matching network is a L network[4].

---

[3] We should note that there is a slight inconsistency in the definition of G_ℓ because $G_\ell \neq \text{Re}\left\{\frac{1}{R_\ell + \frac{1}{\text{j}\omega C_{\ell s}}}\right\}$ as we would expect it to be according to the definitions in (2.13) and (2.7).

[4] However, due to finite capacitances, a "real world" matching network would always be a

4.3.2 Complex load exhibiting an inductive imaginary part

4.3.2.1 π network

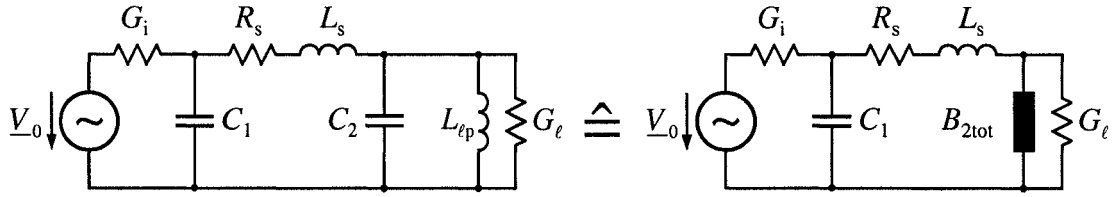

Figure 4.3: Resulting π network's equivalent circuit for matching of a (complex) load admittance consisting of a conductance G_ℓ in parallel to an inductance $L_{\ell p}$ to a (real) source conductance G_i

If the load impedance $\underline{Z}_\ell$, hence the load admittance $\frac{1}{\underline{Z}_\ell}$, exhibits an inductive imaginary part, thus $\mathrm{Im}\{\underline{Z}_\ell\} > 0$ and $\mathrm{Im}\left\{\frac{1}{\underline{Z}_\ell}\right\} < 0$, we may describe the load admittance at matching frequency by a conductance G_ℓ in parallel to an inductance $L_{\ell p}$, where

$$G_\ell = \mathrm{Re}\left\{\frac{1}{\underline{Z}_\ell}\right\}, \quad (4.9) \qquad L_{\ell p} = -\frac{1}{\omega\,\mathrm{Im}\left\{\frac{1}{\underline{Z}_\ell}\right\}}. \quad (4.10)$$

To achieve matching of the π network's input admittance to the source conductance, two completely different solutions arise.

1. (Over-)Compensation of $L_{\ell p}$ by C_2, hence $B_{2tot} \geq 0$ in Figure 4.3 and thus may be described by a capacitance C_{2tot} at matching frequency.

   Similar to Section 4.3.1.1 C_{2tot} is given by (3.18). For the remaining capacitance C_2 of the π network we obtain

   $$C_2 = \frac{1}{\omega^2 L_{\ell p}} + C_{2tot} = \frac{1}{\omega}\left(\frac{1}{\omega L_{\ell p}} + \frac{1}{R_\ell}\sqrt{\frac{R_\ell - R_m}{R_m}}\right). \quad (4.11)$$

   C_2 is a variable capacitance and thus ≥ 0, in particular, $C_2 \geq \frac{1}{\omega^2 L_{\ell p}} > 0$. If the susceptance of C_2 cancels the susceptance of $L_{\ell p}$, B_{2tot} and C_{2tot} may be zero — just equivalent to the case of a purely resistive load with exception of the value of C_2, which is shifted by $\frac{1}{\omega^2 L_{\ell p}}$. All results obtained in Sections 3.5.2.1 and 3.5.2.2 are applicable, but we have to put $R_i = \frac{1}{G_i}$, $R_\ell = \frac{1}{G_\ell}$, and replace

---

T network and could not be set to $G_m = G_{mlim}$, although the maximum capacitances might be remarkably high, e. g. for switchable capacitors in a network similar to [33]. But within this section we investigate the networks' principal behaviour, the impact of minimum and maximum values of C_1, L_s (from parallel-to-series transformation of G_p and L_p), and C_2 will be considered in Section 4.5.2.

C_2 with $C_{2\mathrm{tot}}$ in all formulae derived[5]. However, compared to Section 4.3.1.1, there is no additional limit to R_m, but a minimum value of C_2 given by $\frac{1}{\omega^2 L_{\ell\mathrm{p}}}$.

Similar to Section 3.5.2.2, $g_{\pi,\,\mathrm{inma}}$ increases (or stays constant) with increasing R_m. Thus the highest valid R_m yields the maximum $g_{\pi,\,\mathrm{inma}}$, hence $R_\mathrm{m} = R_\ell$ if $R_\ell \leq R_\mathrm{i} - R_{\mathrm{s}0}$ or $R_\mathrm{m} = R_{\mathrm{mlim}}$ if $R_\ell > R_\mathrm{i} - R_{\mathrm{s}0}$, respectively. For $R_\mathrm{m} = R_\ell$ the resulting type of the **external** matching network is a π network, whose capacitance C_2 cancels $L_{\ell\mathrm{p}}$ at matching frequency, hence π network and $L_{\ell\mathrm{p}}$ build up a L network. For $R_\mathrm{m} = R_{\mathrm{mlim}}$, $C_1 = 0$ holds, and the resulting type of the **external** matching network is a L network[2].

We already might assume that the case of (over-)compensation does not guarantee the lowest losses, because the equivalent circuit's lossless load inductance is "wasted" by (over-)compensation and all inductance needed for matching has to be supplied by the lossy inductor of the matching network.

2. Undercompensation of $L_{\ell\mathrm{p}}$ by C_2, hence $B_{2\mathrm{tot}} < 0$ in Figure 4.3 and thus may be described by an inductance $L_{2\mathrm{tot}}$ at matching frequency.

   According to (3.18) and the notes regarding the signs in parentheses/square brackets we obtain

$$L_{2\mathrm{tot}} = \frac{1}{\frac{1}{L_{\ell\mathrm{p}}} - \omega^2 C_2} = \frac{R_\ell}{\omega}\sqrt{\frac{R_\mathrm{m}}{R_\ell - R_\mathrm{m}}}.$$

   The remaining capacitance C_2 of the π network is then given by

$$C_2 = \frac{1}{\omega}\left(\frac{1}{\omega L_{\ell\mathrm{p}}} - \frac{1}{R_\ell}\sqrt{\frac{R_\ell - R_\mathrm{m}}{R_\mathrm{m}}}\right). \tag{4.12}$$

   As before, we have to put $R_\mathrm{i} = \frac{1}{G_\mathrm{i}}$ and $R_\ell = \frac{1}{G_\ell}$ in all equations derived[5].

   Additionally, according to (3.19) and the notes regarding the signs in parentheses/square brackets we obtain for the inductance L_s of the π network

$$L_\mathrm{s} = \frac{\sqrt{(R_\mathrm{m} + R_\mathrm{s})\,(R_\mathrm{i} - R_\mathrm{m} - R_\mathrm{s})} - \sqrt{R_\mathrm{m}\,(R_\ell - R_\mathrm{m})}}{\omega}. \tag{4.13}$$

   The preceding changes of the equivalent network's elements also involve changes of the limits of parameter R_m.

   One additional limit occurs because C_2 is still a capacitance and ≥ 0. Thus $L_{2\mathrm{tot}} \geq L_{\ell\mathrm{p}}$ holds. Since $L_{2\mathrm{tot}}$ increases with increasing R_m (square root similar

---

[5] We should note that there is a slight inconsistency in the definition of R_ℓ because $R_\ell \neq \mathrm{Re}\left\{\frac{1}{G_\ell + \frac{1}{\mathrm{j}\omega L_{\ell\mathrm{p}}}}\right\}$ as we would expect it to be according to the definitions in (2.7) and (2.13).

to those of $C_{2\mathrm{tot}}$ in Section 4.3.1.2), R_m has to be higher than[6] or equal to

$$R_{\mathrm{m}L_{\ell\mathrm{p}}} = \frac{R_\ell}{1+\left(\frac{R_\ell}{\omega L_{\ell\mathrm{p}}}\right)^2} \left(= \frac{\mathrm{Re}\left\{\frac{1}{\underline{Z}_\ell}\right\}}{\left|\frac{1}{\underline{Z}_\ell}\right|^2} = \mathrm{Re}\{\underline{Z}_\ell\} \right). \tag{4.14}$$

For AC excitation $\omega > 0$ and $R_{\mathrm{m}L_{\ell\mathrm{p}}} < R_\ell$ holds.

Another additional limit, $R_{\mathrm{m}L_{\mathrm{s}}0}$, may occur because L_s is still an inductance and ≥ 0. In the resistive and capacitive cases, the sum of the square roots in L_s could never be lower than zero, but equal to zero if both square roots would be zero. However, the inductive case involves a difference instead of a sum, thus L_s might be lower than zero, if the absolute value of the first square root is lower than the absolute value of the second square root (then we would have to replace the inductance with a capacitance in order to match). In particular, a valid $R_{\mathrm{m}L_{\mathrm{s}}0}$ might occur only if $R_\ell > R_\mathrm{i} - R_{\mathrm{s}0}$ and if additionally $R_{\mathrm{m}L_{\mathrm{s}}0} > R_{\mathrm{m}L_{\ell\mathrm{p}}}$. Since this result is not needed further, all derivations are performed in Appendix C.1.1.1.

The major difference between resistive/capacitive and inductive cases is the different behaviour with respect to the highest $g_{\pi,\mathrm{inma}}$. Although all estimations performed in Section 3.5.2.2 and Appendix B.2.1.1 apply, we have to use

$$\begin{aligned}
\frac{\partial(\omega L_\mathrm{s})}{\partial R_\mathrm{m}} &= \frac{R_\mathrm{i} - 2\,(R_\mathrm{m}+R_\mathrm{s})}{2\sqrt{(R_\mathrm{m}+R_\mathrm{s})\,(R_\mathrm{i}-R_\mathrm{m}-R_\mathrm{s})}} - \frac{R_\ell - 2\,R_\mathrm{m}}{2\sqrt{R_\mathrm{m}\,(R_\ell - R_\mathrm{m})}}, \\
\frac{\partial(\omega L_\mathrm{s})}{\partial R_\mathrm{s}} &= \frac{R_\mathrm{i} - 2\,(R_\mathrm{m}+R_\mathrm{s})}{2\sqrt{(R_\mathrm{m}+R_\mathrm{s})\,(R_\mathrm{i}-R_\mathrm{m}-R_\mathrm{s})}}
\end{aligned}$$

during replacement of $\frac{\partial(\omega L_\mathrm{s})}{\partial R_\mathrm{m}}$ and $\frac{\partial(\omega L_\mathrm{s})}{\partial R_\mathrm{s}}$ in the final checks for numerator and denominator in the case "at least one $a_n > 0$", yielding a difference of the same two terms instead of a sum compared to the resistive/capacitive case. Since we proved that both terms are ≥ 0 if $0 < b_N \leq 2$, their difference might be positive or negative. Thus the method applied gives no indication for the sign of $\frac{\mathrm{d}g_{\pi,\mathrm{inma}}}{\mathrm{d}R_\mathrm{m}}$.

We could try to reconsider the method used, but would not succeed, because calculation of $g_{\pi,\mathrm{inma}}$ for e. g. a constant Q inductor ($R_\mathrm{s} = \frac{1}{Q}\omega L_\mathrm{s}$) yields a maximum of $g_{\pi,\mathrm{inma}}$ within the valid range of R_m if $R_\ell < R_\mathrm{i}$ ($R_{\mathrm{s}0} = 0$ for $R_\mathrm{s} = \frac{1}{Q}\omega L_\mathrm{s}$). In particular, it is a "real" maximum, where $\frac{\mathrm{d}g_{\pi,\mathrm{inma}}}{\mathrm{d}R_\mathrm{m}} = 0$, and which is not located at one of the range's limits — however, if Q is sufficiently high, it is very close to $R_\mathrm{m} = R_\ell$ and its $g_{\pi,\mathrm{inma}}$ does not differ much from $g_{\pi,\mathrm{inma}}(R_\ell)$. Unfortunately such a maximum's $g_{\pi,\mathrm{inma}}$ and the value of its

[6] But $R_\mathrm{m} < R_\ell$, because $R_\mathrm{m} = R_\ell$ would yield $B_{2\mathrm{tot}} = 0$, which is part of the case addressing (over-)compensation where $C_{2\mathrm{tot}} = 0$. Conversely, $R_\mathrm{m} = R_{\mathrm{m}L_{\ell\mathrm{p}}}$ yields $C_2 = 0$ (undercompensation). However, each of those limits may not be within the valid range of R_m if it is limited further by additional conditions, e. g. by minimum/maximum network element values.

location R_m cannot be computed by using inequalities and estimations. Even worse, the constant Q inductor involves two solutions for $R_\mathrm{s}(R_\mathrm{m})$ if $R_\ell > R_\mathrm{i}$, whose according $\frac{\mathrm{d}g_{\pi,\,\mathrm{inma}}}{\mathrm{d}R_\mathrm{m}}$ exhibit opposite signs and thus no single inequality or estimation would apply.

It's interesting to note that if such a (single) maximum would occur, it would always be higher than the highest $g_{\pi,\,\mathrm{inma}}$ in the case of (over-)compensation, because both cases join at $R_\mathrm{m} = R_\ell$, provided that R_m is not limited further when solving for $R_\mathrm{s}(R_\mathrm{m})$.

Summarising the preceding results we may conclude that obviously the maximum $g_{\pi,\,\mathrm{inma}}$ is yielded if the type of the external network is a π network.

4.3.2.2 T network

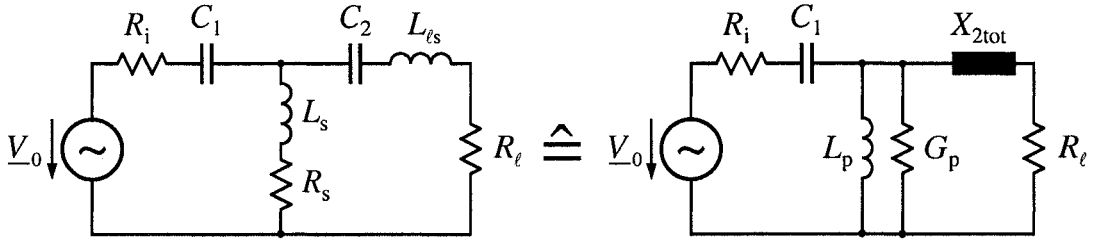

Figure 4.4: Resulting T network's equivalent circuit for matching of a (complex) load impedance consisting of a resistance R_ℓ in series to an inductance $L_{\ell\mathrm{s}}$ to a (real) source resistance R_i

If the load impedance $\underline{Z}_\ell$ exhibits an inductive imaginary part, thus $\mathrm{Im}\{\underline{Z}_\ell\} > 0$, we may describe the load impedance at matching frequency by a resistance R_ℓ in series to an inductance $L_{\ell\mathrm{s}}$, where

$$R_\ell = \mathrm{Re}\{\underline{Z}_\ell\}, \quad (4.15) \qquad L_{\ell\mathrm{s}} = \frac{1}{\omega}\,\mathrm{Im}\{\underline{Z}_\ell\}. \quad (4.16)$$

To achieve matching of the T network's input impedance to the source resistance, two completely different solutions arise.

1. (Over-)Compensation of $L_{\ell\mathrm{s}}$ by C_2, hence $X_{2\mathrm{tot}} \leq 0$ in Figure 4.4 and thus may be described by a capacitance $C_{2\mathrm{tot}}$ at matching frequency.

   Similar to Section 4.3.1.2 $C_{2\mathrm{tot}}$ is given by (3.31). For the remaining capacitance C_2 of the T network we obtain

   $$C_2 = \frac{1}{\omega^2 L_{\ell\mathrm{s}} + \frac{1}{C_{2\mathrm{tot}}}} = \frac{1}{\omega\left(\omega L_{\ell\mathrm{s}} + \frac{1}{G_\ell}\sqrt{\frac{G_\ell - G_\mathrm{m}}{G_\mathrm{m}}}\right)}. \quad (4.17)$$

   C_2 is a variable capacitance and thus ≥ 0, but additionally $C_2 \leq \frac{1}{\omega^2 L_{\ell\mathrm{s}}}$ holds. If the reactance of C_2 cancels the reactance of $L_{\ell\mathrm{s}}$, $X_{2\mathrm{tot}}$ may be zero and

$C_{2\mathrm{tot}}$ may tend to infinity — just equivalent to the case of a purely resistive load with exception of the value of $\frac{1}{C_2}$, which is shifted by $\omega^2 L_{\ell\mathrm{s}}$. All results obtained in Sections 3.5.3.1 and 3.5.3.2 are applicable, but we have to put $G_\mathrm{i} = \frac{1}{R_\mathrm{i}}$, $G_\ell = \frac{1}{R_\ell}$, and replace C_2 with $C_{2\mathrm{tot}}$ in all formulae derived[7]. However, compared to Section 4.3.1.2, there is no additional limit to G_m, but a maximum value of C_2 given by $\frac{1}{\omega^2 L_{\ell\mathrm{s}}}$.

Similar to Section 3.5.3.2, $g_{\mathrm{t,\,inma}}$ increases (or might stay constant) with increasing G_m. Thus the highest valid G_m yields the maximum $g_{\mathrm{t,\,inma}}$, hence $G_\mathrm{m} = G_\ell$ if $G_\ell \leq G_\mathrm{i}$ or $G_\mathrm{m} = G_\mathrm{mlim}$ if $G_\ell > G_\mathrm{i}$, respectively. For $G_\mathrm{m} = G_\ell$ the resulting type of the **external** matching network is a T network, whose capacitance C_2 cancels $L_{\ell\mathrm{s}}$ at matching frequency, hence T network and $L_{\ell\mathrm{s}}$ build up a L network. For $G_\mathrm{m} = G_\mathrm{mlim}$, $C_1 \to \infty$ holds, and the resulting type of the **external** matching network is a L network[4].

We already might assume that the case of (over-)compensation does not guarantee the lowest losses, because the equivalent circuit's lossless load inductance is "wasted" by (over-)compensation and all inductance needed for matching has to be supplied by the lossy inductor of the matching network.

2. Undercompensation of $L_{\ell\mathrm{s}}$ by C_2, hence $X_{2\mathrm{tot}} > 0$ in Figure 4.4 and thus may be described by an inductance $L_{2\mathrm{tot}}$ at matching frequency.

   According to (3.31) and the notes regarding the signs in parentheses/square brackets we obtain

$$L_{2\mathrm{tot}} = L_{\ell\mathrm{s}} - \frac{1}{\omega^2 C_2} = \frac{1}{\omega G_\ell}\sqrt{\frac{G_\ell - G_\mathrm{m}}{G_\mathrm{m}}}.$$

   The remaining capacitance C_2 of the T network is then given by

$$C_2 = \frac{1}{\omega\left(\omega L_{\ell\mathrm{s}} - \frac{1}{G_\ell}\sqrt{\frac{G_\ell - G_\mathrm{m}}{G_\mathrm{m}}}\right)}. \tag{4.18}$$

   As before, we have to put $G_\mathrm{i} = \frac{1}{R_\mathrm{i}}$ and $G_\ell = \frac{1}{R_\ell}$ in all equations derived[7].

   Additionally, according to (3.32) and the notes regarding the signs in parentheses/square brackets we obtain for the inductance L_p of the T network

$$L_\mathrm{p} = \frac{1}{\omega\left(\sqrt{(G_\mathrm{m} + G_\mathrm{p})(G_\mathrm{i} - G_\mathrm{m} - G_\mathrm{p})} - \sqrt{G_\mathrm{m}(G_\ell - G_\mathrm{m})}\right)}. \tag{4.19}$$

   The preceding changes of the equivalent network's elements also involve changes of the limits of parameter G_m.

   One additional limit occurs because C_2 is still a capacitance and ≥ 0. Thus $L_{2\mathrm{tot}} \leq L_{\ell\mathrm{s}}$ holds. Since $L_{2\mathrm{tot}}$ decreases with increasing G_m (square root similar

[7] We should note that there is a slight inconsistency in the definition of G_ℓ because $G_\ell \neq \mathrm{Re}\left\{\frac{1}{R_\ell + \mathrm{j}\omega L_{\ell\mathrm{s}}}\right\}$ as we would expect it to be according to the definitions in (2.13) and (2.7).

to those of $C_{2\mathrm{tot}}$ in Section 4.3.1.1), G_m has to be higher than[8] or equal to

$$G_{\mathrm{m}L_{\ell\mathrm{s}}} = \frac{G_\ell}{1+(\omega L_{\ell\mathrm{s}} G_\ell)^2} \left(= \frac{\mathrm{Re}\{\underline{Z}_\ell\}}{|\underline{Z}_\ell|^2} = \mathrm{Re}\left\{\frac{1}{\underline{Z}_\ell}\right\}\right). \tag{4.20}$$

For AC excitation $\omega > 0$ and $G_{\mathrm{m}L_{\ell\mathrm{s}}} < G_\ell$ holds.

Another additional limit, $G_{\mathrm{m}1/L_\mathrm{p}0}$, may occur because L_p is still an inductance and ≥ 0, hence $\frac{1}{L_\mathrm{p}} \geq 0$. In the resistive and capacitive cases, the sum of the square roots in $\frac{1}{L_\mathrm{p}}$ could never be lower than zero, but equal to zero if both square roots would be zero. However, the inductive case involves a difference instead of a sum, thus $\frac{1}{L_\mathrm{p}}$ or L_p might be lower than zero, if the absolute value of the first square root is lower than the absolute value of the second square root (then we would have to replace the inductance with a capacitance in order to match). In particular, if $R_{\mathrm{s}0} \leq R_\mathrm{i}$, as it would be for the usual $R_\mathrm{i} = 50\,\Omega$, due to (3.33) no valid $G_{\mathrm{m}1/L_\mathrm{p}0}$ occurs. Since this result is not needed further, all derivations (including that for $R_{\mathrm{s}0} > R_\mathrm{i}$) are performed in Appendix C.1.1.2.

The major difference between resistive/capacitive and inductive cases is the different behaviour with respect to the highest $g_{\mathrm{t,\,inma}}$. Although all estimations performed in Section 3.5.3.2 and Appendix B.2.2.1 apply, we have to use

$$\begin{aligned}
\frac{\partial(\frac{1}{\omega L_\mathrm{p}})}{\partial G_\mathrm{m}} &= \frac{G_\mathrm{i} - 2\,(G_\mathrm{m}+G_\mathrm{p})}{2\sqrt{(G_\mathrm{m}+G_\mathrm{p})\,(G_\mathrm{i}-G_\mathrm{m}-G_\mathrm{p})}} - \frac{G_\ell - 2\,G_\mathrm{m}}{2\sqrt{G_\mathrm{m}\,(G_\ell - G_\mathrm{m})}}, \\
\frac{\partial(\frac{1}{\omega L_\mathrm{p}})}{\partial G_\mathrm{p}} &= \frac{G_\mathrm{i} - 2\,(G_\mathrm{m}+G_\mathrm{p})}{2\sqrt{(G_\mathrm{m}+G_\mathrm{p})\,(G_\mathrm{i}-G_\mathrm{m}-G_\mathrm{p})}}
\end{aligned}$$

during replacement of $\frac{\partial(\frac{1}{\omega L_\mathrm{p}})}{\partial G_\mathrm{m}}$ and $\frac{\partial(\frac{1}{\omega L_\mathrm{p}})}{\partial G_\mathrm{p}}$ in the final checks for numerator and denominator in the case "at least one $a_n > 0$", yielding a difference of the same two terms instead of a sum compared to the resistive/capacitive case. Since we proved that both terms are ≥ 0 if $0 < b_N \leq 2$ and $Q \geq 1$, their difference might be positive or negative. Thus the method applied gives no indication for the sign of $\frac{\mathrm{d}g_{\mathrm{t,\,inma}}}{\mathrm{d}G_\mathrm{m}}$.

We could try to reconsider the method used, but would not succeed, because calculation of $g_{\mathrm{t,\,inma}}$ for e. g. a constant Q inductor ($R_\mathrm{s} = \frac{1}{Q}\omega L_\mathrm{s}$, hence $G_\mathrm{p} = \frac{1}{Q}\frac{1}{\omega L_\mathrm{p}}$) yields a maximum of $g_{\mathrm{t,\,inma}}$ within the valid range of G_m if $G_\ell < G_\mathrm{i}$. In particular, it is a "real" maximum, where $\frac{\mathrm{d}g_{\mathrm{t,\,inma}}}{\mathrm{d}G_\mathrm{m}} = 0$, and which is not located at one of the range's limits — however, if Q is sufficiently high, it is very close to $G_\mathrm{m} = G_\ell$ and its $g_{\mathrm{t,\,inma}}$ does not differ much from $g_{\mathrm{t,\,inma}}(G_\ell)$. Unfortunately such a maximum's $g_{\mathrm{t,\,inma}}$ and the value of its location G_m cannot be computed

[8] But $G_\mathrm{m} < G_\ell$, because $G_\mathrm{m} = G_\ell$ would yield $X_{2\mathrm{tot}} = 0$, which is part of the case addressing (over-)compensation where $C_{2\mathrm{tot}} \to \infty$. Conversely, $G_\mathrm{m} = G_{\mathrm{m}L_{\ell\mathrm{s}}}$ yields $C_2 \to \infty$ (undercompensation). However, each of those limits may not be within the valid range of G_m if it is limited further by additional conditions, e. g. by minimum/maximum network element values.

by using inequalities and estimations. Even worse, the constant Q inductor involves two solutions for $G_\mathrm{p}(G_\mathrm{m})$ if $G_\ell > G_\mathrm{i}$, whose according $\frac{\mathrm{d}g_{\mathrm{t,\,inma}}}{\mathrm{d}G_\mathrm{m}}$ exhibit opposite signs and thus no single inequality or estimation would apply.

It's interesting to note that if such a (single) maximum would occur, it would always be higher than the highest $g_{\mathrm{t,\,inma}}$ in the case of (over-)compensation, because both cases join at $G_\mathrm{m} = G_\ell$, provided that G_m is not limited further when solving for $G_\mathrm{p}(G_\mathrm{m})$.

Summarising the preceding results we may conclude that obviously the maximum $g_{\mathrm{t,\,inma}}$ is yielded if the type of the external network is a T network.

4.4 Exact analytical solutions for a constant Q central inductor

4.4.1 Explicit analytical solutions, their valid parameter ranges, and important characteristics

4.4.1.1 π network

To derive an optimum matching strategy, it is important to know more about the solutions' behaviour. Since any inductor can be approximated by an inductor with piecewise constant losses as a function of its number of turns, it is advantageous to derive the exact solutions for the case of a constant Q central inductor which is described by (3.1) if $R_{\mathrm{s}0} = 0$, $N = 1$, $a_1 = \frac{1}{Q}$, and $b_1 = 1$. Furthermore, this approach enables comparison with several works which derived approximate solutions for this case (assuming the network's elements to have the values of a lossless network).

Although the exact solution is derived quickly, it's much more complicated to find the range of the parameter R_m where it's valid within.

The exact solution is computed by solving $R_\mathrm{s} = \frac{1}{Q}\omega L_\mathrm{s}$ for L_s, putting it in Equation (3.19), and solving the resulting equation for R_s, yielding two possible solutions for capacitive/resistive/(over-)compensated inductive loads,

$$R_{\mathrm{scap}\mp} = \frac{R_\mathrm{i} - 2\left(R_\mathrm{m} - Q\sqrt{R_\mathrm{m}\left(R_\ell - R_\mathrm{m}\right)}\right) \mp \sqrt{u_\pi}}{2\left(1+Q^2\right)}, \tag{4.21}$$

where

$$u_\pi = 4\left(1+Q^2\right)\left(R_\mathrm{i} - R_\ell\right)R_\mathrm{m} + \left(R_\mathrm{i} - 2\left(R_\mathrm{m} - Q\sqrt{R_\mathrm{m}\left(R_\ell - R_\mathrm{m}\right)}\right)\right)^2,$$

and two possible solutions for undercompensated inductive loads,

$$R_{\mathrm{sind}\mp} = \frac{R_\mathrm{i} - 2\left(R_\mathrm{m} + Q\sqrt{R_\mathrm{m}\left(R_\ell - R_\mathrm{m}\right)}\right) \mp \sqrt{v_\pi}}{2\left(1+Q^2\right)}, \tag{4.22}$$

where

$$v_\pi = 4\left(1+Q^2\right)\left(R_\mathrm{i}-R_\ell\right)R_\mathrm{m} + \left(R_\mathrm{i}-2\left(R_\mathrm{m}+Q\sqrt{R_\mathrm{m}\left(R_\ell-R_\mathrm{m}\right)}\right)\right)^2.$$

Which solution is valid in which range of the parameter R_m?

Searching of those ranges involves a certain search for zeroes of different terms and comparison of the limits found, but only within the utmost limits derived in Section 3.5.2.1 (applying $R_{\mathrm{s}0}=0$ which holds for $R_\mathrm{s}=\frac{1}{Q}\omega L_\mathrm{s}$), hence $0\le R_\mathrm{m}\le \mathrm{Min}\{R_\mathrm{i},R_\ell\}$. It is simple math, but very lengthy and thus may only be sketched here.

- The first step is to check which parameter range yields real solutions, in particular, in which parameter range is $u_\pi \ge 0$ or $v_\pi \ge 0$, respectively.

  By a careful inspection of u_π, v_π it's quite obvious that u_π and v_π are always ≥ 0 if $R_\ell \le R_\mathrm{i}$.

  If $R_\ell > R_\mathrm{i}$, it is somewhat more complicated.

  If $R_\mathrm{i} < R_\ell \le \frac{1}{4}\left(\left(\sqrt{1+Q^2}-Q\right)^2+4\right)R_\mathrm{i}$, $u_\pi > 0$ within the intervals $0\le R_\mathrm{m}\le R_{\mathrm{mu}01}$ and $R_{\mathrm{mu}02}\le R_\mathrm{m}\le R_\mathrm{i}$, where

$$R_{\mathrm{mu}01} = \frac{R_\ell - Q\left(\sqrt{1+Q^2}+Q\right)R_\mathrm{i} - \sqrt{\left(R_\ell-R_\mathrm{i}\right)\left(R_\ell+\left(\sqrt{1+Q^2}+Q\right)^2R_\mathrm{i}\right)}}{2\left(1+Q^2\right)},$$

$$R_{\mathrm{mu}02} = \frac{R_\ell - Q\left(\sqrt{1+Q^2}+Q\right)R_\mathrm{i} + \sqrt{\left(R_\ell-R_\mathrm{i}\right)\left(R_\ell+\left(\sqrt{1+Q^2}+Q\right)^2R_\mathrm{i}\right)}}{2\left(1+Q^2\right)}.$$

  If $R_\ell > \frac{1}{4}\left(\left(\sqrt{1+Q^2}-Q\right)^2+4\right)R_\mathrm{i}$, only the first interval applies.

  If $R_\mathrm{i} < R_\ell \le \frac{1}{4}\left(\left(\sqrt{1+Q^2}+Q\right)^2+4\right)R_\mathrm{i}$, $v_\pi > 0$ within the intervals $0\le R_\mathrm{m}\le R_{\mathrm{mv}01}$ and $R_{\mathrm{mv}02}\le R_\mathrm{m}\le R_\mathrm{i}$, where

$$R_{\mathrm{mv}01} = \frac{R_\ell - Q\left(\sqrt{1+Q^2}-Q\right)R_\mathrm{i} - \sqrt{\left(R_\ell-R_\mathrm{i}\right)\left(R_\ell+\left(\sqrt{1+Q^2}-Q\right)^2R_\mathrm{i}\right)}}{2\left(1+Q^2\right)}, \qquad (4.23)$$

$$R_{\mathrm{mv}02} = \frac{R_\ell - Q\left(\sqrt{1+Q^2}-Q\right)R_\mathrm{i} + \sqrt{\left(R_\ell-R_\mathrm{i}\right)\left(R_\ell+\left(\sqrt{1+Q^2}-Q\right)^2R_\mathrm{i}\right)}}{2\left(1+Q^2\right)}.$$

  If $R_\ell > \frac{1}{4}\left(\left(\sqrt{1+Q^2}+Q\right)^2+4\right)R_\mathrm{i}$, only the first interval applies.

- The second step is to check which parameter range yields positive solutions.

If $R_\ell < R_\mathrm{i}$, $R_\mathrm{scap-}$ is never positive. If $R_\ell = R_\mathrm{i}$, $R_\mathrm{scap-}$ is never positive, too, but $R_\mathrm{scap-}$ is zero if $0 \leq R_\mathrm{m} \leq \frac{\sqrt{1+Q^2}+Q}{2\sqrt{1+Q^2}} R_\mathrm{i}$. If $R_\ell > R_\mathrm{i}$, $R_\mathrm{scap-}$ is positive within $0 \leq R_\mathrm{m} \leq R_\mathrm{mu01}$ only.

If $R_\ell \leq R_\mathrm{i}$, $R_\mathrm{scap+}$ is positive for $0 \leq R_\mathrm{m} \leq R_\ell$. However, if $R_\ell = R_\mathrm{i}$ it should be noted that $R_\mathrm{scap+}$ is zero if $\frac{\sqrt{1+Q^2}+Q}{2\sqrt{1+Q^2}} R_\mathrm{i} \leq R_\mathrm{m} \leq R_\mathrm{i}$. If $R_\ell > R_\mathrm{i}$, $R_\mathrm{scap+}$ is positive within $0 \leq R_\mathrm{m} \leq R_\mathrm{mu01}$ only.

If $R_\ell < R_\mathrm{i}$, $R_\mathrm{sind-}$ is never positive. If $R_\ell = R_\mathrm{i}$, $R_\mathrm{sind-}$ is never positive, too, but $R_\mathrm{sind-}$ is zero for $0 \leq R_\mathrm{m} \leq R_\mathrm{mv01}$. If $R_\ell > R_\mathrm{i}$, $R_\mathrm{sind-}$ is positive within $0 \leq R_\mathrm{m} \leq R_\mathrm{mv01}$ only.

If $R_\ell < R_\mathrm{i}$, $R_\mathrm{sind+}$ is positive for $0 \leq R_\mathrm{m} \leq R_\ell$. If $R_\ell = R_\mathrm{i}$, $R_\mathrm{sind+}$ is positive for $0 \leq R_\mathrm{m} \leq R_\mathrm{mv01}$ and zero for $R_\mathrm{mv01} \leq R_\mathrm{m} \leq R_\mathrm{i}$. If $R_\ell > R_\mathrm{i}$, $R_\mathrm{sind+}$ is positive within $0 \leq R_\mathrm{m} \leq R_\mathrm{mv01}$ only.

- The third step is to check in which parameter range the solutions are valid with respect to the equation which was solved for. This is performed by putting each solution in Equation (3.19) and checking in which parameter range the resulting $\frac{1}{Q}\,\omega L_\mathrm{s}$ is equal to the solution itself.

  In those cases where the solutions are zero throughout an interval of the parameter R_m, which always involve $R_\ell = R_\mathrm{i}$, it is quite obvious from Equation (3.19) that a zero inductance, hence a valid capacitive solution can only be obtained for $R_\mathrm{m} = R_\mathrm{i}$, whereas a valid inductive solution exists throughout that interval.

  In the remaining cases it is possible to rewrite $(R_\mathrm{m} + R_\mathrm{s})\,(R_\mathrm{i} - R_\mathrm{m} - R_\mathrm{s})$ as $(\ldots)^2$. If $(\ldots) \leq 0$, $\sqrt{(\ldots)^2} = -(\ldots)$, if $(\ldots) \geq 0$, $\sqrt{(\ldots)^2} = (\ldots)$. However, for each of the four possible solutions, only one sign yields a valid solution. Hence the parameter's interval(s) in conjunction with the intervals found in the previous steps limit the applicable range of each solution. The results of the check combined with the limits derived previously are given below:

  $R_\mathrm{scap-}$ is never a valid solution.

  If $0 < R_\ell \leq R_{\ell\mathrm{limofRmlim}}$, where

$$R_{\ell\mathrm{limofRmlim}} = 2\,Q\,(\sqrt{1+Q^2} - Q)\,R_\mathrm{i}, \tag{4.24}$$

  $R_\mathrm{scap+}$ is a valid solution for $0 \leq R_\mathrm{m} \leq R_\ell$. If $R_{\ell\mathrm{limofRmlim}} < R_\ell \leq R_\mathrm{i}$, $R_\mathrm{scap+}$ is a valid solution for $0 \leq R_\mathrm{m} \leq R_\mathrm{mlim1}$ and $R_\mathrm{mlim2} \leq R_\mathrm{m} \leq R_\ell$, where

$$R_\mathrm{mlim1} = \frac{R_\ell + 2Q^2R_\mathrm{i} - \sqrt{R_\ell^2 + 4Q^2R_\mathrm{i}(R_\ell - R_\mathrm{i})}}{2\,(1+Q^2)}, \tag{4.25}$$

$$R_\mathrm{mlim2} = \frac{R_\ell + 2Q^2R_\mathrm{i} + \sqrt{R_\ell^2 + 4Q^2R_\mathrm{i}(R_\ell - R_\mathrm{i})}}{2\,(1+Q^2)}. \tag{4.26}$$

If $R_\ell = R_\mathrm{i}$, $R_\mathrm{mlim1} < \frac{\sqrt{1+Q^2}+Q}{2\sqrt{1+Q^2}} R_\mathrm{i}$, hence $R_\mathrm{scap+}$ is positive throughout the first interval, and the second interval contracts to a single dot at $R_\mathrm{m} = R_\mathrm{mlim2} = R_\mathrm{i}$. If $R_\ell > R_\mathrm{i}$, $R_\mathrm{mlim1} < R_\mathrm{mu01}$ and $R_\mathrm{scap+}$ is a valid solution for $0 \le R_\mathrm{m} \le R_\mathrm{mlim1}$ only.

If $R_\ell \ge R_\mathrm{i}$, $R_\mathrm{sind-}$ is a valid solution for $0 \le R_\mathrm{m} \le R_\mathrm{mv01}$.

If $0 < R_\ell \le R_\mathrm{i}$, $R_\mathrm{sind+}$ is a valid solution for $0 \le R_\mathrm{m} \le R_\ell$. If $R_\ell > R_\mathrm{i}$, $R_\mathrm{sind+}$ is a valid solution for $0 \le R_\mathrm{m} \le R_\mathrm{mv01}$.

It should be noted that the intervals with $R_\mathrm{sind\pm} = 0$ in the case of $R_\ell = R_\mathrm{i}$ simply describe a parallel resonance of C_1 and L_2tot.

Within their valid parameter ranges, the network element values could be calculated using (3.17), (3.19), and (3.18). However, it is much easier to use the defining equation of a constant Q inductor,

$$L_\mathrm{s} = \frac{Q}{\omega} R_\mathrm{s}, \tag{4.27}$$

to compute L_s, and to solve (3.19) for $\sqrt{(R_\mathrm{m}+R_\mathrm{s})(R_\mathrm{i}-R_\mathrm{m}-R_\mathrm{s})}$, to put the solution in (3.17), and to apply (4.27), yielding

$$C_1 = \frac{1}{\omega R_\mathrm{i}} \frac{QR_\mathrm{s} \mp \sqrt{R_\mathrm{m}(R_\ell - R_\mathrm{m})}}{R_\mathrm{m}+R_\mathrm{s}} \tag{4.28}$$

to compute C_1. (The minus sign in the numerator applies to $R_\mathrm{scap+}$, the plus sign to $R_\mathrm{sind-}$ and $R_\mathrm{sind+}$.) Then, as usual, C_2 is computed from (3.18).

The power gain of the π network matched to R_i at its input is easily calculated by (3.24).

Finally, the answers to two important questions regarding the π network are given.

What is the physical meaning of the (applicable) limits derived above?

If $R_\ell \le R_{\ell\mathrm{limofRmlim}}$, C_1 of $R_\mathrm{scap+}$ has a minimum, whose value decreases with increasing R_ℓ until it is zero at $R_\ell = R_{\ell\mathrm{limofRmlim}}$. For higher R_ℓ, it decreases further to negative values. Thus one limit to the left (R_mlim1) and one limit to the right (R_mlim2) exists where $C_1 = 0$ until the right limit reaches its maximum valid value of $R_\mathrm{mlim2} = R_\ell = R_\mathrm{i}$ at $R_\ell = R_\mathrm{i}$. If $R_\ell > R_\mathrm{i}$, only the left limit (R_mlim1) falls within the (utmost) valid range of R_m. (Decreasing of R_mlim1 and increasing of R_mlim2 with increasing R_ℓ will be derived in Section 4.4.2.)

If $R_\ell \ge R_\mathrm{i}$, two inductive solutions exist. At R_mv01, the upper limit of the valid interval of R_m, both inductive solutions join.

Furthermore, if $R_\ell \le R_\mathrm{i}$, $R_\mathrm{scap+}$ and $R_\mathrm{sind+}$ join at $R_\mathrm{m} = R_\ell$, where $C_\mathrm{2tot} = 0$ or $L_\mathrm{2tot} \to \infty$. They would also join at $R_\mathrm{m} = 0$, but due to minimum/maximum

element values and finite load susceptance it is outside the parameter's valid range in practice.

Minimum and solution joining may be observed in the example diagrams depicted in Section 4.4.3.1.

How does the power gain of the matched π network depend on R_m for the different (valid) solutions?

Since the case of a constant Q factor inductor is included in the loss model (3.1) and the conditions of the proof in Section 3.5.2.2 apply, $\frac{\mathrm{d}g_{\pi,\mathrm{inma}}}{\mathrm{d}R_\mathrm{m}} \geq 0$ for $R_{\mathrm{scap}+}$ throughout its valid range of R_m.

For the two inductive solutions, $\frac{\mathrm{d}g_{\pi,\mathrm{inma}}}{\mathrm{d}R_\mathrm{m}}$ has to be computed, numerator and denominator checked for zeroes, and the derivative's sign checked to the right and left of those zeroes. This procedure is quite lengthy and thus only its results are given.

If $R_\ell < R_\mathrm{i}$, there exists a maximum of $\frac{\mathrm{d}g_{\pi,\mathrm{inma}}}{\mathrm{d}R_\mathrm{m}}$ for $R_{\mathrm{sind}+}$ at

$$R_{\mathrm{mgmaxind}+} = \frac{R_\ell \left(R_\ell + (1+2Q^2)\, R_\mathrm{i} + \sqrt{(R_\ell + R_\mathrm{i})^2 + 4Q^2 R_\ell R_\mathrm{i}} \right)}{2\,(1+Q^2)\,(R_\ell + R_\mathrm{i})}, \tag{4.29}$$

where the according power gain's maximum value is given by

$$g_{\pi,\mathrm{inma,maxind}+} = \frac{R_\ell \left(R_\ell + (1+2Q^2)\, R_\mathrm{i} + \sqrt{(R_\ell + R_\mathrm{i})^2 + 4Q^2 R_\ell R_\mathrm{i}} \right)}{R_\mathrm{i} \left(R_\mathrm{i} + (1+2Q^2)\, R_\ell + \sqrt{(R_\ell + R_\mathrm{i})^2 + 4Q^2 R_\ell R_\mathrm{i}} \right)}. \tag{4.30}$$

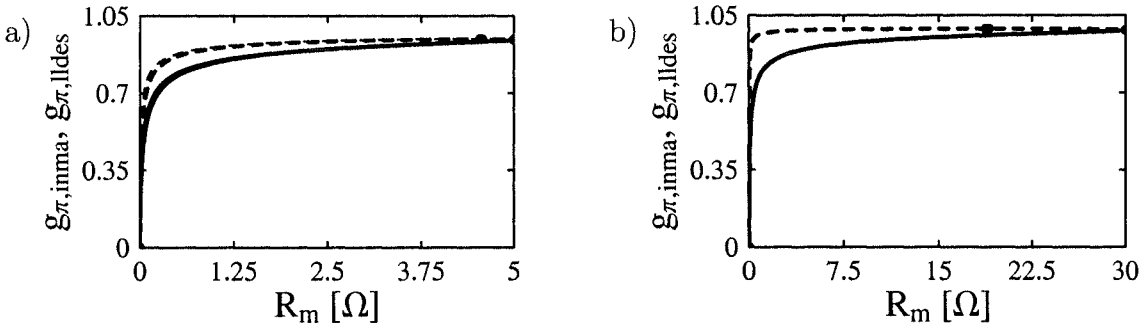

Figure 4.5: Power gain $g_{\pi,\mathrm{llde}}$ of a lossy π network designed as if it would be lossless (thin lines) and $g_{\pi,\mathrm{inma}}$ of a lossy π network exactly matched at its input (thick lines), capacitive (solid) and inductive (dashed) — employing $R_{\mathrm{sind}+}$ for the exactly matched network — solutions at 7.35 MHz, $R_\mathrm{i} = 50\,\Omega$, $Q = 50$, and a) $R_\ell = 5\,\Omega$, b) $R_\ell = 30\,\Omega$

The closer R_ℓ to R_i or the higher Q, the flatter the maximum will be (approximately). Those dependencies are quite obvious when comparing Figure 4.5 and Figure 4.15. Furthermore, the maximum is compared to the highest power gain of the capacitive solution in the last paragraph of Section 4.4.2.

If $R_\ell = R_\mathrm{i}$, $g_{\pi,\mathrm{inma}} = 1 = \mathrm{const.}$ for $R_{\mathrm{sind}-}$ if $0 \leq R_\mathrm{m} \leq R_{\mathrm{mv01}}$ and for $R_{\mathrm{sind}+}$ if $R_{\mathrm{mv01}} \leq R_\mathrm{m} \leq R_\mathrm{i}$ (pure parallel resonance of C_1 and $L_{2\mathrm{tot}}$). If $0 \leq R_\mathrm{m} \leq R_{\mathrm{mv01}}$, $\frac{\mathrm{d}g_{\pi,\mathrm{inma}}}{\mathrm{d}R_\mathrm{m}} > 0$ for $R_{\mathrm{sind}+}$.

If $R_\ell > R_\mathrm{i}$, $\frac{\mathrm{d}g_{\pi,\mathrm{inma}}}{\mathrm{d}R_\mathrm{m}} < 0$ for $R_{\mathrm{sind}-}$ and $\frac{\mathrm{d}g_{\pi,\mathrm{inma}}}{\mathrm{d}R_\mathrm{m}} > 0$ for $R_{\mathrm{sind}+}$ throughout its valid range of R_m.

The behaviour of $g_{\pi,\mathrm{inma}}$ in the different cases may be observed in the example diagrams depicted in Section 4.4.3.1.

4.4.1.2 T network

Since the case of a constant Q central inductor is one of the rare cases mentioned in Footnote [7] (at the end of Section 3.5.3.1), where π and T network are exactly equivalent, the solutions for G_p of the T network may easily be derived from those for R_s of the π network by replacing R_m, R_i, R_ℓ, u_π, and v_π with G_m, G_i, G_ℓ, u_t, and v_t, respectively.

In a similar manner, G_{mu01}, G_{mu02}, G_{mv01}, G_{mv02}, $G_{\ell\mathrm{limofGmlim}}$, G_{mlim1}, and G_{mlim2} are derived. The solution's valid ranges are similar to those of the π network if the previously derived limits are used instead.

However, the intervals with $G_{\mathrm{pind}\pm} = 0$ in the case of $G_\ell = G_\mathrm{i}$ now describe a series resonance of C_1 and $L_{2\mathrm{tot}}$.

Furthermore, there are two more network element values which may be interesting. As with the π network, (3.30), (3.32), and (3.31) could be used to calculate the network element values, but the defining equation of a constant Q inductor,

$$L_\mathrm{p} = \frac{1}{\omega Q}\frac{1}{G_\mathrm{p}}, \tag{4.31}$$

is more convenient to compute L_p. However, the inductor model (3.1) describes a loss resistance R_s as a function of an inductor L_s in series. Thus their values are interesting, too. Applying (4.31) to (A.19) and (A.20) yields

$$R_\mathrm{s} = \frac{1}{1+Q^2}\frac{1}{G_\mathrm{p}}, \tag{4.32}$$

$$L_\mathrm{s} = \frac{Q}{\omega\,(1+Q^2)}\frac{1}{G_\mathrm{p}}. \tag{4.33}$$

Solving (3.32) for $\sqrt{(G_\mathrm{m}+G_\mathrm{p})(G_\mathrm{i}-G_\mathrm{m}-G_\mathrm{p})}$, putting the solution in (3.30), and applying (4.31) gives

$$C_1 = \frac{G_\mathrm{i}}{\omega}\frac{G_\mathrm{m}+G_\mathrm{p}}{QG_\mathrm{p} \mp \sqrt{G_\mathrm{m}(G_\ell - G_\mathrm{m})}} \tag{4.34}$$

to compute C_1. (The minus sign in the denominator applies to $G_{\mathrm{pcap}+}$, the plus sign to $G_{\mathrm{pind}-}$ and $G_{\mathrm{pind}+}$.) Then, as usual, C_2 is computed from (3.31).

C_1, L_p, and C_2 may also be derived from the π network's element values C_1, L_s, and C_2 if they are inverted (except ω) and R_m, R_i, and R_ℓ are replaced with G_m, G_i, and G_ℓ, respectively.

The power gain of the T network matched to G_i at its input is easily calculated by (3.37).

Finally, the answers to two important questions regarding the T network are given.

What is the physical meaning of the (applicable) limits derived above?

If $G_\ell \leq G_{\ell\text{limofGmlim}}$, C_1 of $G_{\text{pcap+}}$ has a maximum, whose value increases with increasing G_ℓ until it is a pole at $G_\ell = G_{\ell\text{limofGmlim}}$. For higher G_ℓ, two poles occur with sign changes (the inverse of the maximum decreases further to negative values). Thus one limit to the left (G_{mlim1}) and one limit to the right (G_{mlim2}) exists where $C_1 \to \infty$ until the right limit reaches its maximum valid value of $G_{\text{mlim2}} = G_\ell = G_\text{i}$ at $G_\ell = G_\text{i}$. If $G_\ell > G_\text{i}$, only the left limit (G_{mlim1}) falls within the (utmost) valid range of G_m. (Decreasing of G_{mlim1} and increasing of G_{mlim2} with increasing G_ℓ will be derived in Section 4.4.2.)

If $G_\ell \geq G_\text{i}$, two inductive solutions exist. At G_{mv01}, the upper limit of the valid interval of G_m, both inductive solutions join.

Furthermore, if $G_\ell \leq G_\text{i}$, $G_{\text{pcap+}}$ and $G_{\text{pind+}}$ join at $G_\text{m} = G_\ell$, where $C_{2\text{tot}} \to \infty$ or $L_{2\text{tot}} = 0$. They would also join at $G_\text{m} = 0$, but due to minimum/maximum element values and finite load reactance it is outside the parameter's valid range in practice.

How does the power gain of the matched T network depend on G_m for the different (valid) solutions?

Due to the exact equivalence of π and T networks in the case of a constant Q factor inductor, the results derived for the π network apply if $R_{\text{scap+}}$, $R_{\text{sind-}}$, $R_{\text{sind+}}$, $g_{\pi,\text{inma}}$, $R_{\text{mgmaxind+}}$, $g_{\pi,\text{inma,maxind+}}$, R_m, R_i, and R_ℓ are replaced with $G_{\text{pcap+}}$, $G_{\text{pind-}}$, $G_{\text{pind+}}$, $g_{\text{t,inma}}$, $G_{\text{mgmaxind+}}$, $g_{\text{t,inma,maxind+}}$, G_m, G_i, and G_ℓ, respectively.

However, there is a slight difference between π and T network. In the case of $G_\ell = G_\text{i}$, $g_{\text{t,inma}} = 1 = \text{const.}$ for $G_{\text{pind-}}$ if $0 \leq G_\text{m} \leq G_{\text{mv01}}$ and for $G_{\text{pind+}}$ if $G_{\text{mv01}} \leq G_\text{m} \leq G_\text{i}$ as with the π network, but a pure series resonance of C_1 and $L_{2\text{tot}}$ occurs instead of the parallel resonance with the π network.

4.4.2 Dependency of the valid intervals' limits on Q and R_ℓ or G_ℓ

To understand the practical importance of the valid intervals' limits derived above their dependency on Q and R_ℓ or G_ℓ has to be investigated. This simply involves calculation of their derivatives with respect to Q and R_ℓ or G_ℓ and checking the sign of those derivatives. Since π and T network are exactly equivalent here, only the π network derivatives are calculated in the following paragraphs, but the results are given for both types of networks.

$$\frac{\partial R_{\ell\text{limofRmlim}}}{\partial Q} = \frac{2\left(\sqrt{1+Q^2}-Q\right)^2}{\sqrt{1+Q^2}}\,R_\text{i}$$

$R_{\ell\text{limofRmlim}}$ or $G_{\ell\text{limofGmlim}}$ increases with increasing Q and tends to R_i or G_i for $Q \to \infty$. (They do not depend on R_ℓ or G_ℓ.)

$$\frac{\partial R_{\text{mlim1,2}}}{\partial Q} = \pm \frac{Q\left(2R_\text{i} - R_\ell \pm \sqrt{R_\ell^2 + 4Q^2R_\text{i}(R_\ell - R_\text{i})}\right)^2}{2\,(1+Q^2)^2\sqrt{R_\ell^2 + 4Q^2R_\text{i}(R_\ell - R_\text{i})}}$$

R_{mlim1} or G_{mlim1} increases with increasing Q, whereas R_{mlim2} decreases with increasing Q. Both tend to R_i or G_i for $Q \to \infty$. (Note that the range of R_ℓ or G_ℓ where those limits exist decreases with increasing Q since $R_{\ell\text{limofRmlim}}$ or $G_{\ell\text{limofGmlim}}$ increases. To compare the limits for increasing Q, R_ℓ or G_ℓ has to be chosen high enough to be valid for those Q.)

$$\frac{\partial R_{\text{mlim1,2}}}{\partial R_\ell} = \mp \frac{R_{\text{mlim1,2}}}{\sqrt{R_\ell^2 + 4Q^2R_\text{i}(R_\ell - R_\text{i})}}$$

R_{mlim1} or G_{mlim1} decreases with increasing R_ℓ or G_ℓ, whereas R_{mlim2} or G_{mlim2} increases with increasing R_ℓ or G_ℓ. Hence R_{mlim2} or G_{mlim2} are valid only till $R_\ell = R_\text{i}$ or $G_\ell = G_\text{i}$, where the highest possible $R_{\text{mlim2}} = R_\text{i}$ or $G_{\text{mlim2}} = G_\text{i}$ is obtained.

Since $\frac{\partial R_{\text{mv01}}}{\partial Q}$ itself and the following the sign check is quite lengthy, only the results are given here. R_{mv01} or G_{mv01} decreases with increasing Q. It tends to zero for $Q \to \infty$.

$$\frac{\partial R_{\text{mv01}}}{\partial R_\ell} = -\frac{R_{\text{mv01}}}{\sqrt{(R_\ell - R_\text{i})\left(R_\ell + (\sqrt{1+Q^2} - Q)^2\,R_\text{i}\right)}}$$

R_{mv01} or G_{mv01} decreases with increasing R_ℓ ($\geq R_\text{i}$) or G_ℓ ($\geq G_\text{i}$). Thus its highest value is given by

$$R_{\text{mv01}}(R_\ell = R_\text{i}) = \frac{\sqrt{1+Q^2}+Q}{2\sqrt{1+Q^2}}\,R_\text{i} \tag{4.35}$$

or

$$G_{\text{mv01}}(G_\ell = G_\text{i}) = \frac{\sqrt{1+Q^2}+Q}{2\sqrt{1+Q^2}}\,G_\text{i}. \tag{4.36}$$

For those limits to be valid, $L_{\ell\text{p}} \leq \frac{R_\text{i}}{\omega\left(\sqrt{1+Q^2}+Q\right)}$ must hold with the π network and $L_{\ell\text{s}} \geq \frac{\sqrt{1+Q^2}+Q}{\omega G_\text{i}}$ with the T network, respectively.

To understand whether those limits are observed in practice additionally the according values of the network's central inductor L_s have to be considered.

In a π network, it is obvious from (4.27) and (4.22) that L_{sind+}, the central inductance of the inductive solution employing R_{sind+}, is always greater than that of the solution employing R_{sind-}, except at $R_m = R_{mv01}$, where both solutions join. The highest L_{sind+} is $L_{sind+}(R_m = 0) = \frac{QR_i}{(1+Q^2)\omega}$ (to prove this simply compute $\frac{L_{sind+}(R_m)}{L_{sind+}(0)}$), although $R_m = 0$ is never reached if realistic loads and element values are considered. For useful Q factors of $Q \geq 1$, $L_{sind+}(0)$ decreases with increasing Q and ω.

Similarily, in a T network, the lowest L_{pind+} is $L_{pind+}(G_m = 0) = \frac{1+Q^2}{Q\omega G_i}$, which increases with increasing Q for useful Q factors of $Q \geq 1$ and decreases with increasing ω (to fit the inductor's series model, the parallel inductance needs to be transformed in a series inductance $L_{sind+}(G_m = 0) = \frac{Q}{\omega G_i}$, but both differ only slightly for sufficiently high Q factors).

Knowing the dependencies given above, which limits are likely to be observed in practice?

If $R_\ell \leq R_i$ or $G_\ell \leq G_i$, even for a quite low $Q = 5$, $R_{\ell limofRmlim} \approx 0.99\,R_i$ or $G_{\ell limofGmlim} \approx 0.99\,G_i$, yielding valid $R_{mlim1,2}$ for $0.99\,R_i \leq R_\ell \leq R_i$ or valid $G_{mlim1,2}$ for $0.99\,G_i \leq G_\ell \leq G_i$. Loads that close to the source resistance or admittance would not require matching, except for a compensation of their susceptance or reactance in case of a complex load. For higher Q, $R_{\ell limofRmlim}$ or $G_{\ell limofGmlim}$ are even closer to R_i or G_i. Thus, for the majority of such loads, $R_{mlim1,2}$ or $G_{mlim1,2}$ do not occur. However, if $R_\ell \geq R_i$ or $G_\ell \geq G_i$, in principle R_{mlim1} or G_{mlim1} are valid, but since C_1 is zero (π network) or tends to infinity (T network) at that limit, minimum or maximum element values provide tighter limits to R_m or G_m.

Regarding R_{mv01} or G_{mv01}, it is very unlikely to observe those limits in practice, too. In a π network, $L_{sind+} < 100\,\text{nH}$ for $Q > 44.2$ and $0 \leq R_m \leq R_{mv01}$ at 1.8 MHz — inductances that low may not be realised by an ordinary variable inductor, but only by a variable capacitor in series to a fixed inductor (Figure 3.12 a)), which is disadvantageous with respect to its losses (although the losses may be reduced by using a switchable tapped inductor as proposed in [3]). In a T network, L_{pind+} of the equivalent region may be within the range of variable inductors at high frequencies, e. g. $L_{pind+} > 26.5\,\mu\text{H}$ for $Q = 100$ and $0 \leq G_m \leq G_{mv01}$ at 30 MHz, but moving the lower limit of the valid parameter range below G_{mv01} would require such high series inductances of the load, e. g. $L_{\ell s} > 53.1\,\mu\text{H}$ for $Q = 100$ at 30 MHz, that even a parasitic parallel capacitance of 1 pF would overcompensate those $L_{\ell s}$, yielding for sure an effective series capacitance of that load.

Besides the intervals' limits, it's also interesting to compare the inductive maximum obtained for $R_\ell < R_\mathrm{i}$ or $G_\ell < G_\mathrm{i}$ to highest power gain of the capacitive solution at $R_\mathrm{m} = R_\ell$ or $G_\mathrm{m} = G_\ell$, where capacitive and inductive solutions join and the inductive load is fully compensated.

Computing $\frac{\partial\left(\frac{g_{\pi,\mathrm{inma,maxind+}}}{g_{\pi,\mathrm{inma,ind+}(R_\mathrm{m}=R_\ell)}}\right)}{\partial R_\ell}$ or $\frac{\partial\left(\frac{g_{\mathrm{t,inma,maxind+}}}{g_{\mathrm{t,inma,ind+}(G_\mathrm{m}=G_\ell)}}\right)}{\partial R_\ell}$ yields a maximum ratio of

$$\left.\frac{g_{\pi,\mathrm{inma,maxind+}}}{g_{\pi,\mathrm{inma,ind+}(R_\mathrm{m}=R_\ell)}}\right|_\mathrm{max} = \frac{\left(1+\sqrt{5}+4Q^2+\sqrt{2\left(3+\sqrt{5}+4\left(\sqrt{5}-1\right)Q^2\right)}\right)\left(1+\left(\sqrt{5}-1\right)Q^2+\sqrt{1+4\left(\sqrt{5}-2\right)Q^2}\right)}{2\left(1+Q^2\right)\left(1+\sqrt{5}+2\left(\sqrt{5}-1\right)Q^2+\sqrt{2\left(3+\sqrt{5}+4\left(\sqrt{5}-1\right)Q^2\right)}\right)}$$

at $R_\ell = \frac{\sqrt{5}-1}{2} R_\mathrm{i} \approx 0.618\, R_\mathrm{i}$ or a similar maximum ratio of $\left.\frac{g_{\mathrm{t,inma,maxind+}}}{g_{\mathrm{t,inma,ind+}(G_\mathrm{m}=G_\ell)}}\right|_\mathrm{max}$ at $G_\ell = \frac{\sqrt{5}-1}{2} G_\mathrm{i} \approx 0.618\, G_\mathrm{i} \approx \frac{1}{1.618\, R_\mathrm{i}}$, respectively[9].

The maximum ratio itself has a maximum value of approximately 1.059 at $Q \approx 2.058$ and quickly approaches 1 for (lower or) higher Q factors. In particular, the maximum ratio is about 1.026 at $Q = 10$, 1.014 at $Q = 20$, 1.006 at $Q = 50$, and 1.003 at $Q = 100$. Thus fully compensating an inductive load does not significantly reduce the power gain compared to the inductive maximum provided the matching network's variable inductor's Q factor is sufficiently high.

4.4.3 Example diagrams

4.4.3.1 Solutions of a π network including comparison to the approximate ones

To gain more insight in the solutions' behaviour, important characteristics of the lossy π network matched exactly at its input are illustrated below in appropriate diagrams. Additionally, the diagrams include the solutions of a lossy π network designed as if it would be lossless, which are quite common in literature — its network elements may be obtained by putting $R_\mathrm{s} = 0$ in (3.17), (3.19), and (3.18). Then R_s is given by the definition of a constant Q factor inductor, $R_\mathrm{s} = \frac{1}{Q}\omega L_\mathrm{s}$. Finally, the formula of its power gain is similar to (3.24), but of course with the previously calculated R_s being put in. It should be noted that there is only one inductive solution if $R_\ell \leq R_\mathrm{i}$, whereas there is no valid inductive solution if $R_\ell > R_\mathrm{i}$.

[9]The derivative of the ratio given is best suited to derive the extremum due to its numerator's simplicity, whereas e. g. the derivative of the inverse ratio is much more complicated.

The π network was chosen as an example because it exhibits zeroes instead of poles for different network element values, thus the diagrams are easier to understand. The relatively low $Q = 5$ ensures better visibility of the exact solutions' different "special" characteristics.

At first C_1 is considered.

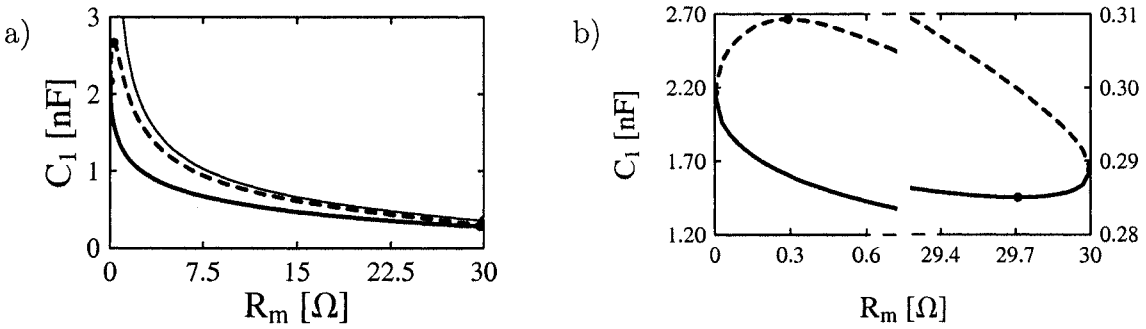

Figure 4.6: C_1 of a lossy π network designed as if it would be lossless (thin lines) and of a lossy π network exactly matched at its input (thick lines), capacitive (solid) and inductive (dashed) — employing $R_{\text{sind+}}$ for the exactly matched network — solutions, a) full range, b) details at 7.35 MHz, $R_\text{i} = 50\,\Omega$, $Q = 5$, and $R_\ell = 30\,\Omega$

If $R_\ell \leq R_\text{i}$, C_1 of the lossy π network designed as if it would be lossless is similar for the capacitive and inductive solution and has a pole at $R_\text{m} = 0$. As indicated in Figure 4.6 b) (note the different scale), the lossy π network exactly matched at its input behaves different. C_1 of the inductive solution (employing $R_{\text{sind+}}$) has a maximum. If $R_\ell \leq R_{\ell\text{limofRmlim}}$, C_1 of the capacitive solution has a minimum. At $R_\text{m} = 0$, both solutions join without a pole.

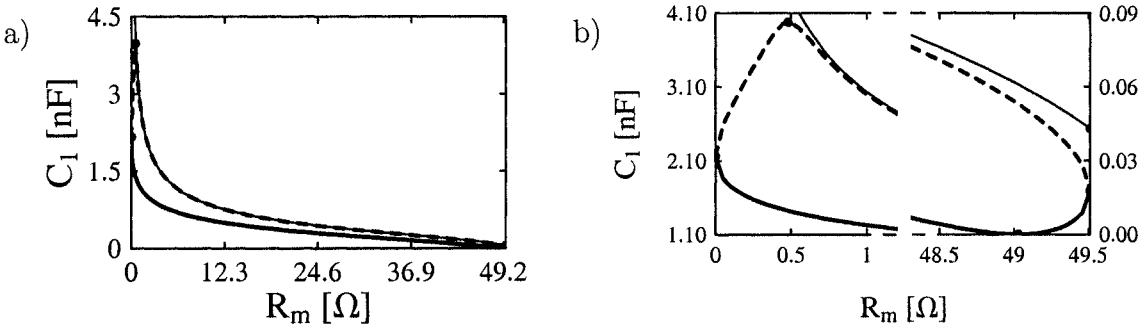

Figure 4.7: C_1 of a lossy π network designed as if it would be lossless (thin lines) and of a lossy π network exactly matched at its input (thick lines), capacitive (solid) and inductive (dashed) — employing $R_{\text{sind+}}$ for the exactly matched network — solutions, a) full range, b) details at 7.35 MHz, $R_\text{i} = 50\,\Omega$, $Q = 5$, and $R_\ell = R_{\ell\text{limofRmlim}} \approx 49.51\,\Omega$

If R_ℓ increases, the value of the minimum decreases until it reaches zero at $R_\ell = R_{\ell\text{limofRmlim}}$ (refer to Figure 4.7 b) — note the different scale).

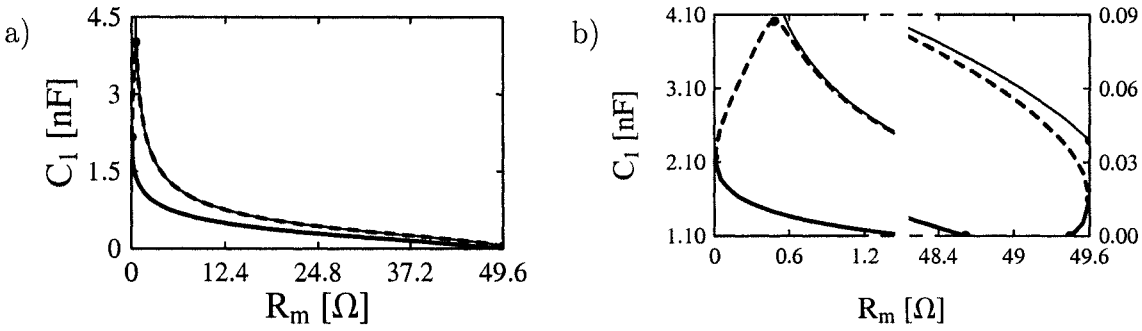

Figure 4.8: C_1 of a lossy π network designed as if it would be lossless (thin lines) and of a lossy π network exactly matched at its input (thick lines), capacitive (solid) and inductive (dashed) — employing $R_{\text{sind+}}$ for the exactly matched network — solutions, a) full range, b) details at 7.35 MHz, $R_\text{i} = 50\,\Omega$, $Q = 5$, and $R_\ell = 49.6\,\Omega$

If R_ℓ increases further, the value of the minimum decreases below zero, yielding two limits of the parameter's valid range (which guarantee that $C_1 \geq 0$ within), R_{mlim1} to the left and R_{mlim2} to the right of the minimum. (An example is given in Figure 4.8 b) — note the different scale).

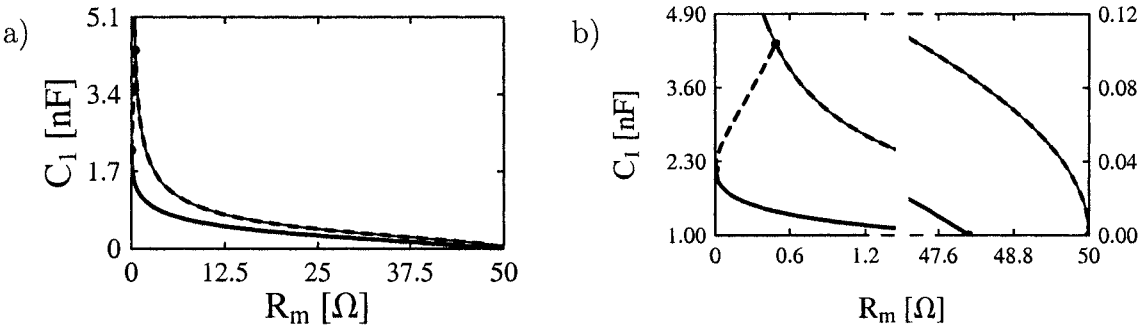

Figure 4.9: C_1 of a lossy π network designed as if it would be lossless (thin lines) and of a lossy π network exactly matched at its input (thick lines), capacitive (solid) and inductive (dashed) — employing $R_{\text{sind-}}$ (long dashes) and $R_{\text{sind+}}$ (short dashes) for the exactly matched network — solutions, a) full range, b) details at 7.35 MHz, $R_\text{i} = 50\,\Omega$, $Q = 5$, and $R_\ell = R_\text{i} = 50\,\Omega$

If $R_\ell = R_\text{i}$, R_{mlim2} reaches its maximum value, $R_{\text{mlim2}} = R_\ell = R_\text{i}$, and the second valid interval of the capacitive solution contracts to a single dot (Figure 4.9 b) — note the different scale). Capacitive and inductive (employing $R_{\text{sind+}}$) solution join at $R_\text{m} = 0$ and $R_\text{m} = R_\ell$ (as they did for lower R_ℓ).

Additionally, the second inductive solution (employing $R_{\text{sind-}}$) becomes valid. Its C_1 tends to infinity if R_m approaches zero. Note that both inductive solutions (employing $R_{\text{sind+}}$, $R_{\text{sind-}}$) join at $R_\text{m} = R_{\text{mv01}}$.

If $0 \leq R_\text{m} \leq R_{\text{mv01}}$, the inductive solution employing $R_{\text{sind-}}$ and, if $R_{\text{mv01}} \leq R_\text{m} \leq R_\text{i}$, the inductive solution employing $R_{\text{sind+}}$ is equal to the inductive solution of the lossy π network designed as if it would be lossless, resulting from the pure parallel resonance of C_1 and $L_{2\text{tot}}$ in this case (R_s and L_s are zero).

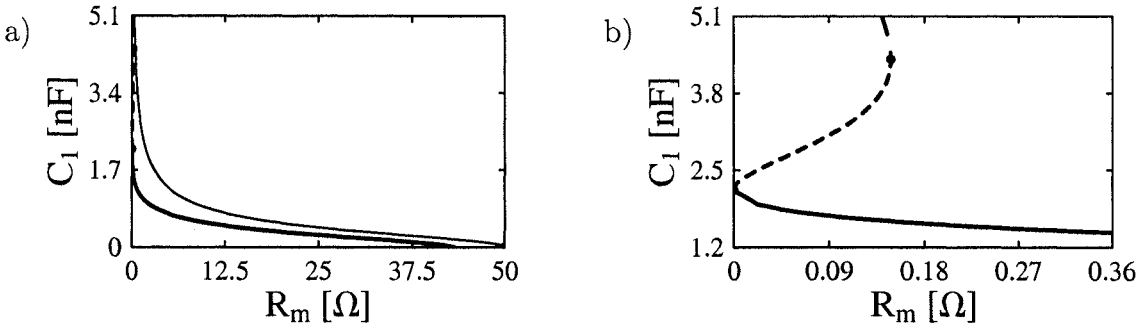

Figure 4.10: C_1 of a lossy π network designed as if it would be lossless (thin lines) and of a lossy π network exactly matched at its input (thick lines), capacitive (solid) and inductive — employing $R_{\text{sind}-}$ (long dashes) and $R_{\text{sind}+}$ (short dashes) — solutions, a) full range, b) details at 7.35 MHz, $R_\text{i} = 50\,\Omega$, $Q = 5$, and $R_\ell = 70\,\Omega$

If $R_\ell > R_\text{i}$, the capacitive solution's valid range is limited by R_{mlim1} only (an example is given in Figure 4.10 a)). Capacitive and inductive (employing $R_{\text{sind}+}$) solution join at $R_\text{m} = 0$.

The second inductive solution (employing $R_{\text{sind}-}$) remains valid. Its C_1 tends to infinity if R_m approaches zero. Note that both inductive solutions (employing $R_{\text{sind}+}$, $R_{\text{sind}-}$) join at $R_\text{m} = R_{\text{mv01}}$ and that there is no valid inductive solution for the lossy π network designed as if it would be lossless (refer to Figure 4.10 b) — note the different scale).

Next L_s is considered. (Since $R_\text{s} = \frac{1}{Q}\omega L_\text{s}$, R_s is not shown separately.)

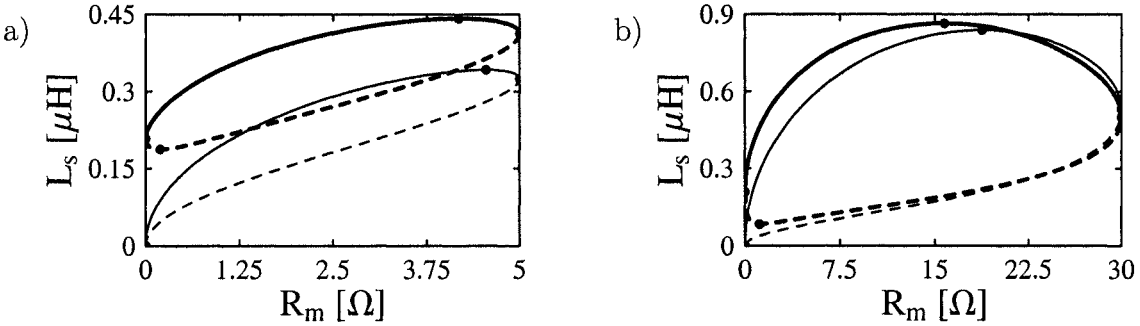

Figure 4.11: L_s of a lossy π network designed as if it would be lossless (thin lines) and of a lossy π network exactly matched at its input (thick lines), capacitive (solid) and inductive (dashed) — employing $R_{\text{sind}+}$ for the exactly matched network — solutions at 7.35 MHz, $R_\text{i} = 50\,\Omega$, $Q = 5$, and a) $R_\ell = 5\,\Omega$, b) $R_\ell = 30\,\Omega$

If $R_\ell \leq R_\text{i}$, L_s of the lossy π network designed as if it would be lossless is zero for the capacitive and inductive solution and L_s of the capacitive solution has a maximum. As indicated in Figure 4.11, the lossy π network exactly matched at its input exhibits a nonzero L_s then and L_s of the capacitive/inductive (employing $R_{\text{sind}+}$) solution has a maximum/minimum. Since $Q > 1$ in the example, $L_\text{s}(R_\text{m} = 0) < L_\text{s}(R_\text{m} = R_\ell)$ for the capacitive and inductive (employing $R_{\text{sind}+}$) solution if $R_\ell < \frac{Q^2+1}{Q^2-1} R_\text{i}$. Two examples are given in Figure 4.11.

Since $\frac{Q^2+1}{Q^2-1}$ increases with increasing Q and is higher than 0.98 if $Q > 10$, yielding loads which do not need to be matched (except for a compensation of their susceptance, if present), it should be noted that even for moderate Q factors $L_s(R_m = 0) < L_s(R_m = R_\ell)$ is usually observed if $R_\ell < R_i$.

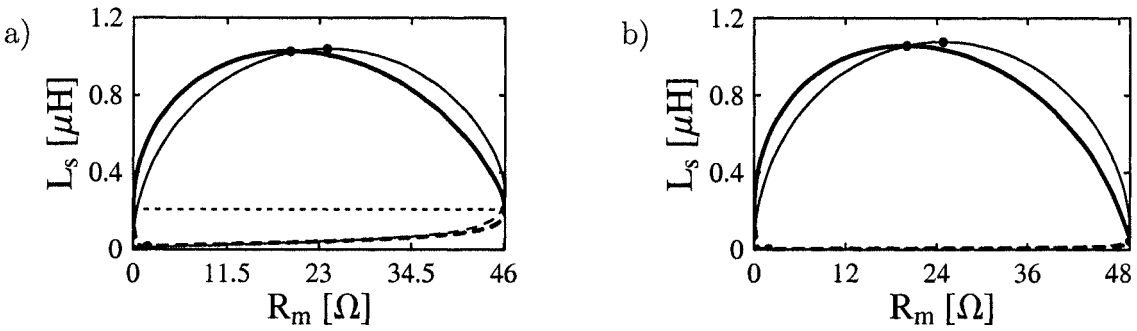

Figure 4.12: L_s of a lossy π network designed as if it would be lossless (thin lines) and of a lossy π network exactly matched at its input (thick lines), capacitive (solid) and inductive (dashed) — employing R_{sind+} for the exactly matched network — solutions at 7.35 MHz, $R_i = 50\,\Omega$, $Q = 5$, and a) $R_\ell = \frac{Q^2+1}{Q^2-1} R_i \approx 46.15\,\Omega$ (horizontal dashed line indicates equal L_s), b) $R_\ell = R_{\ell limofRmlim} \approx 49.51\,\Omega$

If R_ℓ increases, $L_s(R_m = 0)$ and $L_s(R_m = R_\ell)$ come closer until $L_s(R_m = 0) = L_s(R_m = R_\ell)$ at $R_\ell = \frac{Q^2+1}{Q^2-1} R_i$ ($Q > 1$ in the example) for the capacitive and inductive (employing R_{sind+}) solution (refer to Figure 4.12 a)).

If R_ℓ increases further, $L_s(R_m = 0) > L_s(R_m = R_\ell)$ for the capacitive and inductive (employing R_{sind+}) solution (refer to Figure 4.12 b)).

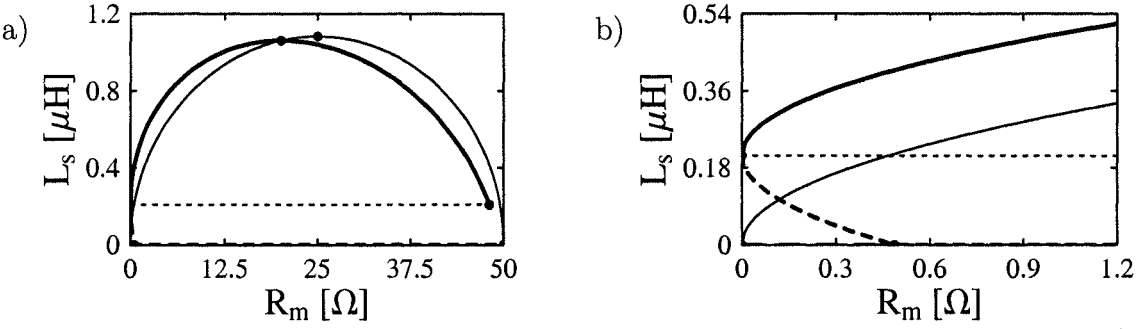

Figure 4.13: L_s of a lossy π network designed as if it would be lossless (thin lines) and of a lossy π network exactly matched at its input (thick lines), capacitive (solid) and inductive (dashed) — employing R_{sind-} (long dashes) and R_{sind+} (short dashes) for the exactly matched network — solutions, a) full range, b) details at 7.35 MHz, $R_i = 50\,\Omega$, $Q = 5$, and $R_\ell = R_i = 50\,\Omega$ (horizontal dashed line indicates equal L_s)

If $R_\ell = R_i$, $L_s(R_m = 0) = L_s(R_m = R_{mlim1})$ for the capacitive solution (Figure 4.13 b) — note the different scale). Since $R_{mlim2} = R_\ell = R_i$, the second valid interval of the capacitive solution contracts to a single dot. Capacitive and inductive (employing R_{sind+}) solution join at $R_m = 0$ and $R_m = R_\ell$ (as they did for lower R_ℓ). Additionally, the second inductive solution (employing R_{sind-}) becomes valid. Note that both inductive solutions (employing R_{sind+}, R_{sind-}) join at $R_m = R_{mv01}$.

If $0 \leq R_m \leq R_{mv01}$, the inductive solution employing R_{sind-} and, if $R_{mv01} \leq R_m \leq R_i$, the inductive solution employing R_{sind+} is equal to the inductive solution of the lossy π network designed as if it would be lossless, resulting from the pure parallel resonance of C_1 and L_{2tot} in this case (R_s and L_s are zero).

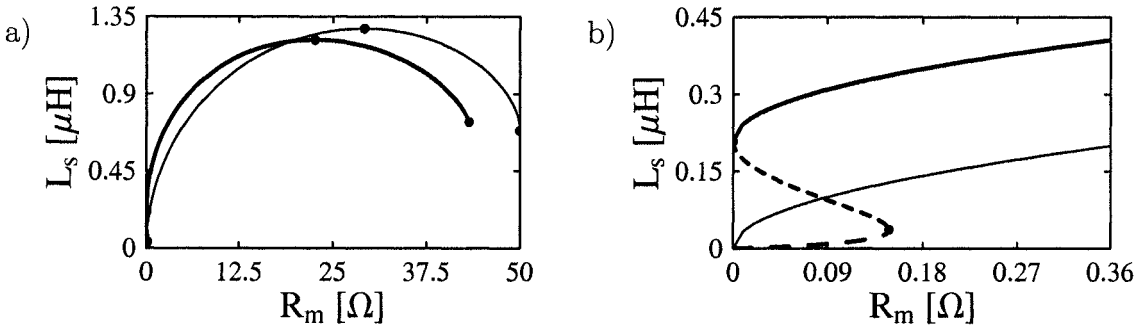

Figure 4.14: L_s of a lossy π network designed as if it would be lossless (thin lines) and of a lossy π network exactly matched at its input (thick lines), capacitive (solid) and inductive — employing R_{sind-} (long dashes) and R_{sind+} (short dashes) — solutions, a) full range, b) details at 7.35 MHz, $R_i = 50\,\Omega$, $Q = 5$, and $R_\ell = 70\,\Omega$

If $R_\ell > R_i$, $L_s(R_m = 0) < L_s(R_m = R_{mlim1})$ for the capacitive solution. Capacitive and inductive (employing R_{sind+}) solution join at $R_m = 0$ (an example is given in Figure 4.14 b) — note the different scale and that the lossy π network designed as if it would be lossless has no valid inductive solution if $R_\ell > R_i$).

The second inductive solution (employing R_{sind-}) remains valid. Its L_s tends to zero if R_m approaches zero. Note that both inductive solutions (employing R_{sind+}, R_{sind-}) join at $R_m = R_{mv01}$ and that there is no valid inductive solution for the lossy π network designed as if it would be lossless.

Next g_π is considered. (Since the value C_2 depends on the load susceptance, it was moved towards the end.)

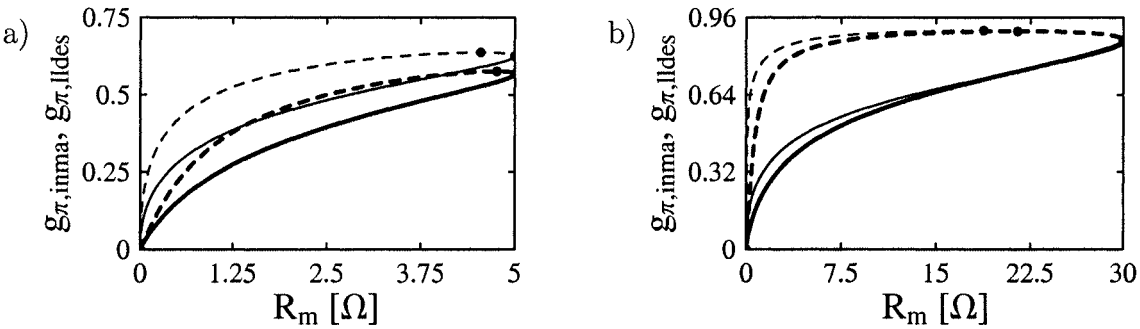

Figure 4.15: Power gain $g_{\pi,llde s}$ of a lossy π network designed as if it would be lossless (thin lines) and $g_{\pi,inma}$ of a lossy π network exactly matched at its input (thick lines), capacitive (solid) and inductive (dashed) — employing R_{sind+} for the exactly matched network — solutions at 7.35 MHz, $R_i = 50\,\Omega$, $Q = 5$, and a) $R_\ell = 5\,\Omega$, b) $R_\ell = 30\,\Omega$

If $R_\ell < R_\mathrm{i}$, the power gain of the capacitive solution increases with increasing R_m (refer to Figure 4.15).

For the lossy π network designed as if it would be lossless, there exists a maximum of $g_{\pi,\mathrm{lldes}}$ for the inductive solution at $R_\mathrm{mgmaxind} = \frac{R_\ell R_\mathrm{i}}{R_\ell + R_\mathrm{i}}$ (the capacitive solution has its maximum L_s at this R_m). For the lossy π network exactly matched at its input, $g_{\pi,\mathrm{inma,maxind+}}$, the maximum of $g_{\pi,\mathrm{inma}}$ in case of the inductive solution employing $R_\mathrm{sind+}$, was given in (4.29).

Since $g_\pi = \frac{R_\ell}{R_\ell + R_\mathrm{s}(1+R_\ell^2 B_\mathrm{2tot}^2)}$, where $B_\mathrm{2tot} = \omega C_\mathrm{2tot} = -\frac{1}{\omega L_\mathrm{2tot}}$, holds for any π network, and C_2tot or L_2tot are similar at a given R_m for a lossy π network matched exactly at its input or a lossy π network designed as if it would be lossless, $g_{\pi,\mathrm{lldes}} > g_{\pi,\mathrm{inma}}$ if the according L_s is lower (easily seen by comparison of Figure 4.11 and Figure 4.15). Thus, (for low Q factors) the exactly matched network may be worse, it matches at the expense of power gain!

Considering this result, which may seem surprisingly at a first glance, one should keep in mind that the concept of maximum transferred active power by achieving a complex conjugate match applies only to lossless matching networks! Depending on the losses, lossy matching networks may behave different. However, the match at the network's input involves other advantages, e. g. reducing of the losses in the line connecting the network to the source.

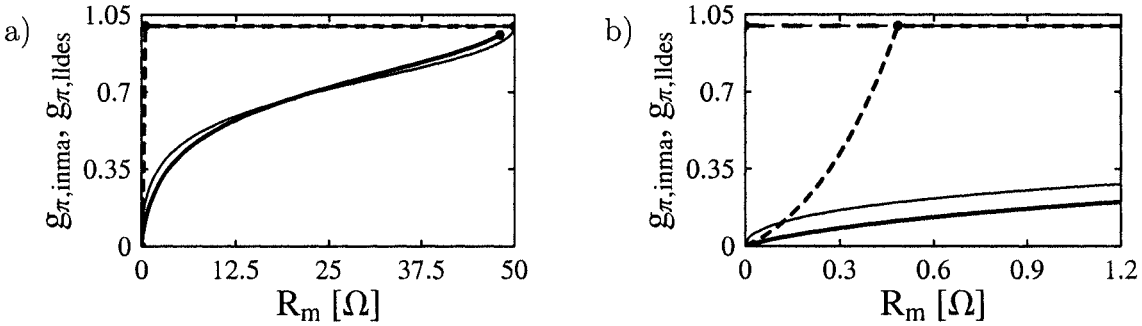

Figure 4.16: Power gain $g_{\pi,\mathrm{lldes}}$ of a lossy π network designed as if it would be lossless (thin lines) and $g_{\pi,\mathrm{inma}}$ of a lossy π network exactly matched at its input (thick lines), capacitive (solid) and inductive (dashed) — employing $R_\mathrm{sind-}$ (long dashes) and $R_\mathrm{sind+}$ (short dashes) for the exactly matched network — solutions, a) full range, b) details at 7.35 MHz, $R_\mathrm{i} = 50\,\Omega$, $Q = 5$, and $R_\ell = R_\mathrm{i} = 50\,\Omega$

If $R_\ell = R_\mathrm{i}$, the power gain of the capacitive solution increases with increasing R_m (refer to Figure 4.16 b) — note the different scale). This also holds for the inductive solution (employing $R_\mathrm{sind+}$) if $0 \leq R_\mathrm{m} \leq R_\mathrm{mv01}$. Since $R_\mathrm{mlim2} = R_\ell = R_\mathrm{i}$, the second valid interval of the capacitive solution contracts to a single dot. Capacitive and inductive (employing $R_\mathrm{sind+}$) solution join at $R_\mathrm{m} = 0$ and $R_\mathrm{m} = R_\ell$ (as they did for lower R_ℓ).

Additionally, the second inductive solution (employing $R_\mathrm{sind-}$) becomes valid. Note that both inductive solutions (employing $R_\mathrm{sind+}$, $R_\mathrm{sind-}$) join at $R_\mathrm{m} = R_\mathrm{mv01}$.

If $0 \leq R_m \leq R_{mv01}$, the inductive solution employing R_{sind-} and, if $R_{mv01} \leq R_m \leq R_i$, the inductive solution employing R_{sind+} is equal to the inductive solution of the lossy π network designed as if it would be lossless, resulting from the pure parallel resonance of C_1 and L_{2tot} in this case (R_s and L_s are zero and thus the power gain is unity and constant).

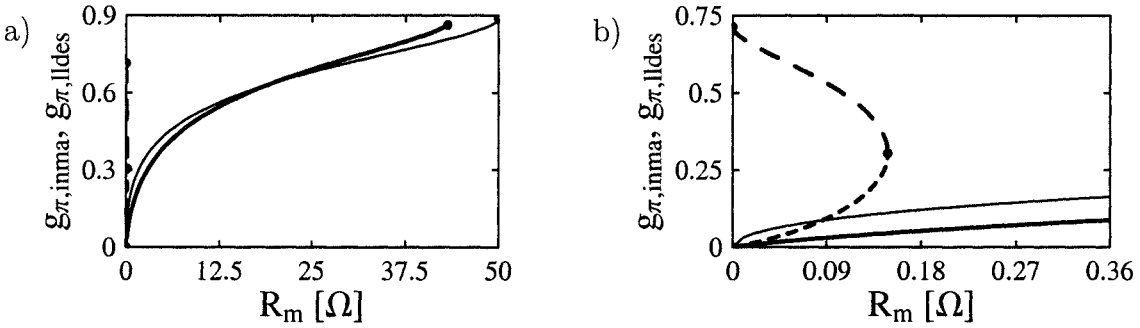

Figure 4.17: Power gain $g_{\pi,llde}$ of a lossy π network designed as if it would be lossless (thin lines) and $g_{\pi,inma}$ of a lossy π network exactly matched at its input (thick lines), capacitive (solid) and inductive — employing R_{sind-} (long dashes) and R_{sind+} (short dashes) — solutions, a) full range, b) details at 7.35 MHz, $R_i = 50\,\Omega$, $Q = 5$, and $R_\ell = 70\,\Omega$

If $R_\ell > R_i$, the power gain of the capacitive solution and the inductive solution (employing R_{sind+}) increases with increasing R_m (refer to Figure 4.17 b) — note the different scale and that the lossy π network designed as if it would be lossless has no valid inductive solution if $R_\ell > R_i$). Capacitive and inductive (employing R_{sind+}) solution join at $R_m = 0$.

The second inductive solution (employing R_{sind-}) remains valid. Its power gain decreases from $\frac{R_i}{R_\ell}$ at $R_m = 0$ with increasing R_m. Note that both inductive solutions (employing R_{sind+}, R_{sind-}) join at $R_m = R_{mv01}$ and that there is no valid inductive solution for the lossy π network designed as if it would be lossless.

Furthermore, Figures 4.15 to 4.17 illustrate the huge advantage of R_m parametrisation in case of a constant Q factor inductor — $\frac{dg_{\pi,inma}}{dR_m}$ of all solutions except the inductive solution employing R_{sind+} for $R_\ell < R_i$ exhibit a unique sign over the entire valid parameter range, yielding an optimum network at one of the range's limits! (The second exception, the pure parallel resonance of C_1 and L_{2tot}, where the power gain stays constant, would require a $L_s = 0$ and $R_s = 0$, which is not realisable. Anyhow, it still would fit the concept because the constant gain is achieved at the parameter range's limits, too.)

Finally C_2 is considered. Its value C_2 depends on the load susceptance, thus only some useful examples are given below. For the chosen R_m parametrisation, C_2 at a given R_m for a lossy π network designed as if it would be lossless and a lossy π network exactly matched at its input is equal. However, the applicable valid parameter ranges differ.

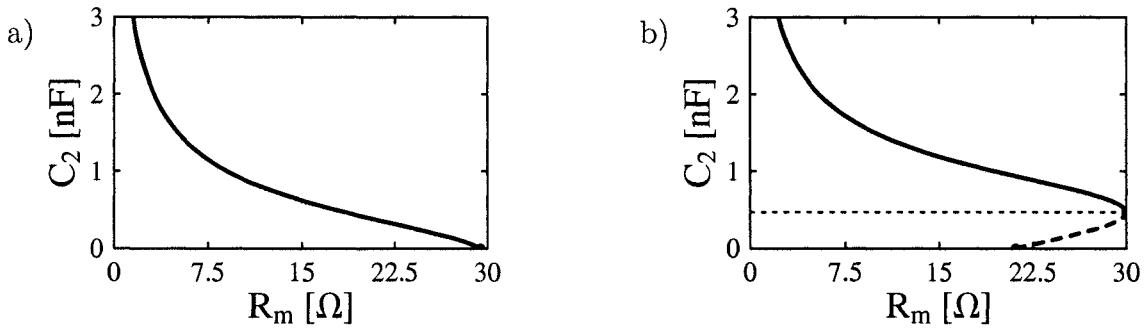

Figure 4.18: C_2 of a lossy π network designed as if it would be lossless (thin lines) and of a lossy π network exactly matched at its input (thick lines) at 7.35 MHz, $R_\mathrm{i} = 50\,\Omega$, $Q = 5$, $R_\ell = 30\,\Omega$, and a) capacitive (solid) solutions for $C_{\ell\mathrm{p}} = 100\,\mathrm{pF}$, b) capacitive (solid, (over-)compensated) and inductive (dashed, undercompensated) — employing $R_{\mathrm{sind+}}$ for the exactly matched network — solutions for $L_{\ell\mathrm{p}} = 1\,\mu\mathrm{H}$ (horizontal dashed line indicates $\omega C_2 = \frac{1}{\omega L_{\ell\mathrm{p}}}$)

As illustrated in Figure 4.18 a) for an example where $R_\ell \leq R_{\ell\mathrm{limofRmlim}}$, $C_{\ell\mathrm{p}}$ limits the maximum possible R_m (the upper limit is below R_ℓ in this case). If the load has an inductive imaginary part, (depending on the minimum value of C_2,) (over-)compensation (capacitive solution) or undercompensation (inductive solution (employing $R_{\mathrm{sind+}}$ in the example)) may occur, refer to Figure 4.18 b). If valid, capacitive and inductive (employing $R_{\mathrm{sind+}}$) solution join at $R_\mathrm{m} = R_\ell$ if $R_\ell \leq R_\mathrm{i}$.

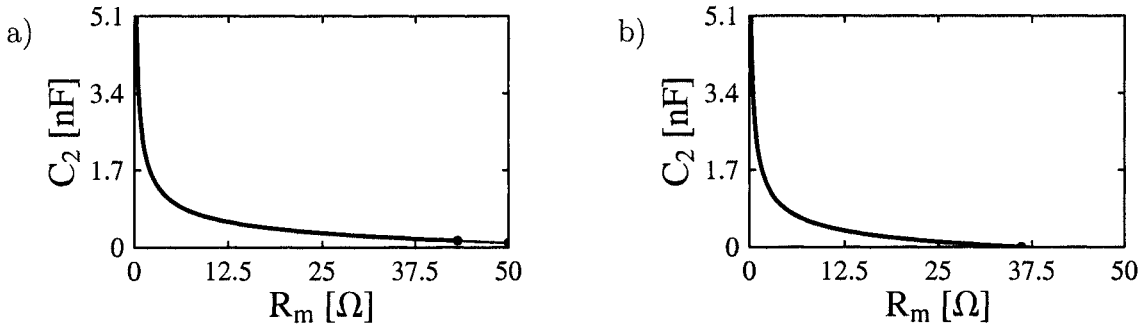

Figure 4.19: C_2 of a lossy π network designed as if it would be lossless (thin lines) and of a lossy π network exactly matched at its input (thick lines), capacitive solutions at 7.35 MHz, $R_\mathrm{i} = 50\,\Omega$, $Q = 5$, $R_\ell = 70\,\Omega$, and a) $C_{\ell\mathrm{p}} = 100\,\mathrm{pF}$, b) $C_{\ell\mathrm{p}} = 300\,\mathrm{pF}$

If $R_\ell > R_\mathrm{i}$, the upper limit in case of the capacitive solution is given by R_i for a lossy π network designed as if it would be lossless and by R_{mlim1} for a lossy π network exactly matched at its input. Thus a load capacitance may be lower (Figure 4.19 a)) or higher (Figure 4.19 b)) than $C_{2\mathrm{tot}}$ at this limit, thus the valid parameter range is not changed or lowered, respectively.

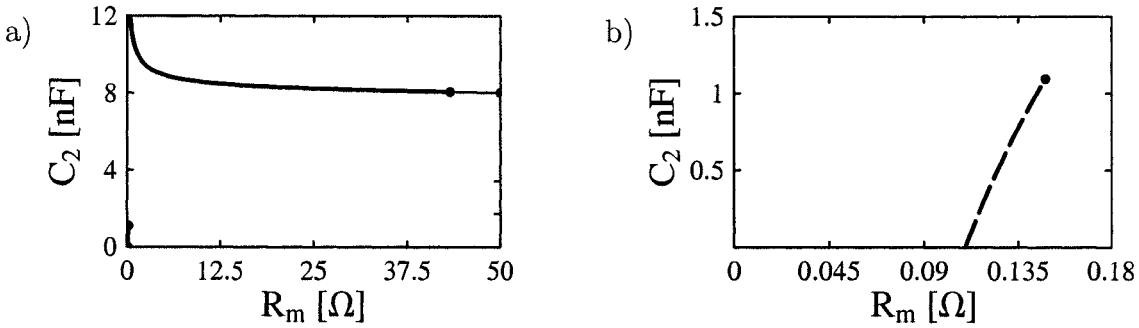

Figure 4.20: C_2 of a lossy π network designed as if it would be lossless (thin lines) and of a lossy π network exactly matched at its input (thick lines), capacitive (solid, (over-)compensated) and inductive — employing $R_{\text{sind}-}$ (long dashes) and $R_{\text{sind}+}$ (short dashes) (both undercompensated) — solutions, a) full range, b) details at 7.35 MHz, $R_\text{i} = 50\,\Omega$, $Q = 5$, $R_\ell = 70\,\Omega$, and $L_{\ell\text{p}} = 60\,\text{nH}$

If $R_\ell > R_\text{i}$, quite low $L_{\ell\text{p}}$ are required for the inductive solutions (employing $R_{\text{sind}+}$, $R_{\text{sind}-}$ with similar C_2) to be valid (an example is given in Figure 4.20). Note the different scales and that there is no valid inductive (undercompensated) solution for the lossy π network designed as if it would be lossless.

4.4.3.2 Power gain's contour line Smith charts for L, π, and T networks

In the following diagrams, power gain's contour line Smith charts for different L, π, and T networks are shown. Their central inductor has a range of $0.1\,\mu\text{H} - 40\,\mu\text{H}$, a constant Q factor of 100, the matching frequency is 7.35 MHz, and the variable capacitor's range is $5\,\text{pF} - 500\,\text{pF}$. The contour lines were calculated from the resulting matching networks of 100 x 100 equally spaced load reflection coefficients whose $\text{Re}\{\underline{r}_\ell\}$, $\text{Im}\{\underline{r}_\ell\} \in [-1, 1]$, where only those with $|\underline{r}_\ell| < 1$ were used.

To gain more insight in the networks' behaviour, a full set of diagrams is given in Appendix C.2.1.1, where the matching frequency is either 1.8 MHz, 7.35 MHz, or 30 MHz and the variable capacitances' ranges resemble different "typical" variable capacitors (a cheap $5\,\text{pF} - 250\,\text{pF}$, a better $5\,\text{pF} - 500\,\text{pF}$, and an expensive $25\,\text{pF} - 4000\,\text{pF}$ vacuum variable).

In case of π and T networks, best and worst networks' power gain is shown.

In case of L networks, it is assumed that the network topology enables implementation of both "complementary" L networks (C_1 only or C_2 only), e. g. by using appropriate switches.

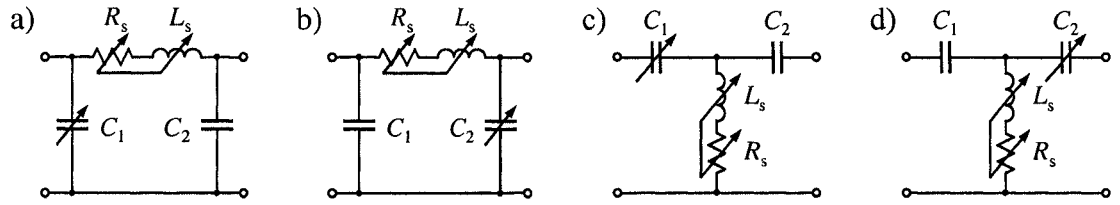

Figure 4.21: Simplified equivalent circuit of L networks derived from π networks with parasitic parallel capacitance a) C_2 or b) C_1 and from T networks with parasitic series capacitance c) C_2 or d) C_1

Additionally, the impact of a parasitic capacitance replacing one variable capacitance of a π or T network is considered (refer to Figure 4.21) — the resulting networks yield a more realistic description of "real world" L networks. Based on [3], the value of that parasitic capacitance was chosen to be equal to the minimum/maximum value of the remaining variable capacitance for L networks derived from π networks/T networks.

Since lossy L networks may theoretically exhibit more than one distinct solutions for a given load, it has to be noted that

- the pure L networks (without parasitic capacitances) and the L networks with a parasitic parallel capacitance derived from π networks yielded only a single valid solution throughout all complete Smith charts for the given network element ranges
- the L networks with a parasitic series capacitance derived from T networks yielded more than one solution within some region of the Smith charts for the given network element ranges, but the differences in power gain of best and worst solutions were low — for the chosen contour line values both diagrams were merely similar — thus only the best diagrams are shown.

Regarding the latter — a more detailed review of the differences between best and worst L networks' power gain is given in Appendix C.2.1.1.

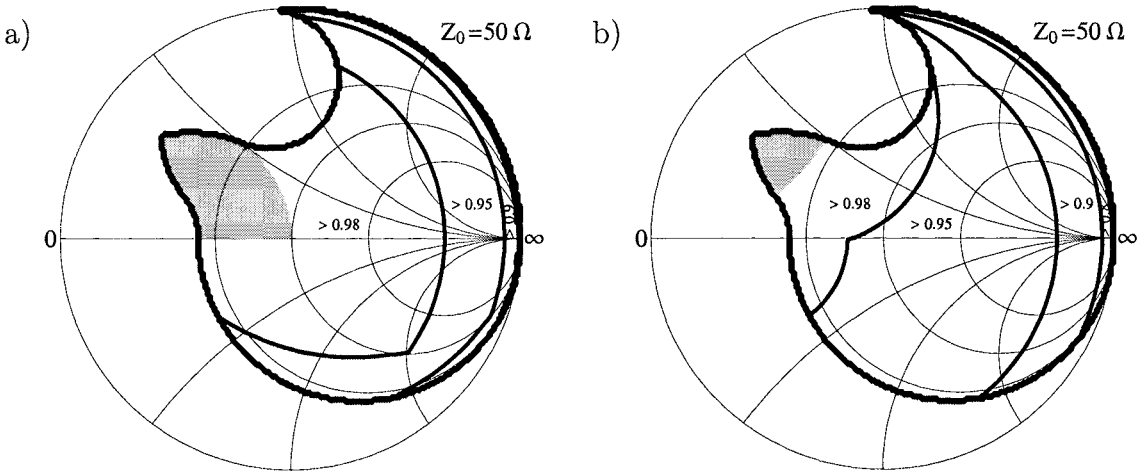

Figure 4.22: a) Best and b) worst $g_{\pi,\mathrm{inma}}$ at 7.35 MHz, $R_\mathrm{i} = 50\,\Omega$, $Q = 100$, $5\,\mathrm{pF} \leq C_{1,2} \leq 500\,\mathrm{pF}$, and $0.1\,\mu\mathrm{H} \leq L_\mathrm{s} \leq 40\,\mu\mathrm{H}$, undercompensation shaded

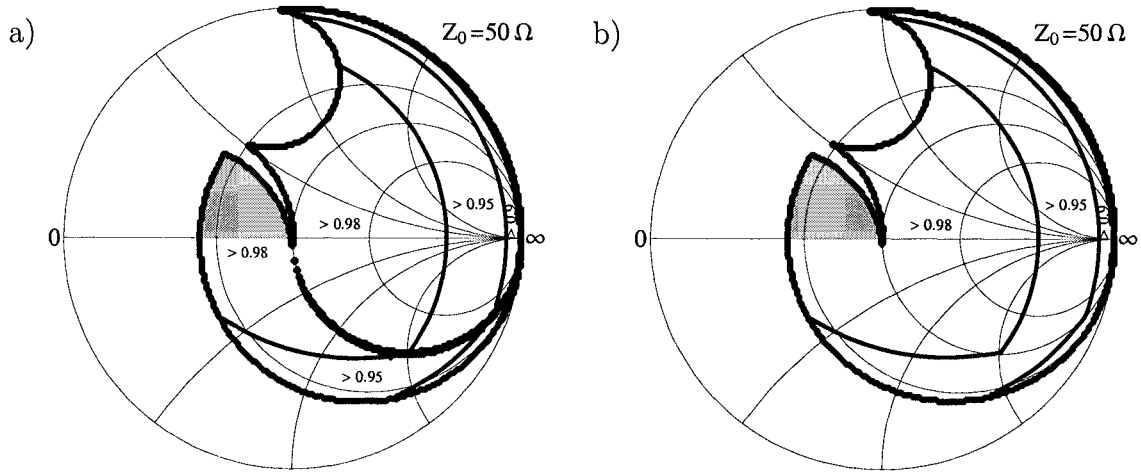

Figure 4.23: $g_{\mathrm{loft}\pi,\mathrm{inma}}$ at 7.35 MHz, $R_\mathrm{i} = 50\,\Omega$, $Q = 100$, $5\,\mathrm{pF} \leq C_{1,2} \leq 500\,\mathrm{pF}$, and $0.1\,\mu\mathrm{H} \leq L_\mathrm{s} \leq 40\,\mu\mathrm{H}$, a) without, b) with 5 pF parasitics, uc. shaded

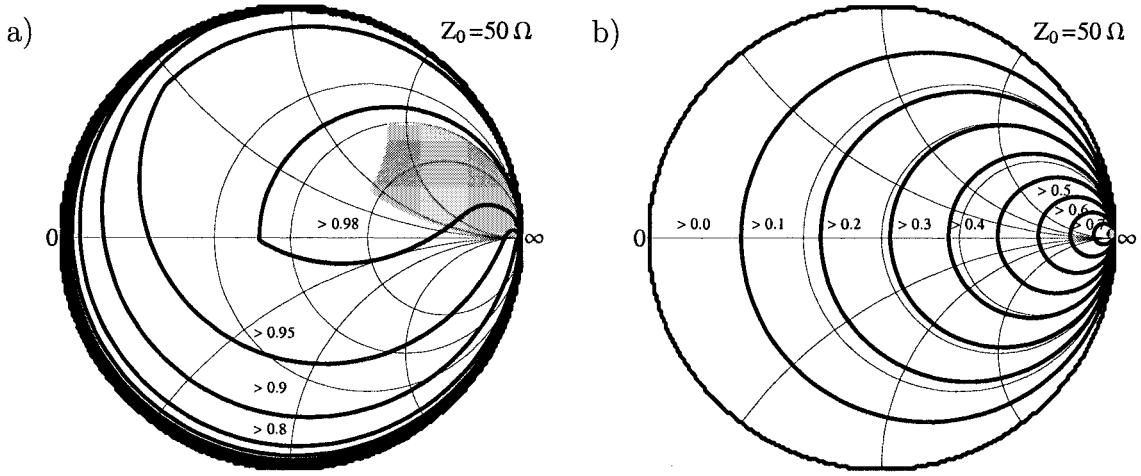

Figure 4.24: a) Best and b) worst $g_{\mathrm{t,inma}}$ at 7.35 MHz, $R_\mathrm{i} = 50\,\Omega$, $Q = 100$, $5\,\mathrm{pF} \leq C_{1,2} \leq 500\,\mathrm{pF}$, and $0.1\,\mu\mathrm{H} \leq L_\mathrm{s} \leq 40\,\mu\mathrm{H}$, undercompensation shaded

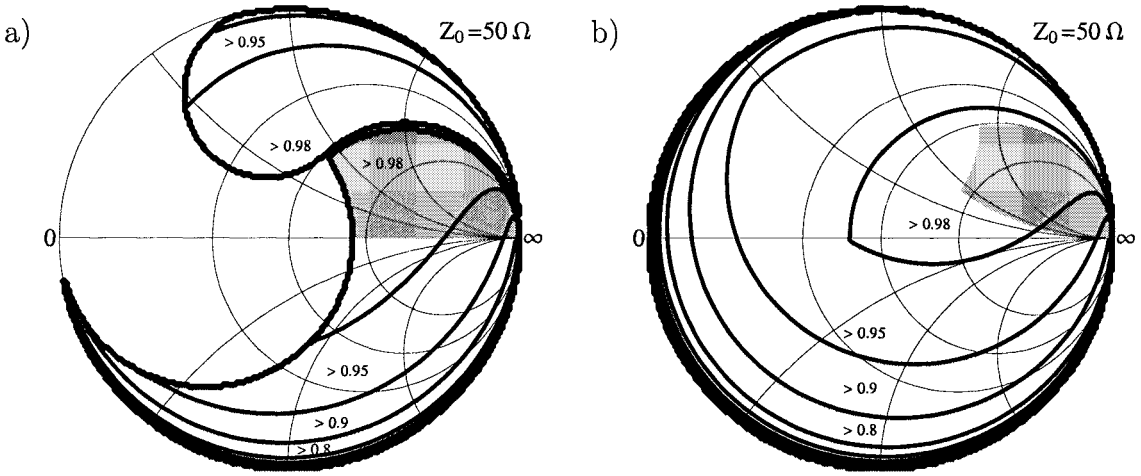

Figure 4.25: $g_{\mathrm{loft,inma}}$ at 7.35 MHz, $R_\mathrm{i} = 50\,\Omega$, $Q = 100$, $5\,\mathrm{pF} \leq C_{1,2} \leq 500\,\mathrm{pF}$, and $0.1\,\mu\mathrm{H} \leq L_\mathrm{s} \leq 40\,\mu\mathrm{H}$, a) without, b) with 5 pF parasitics, uc. shaded

From the preceding diagrams (and those shown in Appendix C.2.1.1), it's quite obvious that the matching range of π and T networks is always greater than that of the derived L networks which seems to be particularly true for L networks derived from T networks at lower frequencies. However, their matching range can be enourmously extended if the omitted variable capacitor is replaced with a fixed capacitance similar to the variable capacitor's minimum/maximum value for L networks derived from π networks/T networks as proposed by [3].

Comparison of π and T networks yields that in our frequency range of interest, the matching range of π networks is lower than that of T networks. Furthermore, π networks require high maximum values of the variable capacitances to obtain a "reasonable" matching range at all. But best and worst π networks' power gains are much closer than T networks' — thus T networks are more vulnerable to careless tuning. As an extreme example, consider the left upper region in Figures 4.24 a) and b) — the best T network's power gain is between 0.95 and 0.98, the worst T network's between 0 and 0.1 which is at least 0.85 lower! The π networks' differences are much lower, although increasing if higher maximum capacitance values are used.

Checking the difference between the networks' best and worst power gains is also useful regarding estimation of the gain's increase due to a proper matching strategy. Depending on the load, frequency, and maximum capacitance values, values well above 10 % are possible. As indicated above, even about 85 % may occur in extreme cases. It's important to note that it's impossible to distinguish matched networks' power gains by simply searching for a good match — all network settings which lie within the region defined by the outer contour line(s) (all settings able to match) yield (theoretically) perfect matches!

Regarding best and worst T networks, approximations were given in [65] for the loads at which highest losses of best T networks occur for a given $|\underline{r}_\ell|$ — approximately at $G_\ell = \frac{1+|\underline{r}_\ell|}{1-|\underline{r}_\ell|} G_\mathrm{i}$. Footnote [3] of [65] contains further approximations for the lowest losses of best T networks. In [65], no indication was given how the formulae were derived and how the contour Smith charts were calculated. However, using the solutions of Section 4.4.1.2, the values of Table 1 and of Table 2 for $Q = 100$ in [65] (load impedance only tabulated for $Q = 100$) were verified and a Smith chart equivalent to Figure 2 of [65] was drawn. Unfortunately the contour line values chosen by [65] are not suited for comparison — e. g. it's impossible to decide whether undercompensation was included in case of loads exhibiting an inductive imaginary part, although it's not likely because the lower bound for best T networks' losses given in Footnote [3] of [65] applies only if that case is not taken into account. For the network element ranges used to derive all Smith charts above (including a set comparable to that used by [65]), it seems that the lowest losses occur at a circle's section which describes best T networks with C_1 and L_s at their maximum values and varying C_2. (That locus may be calculated analytically, but the formulae are quite lengthy — since it was not proven that these are indeed the lowest losses, the formulae are not given herein.) Furthermore, using the solutions of Section 4.4.1.2, it could be proven that if $G_\ell > G_\mathrm{i}$ and G_m is limited by the maximum value of C_2, the

highest losses for a given $|\underline{r}_\ell|$ occur at $\underline{Z}_\ell = G_\ell = \frac{1+|\underline{r}_\ell|}{1-|\underline{r}_\ell|} G_\mathrm{i}$. Calculating numerical examples for the remaining cases yielded highest losses of best T networks close to the approximations given in [65].

4.5 Impact of minimum/maximum elements' values on power gain, optimum networks

4.5.1 π network

In Sections 3.5.2.2 and 4.3.1.1 we observed that the optimum π network of a purely resistive load or a load exhibiting a capacitive imaginary part is an (external) L network. However, minimum/maximum elements' values were not considered. Anyhow, the L network was obtained because the optimisation yielded a maximum power gain if the π network's parameter R_m was at its maximum value.

Which changes have to be made if minimum/maximum elements' values have to be taken into account?

The optimisation remains unchanged. Thus the optimum power gain is still achieved for the highest possible R_m. However, unlike before, it may be limited by the minimum/maximum value of one of the π network's elements instead of the limits derived so far.

How may we ensure that R_m is at its highest value?

In Section 4.3.1.1 we proved that $\frac{\mathrm{d}C_\mathrm{2tot}}{\mathrm{d}R_\mathrm{m}} < 0$ (which also holds for purely resistive loads if C_2tot is replaced with C_2). Thus the value of C_2tot has to be at its lowest value for highest R_m. Since C_2tot is the sum of C_2 and the (given) parallel load capacitance, this condition holds if C_2 is at its lowest value.

Hence the the optimum π network of a purely resistive load or a load exhibiting a capacitive imaginary part is obtained if C_2 is set to the lowest value where matching is still possible.

However, if the parameter's range is limited rather by the minmum/maximum value of L_s or C_1 instead of C_2, there may occur gaps in the range of C_2 where no matching is possible (L_s and C_1 depend on R_s and may exhibit a minimum/maximum throughout the valid range of R_m). Thus if we manually try to find the lowest C_2 where matching is still possible we should initially use the lowest value of C_2 and increase it till a match is achieved.

According to Section 4.3.2.1, the situation changes if loads exhibiting an inductive imaginary part are considered. In case 1 ((over-)compensation), C_2 decreases if R_m increases, whereas in case 2 (undercompensation), C_2 increases if R_m increases — both cases join at $R_\mathrm{m} = R_\ell$, which is an (internal) L network if it's within the parameter's valid range given by (3.20) (in particular, if at least $R_\ell < R_\mathrm{i} - R_\mathrm{s0}$) and

if those range is not further limited by the minimum/maximum value of one of the π network's elements.

How may we distinguish case 1 ((over-)compensation) from case 2 (undercompensation)?

Comparison of (4.11) and (4.12) yields that except of the intersection $C_2 = \frac{1}{\omega^2 L_{\ell p}}$ (at $R_m = R_\ell$ as indicated above), $C_2 > \frac{1}{\omega^2 L_{\ell p}}$ in case 1 and $C_2 < \frac{1}{\omega^2 L_{\ell p}}$ in case 2. Furthermore, by considering the derivative of C_2 with respect to R_m we obtain that C_2 continuously decreases if in case 1 the parameter R_m is increased up to the intersection at $R_m = R_\ell$ (if within the parameter's valid range) and decreases further if R_m is decreased from $R_m = R_\ell$ in case 2. Hence if we decrease C_2 and try to match, the transition from case 1 to case 2 is observed for $C_2 = \frac{1}{\omega^2 L_{\ell p}}$ if $R_\ell < R_i - R_{s0}$ and $R_m = R_\ell$ is not excluded by the minimum/maximum value of one of the π network's elements. If $R_m = R_\ell$ is not within the parameter's valid range, both cases are still distinguishable by comparison of C_2 to $\frac{1}{\omega^2 L_{\ell p}}$.

With respect to the π network's power gain case 1 behaves like the case of a purely resistive load or a load exhibiting a capacitive imaginary part. Thus the highest power gain is obtained if C_2 is set to the lowest value where matching is still possible.

Conversely, case 2 behaves different. As indicated in Section 4.3.2.1, it may involve a maximum which is not located at maximum R_m. In conjunction with the considerations regarding the values of C_2 and its derivatives with respect to R_m we may conclude that if such maximum exists, we should not decrease C_2 beyond the value where the power gain maximum occurs. Thus the highest power gain may not be observed for the lowest C_2 where matching is still possible.

4.5.2 T network

In Sections 3.5.3.2 and 4.3.1.2 we observed that the optimum T network of a purely resistive load or a load exhibiting a capacitive imaginary part is an (external) L network. However, minimum/maximum elements' values were not considered. Anyhow, the L network was obtained because the optimisation yielded a maximum power gain if the T network's parameter G_m was at its maximum value.

Which changes have to be made if minimum/maximum elements' values have to be taken into account?

The optimisation remains unchanged. Thus the optimum power gain is still achieved for the highest possible G_m. However, unlike before, it may be limited by the minimum/maximum value of one of the T network's elements instead of the limits derived so far.

How may we ensure that G_m is at its highest value?

In Section 4.3.1.2 we proved that $\frac{dC_{2tot}}{dG_m} > 0$ (which also holds for purely resistive loads if C_{2tot} is replaced with C_2). Thus the value of C_{2tot} has to be at its highest

value for highest G_m. Since C_2tot is the reciprocal of the sum of the reciprocal of C_2 and the reciprocal of the (given) serial load capacitance, this condition holds if C_2 is at its highest value.

Hence the the optimum T network of a purely resistive load or a load exhibiting a capacitive imaginary part is obtained if C_2 is set to the highest value where matching is still possible.

However, if the parameter's range is limited rather by the minmum/maximum value of L_s (from parallel-to-series transformation of G_p and L_p) or C_1 instead of C_2, there may occur gaps in the range of C_2 where no matching is possible (L_p and C_1 depend on G_p and may exhibit a minimum/maximum throughout the valid range of G_m). Thus if we manually try to find the highest C_2 where matching is still possible we should initially use the highest value of C_2 and decrease it till a match is achieved.

According to Section 4.3.2.2, the situation changes if loads exhibiting an inductive imaginary part are considered. In case 1 ((over-)compensation), C_2 increases if G_m increases, whereas in case 2 (undercompensation), C_2 decreases if G_m increases — both cases join at $G_\mathrm{m} = G_\ell$, which is an (internal) L network if it's within the parameter's valid range given by (3.33) (in particular, if at least $G_\ell < G_\mathrm{i}$) and if those range is not further limited by the minimum/maximum value of one of the T network's elements.

How may we distinguish case 1 ((over-)compensation) from case 2 (undercompensation)?

Comparison of (4.17) and (4.18) yields that except of the intersection $C_2 = \frac{1}{\omega^2 L_{\ell\mathrm{s}}}$ (at $G_\mathrm{m} = G_\ell$ as indicated above), $C_2 < \frac{1}{\omega^2 L_{\ell\mathrm{s}}}$ in case 1 and $C_2 > \frac{1}{\omega^2 L_{\ell\mathrm{s}}}$ in case 2. Furthermore, by considering the derivative of C_2 with respect to G_m we obtain that C_2 continuously increases if in case 1 the parameter G_m is increased up to the intersection at $G_\mathrm{m} = G_\ell$ (if within the parameter's valid range) and increases further if G_m is decreased from $G_\mathrm{m} = G_\ell$ in case 2. Hence if we increase C_2 and try to match, the transition from case 1 to case 2 is observed for $C_2 = \frac{1}{\omega^2 L_{\ell\mathrm{s}}}$ if $G_\ell < G_\mathrm{i}$ and $G_\mathrm{m} = G_\ell$ is not excluded by the minimum/maximum value of one of the T network's elements. If $G_\mathrm{m} = G_\ell$ is not within the parameter's valid range, both cases are still distinguishable by comparison of C_2 to $\frac{1}{\omega^2 L_{\ell\mathrm{s}}}$.

With respect to the T network's power gain case 1 behaves like the case of a purely resistive load or a load exhibiting a capacitive imaginary part. Thus the highest power gain is obtained if C_2 is set to the highest value where matching is still possible.

Conversely, case 2 behaves different. As indicated in Section 4.3.2.2, it may involve a maximum which is not located at maximum G_m. In conjunction with the considerations regarding the values of C_2 and its derivatives with respect to G_m we may conclude that if such maximum exists, we should not increase C_2 beyond the value where the power gain maximum occurs. Thus the highest power gain may not be observed for the highest C_2 where matching is still possible.

4.5.3 Conclusion

Deriving a matching strategy for optimum power gain is particularly easy for all cases considered above except for case 2 (undercompensation) if the load exhibits an inductive imaginary part.

For purely resistive loads, load impedances exhibiting a capacitive imaginary part, or if due to the minimum/maximum network elements' values only (over-)compensation is applicable to load impedances exhibiting an inductive imaginary part, the following matching strategy ensures highest power gain of the network:

- For π networks set C_2 to its lowest value and try to match. If no match is achievable, increase the value of C_2 until matching is possible.
- For T networks set C_2 to its highest value and try to match. If no match is achievable, decrease the value of C_2 until matching is possible.

Conversely, if the load exhibits an inductive imaginary part and the minimum/maximum network elements' values are suitable for undercompensation to apply we need to know the network elements' values and the frequency to compute their settings for highest power gain by applying the solutions derived in Section 4.4.1.1 or Section 4.4.1.2 to a piecewise constant approximation of the inductor's measured Q factor and choosing the optimum settings of the best segment.

It should be noted that pure (external) lossy L networks may exhibit some distinct settings for a given load (for example consider Figure 4.8 b)), although usually only one solution remains valid, in particular if network elements' limits are taken into account. Thus the matching strategy of the type of network the L network was derived from has to be applied, even if both "complementary" L networks (C_1 only or C_2 only) are realisable (e. g. with a switch) and able to match.

Is it likely to observe case 2 if the load exhibits an inductive imaginary part?

Table 4.1: Transition from case 1 ((over-)compensation) to case 2 (undercompensation) at $C_2 = \frac{1}{\omega^2 L_{\ell p,s}}$ for loads exhibiting an inductive imaginary part.

$\omega L_{\ell p,s}$	1.8 MHz		7.35 MHz		30 MHz	
	$L_{\ell p,s}$	$\frac{1}{\omega^2 L_{\ell p,s}}$	$L_{\ell p,s}$	$\frac{1}{\omega^2 L_{\ell p,s}}$	$L_{\ell p,s}$	$\frac{1}{\omega^2 L_{\ell p,s}}$
1 Ω	88 nH	88 nF	22 nH	22 nF	5.3 nH	5.3 nF
2 Ω	180 nH	44 nF	43 nH	11 nF	11 nH	2.7 nF
5 Ω	440 nH	18 nF	110 nH	4.3 nF	27 nH	1.1 nF
10 Ω	880 nH	8.8 nF	220 nH	2.2 nF	53 nH	530 pF
20 Ω	1.8 μH	4.4 nF	430 nH	1.1 nF	110 nH	270 pF
50 Ω	4.4 μH	1.8 nF	1.1 μH	430 pF	270 nH	110 pF
100 Ω	8.8 μH	880 pF	2.2 μH	220 pF	530 nH	53 pF
200 Ω	18 μH	440 pF	4.3 μH	110 pF	1.1 μH	27 pF
500 Ω	44 μH	180 pF	11 μH	43 pF	2.7 μH	11 pF
1000 Ω	88 μH	88 pF	22 μH	22 pF	5.3 μH	5.3 pF
2000 Ω	180 μH	44 pF	43 μH	11 pF	11 μH	2.7 pF

To get a first hint, the values of $C_2 = \frac{1}{\omega^2 L_{\ell p,s}}$ at the transition from case 1 ((over-) compensation) to case 2 (undercompensation) were computed in Table 4.1 for different reciprocals $\omega L_{\ell p}$ of the load's susceptance (π network) or reactances $\omega L_{\ell s}$ of the load (T network) at different frequencies.

Assuming that good vacuum variable capacitors offer an adjustable capacitance range of about 5 pF – 500 pF, expensive ones up to 25 pF – 4 nF (or 100 pF – 5 nF), and parasitic parallel capacitances of about 5 pF may occur, we may conclude that case 2 ($C_2 < \frac{1}{\omega^2 L_{\ell p}}$) is applicable to a π network over a wide range of $\omega L_{\ell p}$ up to 7.35 MHz provided that minimum/maximum values of L_s or C_1 do not involve additional limitations. For higher frequencies, it may be restricted to somewhat lower $\omega L_{\ell p}$, but its range is still broad, which even holds for a minimum capacitance of 30 pF.

However, the applicable range of case 2 in a T network ($C_2 > \frac{1}{\omega^2 L_{\ell s}}$) is severely restricted by the maximum capacitance of C_2. If it's 5 nF, the restrictions are comparable to those of a 30 pF minimum capacitance in a π network, but limit $\omega L_{\ell s}$ to somewhat higher values at lower frequencies. If the maximum capacitance C_2 is 500 pF, or, as in "cheaper" T networks, only 250 pF, the minimum $\omega L_{\ell s}$ required for case 2 to apply is significantly increased, even at 30 MHz.

Another limit is quite obvious if the variable inductor's Q factor is assumed to be reasonably high, say $Q \geq 100$. Then, according to Section 4.4.2, a "real world" π or T network[10] is not able to match a $R_\ell > R_i - R_{s0}$ (π network) or $G_\ell > G_i$ (T network) in our frequency range of interest due to limitations introduced by parasitic elements. (Note: Lossless networks (for which also $R_{s0} = 0$ holds) are not able to match these cases at all).

Summarising the preceding considerations yields that the simple matching strategy proposed above is applicable to the majority of load impedances. However, if the load impedance's imaginary part is inductive, $R_\ell < R_i - R_{s0}$ in a π network or $G_\ell < G_i$ in a T network, and case 2 (undercompensation) is not excluded by the minimum/maximum values of the network's elements, explicit knowledge of the network's elements, the matching frequency, and (e. g.) magnitude and phase of the network's input reflection coefficient is required to obtain the network's settings for highest active power transfer. Then it's also possible to compute the load impedance for any setting and to determine which case applies.

It's interesting to note that the "simple" part of the matching strategy was already proposed for T networks by [66], where the variable inductor was assumed to have a constant Q factor of $Q = 200$, Q-based lossless network design was used, and an iterative calculation algorithm was applied to change the numerical values of L_p and C_1 according to the losses introduced by the inductor's finite Q factor. Due to restriction of the T network's variable capacitances range[11] to 20 pF – 240 pF,

[10] Although "real world" inductor's Q factor is not constant, it can always be approximated by piecewise constant Q factors. The results of Section 4.4.2 apply to any segment and thus to the whole inductor.

[11] Depending on the results, the program used by [66] may further limit the T network's variable capacitances range to 25 pF – 235 pF or 30 pF – 230 pF.

case 2 was not observed by [66], although it should have been obtainable at higher frequencies (at least at 30 MHz) for $G_\ell < \frac{1}{50\,\Omega}$ or $\frac{1}{G_\ell} > 50\,\Omega$.

If we compare the power gain achieved by π or T networks using the (complete) optimum matching strategy described above to those of the popular (external) L networks assuming continuously variable network elements (switchable elements will be considered in Section 4.6) and a switch to realise both complementary L networks, we may conclude that according to Sections 4.3.1.1 and 4.3.1.2, an (external) L network is the optimum choice for purely resistive loads or loads exhibiting a capacitive imaginary part, but its matching range is lower compared to the appropriate π or T network made of similar network elements (refer to Section 4.4.3.2 (and Appendix C.2.1.1) where also a "cure" is given based on [3]). If the load exhibits an inductive imaginary part, it is still the optimum choice if $R_\ell > R_\mathrm{i} - R_\mathrm{s0}$ for the L network derived from a π network or $G_\ell > G_\mathrm{i}$ for the L network derived from a T network, the variable inductor's Q factor is assumed to be reasonably high, say $Q \geq 100$, and the lossy networks' "inductive" case 2 solutions are not realisable as indicated above. Then case 1 (overcompensation) applies and the highest power gain is obtained for $R_\mathrm{m} = R_\mathrm{mlim}$ or $G_\mathrm{m} = G_\mathrm{mlim}$, respectively, which yields an (external) L network. However, if $R_\ell < R_\mathrm{i} - R_\mathrm{s0}$ or $G_\ell < G_\mathrm{i}$, case 2 (undercompensation) applies and the external L network is obtained for $R_\mathrm{m} = R_{\mathrm{m}L_{\ell\mathrm{p}}}$ or $G_\mathrm{m} = G_{\mathrm{m}L_{\ell\mathrm{s}}}$. Unless $R_\ell \ll \omega L_{\ell\mathrm{p}}$ or $G_\ell \ll \frac{1}{\omega L_{\ell\mathrm{s}}}$, the resulting (external) L network's power gain may be close to or far away from the optimum. In particular, considering a variable inductor of a reasonably high constant Q factor, say $Q \geq 100$, yields a flat, broad maximum whose power gain is $\leq 0.3\,\%$ higher (derived in the last paragraph of Section 4.4.2) than the power gain of the internal L network (C_2 set to compensate $L_{\ell\mathrm{p,s}}$, and $L_\mathrm{s,p}$ and C_1 tuned to match) where case 1 and case 2 join. Depending on $L_{\ell\mathrm{p,s}}$, the external L network's $R_{\mathrm{m}L_{\ell\mathrm{p,s}}}$ may be higher or lower than the optimum R_m. If it is higher, its power gain is close to the maximum, if it is lower, its power gain may be much lower than the maximum, although the maximum's flatness helps to increase the range of $L_{\ell\mathrm{p,s}}$ where the external L network does not waste too much active power. The advantages of using an external L network are its low number of network elements and its simple tunability by measuring the magnitude of the network's input reflection coefficient.

If the variable inductor's Q factor is sufficiently high, say $Q \geq 100$, a matching strategy may be proposed based on the considerations regarding external L networks which is somewhat simpler than the optimum strategy given above. If the network's load impedance is purely resistive, exhibits a capacitive imaginary part, or an inductive imaginary part if $R_\ell > R_\mathrm{i} - R_\mathrm{s0}$ for the π network or $G_\ell > G_\mathrm{i}$ for the T network, the "simple" part of the matching strategy described above is used. If the network's load impedance exhibits an inductive imaginary part if $R_\ell < R_\mathrm{i} - R_\mathrm{s0}$ (which is approximately $R_\ell < R_\mathrm{i}$ if $R_\mathrm{i} = 50\,\Omega$ and Q is high) for the π network or $G_\ell < G_\mathrm{i}$ for the T network, we set the network's elements as close as possible to the applicable internal L network (C_2 is set to compensate as much as possible, but not to overcompensate the inductive part of the load, and $L_\mathrm{s,p}$ and C_1 are tuned to match). Then a magnitude and phase measurement of the network's in-

put reflection coefficient suffices if we (approximately) determine the network's load impedance by setting all elements of a π network to their minimum value or all elements of a T network to their maximum value and, if required, compensate the load's inductive part using C_2. The disadvantages of this matching strategy are that the minimum/maximum values may not be low/high enough at the upper/lower end of our frequency range of interest to determine the load impedance with sufficient accuracy and that in case no match gaps occur in the network's settings there is no indication which limit of the gap would yield the higher power gain. Additionally, "steps" in time varying loads would require a restart from minimum/maximum element values. All disadvantages vanish if we know the network's elements explicitly and measure the matching frequency, but then the amount of simplification compared to the optimum strategy is lowered.

Thus, depending on the affordable effort, the optimum matching stragtegy or its simplified descendant should be applied to a π or T network to obtain a high power gain. External L networks (which are somehow equal to using only the "simple" part of the optimum matching strategy in π or T networks) do not guarantee high power gains for certain loads, but are a good choice for the majority of loads.

4.6 Applicability of the optimisation method to switchable matching networks

4.6.1 Simplifying assumptions for matching networks using switchable elements

To check if the optimisation method presented above is applicable to matching networks using switchable elements instead of continuously variable elements we need to consider which simplifying assumptions may apply and what the differences are compared to continuously variable networks. (The other remaining case of a fixed inductor in series or in parallel to a continuously variable capacitor is completely described by (3.1) at matching frequency and thus part of the solution derived above.)

Firstly we assume that high-Q capacitors are used in the switchable network, whose losses are small and negligible compared to the losses of the inductor losses, which are usually made of ferrite or iron powder toroidal cores involving additional core losses.

Secondly we assume that the minimum step size of the network's capacitances and inductances is low enough to allow approximation of those capacitances and inductances by continously variable ones at matching frequency. In particular, this assumption implies the possibility of an "exact" match at the switchable network's input.

However, the losses involved do not change continuously and still exhibit resistance steps. This behaviour is clearly visible if we consider combinations of low inductance

coils, where the connecting wires' losses may not be small and thus not be negligible — e. g. switching from 80 nH + 160 nH + 320 nH = 560 nH (three coils) to 640 nH (one coil) will definitely cause a loss resistance step. Since we cannot predict the step's direction unless we know which cores and wiring are used, switchable networks behave different than continously variable ones, because the latters' losses could be described by (3.1), indicating that for an increasing inductance the losses stay constant or increase, but never decrease!

4.6.2 π network

If the parameter R_m is increased by $\Delta R_\mathrm{m} \ll R_\mathrm{m}$, thus changed from R_m to $R_\mathrm{m} + \Delta R_\mathrm{m}$, the (switchable) inductance also changes, which is accompanied by a resistance step in R_s.

We have to distinguish two cases:

1. $R_\mathrm{s}(R_\mathrm{m}) < R_\mathrm{s}(R_\mathrm{m} + \Delta R_\mathrm{m})$:
   $\Delta R_\mathrm{m} \ll R_\mathrm{m}$, thus $\frac{R_\mathrm{s}(R_\mathrm{m}+\Delta R_\mathrm{m})}{R_\mathrm{m}+\Delta R_\mathrm{m}} \approx \frac{R_\mathrm{s}(R_\mathrm{m}+\Delta R_\mathrm{m})}{R_\mathrm{m}}$ holds. Hence $\frac{R_\mathrm{s}(R_\mathrm{m})}{R_\mathrm{m}} < \frac{R_\mathrm{s}(R_\mathrm{m}+\Delta R_\mathrm{m})}{R_\mathrm{m}}$ or $\frac{1}{1+\frac{R_\mathrm{s}(R_\mathrm{m})}{R_\mathrm{m}}} > \frac{1}{1+\frac{R_\mathrm{s}(R_\mathrm{m}+\Delta R_\mathrm{m})}{R_\mathrm{m}}}$.
   Then $g_{\pi,\,\mathrm{inma}}(R_\mathrm{m}) > g_{\pi,\,\mathrm{inma}}(R_\mathrm{m} + \Delta R_\mathrm{m})$.

2. $R_\mathrm{s}(R_\mathrm{m}) > R_\mathrm{s}(R_\mathrm{m} + \Delta R_\mathrm{m})$:
   $\Delta R_\mathrm{m} \ll R_\mathrm{m}$, thus $\frac{R_\mathrm{s}(R_\mathrm{m}+\Delta R_\mathrm{m})}{R_\mathrm{m}+\Delta R_\mathrm{m}} \approx \frac{R_\mathrm{s}(R_\mathrm{m}+\Delta R_\mathrm{m})}{R_\mathrm{m}}$ holds. Hence $\frac{R_\mathrm{s}(R_\mathrm{m})}{R_\mathrm{m}} > \frac{R_\mathrm{s}(R_\mathrm{m}+\Delta R_\mathrm{m})}{R_\mathrm{m}}$ or $\frac{1}{1+\frac{R_\mathrm{s}(R_\mathrm{m})}{R_\mathrm{m}}} < \frac{1}{1+\frac{R_\mathrm{s}(R_\mathrm{m}+\Delta R_\mathrm{m})}{R_\mathrm{m}}}$.
   Then $g_{\pi,\,\mathrm{inma}}(R_\mathrm{m}) < g_{\pi,\,\mathrm{inma}}(R_\mathrm{m} + \Delta R_\mathrm{m})$.

Choosing the optimum value of R_m for continuously variable networks by the method presented above involved proving of $g_{\pi,\,\mathrm{inma}}(R_\mathrm{m}) \leq g_{\pi,\,\mathrm{inma}}(R_\mathrm{m} + \Delta R_\mathrm{m})$. Since case 2 exhibits similar behaviour of $g_{\pi,\,\mathrm{inma}}$, the method would be applicable to it. However, case 1 is critical because $g_{\pi,\,\mathrm{inma}}$ steps downward for a certain R_m and we do not know if $g_{\pi,\,\mathrm{inma}}$ will be as high or even higher than its value prior to the step within the remaining range of R_m unless we know the exact functional description of $R_\mathrm{s}(R_\mathrm{m})$ and the load and source admittance.

Usually both cases are possible — in a continuously variable matching network with a constant Q inductor and a resistive load the inductance would have a maximum throughout the (utmost) valid range of R_m indicated in (3.20) — thus it's quite likely that for increasing R_m the switchable network's inductance may pass a certain value twice for increasing and decreasing inductances, and both resistance step directions occur.

Hence there is no common optimisation for π networks using switchable elements. However, if we know the losses involved and load and source admittances, we may optimise the network elements' values for minimum losses in this particular case.

Only if the resistance steps would be small compared to the total loss resistance for a minimum inductance step between any two possible total switchable inductance values, the continuously variable network's optimisation method would be approximately applicable for the switchable network — but this assumption might not hold for small inductance values where the losses in the connecting wires might not be small and thus not be negligible.

4.6.3 T network

If the parameter G_m is increased by $\Delta G_\mathrm{m} \ll G_\mathrm{m}$, thus changed from G_m to $G_\mathrm{m} + \Delta G_\mathrm{m}$, the (switchable) inductance also changes, which is accompanied by a resistance step in R_s, hence an admittance step in G_p.

According to (A.16) $G_\mathrm{p} = \frac{R_\mathrm{s}}{R_\mathrm{s}^2+\omega^2 L_\mathrm{s}^2}$ holds. Since we assumed that L_s might be approximately descibed by a continuously variable inductance, the inductance steps are small enough to simplify calculations by using $L_\mathrm{s}(G_\mathrm{m}) \approx L_\mathrm{s}(G_\mathrm{m}+\Delta G_\mathrm{m})$. During optimisation, we additionally restricted the inductor's Q factor to $Q > 1$ (which is equal to $\omega L_\mathrm{s} > R_\mathrm{s}$), thus $\frac{\partial G_\mathrm{p}}{\partial R_\mathrm{s}} = \frac{(\omega L_\mathrm{s}-R_\mathrm{s})\,(\omega L_\mathrm{s}+R_\mathrm{s})}{(R_\mathrm{s}^2+\omega^2 L_\mathrm{s}^2)^2} > 0$ holds. Hence if there is a step in R_s, there is a step of similar direction in G_p.

Again we have to distinguish two cases:

1. $R_\mathrm{s}(G_\mathrm{m}) < R_\mathrm{s}(G_\mathrm{m} + \Delta G_\mathrm{m})$, hence $G_\mathrm{p}(G_\mathrm{m}) < G_\mathrm{p}(G_\mathrm{m} + \Delta G_\mathrm{m})$:
   $\Delta G_\mathrm{m} \ll G_\mathrm{m}$, thus $\frac{G_\mathrm{p}(G_\mathrm{m}+\Delta G_\mathrm{m})}{G_\mathrm{m}+\Delta G_\mathrm{m}} \approx \frac{G_\mathrm{p}(G_\mathrm{m}+\Delta G_\mathrm{m})}{G_\mathrm{m}}$ holds. Hence $\frac{G_\mathrm{p}(G_\mathrm{m})}{G_\mathrm{m}} < \frac{G_\mathrm{p}(G_\mathrm{m}+\Delta G_\mathrm{m})}{G_\mathrm{m}}$ or $\frac{1}{1+\frac{G_\mathrm{p}(G_\mathrm{m})}{G_\mathrm{m}}} > \frac{1}{1+\frac{G_\mathrm{p}(G_\mathrm{m}+\Delta G_\mathrm{m})}{G_\mathrm{m}}}$.
   Then $g_{\mathrm{t,\,inma}}(G_\mathrm{m}) > g_{\mathrm{t,\,inma}}(G_\mathrm{m} + \Delta G_\mathrm{m})$.

2. $R_\mathrm{s}(G_\mathrm{m}) > R_\mathrm{s}(G_\mathrm{m} + \Delta G_\mathrm{m})$, hence $G_\mathrm{p}(G_\mathrm{m}) > G_\mathrm{p}(G_\mathrm{m} + \Delta G_\mathrm{m})$:
   $\Delta G_\mathrm{m} \ll G_\mathrm{m}$, thus $\frac{G_\mathrm{p}(G_\mathrm{m}+\Delta G_\mathrm{m})}{G_\mathrm{m}+\Delta G_\mathrm{m}} \approx \frac{G_\mathrm{p}(G_\mathrm{m}+\Delta G_\mathrm{m})}{G_\mathrm{m}}$ holds. Hence $\frac{G_\mathrm{p}(G_\mathrm{m})}{G_\mathrm{m}} > \frac{G_\mathrm{p}(G_\mathrm{m}+\Delta G_\mathrm{m})}{G_\mathrm{m}}$ or $\frac{1}{1+\frac{G_\mathrm{p}(G_\mathrm{m})}{G_\mathrm{m}}} < \frac{1}{1+\frac{G_\mathrm{p}(G_\mathrm{m}+\Delta G_\mathrm{m})}{G_\mathrm{m}}}$.
   Then $g_{\mathrm{t,\,inma}}(G_\mathrm{m}) < g_{\mathrm{t,\,inma}}(G_\mathrm{m} + \Delta G_\mathrm{m})$.

Choosing the optimum value of G_m for continuously variable networks by the method presented above involved proving of $g_{\mathrm{t,\,inma}}(G_\mathrm{m}) \leq g_{\mathrm{t,\,inma}}(G_\mathrm{m} + \Delta G_\mathrm{m})$. Since case 2 exhibits similar behaviour of $g_{\mathrm{t,\,inma}}$, the method would be applicable to it. However, case 1 is critical because $g_{\mathrm{t,\,inma}}$ steps downward for a certain G_m and we do not know if $g_{\mathrm{t,\,inma}}$ will be as high or even higher than its value prior to the step within the remaining range of G_m unless we know the exact functional description of $G_\mathrm{p}(G_\mathrm{m})$ and the load and source impedance.

Usually both cases are possible — in a continuously variable matching network with a constant Q inductor and a resistive load the inductance would have a minimum throughout the (utmost) valid range of G_m indicated in (3.33) — thus it's quite likely that for increasing G_m the switchable network's inductance may pass a certain value

twice for decreasing and increasing inductances, and both resistance step directions occur.

Hence there is no common optimisation for T networks using switchable elements. However, if we know the losses involved and load and source admittances, we may optimise the network elements' values for minimum losses in this particular case.

Only if the resistance steps would be small compared to the total loss resistance for a minimum inductance step between any two possible total switchable inductance values, the continuously variable network's optimisation method would be approximately applicable for the switchable network — but this assumption might not hold for small inductance values where the losses in the connecting wires might not be small and thus not be negligible.

Chapter 5

Transmission Lines' and Total Losses in a Source, Line 1, Matching Network, Line 2, and Load System

5.1 Introduction

The active power transfer of a transmission line (Figure 2.1) or of a system consisting of a matching network enclosed by two transmission lines (Figure 2.3) was already derived in Section 2.6 or 2.7, respectively.

In the following chapter, we optimise the active power transfer of those systems.

Firstly we consider a transmission line, secondly the matching system involving lossless and lossy matching networks to distinguish different loss origins. Optimisation of the matching system includes optimised splitting of the total line length (although the total line length is usually fixed by a given distance between source and load, the position of the matching network may be optimised). Finally an optimum compromise is proposed which is applicable to unknown or changing load impedances.

Throughout the chapter, all transmission lines are considered to have a complex characteristic impedances. Based on the equations derived, we will be able to distinguish parts of the system where we may approximately use real characteristic impedances instead from parts where we always have to use complex ones.

5.2 Definitions/notations

From this chapter on, the following definitions/notations will be used:

Latin letters

$B_{\ell,\,\mathrm{MB}}$	Load susceptance of a matchbox
$C_{0\mathrm{p}}$	(Equivalent) parallel capacitance calculated from the imaginary part of $\frac{1}{\underline{Z}_0}$
$C_{0\mathrm{s}}$	(Equivalent) series capacitance calculated from the imaginary part of $\underline{Z}_0$
$C_{1\mathrm{tot}}$	Total source capacitance (including C_1 of the network and the source's (equivalent) capacitance)
$C_{\ell\mathrm{p},\,\mathrm{MB}}$	(Equivalent) parallel load capacitance of a matchbox, calculated from $B_{\ell,\,\mathrm{MB}}$ (π network)
$C_{\ell\mathrm{s},\,\mathrm{MB}}$	(Equivalent) series load capacitance of a matchbox, calculated from $X_{\ell,\,\mathrm{MB}}$ (T network)
$g_{\mathrm{tot},\,\mathrm{ll},\,\mathrm{inma}}$	Power gain of the complete matching system whose lossless matchbox is exactly matched at its input
$g_{\mathrm{tot},\,\mathrm{inma}}$	Power gain of the complete matching system whose matchbox is exactly matched at its input
$g_{\mathrm{tot},\,\mathrm{t},\,\mathrm{inma}}$	Power gain of the complete matching system whose T network is exactly matched at its input
$g_{\mathrm{tot},\,\pi,\,\mathrm{inma}}$	Power gain of the complete matching system whose π network is exactly matched at its input
g_{Lopt}	Power gain of a transmission line with $X_0 \neq 0$ whose load is the optimum load impedance $\underline{Z}_{\ell\mathrm{opt}}$
$g_{\mathrm{MB},\,\mathrm{inma}}$	Power gain of a matchbox exactly matched at its input
$g_{\mathrm{MB},\,\mathrm{inma}}(\underline{r}_{\ell\mathrm{MB}})$	Power gain of a matchbox exactly matched at its input as a function of $\underline{r}_{\ell\mathrm{MB}}$
$g_{\mathrm{MB},\,\mathrm{ll},\,\mathrm{inma}}$	Power gain of a lossless matchbox exactly matched at its input
$g_{\mathrm{MB},\,\mathrm{ll},\,\mathrm{inma}}(\underline{r}_{\ell\mathrm{MB}})$	Power gain of a lossless matchbox exactly matched at its input as a function of $\underline{r}_{\ell\mathrm{MB}}$
$g_{\mathrm{T,Lopt}}$	Transducer power gain of a transmission line with $X_0 \neq 0$ whose load is the optimum load impedance $\underline{Z}_{\ell\mathrm{opt}}$
$g_{\mathrm{Ttot},\,\mathrm{inma}}$	Transducer power gain of the complete matching system whose matchbox is exactly matched at its input
G'	Per-unit-length conductance of a transmission line
$G_{0\mathrm{s}}$	Inverse of the real part of $\underline{Z}_0$
$G_{\ell,\,\mathrm{MB}}$	In case of a π network, load conductance (real part of load admittance) of that network (matchbox), in case of a T network, $G_{\ell,\,\mathrm{MB}} = \frac{1}{R_{\ell,\,\mathrm{MB}}}$, where R_ℓ is the load resistance (real part of load impedance of that network (matchbox))
$l_{2,m,\pm}$	Length of transmission line 2 where (depending on sign $\pm$) the m-th maximum or minimum of $\mathrm{e}^{2\alpha l_{\mathrm{tot}}}\, g_{\mathrm{tot},\,\mathrm{ll},\,\mathrm{inma}}$ occurs
l_{tot}	Total length of lines in a complete matching system ($l_{\mathrm{tot}} = l_1 + l_2$)
L'	Per-unit-length inductance of a transmission line
$L_{1\mathrm{tot}}$	Total source inductance (including C_1 of the network and the source's (equivalent) inductance)
$L_{\ell\mathrm{p},\,\mathrm{MB}}$	(Equivalent) parallel load inductance of a matchbox, calculated from $B_{\ell,\,\mathrm{MB}}$ (π network)
$L_{\ell\mathrm{s},\,\mathrm{MB}}$	(Equivalent) series load inductance of a matchbox, calculated from $X_{\ell,\,\mathrm{MB}}$ (T network)
m	Whole number (integer)
$P_{\mathrm{act}}(z)$	Active power transferred to the "load" of a transmission line at location z
P_{act1opt}	Active power transferred to the input of a transmission line whose $X_0 \neq 0$ terminated with $\underline{Z}_{\ell\mathrm{opt}}$
$\underline{r}_{1\mathrm{t},\,\mathrm{inma}}$	Reflection coefficient at the input of a T network exactly matched at its input (referred to $\underline{Z}_0$)
$\underline{r}_{1\pi,\,\mathrm{inma}}$	Reflection coefficient at the input of a π network exactly matched at its input (referred to $\underline{Z}_0$)
$\underline{r}_{1\mathrm{MB}}$	Reflection coefficient at the input of a matchbox (referred to $\underline{Z}_0$)
$\underline{r}_{1\mathrm{MB},\,\mathrm{inma}}$	Reflection coefficient at the input of a matchbox exactly matched at its input (referred to $\underline{Z}_0$)
$\underline{r}_{\ell\mathrm{opt}}$	Resulting valid reflection coefficient of the optimum load impedance of a transmission line with $X_0 \neq 0$ (referred to $\underline{Z}_0$)
$\underline{r}_{\ell\mathrm{MB}}$	Reflection coefficient at a matchbox's load (referred to $\underline{Z}_0$)
$R_{0\mathrm{p}}$	Inverse of the real part of $\frac{1}{\underline{Z}_0}$

$R_{\ell,\,\mathrm{MB}}$	In case of a T network, load resistance (real part of load impedance) of that network (matchbox), in case of a π network, $R_{\ell,\,\mathrm{MB}} = \frac{1}{G_{\ell,\,\mathrm{MB}}}$, where $G_{\ell,\,\mathrm{MB}}$ is the load conductance (real part of load admittance of that network (matchbox))
$X_{\ell,\,\mathrm{MB}}$	Load reactance of a matchbox
z	Location along a transmission line, range 0 to length of transmission line
$\underline{Z}_{0\mathrm{MB1}}$	Reference impedance of the reflection coefficients at a matchbox's input
$\underline{Z}_{0\mathrm{MB2}}$	Reference impedance of the reflection coefficients at a matchbox's output
$\underline{Z}_1$	Impedance at the beginning of a transmission line (at its input)
$\underline{Z}_{\mathrm{iopt}}$	Optimum source impedance for a transmission line with $X_0 \neq 0$ whose load is the optimum load impedance $\underline{Z}_{\ell\mathrm{opt}}$
$\underline{Z}_{\ell\mathrm{MB}}$	Load impedance of a matchbox
$\underline{Z}_{\ell\mathrm{opt}}$	Resulting optimum load impedance of a transmission line with $X_0 \neq 0$

Greek letters

$\varphi_{\underline{r}\,\ell}$	Phase of reflection coefficient $\underline{r}_\ell$

5.3 Losses and matching in a source, transmission line, and load system

The power gain g_L of a source, transmission line, and load system (depicted in Figure 2.1) is given by (2.23),

$$g_\mathrm{L} = \mathrm{e}^{-2\alpha l}\,\frac{R_0\,(1-|\underline{r}_\ell|^2) - 2X_0\,\mathrm{Im}\{\underline{r}_\ell\}}{R_0\,(1-\mathrm{e}^{-4\alpha l}\,|\underline{r}_\ell|^2) - 2X_0\,\mathrm{e}^{-2\alpha l}\,\mathrm{Im}\{\underline{r}_\ell\,\mathrm{e}^{-\mathrm{j}2\beta l}\}}$$

$$g_\mathrm{L} = \mathrm{e}^{-2\alpha l}\,\frac{R_0\,(1-\underline{r}_\ell\,\underline{r}_\ell^*) + \mathrm{j}X_0\,(\underline{r}_\ell - \underline{r}_\ell^*)}{R_0\,(1-\mathrm{e}^{-4\alpha l}\,\underline{r}_\ell\,\underline{r}_\ell^*) + \mathrm{j}X_0\,\mathrm{e}^{-2\alpha l}\,(\underline{r}_\ell\,\mathrm{e}^{-\mathrm{j}2\beta l} - \underline{r}_\ell^*\,\mathrm{e}^{\mathrm{j}2\beta l})},$$

which will be optimised for a fixed[1] length $l > 0$ by changing $\underline{r}_\ell$. If the method described in [26g] is applied (as mentioned at the end of Appendix A.3, calculation of $P_\mathrm{act}(z)$ in [26g] does not include all dependencies on $\underline{r}_\ell$ and, furthermore, then $P_\mathrm{act}(z)$ is optimised in [26g] instead of g_L, where $P_\mathrm{act}(z)$ is the active power transferred to the "load" of a transmission line at location z as defined in (A.8)), we obtain

$$\begin{aligned}\frac{\partial g_\mathrm{L}}{\partial \underline{r}_\ell^*} = {} & \big[\mathrm{j}R_0X_0\,\mathrm{e}^{-2\alpha l}\,(\mathrm{e}^{-2\alpha l} - \mathrm{e}^{-\mathrm{j}2\beta l})\,\underline{r}_\ell^2 \\ & - \big(R_0^2\,(1-\mathrm{e}^{-4\alpha l}) + X_0^2\,\mathrm{e}^{-2\alpha l}\,(\mathrm{e}^{\mathrm{j}2\beta l} - \mathrm{e}^{-\mathrm{j}2\beta l})\big)\,\underline{r}_\ell \\ & - \mathrm{j}R_0X_0\,(1-\mathrm{e}^{-2\alpha l}\,\mathrm{e}^{\mathrm{j}2\beta l})\big]\,\frac{\mathrm{e}^{-2\alpha l}}{\big(R_0(1-\mathrm{e}^{-4\alpha l}\,\underline{r}_\ell\,\underline{r}_\ell^*) + \mathrm{j}X_0\,\mathrm{e}^{-2\alpha l}\,(\underline{r}_\ell\,\mathrm{e}^{-\mathrm{j}2\beta l} - \underline{r}_\ell^*\,\mathrm{e}^{\mathrm{j}2\beta l})\big)^2},\end{aligned}$$

[1] An optimisation with respect to the transmission line's length l is impossible because lossy transmission lines are passive. Thus $\frac{\partial g_\mathrm{L}}{\partial l} \leq 0$, causing g_L to decrease from $g_\mathrm{L} = 1$ at $l = 0$ for increasing l and a given (constant) $\underline{r}_\ell$. $\frac{\partial g_\mathrm{L}}{\partial l} = 0$ may indicate a (single) maximum if $l = 0$, but only an inflexion point if $l > 0$.

$$\frac{\partial g_{\mathrm{L}}}{\partial \underline{r}_\ell} = \left[-\mathrm{j}R_0X_0\,\mathrm{e}^{-2\alpha l}\left(\mathrm{e}^{-2\alpha l}-\mathrm{e}^{\mathrm{j}2\beta l}\right)\left(\underline{r}_\ell^*\right)^2 - \left(R_0^2\left(1-\mathrm{e}^{-4\alpha l}\right)+X_0^2\,\mathrm{e}^{-2\alpha l}\left(\mathrm{e}^{-\mathrm{j}2\beta l}-\mathrm{e}^{\mathrm{j}2\beta l}\right)\right)\underline{r}_\ell^* + \mathrm{j}R_0X_0\left(1-\mathrm{e}^{-2\alpha l}\,\mathrm{e}^{-\mathrm{j}2\beta l}\right)\right] \frac{\mathrm{e}^{-2\alpha l}}{\left(R_0\left(1-\mathrm{e}^{-4\alpha l}\,\underline{r}_\ell\,\underline{r}_\ell^*\right)+\mathrm{j}X_0\,\mathrm{e}^{-2\alpha l}\left(\underline{r}_\ell\,\mathrm{e}^{-\mathrm{j}2\beta l}-\underline{r}_\ell^*\,\mathrm{e}^{\mathrm{j}2\beta l}\right)\right)^2}.$$

The ratio following the term in squared brackets never equals zero, thus an extremum exists only if the term in squared brackets equals zero. Since the terms in squared brackets of $\frac{\partial g_{\mathrm{L}}}{\partial \underline{r}_\ell^*}$ and $\frac{\partial g_{\mathrm{L}}}{\partial \underline{r}_\ell}$ are just the conjugate complex of each other, both partial derivatives are simultaneously zero, hence the extremum of g_{L} requires $\frac{\partial g_{\mathrm{L}}}{\partial \underline{r}_\ell^*} = 0 = \frac{\partial g_{\mathrm{L}}}{\partial \underline{r}_\ell}$ to hold and only one of both partial derivatives has to be considered — $\frac{\partial g_{\mathrm{L}}}{\partial \underline{r}_\ell^*}$ is more convenient for optimisation with respect to $\underline{r}_\ell$.

Since derivation of the optimum load and source impedance is quite lengthy, it is performed in Appendix D.2. The results are summarised below.

The solution involves two different cases, in particular:

1. $X_0 = 0$

   If $\alpha > 0$, the transmission line is either Heaviside's distortionless transmission line obtained for $\frac{R'}{\omega L'} = \frac{G'}{\omega C'} > 0$ and $\underline{Z}_0 = Z_{0\mathrm{ll}}$ (where G' is the per-unit-length conductance and $L' = Z_{0\mathrm{ll}}^2 C'$ the per-unit-length inductance of that line, defined in [26a]) or the approximation (2.5) is used. Then $\underline{r}_\ell = 0$ uniquely solves the equation, thus $\underline{Z}_\ell = Z_{0\mathrm{ll}}$ yields the maximum g_{L}. If we terminate the line accordingly, its input resistance $\underline{Z}_1 = Z_{0\mathrm{ll}}$, hence the source's impedance has to be $\underline{Z}_{\mathrm{i}} = Z_{0\mathrm{ll}}$ to achieve maximum active input power. In particular, optimum source and load impedance is independent of (frequency and) line length.

   If $\alpha = 0$, the transmission line is lossless, hence $\frac{R'}{\omega L'} = \frac{G'}{\omega C'} = 0$. Then $g_{\mathrm{L}} = 1$ for any $\underline{Z}_\ell$. However, according to (2.20) only a choice of $\underline{Z}_\ell = \underline{Z}_0 = Z_{0\mathrm{ll}}$ combined with $\underline{Z}_{\mathrm{i}} = Z_{0\mathrm{ll}}$ yields a source impedance for maximum active power input which is independent of (frequency and) line length — thus no other choice is appropriate.

2. $X_0 \neq 0$

   In (D.1), (D.2), and (D.3), the optimum load reflection coefficient is given by

$$\underline{r}_{\ell\mathrm{opt}} = \frac{\sqrt{\left(R_0^2\cosh(2\alpha l)+X_0^2\cos(2\beta l)\right)^2-|\underline{Z}_0|^4}-R_0^2\sinh(2\alpha l)-\mathrm{j}X_0^2\sin(2\beta l)}{\mathrm{j}R_0X_0\,\mathrm{e}^{-\mathrm{j}2\beta l}\left(1-\mathrm{e}^{-2\alpha l}\,\mathrm{e}^{\mathrm{j}2\beta l}\right)}, \tag{5.1}$$

   yielding an optimum load impedance of

$$\underline{Z}_{\ell\mathrm{opt}} = \frac{\sqrt{\left(R_0^2\cosh(2\alpha l)+X_0^2\cos(2\beta l)\right)^2-|\underline{Z}_0|^4}-\mathrm{j}R_0X_0(\cosh(2\alpha l)-\cos(2\beta l))}{R_0\sinh(2\alpha l)+X_0\sin(2\beta l)} \tag{5.2}$$

and an optimum power gain of

$$g_{\mathrm{Lopt}} = \frac{R_0^2\cosh(2\alpha l)+X_0^2\cos(2\beta l)-\sqrt{\left(R_0^2\cosh(2\alpha l)+X_0^2\cos(2\beta l)\right)^2-|\underline{Z}_0|^4}}{|\underline{Z}_0|^2}. \tag{5.3}$$

If the transmission line is terminated by its optimum load impedance, its input impedance is the complex conjugate of the optimum load impedance.

To achieve maximum active input power, the source impedance has to be equal to the complex conjugate of the line's input impedance, hence $\underline{Z}_{\mathrm{iopt}} = \underline{Z}_{\ell\mathrm{opt}}$. If the source impedance is chosen accordingly, the active input power is $P_{\mathrm{act1opt}} = P_{\mathrm{actmaxi}}$, thus $g_{\mathrm{T,Lopt}} = g_{\mathrm{Lopt}}$. Additionally, the line's output impedance is equal to the complex conjugate of its optimum load impedance. Optimum active power input and transfer involves complex conjugate matching at the line's in- and output.

But, compared to a transmission line whose characteristic impedance is real ($X_0 = 0$), the optimum load in case of a complex characteristic has a severe disadvantage — it depends on **frequency and line length** — thus, depending on frequency and line length, different load and source impedances would have to be used.

To choose a useful length independent load impedance close to the optimised load, the limits for $l \to 0$ and $l \to \infty$ were considered in Appendix D.2. Those limits give us a hint which length independent choice of source and load impedance is recommendable. $\underline{Z}_\ell = \underline{Z}_0^* = \underline{Z}_{\mathrm{i}}$ (which is still frequency dependent), is far from the optimum value if the line's length is short, but increasingly close to the optimum value[2], if the line's length increases, in particular, if $\alpha l \geq 1.5$ holds.

Considering a coaxial transmission line whose complex characteristic impedance is given by $\underline{Z}_0 \approx Z_{0\mathrm{ll}}\left(1 - \mathrm{j}\,\frac{\alpha}{\beta}\right)$ according to (2.4) where $\frac{\alpha}{\beta} \ll 1$, the typical choice of $\underline{Z}_\ell = \underline{Z}_{\mathrm{i}} = R_0 \approx Z_{0\mathrm{ll}}$ (which is independent of length and frequency!) slightly differs from the preceding one[3].

Nevertheless, since αl should be low to ensure low line losses, it's not obvious that the choice indicated above is truly recommendable, but we should keep

---

[2]However, if source and load impedances are chosen accordingly, a complex conjugate match at the line's input can only be achieved for high values of l because $\underline{Z}_1 \neq \underline{Z}_0$ (except for $l \to \infty$), hence $g_{\mathrm{L}} = \frac{|\underline{Z}_0|^2}{R_0^2+X_0^2\,\mathrm{e}^{-2\alpha l}(2\cos(2\beta l)-\mathrm{e}^{-2\alpha l})}\,\mathrm{e}^{-2\alpha l}$ differs from $g_{\mathrm{T,L}} = \frac{R_0^2|\underline{Z}_0|^2}{R_0^4+2R_0^2X_0^2\,\mathrm{e}^{-2\alpha l}\cos(2\beta l)+X_0^4\,\mathrm{e}^{-4\alpha l}}\,\mathrm{e}^{-2\alpha l}$ (except for $l \to \infty$).

[3] However, if source and load impedances are equal to R_0, thus $\underline{r}_\ell = \underline{r}_{\mathrm{i}} = \frac{X_0}{\mathrm{j}2R_0-X_0}$, a complex conjugate match at the line's input cannot be achieved for any value of l because $\underline{Z}_1 \neq R_0$, hence $g_{\mathrm{L}} = \frac{2R_0|\underline{Z}_0|^2}{2R_0^3+X_0^2\,\mathrm{e}^{-2\alpha l}(R_0(\sinh(2\alpha l)+2\cos(2\beta l))-X_0\sin(2\beta l))}\,\mathrm{e}^{-2\alpha l}$ differs from $g_{\mathrm{T,L}} = \frac{16R_0^2|\underline{Z}_0|^2}{\left(4R_0^2+X_0^2\right)^2+X_0^2\,\mathrm{e}^{-2\alpha l}\left(8R_0(R_0\cos(2\beta l)-X_0\sin(2\beta l))+X_0^2(\mathrm{e}^{-2\alpha l}-2\cos(2\beta l))\right)}\,\mathrm{e}^{-2\alpha l}$.

in mind that the goal is not to choose source and load impedances as close as possible to its optimum impedance values, but to achieve a power gain as close as possible to its optimum value.

The latter holds for coaxial transmission line whose complex characteristic impedance is given by (2.4) and $\frac{\alpha}{\beta} \ll 1$. Then either a choice of source and load impedances equal to $\underline{Z}_0^*$ or equal to R_0 ensures a low deviation of power gain and transducer power gain from its optimum values, which would be 1.6% higher at 1.8 MHz and 0.4% higher at 30 MHz if e. g. a RG-213/U coaxial cable would be used.

5.4 Losses and matching in a source, line 1, matching network, line 2, and load system

5.4.1 Power gain of the system

In the preceding section, we investigated the active power transfer in transmission lines whose characteristic impedances were complex. We derived the optimum load impedance for maximum active power transfer and its according optimum source impedance for maximum active input power, which were both equal and depended on line length and frequency.

Compared to a (lossy) transmission line whose characteristic impedance is real or is approximated as real, it's not obvious that the insertion of a two-port, a matching network which is designed to match the line's characteristic impedance at its input, is suited to optimise the active power transfer to the load.

However, in our application all transmission lines have a complex characteristic impedance of the kind $\underline{Z}_0 \approx Z_{0\mathrm{II}}\,(1 - \mathrm{j}\,\frac{\alpha}{\beta})$, where $\frac{\alpha}{\beta} \ll 1$, and the source impedance is real and equal to $Z_{0\mathrm{II}} \approx R_0$.

At the end of the preceding section, we discovered that the active power transfer in such transmission lines is close to maximum if source and load impedances are equal to R_0. Hence we suppose that the insertion of a matching network as indicated above is recommendable, decreases line losses, and increases the active power transfer to the load. Another advantage is that the network may be tuned quite easily by measuring its input reflection coefficient.

Besides network element values, the position of the matching network is variable. Thus we have to consider a matching network embedded in two transmission lines of variable lengths connecting to source and load. Both lines have complex characteristic impedances to investigate its impact on active power transfer.

To derive the power gain $g_{\mathrm{tot,\,inma}}$ of the complete system depicted in Figure 2.3 consisting of a source (source impedance $\underline{Z}_\mathrm{i}$), a transmission line 1 connecting it to the input of a matching network, a transmission line 2 connecting the output of the matching network to the load (load impedance $\underline{Z}_\ell$). The matching network

is tuned to match the characteristic impedance of line 1 at its input. To denote network specific variables, the index "MB" (matchbox) is used instead of the index "tp" (two-port) which was used in Section 2.7.

To simplify calculations, we assume line 1 and 2 to be similar, hence both complex characteristic impedances, attenuation constants, and phase constants are equal, and we define $\underline{Z}_0 = \underline{Z}_{01} = \underline{Z}_{02}$, $\alpha = \alpha_1 = \alpha_2$, and $\beta = \beta_1 = \beta_2$. Then the matching network's reference impedances should also be similar and equal to the characteristic impedance of the lines, $\underline{Z}_0 = \underline{Z}_{0\mathrm{MB1}} = \underline{Z}_{0\mathrm{MB2}}$.

The lengths of the transmission lines, l_1 and l_2, may be chosen arbitrarily, but the total length

$$l_{\mathrm{tot}} = l_1 + l_2 \tag{5.4}$$

is given.

We (usually) also need to know $\underline{Z}_\ell$ or $\underline{r}_\ell$, respectively, which is transformed to $\underline{r}_{\ell\mathrm{MB}} = \underline{r}_{12} = \underline{r}_\ell \, \mathrm{e}^{-2\alpha l_2} \, \mathrm{e}^{-\mathrm{j}2\beta l_2}$ at the input of line 2 according to (2.20).

It's further transformed by the matching network, which is designed (or tuned) to match the characteristic impedance of line 1 at its input, hence

$$\underline{r}_{1\mathrm{MB}} = \underline{r}_{1\mathrm{MB,\,inma}} = 0.$$

The matched network's power gain is given by

$$g_{\mathrm{MB,\,inma}}(\underline{r}_{\ell\mathrm{MB}}) = g_{\mathrm{MB,\,inma}}\left(\underline{r}_\ell \, \mathrm{e}^{-2\alpha l_2} \, \mathrm{e}^{-\mathrm{j}2\beta l_2}\right).$$

From (2.27) we obtain

$$\begin{aligned} g_{\mathrm{tot,\,inma}} \;=\; & \mathrm{e}^{-2\alpha l_{\mathrm{tot}}} \cdot 1 \cdot g_{\mathrm{MB,\,inma}}\left(\underline{r}_\ell \, \mathrm{e}^{-2\alpha l_2} \, \mathrm{e}^{-\mathrm{j}2\beta l_2}\right) \\ & \cdot \frac{R_0\left(1 - |\underline{r}_\ell|^2\right) - 2X_0 \,\mathrm{Im}\{\underline{r}_\ell\}}{R_0\left(1 - \mathrm{e}^{-4\alpha l_2}\,|\underline{r}_\ell|^2\right) - 2X_0\,\mathrm{e}^{-2\alpha l_2}\,\mathrm{Im}\left\{\underline{r}_\ell\,\mathrm{e}^{-\mathrm{j}2\beta l_2}\right\}}, \end{aligned} \tag{5.5}$$

which has to be maximised in the following sections.

However, prior to the optimisation we have to consider the source impedance $\underline{Z}_{\mathrm{i}}$ because the active input power will depend on it. The matching network is designed to match the characteristic impedance of line 1 at its input, $\underline{r}_{1\mathrm{MB}} = \underline{r}_{21} = 0$. Then $\underline{r}_{11} = 0$ or $\underline{Z}_{11} = \underline{Z}_0$ according to (2.20). If $\underline{r}_{\mathrm{i}}$ is chosen arbitrarily, application of (2.26) gives

$$\begin{aligned} g_{\mathrm{Ttot,\,inma}} \;=\; & \mathrm{e}^{-2\alpha l_{\mathrm{tot}}} \cdot \frac{R_0\left(R_0\left(1 - |\underline{r}_{\mathrm{i}}|^2\right) - 2X_0\,\mathrm{Im}\{\underline{r}_{\mathrm{i}}\}\right)}{|\underline{Z}_0|^2} \cdot g_{\mathrm{MB,\,inma}}\left(\underline{r}_\ell \, \mathrm{e}^{-2\alpha l_2} \, \mathrm{e}^{-\mathrm{j}2\beta l_2}\right) \\ & \cdot \frac{R_0\left(1 - |\underline{r}_\ell|^2\right) - 2X_0\,\mathrm{Im}\{\underline{r}_\ell\}}{R_0\left(1 - \mathrm{e}^{-4\alpha l_2}\,|\underline{r}_\ell|^2\right) - 2X_0\,\mathrm{e}^{-2\alpha l_2}\,\mathrm{Im}\left\{\underline{r}_\ell\,\mathrm{e}^{-\mathrm{j}2\beta l_2}\right\}}. \end{aligned} \tag{5.6}$$

Maximisation of the active input power requires $\underline{Z}_{\mathrm{i}} = \underline{Z}_0^*$, which is equivalent to $\underline{r}_{\mathrm{i}} = -\mathrm{j}\,\frac{X_0}{R_0}$ as indicated in (2.19) and yields an active input power of P_{actmaxi}. Then the source and load related "correction factor" of line 1 in $g_{\mathrm{Ttot,\,inma}}$ becomes

$$\frac{R_0\left(R_0\left(1 - |\underline{r}_{\mathrm{i}}|^2\right) - 2X_0\,\mathrm{Im}\{\underline{r}_{\mathrm{i}}\}\right)}{|\underline{Z}_0|^2} = 1.$$

However, in our application the line's characteristic impedance is $\underline{Z}_0 \approx Z_{0\mathrm{ll}}\,(1 - \mathrm{j}\,\frac{\alpha}{\beta})$ and the source impedance is $\underline{Z}_\mathrm{i} = Z_{0\mathrm{ll}}\ (\approx R_0)$.
From (2.9) we obtain $\underline{r}_\mathrm{i} = \frac{-\mathrm{j}X_0}{2R_0+\mathrm{j}X_0} \approx \frac{\mathrm{j}\frac{\alpha}{\beta}}{2\,(1-\mathrm{j}\frac{\alpha}{2\beta})} \approx \frac{\alpha}{2\beta}\,(\mathrm{j} - \frac{\alpha}{2\beta})$. Then the source and load related "correction factor" of line 1 in $g_{\mathrm{Ttot,\,inma}}$ is given by

$$\frac{R_0\left(R_0\left(1-|\underline{r}_\mathrm{i}|^2\right)-2X_0\,\mathrm{Im}\{\underline{r}_\mathrm{i}\}\right)}{|\underline{Z}_0|^2} = \frac{4R_0^2}{4R_0^2+X_0^2} \approx \frac{1}{1+\frac{\alpha^2}{4\beta^2}} \approx 1 - \frac{\alpha^2}{4\beta^2},$$

which is close to 1 because $\frac{\alpha}{\beta} \ll 1$, e. g. for a RG-213/U coaxial cable it's 0.999927 at 1.8 MHz and 0.999995 at 30 MHz.

The situation changes if the matching network is designed to match $Z_{0\mathrm{ll}}$, which is approximately equal to $\underline{Z}_0$. Then $\underline{r}_\mathrm{i} = \underline{r}_{1\mathrm{MB}} = \frac{-\mathrm{j}X_0}{2R_0+\mathrm{j}X_0} \approx \frac{\mathrm{j}\frac{\alpha}{\beta}}{2\,(1-\mathrm{j}\frac{\alpha}{2\beta})} \approx \frac{\alpha}{2\beta}\,(\mathrm{j} - \frac{\alpha}{2\beta})$ and the matching network's input is not (exactly) matched to the line's charateristic impedance.

According to (2.27) and g_L in Footnote [3], the load related "correction factor" of line 1 in $g_{\mathrm{tot,\,inma}}$ changes from 1 to

$$\begin{aligned}
&\frac{R_0\left(1-|\underline{r}_{1\mathrm{MB}}|^2\right)-2X_0\,\mathrm{Im}\{\underline{r}_{1\mathrm{MB}}\}}{R_0\left(1-\mathrm{e}^{-4\alpha l_1}\,|\underline{r}_{1\mathrm{MB}}|^2\right)-2X_0\,\mathrm{e}^{-2\alpha l_1}\,\mathrm{Im}\{\underline{r}_{1\mathrm{MB}}\,\mathrm{e}^{-\mathrm{j}2\beta l_1}\}} \\
&= \frac{2R_0|\underline{Z}_0|^2}{2R_0^3+X_0^2\,\mathrm{e}^{-2\alpha l_1}\,(R_0(\sinh(2\alpha l_1)+2\cos(2\beta l_1))-X_0\sin(2\beta l_1))} \\
&= \frac{1+\frac{\alpha^2}{\beta^2}}{1+\frac{\alpha^2}{2\beta^2}\,\mathrm{e}^{-2\alpha l_1}\left(\sinh(2\alpha l_1)+2\cos(2\beta l_1)+\frac{\alpha}{\beta}\sin(2\beta l_1)\right)} \\
&\approx 1 - \frac{\alpha^2}{4\beta^2}\left(\mathrm{e}^{-2\alpha\,(l_\mathrm{tot}-l_2)}\left(4\cos(2\beta\,(l_\mathrm{tot}-l_2)\right) - \mathrm{e}^{-2\alpha\,(l_\mathrm{tot}-l_2)}\right) - 3\Big),
\end{aligned}$$

where $l_1 = l_\mathrm{tot} - l_2$ was applied. Since $\frac{\alpha}{\beta} \ll 1$, the "correction factor" is still close to 1, e. g. for a RG-213/U coaxial cable it's between 1 and 1.0003 at 1.8 MHz and between 1 and 1.00004 at 30 MHz.

According to (2.26) and $g_{\mathrm{T,\,L}}$ in Footnote [3], the source and load related "correction factor" of line 1 in $g_{\mathrm{Ttot,\,inma}}$ changes from $\frac{R_0\left(R_0\left(1-|\underline{r}_\mathrm{i}|^2\right)-2X_0\,\mathrm{Im}\{\underline{r}_\mathrm{i}\}\right)}{|\underline{Z}_0|^2}$ to

$$\begin{aligned}
&\frac{\left(R_0\,(1-|\underline{r}_\mathrm{i}|^2)-2X_0\,\mathrm{Im}\{\underline{r}_\mathrm{i}\}\right)^2}{|\underline{Z}_0|^2\,|1-\underline{r}_\mathrm{i}^2\,\mathrm{e}^{-2\alpha l_1}\,\mathrm{e}^{-\mathrm{j}2\beta l_1}|^2} \\
&= \frac{16R_0^2\,|\underline{Z}_0|^2}{\left(4R_0^2+X_0^2\right)^2+X_0^2\,\mathrm{e}^{-2\alpha l_1}\left(8R_0(R_0\cos(2\beta l_1)-X_0\sin(2\beta l_1))+X_0^2\left(\mathrm{e}^{-2\alpha l_1}-2\cos(2\beta l_1)\right)\right)} \\
&= \frac{1+\frac{\alpha^2}{\beta^2}}{1+\frac{\alpha^2}{2\beta^2}\left(1+\mathrm{e}^{-2\alpha l_1}\left(\cos(2\beta l_1)+\frac{\alpha}{\beta}\sin(2\beta l_1)\right)+\frac{\alpha^2}{8\beta^2}\left(1+\mathrm{e}^{-2\alpha l_1}\left(\mathrm{e}^{-2\alpha l_1}-2\cos(2\beta l_1)\right)\right)\right)} \\
&\approx 1 - \frac{\alpha^2}{2\beta^2}\left(\mathrm{e}^{-2\alpha\,(l_\mathrm{tot}-l_2)}\cos(2\beta\,(l_\mathrm{tot}-l_2)) - 1\right),
\end{aligned}$$

where $l_1 = l_\mathrm{tot} - l_2$ was applied. Since $\frac{\alpha}{\beta} \ll 1$, the "correction factor" is close to 1, e. g. for a RG-213/U coaxial cable it's between 1 and 1.0006 at 1.8 MHz and between 1 and 1.00002 at 30 MHz.

Regarding the values of the "correction factors" of line 1, we should keep in mind that both are multiplied by $\mathrm{e}^{-2\alpha l_1}$, thus the "complete" factors are always ≤ 1. Surprisingly the approximate design is slightly better than exact matching and its according source impedance choice, but that just reflects that both cases differ from the optimum derived in the preceding section (since $g_{\mathrm{Lopt}} = g_{\mathrm{T,\,Lopt}}$, the "correction factors" of the optimum are equal, e. g. for a RG-213/U coaxial cable they are between 1 and 1.016 at 1.8 MHz and between 1 and 1.0042 at 30 MHz, which is also quite close to 1).

Nevertheless we may conclude that in our frequency range of interest, the "matched" line 1 behaves as an idealised matched line (source impedance $Z_{0\mathrm{II}}$, characteristic impedance $Z_{0\mathrm{II}}$ of line 1, matching network's input matched to $Z_{0\mathrm{II}}$) would do, in particular if low loss coaxial cables are used. This holds either for termination by an exactly matched network and a source impedance of $\underline{Z}_0^* \approx Z_{0\mathrm{II}}\,(1 + \mathrm{j}\,\frac{\alpha}{\beta})$ or $Z_{0\mathrm{II}}$ or for termination by a network matched to $Z_{0\mathrm{II}}$ and a source impedance of $Z_{0\mathrm{II}}$, where the latter is usually applied. Hence the active power transfer of the "matched" line 1 does not necessarily involve complex characteristic impedance calculations because the mismatch introduced is small. However, the impact of the small mismatch caused by the source impedance $Z_{0\mathrm{II}}$ on the matching network's design will have to be considered later.

Conversely, depending on the load impedance $\underline{Z}_\ell$, the mismatch of line 2 may be large, thus active power transfer of line 2 requires complex characteristic impedance calculations.

5.4.2 Lossless matching network

A lossless matching network is characterised by a power gain equal to unity for any load impedance attached (and any source impedance it is designed to match to), hence

$$g_{\mathrm{MB,\,II,\,inma}}\left(\underline{r}_\ell\,\mathrm{e}^{-2\alpha l_2}\,\mathrm{e}^{-\mathrm{j}2\beta l_2}\right) = 1.$$

Then (5.5) becomes

$$g_{\mathrm{tot,\,II,\,inma}} = \mathrm{e}^{-2\alpha l_{\mathrm{tot}}}\,\frac{R_0\,(1 - |\underline{r}_\ell|^2) - 2X_0\,\mathrm{Im}\{\underline{r}_\ell\}}{R_0\,(1 - \mathrm{e}^{-4\alpha l_2}\,|\underline{r}_\ell|^2) - 2X_0\,\mathrm{e}^{-2\alpha l_2}\,\mathrm{Im}\,\{\underline{r}_\ell\,\mathrm{e}^{-\mathrm{j}2\beta l_2}\}}. \tag{5.7}$$

According to (5.4), l_{tot} seems to depend on l_2. However, in our application the total length l_{tot} is given, thus l_1 is chosen to keep the total length constant and $\mathrm{e}^{-2\alpha l_{\mathrm{tot}}}$ does not depend on l_2.

To optimise $g_{\mathrm{tot,\,II,\,inma}}$ by varying l_2, we have to solve

$$\frac{\mathrm{d}(\mathrm{e}^{2\alpha l_{\mathrm{tot}}}\,g_{\mathrm{tot,\,II,\,inma}})}{\mathrm{d}l_2} = 0$$

for l_2.

Application of (5.7) yields

$$\frac{\mathrm{d}(\mathrm{e}^{2\alpha l_{\mathrm{tot}}}\, g_{\mathrm{tot,\,ll,\,inma}})}{\mathrm{d}l_2} = -4\,\mathrm{e}^{-2\alpha l_2}\, \frac{R_0\,(1-|\underline{r}_\ell|^2) - 2X_0\,\mathrm{Im}\{\underline{r}_\ell\}}{\left(R_0\,(1-\mathrm{e}^{-4\alpha l_2}\,|\underline{r}_\ell|^2) - 2X_0\,\mathrm{e}^{-2\alpha l_2}\,\mathrm{Im}\left\{\underline{r}_\ell\,\mathrm{e}^{-\mathrm{j}2\beta l_2}\right\}\right)^2} \cdot \left[R_0\alpha\,|\underline{r}_\ell|^2\,\mathrm{e}^{-2\alpha l_2} + X_0\left(\alpha\,\mathrm{Im}\left\{\underline{r}_\ell\,\mathrm{e}^{-\mathrm{j}2\beta l_2}\right\} + \beta\,\mathrm{Re}\left\{\underline{r}_\ell\,\mathrm{e}^{-\mathrm{j}2\beta l_2}\right\}\right)\right].$$

The derivative equals zero only if the term in squared brackets equals zero, because $-4\,\mathrm{e}^{-2\alpha l_2} < 0$ and applying (2.9), (2.8), and (2.7) to numerator and denominator of the second term yields

$$\begin{aligned} & R_0\,(1-|\underline{r}_\ell|^2) - 2X_0\,\mathrm{Im}\{\underline{r}_\ell\} \\ &= \frac{4\,\mathrm{Re}\{\underline{Z}_\ell\}\,|\underline{Z}_0|^2}{(\mathrm{Re}\{\underline{Z}_\ell\}+R_0)^2 + (\mathrm{Im}\{\underline{Z}_\ell\}+X_0)^2} > 0, \\ & R_0\,(1-\mathrm{e}^{-4\alpha l_2}\,|\underline{r}_\ell|^2) - 2X_0\,\mathrm{e}^{-2\alpha l_2}\,\mathrm{Im}\left\{\underline{r}_\ell\,\mathrm{e}^{-\mathrm{j}2\beta l_2}\right\} \\ &= \frac{4\,\mathrm{Re}\{\underline{Z}_{\ell\mathrm{MB}}\}\,|\underline{Z}_0|^2}{(\mathrm{Re}\{\underline{Z}_{\ell\mathrm{MB}}\}+R_0)^2 + (\mathrm{Im}\{\underline{Z}_{\ell\mathrm{MB}}\}+X_0)^2} > 0, \end{aligned}$$

which hold since $R_0 > 0$ according to [26c], $\mathrm{Re}\{\underline{Z}_\ell\} > 0$ because the load is passive and it should be possible to transfer active power to the load[4], and $\mathrm{Re}\{\underline{Z}_{\ell\mathrm{MB}}\} > 0$ if $\mathrm{Re}\{\underline{Z}_\ell\} > 0$ since line 2 is lossy and passive ($\underline{Z}_{\ell\mathrm{MB}}$ may be computed from $\underline{r}_{\ell\mathrm{MB}} = \underline{r}_\ell\,\mathrm{e}^{-2\alpha l_2}\,\mathrm{e}^{-\mathrm{j}2\beta l_2}$ if (2.10) is applied ($\underline{r}_{\ell\mathrm{MB}}$ was derived in Section 5.4.1)).

Using the definition

$$\underline{r}_\ell := |\underline{r}_\ell|\,\mathrm{e}^{\mathrm{j}\varphi_{\underline{r}_\ell}} \tag{5.8}$$

we obtain for the term in squared brackets

$$\begin{aligned} & R_0\alpha\,|\underline{r}_\ell|^2\,\mathrm{e}^{-2\alpha l_2} + X_0\left(\alpha\,\mathrm{Im}\left\{\underline{r}_\ell\,\mathrm{e}^{-\mathrm{j}2\beta l_2}\right\} + \beta\,\mathrm{Re}\left\{\underline{r}_\ell\,\mathrm{e}^{-\mathrm{j}2\beta l_2}\right\}\right) \\ &= R_0\alpha\,|\underline{r}_\ell|^2\,\mathrm{e}^{-2\alpha l_2} + X_0\left(\alpha\,|\underline{r}_\ell|\,\sin(\varphi_{\underline{r}_\ell} - 2\beta l_2) + \beta\,|\underline{r}_\ell|\,\cos(\varphi_{\underline{r}_\ell} - 2\beta l_2)\right), \end{aligned}$$

which may be rewritten to

$$\begin{aligned} & R_0\alpha\,|\underline{r}_\ell|^2\,\mathrm{e}^{-2\alpha l_2} + X_0\left(\alpha\,\mathrm{Im}\left\{\underline{r}_\ell\,\mathrm{e}^{-\mathrm{j}2\beta l_2}\right\} + \beta\,\mathrm{Re}\left\{\underline{r}_\ell\,\mathrm{e}^{-\mathrm{j}2\beta l_2}\right\}\right) \\ &= R_0\alpha\,|\underline{r}_\ell|^2\,\mathrm{e}^{-2\alpha l_2} + X_0\,|\underline{r}_\ell|\,|\underline{\gamma}|\,\cos\left(\varphi_{\underline{r}_\ell} - 2\beta l_2 - \arctan\left(\frac{\alpha}{\beta}\right)\right) \end{aligned}$$

if we take into account that $\beta > 0$ if $\omega > 0$ according to [26b].

Then we have to distinguish two different cases.

If $\underline{r}_\ell = 0$, $\mathrm{e}^{2\alpha l_{\mathrm{tot}}}\, g_{\mathrm{tot,\,ll,\,inma}} = 1 = \text{const.}$ or $g_{\mathrm{tot,\,ll,\,inma}} = \mathrm{e}^{-2\alpha l_{\mathrm{tot}}}$ holds, causing $\frac{\mathrm{d}(\mathrm{e}^{2\alpha l_{\mathrm{tot}}}\, g_{\mathrm{tot,\,ll,\,inma}})}{\mathrm{d}l_2} = 0$ although no extremum occurs.

[4] $\mathrm{Re}\{\underline{Z}_\ell\} = 0$ would apply if the load is a pure capacitance, a pure inductance, or an ideal short circuit. Although those loads would be entirely passive, no active power could be transferred to such loads.

If $\underline{r}_\ell \neq 0$ we have to consider two subcases:

1. $X_0 = 0$

   Then we have to solve

   $$0 = R_0 \alpha \, |\underline{r}_\ell|^2 \, \mathrm{e}^{-2\alpha l_2}.$$

   According to [26c] $R_0 > 0$. Additionally, [26b] indicates that $\alpha \geq 0$.

   If $\alpha > 0$, the transmission line is either Heaviside's distortionless transmission line obtained for $\frac{R'}{\omega L'} = \frac{G'}{\omega C'} > 0$ and $\underline{Z}_0 = Z_{0\mathrm{II}}$ (where G' is the per-unit-length conductance and $L' = Z_{0\mathrm{II}}^2 C'$ the per-unit-length inductance of that line, defined in [26a]) or the approximation (2.5) is used. Since $\underline{r}_\ell \neq 0$ if $l_2 \in \mathbb{R}_0^+$, $R_0 \alpha \, |\underline{r}_\ell|^2 \, \mathrm{e}^{-2\alpha l_2} > 0$ holds. Combined with the preceding considerations regarding the sign of the remaining terms yields $\frac{\mathrm{d}(\mathrm{e}^{2\alpha l_{\mathrm{tot}}} \, g_{\mathrm{tot,\,II,\,inma}})}{\mathrm{d}l_2} < 0$, thus the maximum $\mathrm{e}^{2\alpha l_{\mathrm{tot}}} \, g_{\mathrm{tot,\,II,\,inma}}$ is obtained if $l_2 = 0$.

   If $\alpha = 0$, the transmission line is lossless, hence $\frac{R'}{\omega L'} = \frac{G'}{\omega C'} = 0$. Then $\mathrm{e}^{2\alpha l_{\mathrm{tot}}} \, g_{\mathrm{tot,\,II,\,inma}} = 1 = \text{const.}$ or $g_{\mathrm{tot,\,II,\,inma}} = 1$ holds, causing $\frac{\mathrm{d}(\mathrm{e}^{2\alpha l_{\mathrm{tot}}} \, g_{\mathrm{tot,\,II,\,inma}})}{\mathrm{d}l_2} = 0$ although no extremum occurs.

2. $X_0 \neq 0$

   We assumed $l_{\mathrm{tot}} > 0$ and, according to [26c], $R_0 > 0$. Additionally, [26b] indicates that $\alpha \geq 0$, but in conjunction with [26c] we may conclude that $X_0 \neq 0$ is accompanied by $\alpha > 0$, hence we have to consider $\alpha > 0$ only.

   Then we have to solve

   $$\cos\left(\varphi_{\underline{r}_\ell} - 2\beta l_2 - \arctan\left(\frac{\alpha}{\beta}\right)\right) = -\frac{R_0 \alpha \, |\underline{r}_\ell| \, \mathrm{e}^{-2\alpha l_2}}{X_0 \, |\underline{\gamma}|}.$$

   Due to periodicity and symmetry of the cosine function and the applicable range of the arc cosine function (which is $[0, \pi]$) we obtain

   $$\pm\left(\varphi_{\underline{r}_\ell} - 2\beta l_{2,m,\pm} - \arctan\left(\frac{\alpha}{\beta}\right) + 2\pi m\right) = \arccos\left(-\frac{R_0 \alpha \, |\underline{r}_\ell| \, \mathrm{e}^{-2\alpha l_{2,m,\pm}}}{X_0 \, |\underline{\gamma}|}\right),$$

   where $m \in \mathbb{Z}$.

   Numerical solution[5] of

   $$l_{2,m,\pm} = \frac{\varphi_{\underline{r}_\ell} - \arctan\left(\frac{\alpha}{\beta}\right) \mp \arccos\left(-\frac{R_0 \alpha \, |\underline{r}_\ell| \, \mathrm{e}^{-2\alpha l_{2,m,\pm}}}{X_0 \, |\underline{\gamma}|}\right) + 2\pi m}{2\beta}$$

   yields the line length $l_{2,m,\pm}$ of each extremum, where $l_{2,m,\pm} \in [0, \, l_{\mathrm{tot}}]$.

---

[5] A (positive) real solution requires $\left|-\frac{R_0 \alpha \, |\underline{r}_\ell| \, \mathrm{e}^{-2\alpha l_{2,m,\pm}}}{X_0 \, |\underline{\gamma}|}\right| \leq 1$ to hold. Since $l_2 \leq l_{\mathrm{tot}}$, at least one extremum might exist only if $l_{\mathrm{tot}} \geq \frac{1}{2\alpha} \ln\left(\frac{R_0 \alpha \, |\underline{r}_\ell|}{|X_0| \, |\underline{\gamma}|}\right)$ — then the initial numerical value is given by $\mathrm{Max}\left\{0, \, \frac{1}{2\alpha} \ln\left(\frac{R_0 \alpha \, |\underline{r}_\ell|}{|X_0| \, |\underline{\gamma}|}\right)\right\}$.

If the sign of $R_0\alpha\,|\underline{r}_\ell|^2\,\mathrm{e}^{-2\alpha l_2} + X_0\,|\underline{r}_\ell|\,|\underline{\gamma}|\,\cos(\varphi_{\underline{r}_\ell} - 2\beta l_2 - \arctan(\frac{\alpha}{\beta}))$ changes at $l_{2,m,\pm}$ from $-$ to $+$ or from $+$ to $-$, a maximum or minimum exists at $l_{2,m,\pm}$ (the product of the remaining terms of $\frac{\mathrm{d}(\mathrm{e}^{2\alpha l_{\mathrm{tot}}}\, g_{\mathrm{tot,\,ll,\,inma}})}{\mathrm{d}l_2}$ is always < 0 as indicated above). Additionally, the sign of this term at $l_2 = 0$ is important, because it indicates if the first extremum is a maximum or a minimum, provided an extremum exists within the range $[0,\, l_{\mathrm{tot}}]$. Alternatively we may plot $\mathrm{e}^{2\alpha l_{\mathrm{tot}}}\, g_{\mathrm{tot,\,ll,\,inma}}$ as a function of l_2, which also helps to choose good initial numerical values for the numerical solution.

However, the goal is to derive the $l_2 \in [0,\, l_{\mathrm{tot}}]$ which yields the highest $\mathrm{e}^{2\alpha l_{\mathrm{tot}}}\, g_{\mathrm{tot,\,ll,\,inma}}$. Hence, if one or more maxima exist within the range $[0,\, l_{\mathrm{tot}}]$, those (local) maxima have to be compared to the values at $l_2 = 0$ and $l_2 = l_{\mathrm{tot}}$. Then the highest value[6] belongs to the optimum length of l_2. Conversely, if there is no maximum within the range $[0,\, l_{\mathrm{tot}}]$, we just have to compare the values at $l_2 = 0$ and $l_2 = l_{\mathrm{tot}}$ to determine the optimum length of l_2.

If the line's complex characteristic impedance is given by $\underline{Z}_0 \approx Z_{0\mathrm{ll}}\,(1 - \mathrm{j}\,\frac{\alpha}{\beta})$ according to (2.4), we have to solve

$$l_{2,m,\pm} \approx \frac{\varphi_{\underline{r}_\ell} - \arctan\left(\frac{\alpha}{\beta}\right) \mp \arccos\left(\frac{\beta\,|\underline{r}_\ell|\,\mathrm{e}^{-2\alpha l_{2,m,\pm}}}{|\underline{\gamma}|}\right) + 2\pi m}{2\beta}$$

$$l_{2,m,\pm} \approx \frac{\varphi_{\underline{r}_\ell} - \frac{\alpha}{\beta} \mp \arccos\left((1 - \frac{\alpha^2}{2\beta^2})\,|\underline{r}_\ell|\,\mathrm{e}^{-2\alpha l_{2,m,\pm}}\right) + 2\pi m}{2\beta}$$

numerically[7] for $l_{2,m,\pm} \in [0,\, l_{\mathrm{tot}}]$.

Thus the small imaginary part of $\underline{Z}_0$ causes an optimum $l_{2,m,\pm} > 0$. Taking into account "real world" coaxial cable data in our frequency range of interest yields maximum values of $\mathrm{e}^{2\alpha l_{\mathrm{tot}}}\, g_{\mathrm{tot,\,ll,\,inma}}$ which are just some percent (max. 2% at 1.8 MHz, max. 0.5% at 30 MHz for a RG-213/U) higher[6] than 1, the value at $l_2 = 0$, but it depends on l_{tot} if l_2 may be chosen accordingly. If not, the maximum possible increase of power gain may be significantly lower. It's interesting to note that increasing of l_{tot} to enable a choice of $l_2 = l_{2,m,\pm}$ for maxi-

[6] Although $\mathrm{e}^{2\alpha l_{\mathrm{tot}}}\, g_{\mathrm{tot,\,ll,\,inma}} > 1$ is possible ($\mathrm{e}^{2\alpha l_{\mathrm{tot}}}\, g_{\mathrm{tot,\,ll,\,inma}} = 1$ at $l_2 = 0$), the factor $\mathrm{e}^{-2\alpha l_{\mathrm{tot}}}$ causes the power gain $g_{\mathrm{tot,\,ll,\,inma}}$ to be always ≤ 1.

[7] As indicated in Footnote [5], a (positive) real solution requires $l_{\mathrm{tot}} \geq \frac{1}{2\alpha}\,\ln\left(\frac{\beta\,|\underline{r}_\ell|}{|\underline{\gamma}|}\right)$ to hold, because $\left(\frac{\beta\,|\underline{r}_\ell|\,\mathrm{e}^{-2\alpha l_{2,m,\pm}}}{|\underline{\gamma}|}\right)_{\max} > 1$ is possible according to Footnote [3] of Appendix D.2. Then the initial numerical value is given by $\mathrm{Max}\left\{0,\, \frac{1}{2\alpha}\,\ln\left(\frac{\beta\,|\underline{r}_\ell|}{|\underline{\gamma}|}\right)\right\}$.

mum $e^{2\alpha l_{tot}}\, g_{tot,\,ll,\,inma} > 1$ is not useful because $g_{tot,\,ll,\,inma}$ decreases if l_{tot} increases[8].

Conversely, if the imaginary part of $\underline{Z}_0$ would be more significant, hence $\frac{|X_0|}{R_0} \not\ll 1$ (but $\frac{|X_0|}{R_0} < 1$ according to [26c]), the maximum value of $e^{2\alpha l_{tot}}\, g_{tot,\,ll,\,inma}$ could be some ten percent higher[6] than 1. However, as indicated above and in Section 2.4, coaxial cables in our frequency range of interest do not involve such high imaginary parts of $\underline{Z}_0$.

5.4.3 Lossy matching network

5.4.3.1 π network

According to Section 5.4.1, the π network is used to transform its load admittance (described by its reflection coefficient $\underline{r}_{\ell MB} = \underline{r}_\ell\, e^{-2\alpha l_2}\, e^{-j2\beta l_2}$) in the line's complex characteristic impedance $\underline{Z}_0$ at its input (hence $\underline{r}_{1MB,\,inma} = \underline{r}_{1\pi,\,inma} = 0$).

To design such a π network, real and imaginary part of its load impedance have to be known which might be computed based on the load's reflection coefficient $\underline{r}_{\ell MB}$ either separately using (2.14) and (2.15) or together using the reciprocal of (2.10).

Performing the former yields

$$R_{\ell,\,MB} = \frac{1}{G_{\ell,\,MB}} = \frac{|\underline{Z}_0|^2\,|1+\underline{r}_\ell\, e^{-2\alpha l_2}\, e^{-j2\beta l_2}|^2}{R_0\,(1-e^{-4\alpha l_2}\,|\underline{r}_\ell|^2)-2X_0\, e^{-2\alpha l_2}\,\mathrm{Im}\{\underline{r}_\ell\, e^{-j2\beta l_2}\}},$$

$$\left.\begin{matrix} C_{\ell p,\,MB} \\ L_{\ell p,\,MB} \end{matrix}\right\} = \begin{cases} \frac{B_{\ell,\,MB}}{\omega} = -\frac{2R_0\, e^{-2\alpha l_2}\,\mathrm{Im}\{\underline{r}_\ell\, e^{-j2\beta l_2}\}+X_0\,(1-e^{-4\alpha l_2}\,|\underline{r}_\ell|^2)}{\omega\,|\underline{Z}_0|^2\,|1+\underline{r}_\ell\, e^{-2\alpha l_2}\, e^{-j2\beta l_2}|^2} \\ -\frac{1}{\omega B_{\ell,\,MB}} = \frac{|\underline{Z}_0|^2\,|1+\underline{r}_\ell\, e^{-2\alpha l_2}\, e^{-j2\beta l_2}|^2}{\omega\left(2R_0\, e^{-2\alpha l_2}\,\mathrm{Im}\{\underline{r}_\ell\, e^{-j2\beta l_2}\}+X_0\,(1-e^{-4\alpha l_2}\,|\underline{r}_\ell|^2)\right)} \end{cases}.$$

Depending on the sign of the load admittance's imaginary part we then apply the optimisation given in Section 4.3.1.1 (if $C_{\ell p,\,MB} \geq 0$) or Section 4.3.2.1 (if $L_{\ell p,\,MB} > 0$) and the appropriate inclusion of minimum/maximum element values in Section 4.5.1. However, due to the line's complex characteristic impedance, they might have to be extended to complex source admittances.

To check the impact of source admittance transformation by the line on network design, in particular the necessity of extending the optimisation to complex source admittances, we have to consider the achieved susceptances if the source impedance is chosen from the three "useful" cases — the line's characteristic impedance, its complex conjugate, or its real part — and low loss coaxial cables are used.

However, calculation of those susceptances is quite lengthy and was moved to the appendix to enhance readability. The minimum/maximum (equivalent) capacitances

[8]Depending on l_{tot}, choosing of optimum lengths involves intervals where either l_1 is constant and l_2 increases if l_{tot} increases or l_2 is constant and l_1 increases if l_{tot} increases. Since $g_{tot,\,ll,\,inma}$ is continuous at the intervals' limits, $g_{MB,\,ll,\,inma} = 1 = \text{const.}$, and $g_{L1,2}$ decreases if $l_{1,2}$ increases (as indicated in Footnote [1]), $g_{tot,\,ll,\,inma}$ decreases if l_{tot} increases.

or inductances obtained from transformation of the three possible source impedances considered herein are derived in Appendix D.3.1.1. The resulting formulae were used to compute the values below.

In our frequency range of interest, coaxial cables involve $\frac{\alpha}{\beta} \ll 1$. Thus the real part of the source admittance is only slightly changed by line transformation. Regarding its imaginary part, we have to compute its actual values using low loss cable data to determine its impact on optimised network design derived in Sections 4.3.1.1 and 4.3.2.1.

Performing those calculations for low loss coaxial cables (RG-213/U or better) yields:

1. If the source impedance is equal to the line's characteristic impedance, its (transformed) admittance at the matching network's input is equal to the reciprocal of the line's characteristic impedance which exhibits a parallel capacitance of about $30-0.47\,\mathrm{pF}$ at $1.8-30\,\mathrm{MHz}$.

2. If the source impedance is equal to the complex conjugate of the line's characteristic impedance, its transformed admittance at the matching network's input exhibits a maximum parallel capacitance of about $91-1.4\,\mathrm{pF}$ or a minimum parallel inductance of about $260-59\,\mu\mathrm{H}$ at $1.8-30\,\mathrm{MHz}$, respectively. Compensation of those inductances would require a parallel capacitance greater or equal than $30-0.48\,\mathrm{pF}$.

3. If the source impedance is equal to the real part of the line's characteristic impedance, its transformed admittance at the matching network's input exhibits a maximum parallel capacitance of about $60-0.95\,\mathrm{pF}$ or a minimum parallel inductance[9] of about $7.1-24\,\mathrm{H}$ at $1.8-30\,\mathrm{MHz}$, respectively. Compensation of those inductances would require a parallel capacitance greater or equal than $1.1\,\mathrm{fF}-1.2\,\mathrm{aF}$.

For any source impedance considered above, the maximum parallel capacitance of the transformed source admittance or the parallel capacitance required to compensate the minimum inductance of the transformed source admittance does not exceed (typical) minimum values of variable capacitances and/or (typical) values of parasitic capacitances if the matching frequency is higher than 10 MHz.

But even at lower frequencies, the mismatch introduced by the parallel susceptance is low (in theory, matching is "perfect" in case 1, better than 35 dB in case 2, and better than 40 dB in case 3). Additionally, if we take into account that parasitics change the values of the network's elements and, if a transmission line connects the network's output to a load, characteristic impedance discontinuities introduced by connectors, cable bending, etc. may change the (calculated) load of the network,

[9] Exact calculation considering the spiral reveals that even for a low loss RG-213/U, the transformed susceptance stays entirely capacitive. At 1.8/10/30 MHz, the maximum parallel capacitance of 59/4.6/0.95 pF is achieved for a line length of about 27.7/4.97/1.65 m. Further maxima with decreasing maximum parallel capacitances occur at odd multiples of those lengths.

it's always recommendable to tune the designed π network, e. g. by measuring its input reflection coefficient using a directional coupler. However, tuning involves measurement uncertainties which are higher than the mismatch indicated above.

In particular, in our application the matching network is designed or tuned to match $Z_{0\mathrm{ll}} \approx R_0$ at its input, which is further transformed to the line's input. The resulting admittance at the line's input is similar to that derived in case 3 (a line is a reciprocal "network") — in theory the match at the source would be better than 40 dB — of course it's worse in practice.

Thus we may conclude that the π network may be designed to match $Z_{0\mathrm{ll}} \approx R_0$ at its input — the "error" involved is low.

Which power gain is obtained then?

If the π network is designed (or tuned) to match (exactly) the reciprocal of the line's characteristic impedance at its input, $\underline{r}_{1\mathrm{MB,\,inma}} = \underline{r}_{1\pi,\,\mathrm{inma}} = 0$ holds and the π network's power gain is given by $g_{\mathrm{MB,\,inma}} = g_{\pi,\,\mathrm{inma}}$ according to (3.24). Hence (5.5) gives

$$g_{\mathrm{tot},\,\pi,\,\mathrm{inma}} = \mathrm{e}^{-2\alpha l_{\mathrm{tot}}} \frac{1}{1+\frac{R_{\mathrm{s}}(R_{\mathrm{m}})}{R_{\mathrm{m}}}} \frac{R_0\left(1-|\underline{r}_\ell|^2\right)-2X_0\,\mathrm{Im}\{\underline{r}_\ell\}}{R_0\left(1-\mathrm{e}^{-4\alpha l_2}\,|\underline{r}_\ell|^2\right)-2X_0\,\mathrm{e}^{-2\alpha l_2}\,\mathrm{Im}\left\{\underline{r}_\ell\,\mathrm{e}^{-\mathrm{j}2\beta l_2}\right\}}, \tag{5.9}$$

where, as indicated in Sections 4.3.1.1 and 4.3.2.1, R_{m} is restricted by $R_{\ell,\,\mathrm{MB}}$ and $C_{\ell\mathrm{p,\,MB}}$ or $L_{\ell\mathrm{p,\,MB}}$, respectively[10], or by the minimum/maximum values of the network's elements according to Section 4.5.1.

If the π network is designed to match $Z_{0\mathrm{ll}} \approx R_0$ at its input, (3.24) is still applicable[11] (a network's power gain depends on its elements' settings and its load, but not on its source), but R_{i} used for design is (slightly) different from the inverse of the real part of the exact admittance to match and the susceptance of the exact admittance to match is neglected. Then, of course, $\underline{r}_{1\mathrm{MB,\,inma}} = \underline{r}_{1\pi,\,\mathrm{inma}} \neq 0$. Thus exact calculation of the total power gain would involve the load related "correction

[10] As exact matching involves an extension to complex sources, R_{m} may be restricted further and optimisation may be different. For example, matching the line's characteristic impedance (case 1) involves either a total capacitance $C_{1\mathrm{tot}}$ replacing C_1 in all π network design formulae, then, using the definitions of Appendix D.3.1.1, $C_1 = C_{0\mathrm{p}} + C_{1\mathrm{tot}} = C_{0\mathrm{p}} + \frac{1}{\omega R_{0\mathrm{p}}}\sqrt{\frac{R_{0\mathrm{p}}-R_{\mathrm{m}}-R_{\mathrm{s}}}{R_{\mathrm{m}}+R_{\mathrm{s}}}}$ (comparable to case 1 in Section 4.3.2.1), or a total inductance $L_{1\mathrm{tot}}$, then $C_1 = C_{0\mathrm{p}} - \frac{1}{\omega^2 L_{1\mathrm{tot}}} = C_{0\mathrm{p}} - \frac{1}{\omega R_{0\mathrm{p}}}\sqrt{\frac{R_{0\mathrm{p}}-R_{\mathrm{m}}-R_{\mathrm{s}}}{R_{\mathrm{m}}+R_{\mathrm{s}}}}$ and in (3.19) the minus in parentheses applies (comparable to case 2 in Section 4.3.2.1).
The former does not change the range of R_{m} or the optimisation (because the minimum capacitance of the variable capacitor is not considered). The latter is not applicable in conjunction with case 2 in Section 4.3.2.1 (transformation of a resistor by three inductors is never capacitive), restricts R_{m} further by $R_{\mathrm{m}} + R_{\mathrm{s}} \geq \frac{R_{0\mathrm{p}}}{1+\omega^2 R_{0\mathrm{p}}^2 C_{0\mathrm{p}}^2}$, changes optimisation (comparable to case 2 in Section 4.3.2.1, but in the final checks for numerator and denominator in the case "at least one $a_n > 0$" the first term is subtracted from the second term due to different signs in ωL_{s} and its derivatives), requires explicit knowledge of R_{s}, and may be applicable only in a certain range of $R_{\ell,\,\mathrm{MB}}$.

[11] It should be noted that the index "inma" is still valid in (3.24) because it indicates that the π network is designed to match a certain impedance (which has not necessarily to be equal to the line's characteristic impedance).

factor" of line 1, whose value is indicated at the end of Section 5.4.1. However, it's close to 1 due to the small mismatch. Hence the equation for $g_{\mathrm{tot},\pi,\mathrm{inma}}$ given above is (approximately) applicable and π network design is simplified because the susceptance of the exact admittance to match to is not included (the network's input admittance has to resemble a conductance instead of the complex conjugate of an admittance).

Additionally, if we would like to tune the network, e. g. by inserting a directional coupler, the optimisation remains (approximately) unchanged — if the network is tuned, the coupler is (approximately) matched at its input and output. Thus it just introduces an additional, (approximately) constant loss factor.

Unfortunately, there is no common optimisation for the power gain due to several reasons. Firstly, a load exhibiting a capacitive imaginary part may be transformed by line 2 in a load exhibiting an inductive imaginary part and vice versa. Secondly, optimisation involves three concurrent objectives — the optimum load resistance (derived for resistive loads in Section 3.5.2.3) which is equal to $\frac{1}{\mathrm{Re}\{\underline{Y}_{\mathrm{iMB}}\}} - R_{\mathrm{s0}} \approx Z_{\mathrm{0ll}} - R_{\mathrm{s0}} \approx Z_{\mathrm{0ll}}$ in all three cases considered above ($R_{\mathrm{s0}} \ll Z_{\mathrm{0ll}}$ for useful variable inductors), the restrictions on the valid range of parameter R_{m} (given in Sections 4.3.1.1 and 4.3.2.1) which depend on the transformed load admittance, hence on l_2, and optimum length l_2 for minimum line losses (similar to Section 5.4.2, but in conjunction with lossy matching networks). Additionally, both objectives depending on l_2 depend on frequency, too.

Thus optimum length l_2 and its according optimum π network design usually apply only to a given total line length, network characteristics (in particular, explicitly known losses), load admittance, and frequency. Unlike lossless π networks, increasing of the total line length may be recommendable for lossy π networks if the decrease of the network's losses exceeds the increase of the line's losses. It's interesting to note that the maximum possible loss reduction increases if the inductor's Q factor decreases.

Calculations always require usage of the line's complex characteristic impedance with two exceptions — the matched line's power gain may be computed using the real characteristic impedance approximation and the π network may be designed to match the real characteristic impedance.

5.4.3.2 T network

According to Section 5.4.1, the T network is used to transform its load impedance (described by its reflection coefficient $\underline{r}_{\ell\mathrm{MB}} = \underline{r}_{\ell}\,\mathrm{e}^{-2\alpha l_2}\,\mathrm{e}^{-\mathrm{j}2\beta l_2}$) in the line's complex characteristic impedance $\underline{Z}_0$ at its input (hence $\underline{r}_{\mathrm{1MB,\,inma}} = \underline{r}_{\mathrm{1t,\,inma}} = 0$).

To design such a T network, real and imaginary part of its load impedance have to be known which might be computed based on the load's reflection coefficient $\underline{r}_{\ell\mathrm{MB}}$ either separately using (2.11) and (2.12) or together using (2.10).

Performing the former yields

$$G_{\ell,\mathrm{MB}} = \frac{1}{R_{\ell,\mathrm{MB}}} = \frac{|1-\underline{r}_\ell\,\mathrm{e}^{-2\alpha l_2}\,\mathrm{e}^{-\mathrm{j}2\beta l_2}|^2}{R_0\,(1-\mathrm{e}^{-4\alpha l_2}\,|\underline{r}_\ell|^2)-2X_0\,\mathrm{e}^{-2\alpha l_2}\,\mathrm{Im}\{\underline{r}_\ell\,\mathrm{e}^{-\mathrm{j}2\beta l_2}\}},$$

$$\left.\begin{matrix} C_{\ell\mathrm{s},\mathrm{MB}} \\ L_{\ell\mathrm{s},\mathrm{MB}} \end{matrix}\right\} = \begin{cases} -\dfrac{1}{\omega X_{\ell,\mathrm{MB}}} = -\dfrac{|1-\underline{r}_\ell\,\mathrm{e}^{-2\alpha l_2}\,\mathrm{e}^{-\mathrm{j}2\beta l_2}|^2}{\omega\left(2R_0\,\mathrm{e}^{-2\alpha l_2}\,\mathrm{Im}\{\underline{r}_\ell\,\mathrm{e}^{-\mathrm{j}2\beta l_2}\}+X_0\,(1-\mathrm{e}^{-4\alpha l_2}\,|\underline{r}_\ell|^2)\right)} \\ \dfrac{X_{\ell,\mathrm{MB}}}{\omega} = \dfrac{2R_0\,\mathrm{e}^{-2\alpha l_2}\,\mathrm{Im}\{\underline{r}_\ell\,\mathrm{e}^{-\mathrm{j}2\beta l_2}\}+X_0\,(1-\mathrm{e}^{-4\alpha l_2}\,|\underline{r}_\ell|^2)}{\omega\,|1-\underline{r}_\ell\,\mathrm{e}^{-2\alpha l_2}\,\mathrm{e}^{-\mathrm{j}2\beta l_2}|^2} \end{cases}.$$

Depending on the sign of the load impedance's imaginary part we then apply the optimisation given in Section 4.3.1.2 (if $C_{\ell\mathrm{s},\mathrm{MB}} \geq 0$) or Section 4.3.2.2 (if $L_{\ell\mathrm{s},\mathrm{MB}} > 0$) and the appropriate inclusion of minimum/maximum element values in Section 4.5.2. However, due to the line's complex characteristic impedance, they might have to be extended to complex source admittances.

To check the impact of source impedance transformation by the line on network design, in particular the necessity of extending the optimisation to complex source impedances, we have to consider the achieved reactances if the source impedance is chosen from the three "useful" cases — the line's characteristic impedance, its complex conjugate, or its real part — and low loss coaxial cables are used.

However, calculation of those reactances is quite lengthy and was moved to the appendix to enhance readability. The minimum/maximum (equivalent) capacitances or inductances obtained from transformation of the three possible source impedances considered herein are derived in Appendix D.3.1.2. The resulting formulae were used to compute the values below.

In our frequency range of interest, coaxial cables involve $\frac{\alpha}{\beta} \ll 1$. Thus the real part of the source impedance is only slightly changed by line transformation. Regarding its imaginary part, we have to compute its actual values using low loss cable data to determine its impact on optimised network design derived in Sections 4.3.1.2 and 4.3.2.2.

Performing those calculations for low loss coaxial cables (RG-213/U or better) yields:

1. If the source impedance is equal to the line's characteristic impedance, its (transformed) impedance at the matching network's input is equal to the line's characteristic impedance which exhibits a series capacitance of about 100 – 24 nF at 1.8 – 30 MHz.

2. If the source impedance is equal to the complex conjugate of the line's characteristic impedance, its transformed impedance at the matching network's input exhibits a minimum series capacitance of about 34 – 7.9 nF or a maximum series inductance of about 76 – 1.2 nH at 1.8 – 30 MHz, respectively. Compensation of those inductances would require a series capacitance lower or equal than 100 – 24 nF.

3. If the source impedance is equal to the real part of the line's characteristic impedance, its transformed impedance at the matching network's input exhibits a minimum series capacitance of about 52 – 12 nF or a maximum series inductance[12] of about 2.8 pH – 3.0 fH at 1.8 – 30 MHz, respectively. Compensation of those inductances would require a series capacitance lower or equal than 2.8 – 9.5 mF.

For any source impedance considered above, the minimum series capacitance of the transformed source impedance or the series capacitance required to compensate the maximum inductance of the transformed source impedance exceeds (typical) maximum values of variable capacitances by at least one order of magnitude (typical variable capacitors have a maximum capacitance of about 500 pF to 1 nF, although vacuum variables are available up to 5 nF, but those high values are usually required only at the lower end of our frequency range of interest).

Anyhow, the mismatch introduced by the series reactance is low (in theory, matching is "perfect" in case 1, better than 35 dB in case 2, and better than 40 dB in case 3). Additionally, if we take into account that parasitics change the values of the network's elements and, if a transmission line connects the network's output to a load, characteristic impedance discontinuities introduced by connectors, cable bending, etc. may change the (calculated) load of the network, it's always recommendable to tune the designed T network, e. g. by measuring its input reflection coefficient using a directional coupler. However, tuning involves measurement uncertainties which are higher than the mismatch indicated above.

In particular, in our application the matching network is designed or tuned to match $Z_{0\mathrm{ll}} \approx R_0$ at its input, which is further transformed to the line's input. The resulting impedance at the line's input is similar to that derived in case 3 (a line is a reciprocal "network") — in theory the match at the source would be better than 40 dB — of course it's worse in practice.

Thus we may conclude that the T network may be designed to match $Z_{0\mathrm{ll}} \approx R_0$ at its input — the "error" involved is low.

Which power gain is obtained then?

If the T network is designed (or tuned) to match (exactly) the line's characteristic impedance at its input, $\underline{r}_{1\mathrm{MB,\,inma}} = \underline{r}_{1\mathrm{t,\,inma}} = 0$ holds and the T network's power gain is given by $g_{\mathrm{MB,\,inma}} = g_{\mathrm{t,\,inma}}$ according to (3.37). Hence (5.5) gives

$$g_{\mathrm{tot,\,t,\,inma}} = \mathrm{e}^{-2\alpha l_{\mathrm{tot}}} \frac{1}{1+\frac{G_{\mathrm{p}}(G_{\mathrm{m}})}{G_{\mathrm{m}}}} \frac{R_0\left(1-|\underline{r}_\ell|^2\right)-2X_0\,\mathrm{Im}\{\underline{r}_\ell\}}{R_0\left(1-\mathrm{e}^{-4\alpha l_2}\,|\underline{r}_\ell|^2\right)-2X_0\,\mathrm{e}^{-2\alpha l_2}\,\mathrm{Im}\left\{\underline{r}_\ell\,\mathrm{e}^{-\mathrm{j}2\beta l_2}\right\}}, \tag{5.10}$$

where, as indicated in Sections 4.3.1.2 and 4.3.2.2, G_{m} is restricted by $G_{\ell,\mathrm{MB}}$ and

[12] Exact calculation considering the spiral reveals that even for a low loss RG-213/U, the transformed reactance stays entirely capacitive. At 1.8/10/30 MHz, the minimum series capacitance of 53/22/12 nF is achieved for a line length of about 27.1/4.92/1.64 m. Further minima with increasing minimum series capacitances occur at odd multiples of those lengths.

$C_{\ell s,\,\mathrm{MB}}$ or $L_{\ell s,\,\mathrm{MB}}$, respectively[13], or by the minimum/maximum values of the network's elements according to Section 4.5.2.

If the T network is designed to match $Z_{0\mathrm{ll}} \approx R_0$ at its input, (3.37) is still applicable[14] (a network's power gain depends on its elements' settings and its load, but not on its source), but G_i used for design is (slightly) different from the inverse of the real part of the exact impedance to match and the reactance of the exact impedance to match is neglected. Then, of course, $\underline{r}_{1\mathrm{MB},\,\mathrm{inma}} = \underline{r}_{1\mathrm{t},\,\mathrm{inma}} \neq 0$. Thus exact calculation of the total power gain would involve the load related "correction factor" of line 1, whose value is indicated at the end of Section 5.4.1. However, it's close to 1 due to the small mismatch. Hence the equation for $g_{\mathrm{tot,\,t,\,inma}}$ given above is (approximately) applicable and T network design is simplified because the reactance of the exact impedance to match is not included (the network's input impedance has to resemble a resistance instead of the complex conjugate of an impedance).

Additionally, if we would like to tune the network, e. g. by inserting a directional coupler, the optimisation remains (approximately) unchanged — if the network is tuned, the coupler is (approximately) matched at its input and output. Thus it just introduces an additional, (approximately) constant loss factor.

Unfortunately, there is no common optimisation for the power gain due to several reasons. Firstly, a load exhibiting a capacitive imaginary part may be transformed by line 2 in a load exhibiting an inductive imaginary part and vice versa. Secondly, optimisation involves three concurrent objectives — the optimum load conductance (derived for resistive loads in Section 3.5.3.3) which is equal to $\frac{1}{\mathrm{Re}\{\underline{Z}_{\mathrm{iMB}}\}} = \frac{1}{R_0} \approx \frac{1}{Z_{0\mathrm{ll}}}$ in all three cases considered above, the restrictions on the valid range of parameter G_m (given in Sections 4.3.1.2 and 4.3.2.2) which depend on the transformed load impedance, hence on l_2, and optimum length l_2 for minimum line losses (similar to Section 5.4.2, but in conjunction with lossy matching networks). Additionally, both objectives depending on l_2 depend on frequency, too.

---

[13] As exact matching involves an extension to complex sources, G_m may be restricted further and optimisation may be different. For example, matching the line's characteristic impedance (case 1) involves either a total capacitance $C_{1\mathrm{tot}}$ replacing C_1 in all T network design formulae, then, using the definitions of Appendix D.3.1.2, $C_1 = \frac{1}{\frac{1}{C_{0\mathrm{s}}} + \frac{1}{C_{1\mathrm{tot}}}} = \frac{1}{\frac{1}{C_{0\mathrm{s}}} + \frac{\omega}{G_{0\mathrm{s}}}\sqrt{\frac{G_{0\mathrm{s}} - G_\mathrm{m} - G_\mathrm{p}}{G_\mathrm{m} + G_\mathrm{p}}}}$ (comparable to case 1 in Section 4.3.2.2), or a total inductance $L_{1\mathrm{tot}}$, then $C_1 = \frac{1}{\frac{1}{C_{0\mathrm{s}}} - \omega^2 L_{1\mathrm{tot}}} = \frac{1}{\frac{1}{C_{0\mathrm{s}}} - \frac{\omega}{G_{0\mathrm{s}}}\sqrt{\frac{G_{0\mathrm{s}} - G_\mathrm{m} - G_\mathrm{p}}{G_\mathrm{m} + G_\mathrm{p}}}}$ and in (3.32) the minus in parentheses applies (comparable to case 2 in Section 4.3.2.2).
The former does not change the range of G_m or the optimisation (because the maximum capacitance of the variable capacitor is not considered). The latter is not applicable in conjunction with case 2 in Section 4.3.2.2 (transformation of a resistor by three inductors is never capacitive), restricts G_m further by $G_\mathrm{m} + G_\mathrm{p} \geq \frac{G_{0\mathrm{s}}}{1 + \frac{G_{0\mathrm{s}}^2}{\omega^2 C_{0\mathrm{s}}^2}}$, changes optimisation (comparable to case 2 in Section 4.3.2.2 with similar final checks for numerator and denominator in the case "at least one $a_n > 0$" although signs are different in $\frac{1}{\omega L_\mathrm{p}}$ and its derivatives), requires explicit knowledge of G_p, and may be applicable only in a certain range of $G_{\ell,\,\mathrm{MB}}$.

[14] It should be noted that the index "inma" is still valid in (3.37) because it indicates that the T network is designed to match a certain impedance (which has not necessarily to be equal to the line's characteristic impedance).

Thus optimum length l_2 and its according optimum T network design usually apply only to a given total line length, network characteristics (in particular, explicitly known losses), load impedance, and frequency. Unlike lossless T networks, increasing of the total line length may be recommendable for lossy T networks if the decrease of the network's losses exceeds the increase of the line's losses. It's interesting to note that the maximum possible loss reduction increases if the inductor's Q factor decreases.

Calculations always require usage of the line's complex characteristic impedance with two exceptions — the matched line's power gain may be computed using the real characteristic impedance approximation and the T network may be designed to match the real characteristic impedance.

5.4.3.3 Optimum compromise

Summarising the preceding sections, we may conclude that optimisation usually applies only to a given total line length, network characteristics, load impedance, and frequency. Calculations always require usage of the line's complex characteristic impedance with two exceptions — the matched line's power gain may also be computed using the real characteristic impedance approximation and the network may be designed to match the real characteristic impedance. Although some parts of the optimisation procedure may yield values close to those of a real characteristic impedance, we should keep in mind that the error in power gain calculation may be high, in particular for the mismatched line to the load (an example is given in Figure 2.2), and some issues (as the impact of source impedance transformation) cannot be addressed properly by a real characteristic impedance.

Additionally, optimisation may involve increasing of the total line length if the decrease of the network's losses exceeds the increase of the line's losses. It's interesting to note that the maximum possible loss reduction increases if the inductor's Q factor decreases.

Due to the optimisation's dependencies, an optimisation is recommendable only in applications where frequency and load are (approximately) fixed.

Nevertheless, if a matching network is used for varying loads and/or varying frequencies, it's always a good compromise to put the π or T network as close as possible to the load and set the network's elements according to one of the matching strategies given in Section 4.5.3.

The former ensures low, but not minimal line losses. Depending on the matching strategy used, the latter ensures maximum or at least high power gain of the network depending on matching strategy and effort involved.

The simplest matching strategy would be to set C_2 to the lowest value where matching is possible in a π network or to the highest value where matching is possible in a T network. Alternatively an L network switchable to realise both complementary types could be used. These simple approaches will require measuring the magnitude of the network's input reflection coefficient only and do not guarantee high power

gains for certain loads, but are a good choice for the majority of loads if the variable inductor's Q factor is sufficiently high (which holds for "well designed" variable air-core inductors).

However, setting π or T networks' elements for highest power gain usually requires explicit knowledge of the elements' values, the matching frequency, and measuring magnitude and phase of the network's input reflection coefficient — the appropriate optimum matching strategy is described in Section 4.5.3.

Chapter 6

Experimental Validation of the Network's Matching Strategy

6.1 Introduction

In the following chapter, the experimental setup designed to test the network's matching strategy is described. The performed measurements are explained and results are given validating the proposed matching strategy for optimum power gain of the network.

6.2 Experimental setup

Regarding the experimental setup, several different considerations have to be taken into account.

Firstly, all measurements should be repeatable. Thus it's important to reduce the influence of the (possibly changing) environment and keep all matching elements within a metal housing (although generally shielding would not be required for matching networks). In addition, the motors used to turn the elements need to be capable of setting the elements' positions with sufficient accuracy. Hence a suitable combination of encoder resolution and gearbox reduction is essential.

Secondly, in order to reduce unwanted losses introduced by parasitics, it's important to obey some general network design rules. The distance between the inductor's windings and any metal part (such as walls or the adjacent capacitors) has to be at least five times of the wire's width and that between an end of the coil and the adjacent metal wall at least half of the coil's diameter, or, even better, equal to the coil's diameter. This ensures that the magnetic fields are low enough that the eddy-currents induced in any surrounding metal part does not increase the inductor's losses significantly. Furthermore, the parasitic capacitances are kept low, too. The latter also holds for the capacitors if they are mounted not too close to the metal walls. Additionally, the cross-section of the "wires" connecting plugs, capacitors,

and the inductor has to be high enough to reduce their parasitic resistance and inductance.

Thirdly, the components themselves and the connectors have to be of good quality. In particular, it's advantageous to use vacuum variable capacitors. They offer a high ratio of maximum to minimum capacitance and introduce low losses. Regarding the variable inductance, a high-power type should be chosen. Furthermore, 7 mm connectors yield the highest measurement accuracy of the vector network analyser obtainable in the frequency range of interest.

Finally, the experimental setup should be convertible to both network types (π and T network) for further measurements.

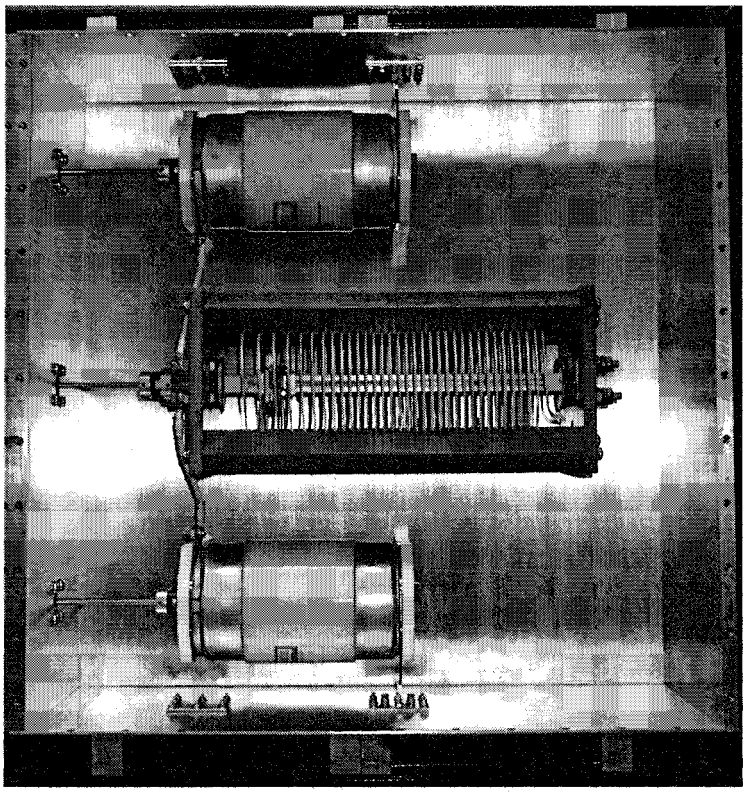

Figure 6.1: Matching compartment, T network built with elements of high values

Figure 6.1 shows one possible realisation of a T network. It consists of two Jennings Technology CMV1-4000-0005 vacuum variable capacitors (25 – 4000 pF) and one (IRV) RI-40 variable inductor (0.1 – 40 μH) from Surplus Sales of Nebraska (made of wire of rectangular cross-section). As indicated above, the network is surrounded by a metal housing made of brass.

Note that the capacitors are connected to the plug on the right side, mounted on Teflon holders, and that the wire which makes the ground connection of the variable inductor is not visible from the chosen point of view.

The distance from the inductor's windings to the adjacent variable capacitors and the surrounding walls is about 5 cm (about five times the wire's width of $l_{\mathrm{rad}} \approx 0.92$ cm)

and its ends are at least 10 cm apart from the walls (equal to the coil's mean diameter of $d_C \approx 10.2\,\text{cm}$).

The capacitors are mounted about 3 cm apart from the adjacent wall where the according plug is mounted. Since both capacitors (and the inductor) are mounted at an equal height of 10 cm, and the capacitor's diameter is about 7.6 cm, their distance to the remaining walls is even higher.

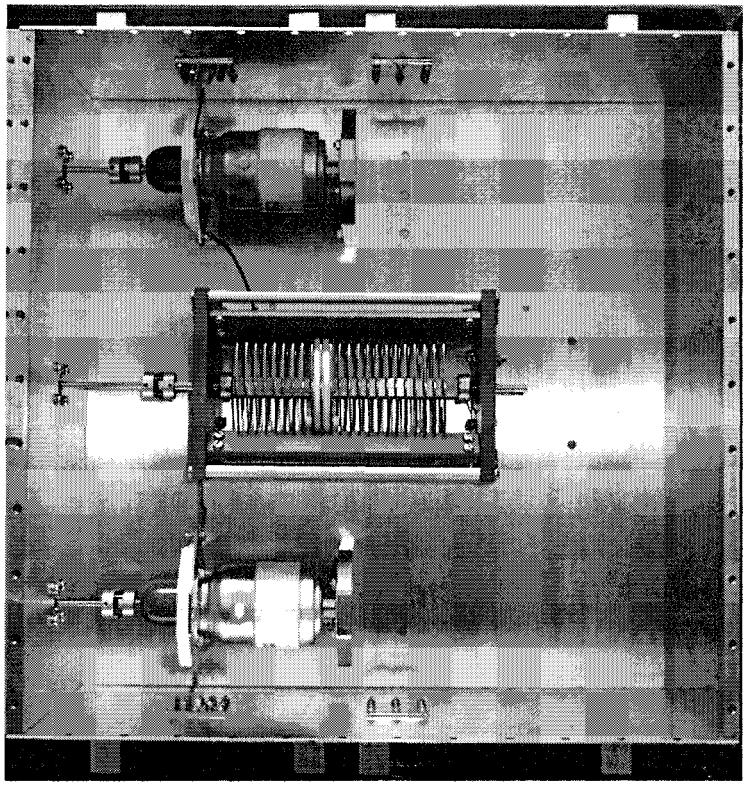

Figure 6.2: Matching compartment, π network built with elements of low values

Figure 6.2 shows one possible realisation of a π network. It consists of two Jennings Technology CSV1-500-0005 vacuum variable capacitors ($5-500\,\text{pF}$) and one (IRV) L32017 variable inductor ($0.1-24\,\mu\text{H}$) from Surplus Sales of Nebraska (made of wire of rectangular cross-section). The latter contained several additional parts, e. g. a potentiometer for position detection, which were removed completely prior to mounting.

Note that the capacitors are connected to the plug on the left side, mounted on one Teflon and one brass holder, and that there is no ground connection of the variable inductor.

Since the diameter of the capacitors and the inductor is lower than those of the T network elements of Figure 6.1, all distances checked above are even higher herein.

In both networks of Figure 6.1 and Figure 6.2, insulating backlash-free Oldham couplings are used to connect the driving axes to the variable elements.

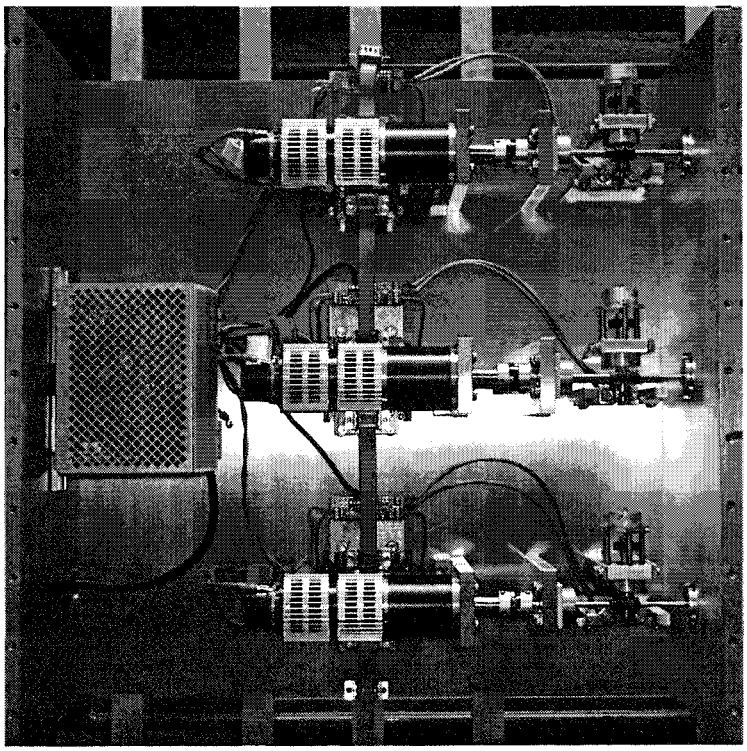

Figure 6.3: Motor, motor control, and power supply compartment

To set the network's elements to the given values (positions), servo motors in conjunction with position encoders and gearboxes are employed. To prevent interference with the high frequencies of the network, they were mounted in a separate compartment together with the power supply and the start/end point switches (refer to Figure 6.3).

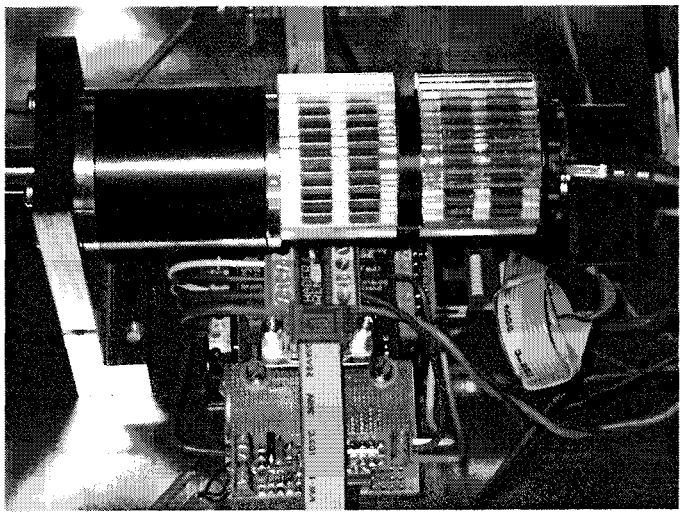

Figure 6.4: Gearbox, motor, position encoder, and motor control

As shown in Figure 6.4, each motor "unit" consists (from left to right) of a Maxon

planetary gearhead GP42C (91:6 reduction), a Maxon RE36 servo motor (24 V), and an Agilent HEDL5540 position encoder (500 cycles/revolution). The motor is controlled by a Faulhaber MCDC2805 via a RS232 interface. Since the motor contol uses edge detection, the resulting resolution is $4 \cdot 500\,\text{counts} \cdot 91/6 \approx 30333\,\text{counts}$ per revolution or 0.012° at the output of the gearbox.

However, the gearbox has a avearge backlash (no load) of 0.4° or 33.7 counts. Thus, if a small movement is intended, it has to be performed in two steps. At first, the motor control has to move back beyond the backlash (plus tolerances) and then, in a second step, forward towards the intended position.

a) 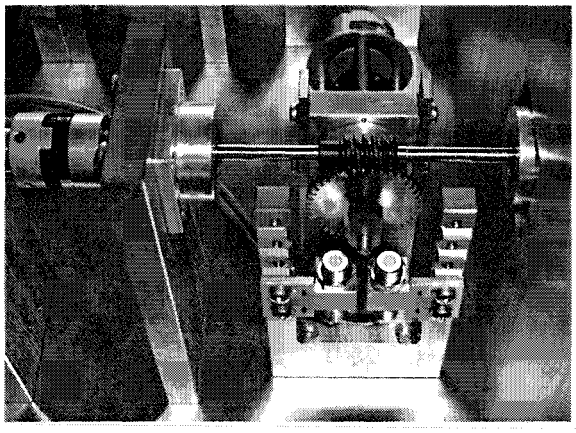 b) 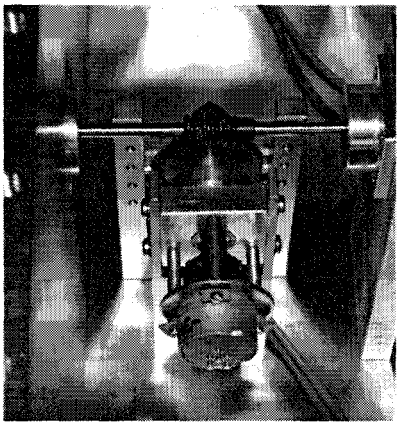

Figure 6.5: a) Worm gear driving end point switch actuator and two end point switches, and b) a servopotentiometer

Furthermore, start and end point switches are needed, the former to detect the zero position with sufficient repeatability during power-up, and both after power-up to prevent the motor from moving beyond the element's physical limits in case of programming errors. Those switches are Baumer Electric MY-COM G75N types offering a repeatability below 1 μm (since the actuator employs a worm gear with backlash, the total repeatability is worse, but still sufficiently well).

The switching itself is performed using a steel actuator driven by a worm gear (refer to Figure 6.5 a)). Different gears are employed to accomodate for the different total number of turns of the element to be driven. For example, the CMV1-4000-0005 vacuum variable capacitor has about 14 turns requiring a 20:1 worm gear/gear reduction compared to 32 turns of the (IRV) RI-40 variable inductor requiring a 40:1 worm gear/gear reduction. Note the different discrete positions available at the switch holders and the variable mounting of the switches which takes the different gear sizes into account.

Additionally, as shown in Figure 6.5 b), the worm gear drives a servopotentiometer, which will be used in the future to speed up the homing procedure during power-up.

6.3 Measurements performed to test and validate the matching algorithm for optimum power gain of the network

6.3.1 Experimental setup used

In the following measurements, the setup of Figure 6.1 — hence a T network — is used. Although it may seem disadvantageous with respect to the vulnerability of its series variable capacitors to parasitics, it's mainly the variable inductor and its Q factor we are interested in, and on this behalf it's advantageous that one end of the variable inductor is connected to ground.

Furthermore, if the frequency used in the measurement is sufficiently low, nearly the whole range of the available inductance is employed. Thus a frequency of 1.8 MHz is used in all measurements, which, in addition, reduces the influence of any parasitics.

6.3.2 Calculation of the network elements (and the coil's Q)

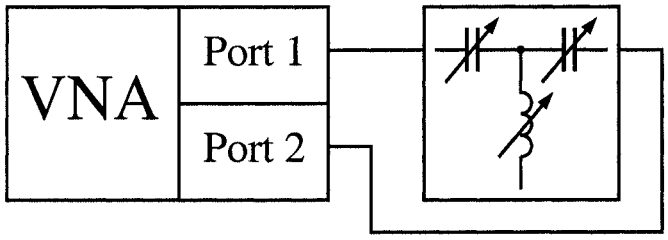

Figure 6.6: S-parameter measurement setup used to calculate network element values

To calculate the values of the network elements (and the coil's Q) at 1.8 MHz, the matching network's ports were connected to the ports of an Agilent 8753E vector network analyser (VNA) (refer to Figure 6.6). The vector network analyser was set to a source power of -10 dBm, an IF bandwidth of 10 Hz, and a full 12-term adapter removal calibration was performed using an Agilent 85031B 7 mm CalKit and a 48 cm long precision cable with 7 mm connectors (a Micro-Coax UFA210B). The cable serves as an "adapter" resembling the distance of the two 7 mm connectors of the network — thus the bending of the precision cables connecting the network and the vector network analyser is similar during calibration and measurement.

In any measurement, C_2 was incremented and the basic matching algorithm tuned the network to a match of at least -66.8 dB (most times even below -75 dB), which is well below the measurement uncertainty of -55 dB. Hence the overall error is dominated by the measurement uncertainty and as low as possible for the given setup.

If depicted, the error of any calculation given was derived applying sensititvity analysis. In case matched T network formulae are involved, it consists of two parts — the measurement error and the adjustment error (taking into account that a formula of the exactly matched T network was used although the real T network may deviate from the exact match due to measurement uncertainties).

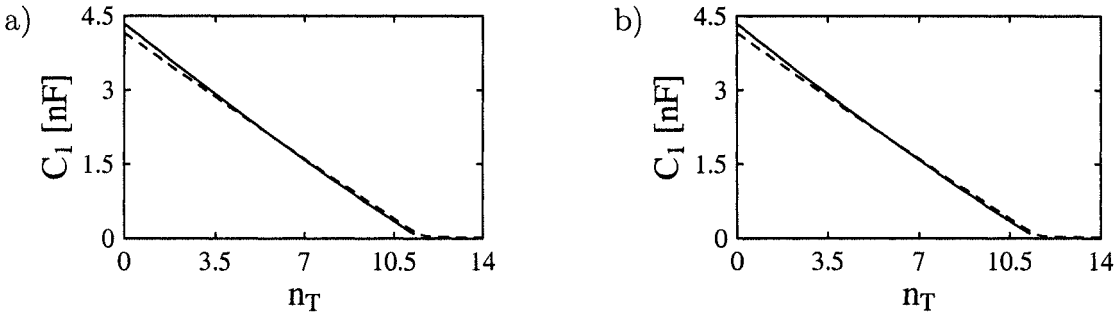

Figure 6.7: a) C_1 and b) C_2 of the equivalent T network, calculated from S-parameter measurements (solid line) and the single capacitances measured with a capacitance meter (dashed line)

Calculation of the equivalent T network's elements from S-parameters (applying admittance matrix to S-parameter matrix conversion) yields the capacitances C_1 and C_2 shown in Figure 6.7. Compared to the values of the single elements measured previously using an AADE L/C meter IIB, they are somewhat higher — this just resembles the parasitic series inductances of the wires connecting those capacitors to the 7 mm connectors and the central inductor.

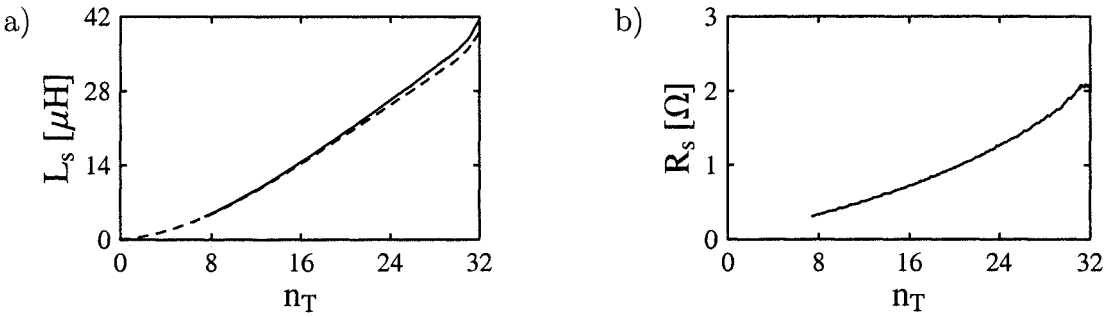

Figure 6.8: a) L_s of the equivalent T network, calculated from S-parameter measurements (solid line), the single inductance measured with an inductance meter (dashed line), and b) R_s calculated from S-parameter measurements and matched T network formulae

As indicated in Figure 6.8 a), the values of the equivalent inductance (calculated in a manner similar to that of the capacitors) and of the single inductor measured previously using an AADE L/C meter IIB differ in similar manner — this resembles the parasitic parallel capacitances, in particular between the windings of the inductor (the distance between the windings and the brass walls is relatively high).

However, since equivalent and measured values are quite close, the parasitics seem to be quite low for all elements of the network.

Regarding the accuracy of the calculated losses (and of the Q factor), the useful range of the measurement is limited.

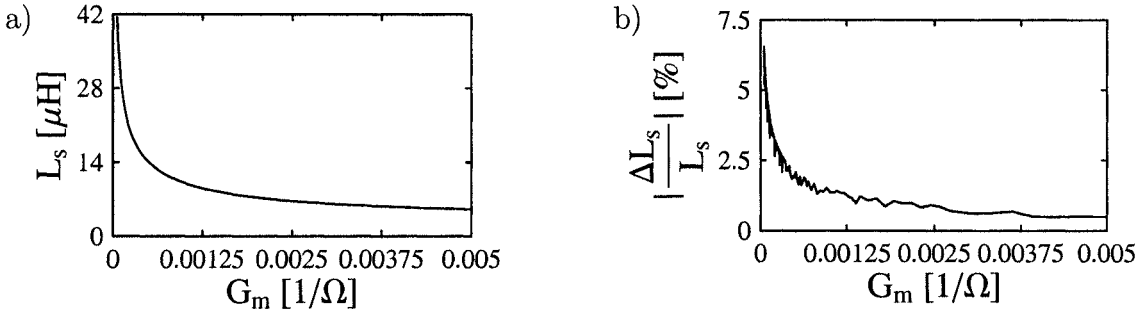

Figure 6.9: a) L_s and b) its percentage error when calculated from S-parameters

Fortunately the inductance required to match is approximately symmetrical to the middle ($G_m \approx 0.01\,\frac{1}{\Omega}$) of the full (theoretical) matching range and does not change much towards the middle provided its Q factor is sufficiently high.

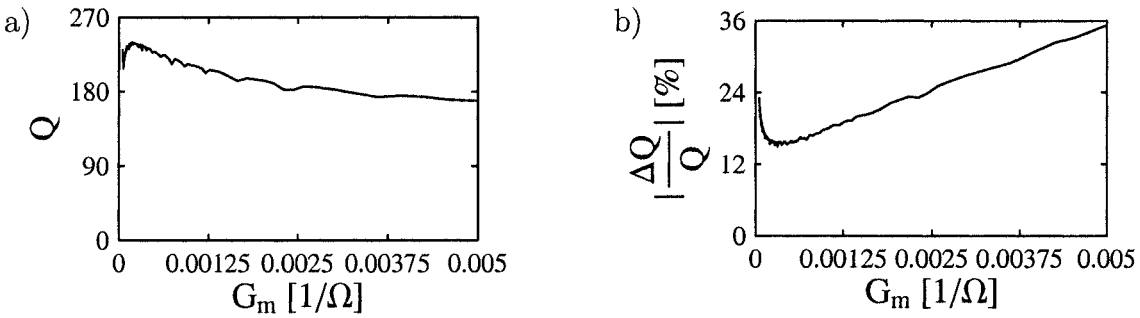

Figure 6.10: a) Q factor of the inductor and b) its percentage error when calculated from S-parameters and matched T network formulae

Thus the lower quarter of the full range contains nearly all possible inductance values (Figure 6.9 a)) and yields a Q factor whose accuracy is reasonable (Figure 6.10 b)). (If the inductor's Q factor would be lower, the useful range would be higher.)

However, it should be noted that although the theoretical accuracy is poor, the values of the Q factor obtained to the right of the middle are similar to those obtained to the left as one would expect from symmetry!

Furthermore, the Q factor's magnitude is comparable to those given in [67] — although different coils were measured in this work.

From the calculated Q factors of Figure 6.10 a) and the previously computed L_s and L_p (which is not shown), the series resistance R_s is calculated and depicted in Figure 6.8 b). It behaves as expected.

Finally, as a cross-check, the calculated Q factors of Figure 6.10 a) were used to compute the values of the elements and $g_{t,inma}$ of the T network based on piecewise constant Q factors between two measured points (equal to the arithmetic mean

of the calculated Q factors of those points) and the minimum/maximum element values.

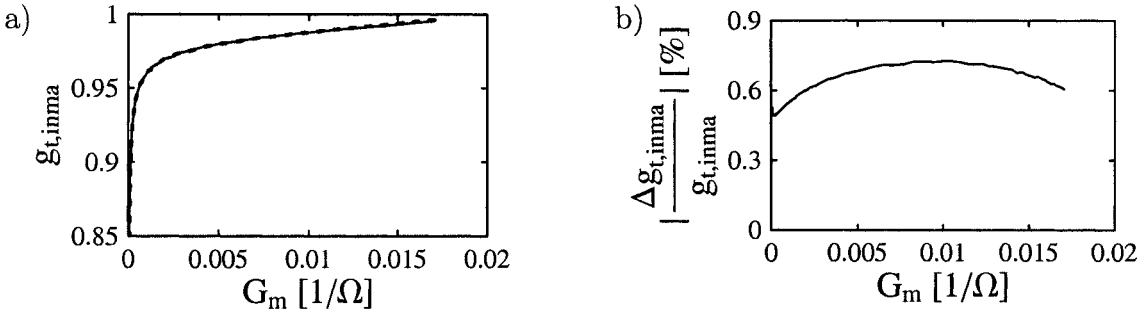

Figure 6.11: a) Comparison of $g_{t,inma}$ calculated from S-parameters (dashed line) and $g_{t,inma}$ calculated from the piecewise constant Q factors and minimum/maximum element values (solid line) for a load of 50 Ω and b) its percentage error when calculated from S-parameters

The resulting $g_{t,inma}$ is shown in Figure 6.11 a) and agrees well with the $g_{t,inma}$ calculated from S-parameters. In addition, it behaves as expected — the optimum power gain is achieved for the highest possible G_m.

6.3.3 Validation of the matching algorithm setting the network to optimum power gain

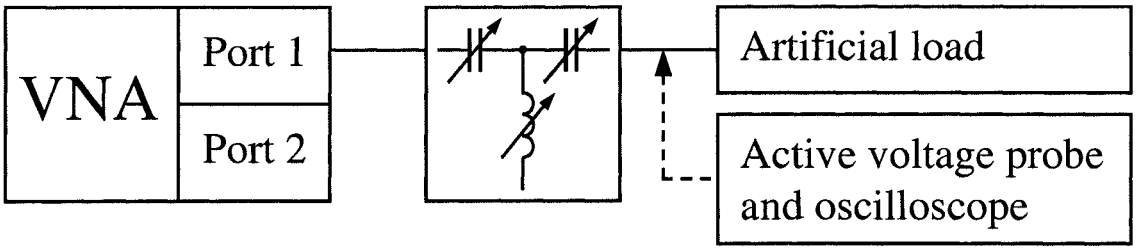

Figure 6.12: Additional S-parameter measurement setup used to validate the matching algorithm setting the network to optimum power gain

To validate the matching algorithm setting the network to optimum power gain, two measurements were performed at 1.8 MHz for each increment of C_2.

Firstly, the vector network analyser was set to a source power of 0 dBm, an IF bandwidth of 10 Hz, and a 3-term reflection calibration was performed using an Agilent 85031B 7 mm CalKit. Then the network was terminated with an artificial load as depicted in Figure 6.12 and, as before, the basic matching algorithm was used to tune the network to a match better than -70 dB. After achieving the match, the amplitude of the voltage at the load was measured using a LeCroy WaveRunner 104MXi oscilloscope (10 GS/s, noise filter set to 11 bit resolution — limiting the bandwith to 80 MHz — and averaging set to 256) with a ZS1000 active probe.

Secondly, the artificial load was replaced with a connection to port 2 of the vector network analyser (similar to Figure 6.6) and all S-parameters were measured using the settings and the according full 12-term adapter removal calibration described in Section 6.3.2.

The second S-parameter measurement enables calculation of the load including parasitics, of the network element values, and of the network's power gain. Since the amplitude measurement's accuracy is difficult to estimate and the absolute value of the input power is not known sufficiently well (±1 dB), the first amplitude measurement serves only as a cross-check for the measured power gain.

Two artificial loads were built — 82 Ω in series to 10 μH or 680 pF. However, due to parasitics (and depending on frequency) the actual resistance and reactance is different. Thus the actual values were calculated from the second S-parameter measurement and given in the captions of the figures below.

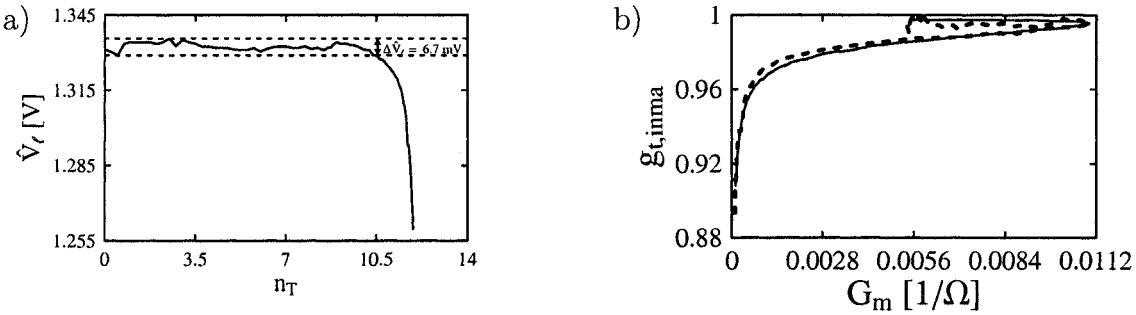

Figure 6.13: a) Amplitude measured with the oscilloscope and b) comparison of $g_{t,inma}$ calculated from that amplitude (dashed line) and $g_{t,inma}$ calculated from the piecewise constant Q factors and minimum/maximum element values (solid line) for a load of 91 Ω in series to 9.7 μH

As shown in Figure 6.13 a), in case of the inductive load there is a broad region where the change of the amplitude at the load is very low — it's within 6.7 mV or 0.5 % of the measured amplitude!

To compare the squared amplitudes with the $g_{t,inma}$ calculated from piecewise constant Q factors of Figure 6.10 a) and minimum/maximum element values (as described above) in Figure 6.13 b), it was assumed that both power gains are equal at the highest G_m (where the load's inductance is just compensated).

Note that the values whose $g_{t,inma}$ is higher than that of the highest G_m belong to the inductive solution (undercompensation), whereas the lower ones belong to the capacitive solution (overcompensation).

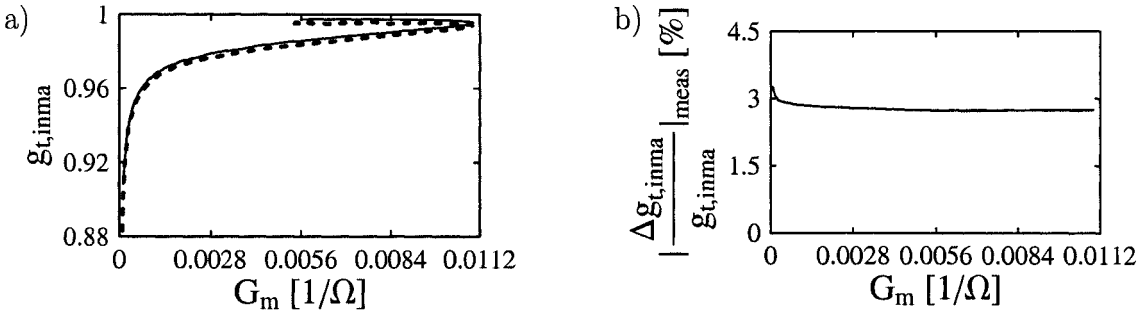

Figure 6.14: a) Comparison of $g_{t,inma}$ calculated from S-parameters (dashed line) and $g_{t,inma}$ calculated from the piecewise constant Q factors and minimum/maximum element values (solid line) for a load of 91 Ω in series to 9.7 μH and b) its percentage measurement error when calculated from S-parameters

In addition, a similar comparison with $g_{t,inma}$ calculated from measured S-parameters is performed in Figure 6.14 a).

Both figures show a that the calculation using piecewise constant Q factors of Figure 6.10 a) agrees well with the measured values, hence the matching algorithm setting the network to optimum power gain using the best setting obtained by that calculation will work as expected.

Note that the measured values extend the calculated values at both line's ends — this is related to the minimum/maximum element values used in the calculation, which were derived from Figure 6.7 — however, parasitics of C_2 changed and Figure 6.7 does not contain the lowest possible values of C_1 and C_2.

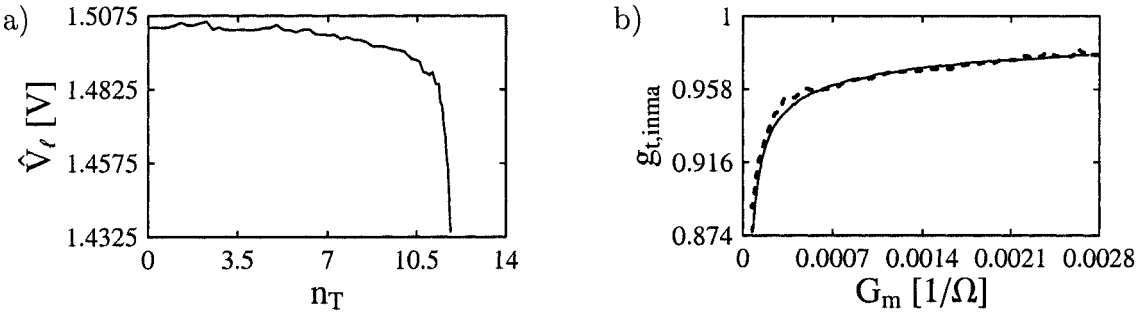

Figure 6.15: a) Amplitude measured with the oscilloscope and b) comparison of $g_{t,inma}$ calculated from that amplitude (dashed line) and $g_{t,inma}$ calculated from the piecewise constant Q factors and minimum/maximum element values (solid line) for a load of 84 Ω in series to 660 pF

As shown in Figure 6.15 a), in case of the capacitive load the amplitude at the load continuously decreases.

To compare the squared amplitudes with the $g_{t,inma}$ calculated from piecewise constant Q factors of Figure 6.10 a) and minimum/maximum element values (as described above) in Figure 6.15 b), it was assumed that both power gains are equal at the highest G_m.

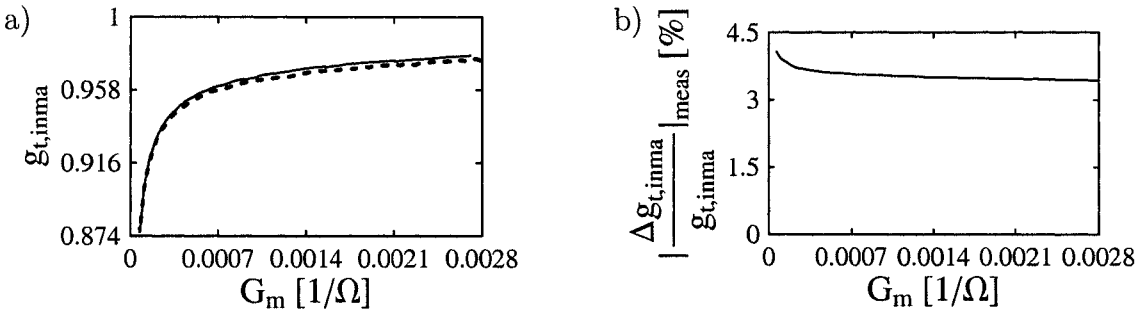

Figure 6.16: a) Comparison of $g_{t,inma}$ calculated from S-parameters (dashed line) and $g_{t,inma}$ calculated from the piecewise constant Q factors and minimum/maximum element values (solid line) for a load of 84 Ω in series to 660 pF and b) its percentage measurement error when calculated from S-parameters

In addition, a similar comparison with $g_{t,inma}$ calculated from measured S-parameters is performed in Figure 6.16 a).

Both figures show a that the calculation using piecewise constant Q factors of Figure 6.10 a) agrees well with the measured values. Furthermore, those calculations are not necessary in the capacitive case since, as expected, the highest power gain is achieved for the highest G_m (which was also observed in measurements mentioned in [68]). Hence the matching algorithm setting the network to optimum power gain using the best setting obtained (or the highest value of C_2 yielding a match) will work as expected.

Note that once again the measured values extend the calculated values at both line's ends for the same reason than that given above.

6.4 Conclusion

In the measurements described above, the proposed matching strategy tuning the network to optimum power gain was validated.

This is not surprising since it's always possible to replace any Q factor by its piecewise constant approximation with sufficient accuracy provided the intervals are sufficiently small.

In addition, the measurements illustrate the simpler part of the matching strategy. For capacitive loads, the maximum power gain is achieved for the highest G_m obtainable with the network's elements. For inductive loads — provided the inductive maximum occurs — it's flat enough due to the relatively high Q factor of the variable inductor that the power gain at the highest G_m (where compensation occurs) is very close to the maximum power gain and thus a good compromise.

Chapter 7

Conclusions and Recommendations for Further Work

7.1 Conclusions

Since the optimum matching strategy and matching system optimisation are already summarised in Sections 4.5.3 and 5.4.3.3, respectively, only a brief conclusion is given herein.

In this work, a matching strategy was derived that is suitable for automatic and continuous adjustment of L, π, and T matching networks for optimum active power transfer to their load while matching the network's input impedance to a resistive source applicable in a frequency range of 1.8 – 30 MHz.

It is splitted in two parts — one (simple) strategy for purely resistive or capacitive complex loads which always applies — provided the network's losses are properly described by the general loss model — and a more complicated strategy for inductive complex loads which involves real-time calculations and requires knowledge of the losses of the inductor and all network elements' values.

Unlike other works existing in the literature, the approach of this work was proven analytically and not limited to constant Q factor central inductors. The model used was validated by comparison to models of several previous works which fit a large amount of measurements including the frequency range of interest.

Moreover, besides using the optimisation based on the model, it's possible to perform an optimisation calculated from piecewise constant approximation of the inductor's Q factor and known elements' values similar to the optimisation derived for inductive complex loads. It never fails provided the network elements' values and the inductor's Q factor were measured in advance over the network elements' ranges in sufficiently small steps.

The network design presented in this work can also be used to estimate the losses in the network's low loss variable capacitors (see Appendices B.5.1 and B.5.2).

Furthermore, the influence of the transmission lines' lengths (which connect the matching network to source and load) on power gain of the matching system and an optimum split of the total line length was derived, where the transmission lines' characteristic impedance was complex.

However, an optimisation of the whole matching system is recommendable only in case of a fixed load. Varying loads involve a compromise, putting the matching network as close as possible to the load which is similar to the optimum position derived from the real characteristic impedance approximation (losses described solely by the attenuation) of lossy transmission lines.

Finally, an experimental setup was designed to test and validate the optimum matching strategy of the network. The experimental results are close to those predicted theoretically as well as they illustrate the simpler part and the proposed simpler approximations of the matching strategy given in Section 4.5.3.

7.2 Further work

The emphasis of this work was on deriving an optimum matching strategy for π and T networks suitable for any complex load. If the load's imaginary part is inductive, achieving the highest power gain involved a piecewise constant approximation of the known (measured) Q factor as a function of the inductor's reactance or its number of turns. Then the optimum network settings are computed for each interval, from which the best settings are chosen yielding the optimum network. However, describing the nonlinear Q factor by a piecewise constant approximation with sufficient accuracy may require a large number of relatively small intervals, thereby significantly increasing calculation time. This may be particularly disadvantageous in real time applications where the network has to match varying loads.

If a piecewise linearisation would be used instead, a lower number of intervals should suffice to approximate the nonlinear Q factor with similar accuracy, thereby reducing calculation time.

Thus deriving of an exact analytical solution for piecewise linearised losses, in particular for

$$R_\mathrm{s} = R_\mathrm{s0} + a_1 \omega L_\mathrm{s} \text{ or } G_\mathrm{p} = G_\mathrm{p0} + a_1 \frac{1}{\omega L_\mathrm{p}},$$

the former for π, the latter for T networks, may be recommendable.

However, solutions and applicable parameter ranges' limits are much more complicated than those of the constant Q factor approximation. Additional limits are introduced as indicated in Appendices C.1.1.1 and C.1.1.2. Moreover, the network's power gain may stay constant in some parameter region[1] if $a_1 = 0$.

[1] If, for example, a π network is considered and $R_\mathrm{s} = R_\mathrm{s0}$, the optimum power gain for resistive (and capacitive complex) loads is given by $g_{\pi,\,\mathrm{inma}} = 1 - \frac{R_\mathrm{s0}}{R_\mathrm{i}} = \text{const.}$ if $R_\ell > R_\mathrm{i} - R_\mathrm{s0}$ (yielding $R_\mathrm{mlim} = R_\mathrm{i} - R_\mathrm{s0} = \text{const.}$).

Another (at least theoretically) interesting extension would be the derivation of the exact analytical solutions if all three network elements are lossy and those losses are described by constant Q factors as sketched in Appendices B.3.2 and B.3.3.

Unfortunately, four possible solutions are obtained instead of two, hence it may be very complicated to prove which solution applies and to calculate the according parameter's limits.

Since high power applications — where an optimisation is essential — require usage of low loss variable capacitors, whose losses can be estimated as indicated in Appendices B.5.1 and B.5.2, the question of whether their exact inclusion significantly improves matching network design needs to be investigated.

On the other hand, there are other useful extensions of the network design presented in this work:

The theory may be extended to networks with two (lossy) inductors and one central capacitor (whose losses are negligible). Network parametrisation may be adapted from those given in Appendices B.3.2 and B.3.3. For example, in a T network, the resulting formulae are similar to those of Appendix B.3.3 except that L_p is replaced with C_p, whose loss $G_\mathrm{p} = 0$, and $C_{1,2}$ is replaced with $L_{1,2}$, whose losses $R_{\mathrm{sL}_{1,2}} = \frac{1}{G_{\mathrm{sL}_{1,2}}}$ are described by individual series loss models given by (3.1). But, since two series loss models are involved, the problem's difficulty is increased. In addition, the parametrisation cannot be adapted to "remove" the losses from the design formula of L_2 or L_1 to simplify the extension to complex loads or sources, respectively.

Another possibility is that the method extended to complex loads may be extended further to complex sources as indicated in Footnotes [10] and [13] in Section 5.4.3.1 and 5.4.3.2, respectively, yielding an extension to complex loads and sources. Since minima/maxima of $C_{1\mathrm{tot}}$ may occur (refer to Figures 4.6 to 4.9) and additional inductive solutions (and parameter limits) for $L_{1\mathrm{tot}}$ have to be derived, this task is also quite difficult.

Furthermore, the network design presented in this work may be employed to design loads for optimum network efficiency. For example, if the load's imaginary part is considered, it's always recommendable to keep a capacitive imaginary part as small as possible. Conversely, an inductive imaginary part should be kept as high as possible provided the network may be chosen arbitrarily — then either a T network ($\frac{1}{\mathrm{Re}\{\underline{Z}_\ell\}} < G_\mathrm{i}$) or a π network ($\frac{1}{\mathrm{Re}\{\frac{1}{\underline{Z}_\ell}\}} < R_\mathrm{i}$) will be the optimum choice.

Moreover, the lossy network design theory derived in this work is not limited to the order three networks considered herein. Higher order networks may be obtained by splitting those networks into lower order ones — then one approach would be to design those networks for optimum power gain depending on the impedances at the interfaces between those (partial) networks whose optimum values would have to be derived. Generally, this would require at least the extension to complex loads and sources mentioned above.

At a first glance, matching of a resistive load to a resistive source seems to be obtainable by a combination of a second or third order network designed to match a complex load to a resistive source and a second or third order network designed to match a complex source to a resistive load (both derived within this work) to generate lossy matching networks of up to fifth order — even up to sixth order if the extension to networks with two (lossy) inductors and one central capacitor would be derived. However, since lossy networks achieve a complex conjugate match in one direction only, this approach would not yield the intended result. Although such a combination would still be able to match in one direction, the part of the network with opposite "matching design" direction would be expected to be suboptimal.

In addition, the applicable frequency range may be extended provided the (equivalent) network elements still consist of lumped elements and narrowband matching is required. In particular, the former is true for CMOS integrated RF circuits up to the GHz range. Nowadays, as for wireless applications, integration density is increasing. Thus matching networks are implemented within the integrated circuit. However, as indicated in [69], the inductors employed are quite lossy. Since it's always possible to use a piecewise constant approximation of the losses if there would be any case where the inductor's losses would not fit the model, the network design presented in this work is ideally suited to optimise the power gain of those networks.

Finally, the lossy networks' power gain optimisation strategy derived in this work may serve to implement an improved cost function in a broadband (or higher order) network design optimisation (an example for a filter optimisation employing a cost function combined with other methods is given in [70]), to enhance the parametrisation of such networks, or to find better initial values in a lossy network optimisation like in [71].

Appendix A

RF Basics

A.1 Definitions/notations

From this chapter on, the following definitions/notations will be used:

Latin letters

B_i	Defined as $-\omega C_1$ in Figure A.4 and subsequent calculations
B_i	Defined as $\frac{1}{\omega L_\mathrm{p}}$ in Figure A.6 and subsequent calculations
B_ℓ	Load susceptance (in parallel to load conductance G_ℓ)
$g_\mathrm{tp}(\underline{r}_{\ell\mathrm{tp},\,50\,\Omega})$	Power gain of a two-port as a function of reflection coefficient $\underline{r}_{\ell\mathrm{tp},\,50\,\Omega}$
$\underline{I}(z)$	Complex amplitude of the current in a transmission line at location z
$\underline{I}_1$	Complex amplitude a current of flowing in a network's input
$\underline{I}_\ell$	Complex amplitude of a current flowing through the load impedance $\underline{Z}_\ell$
$\underline{p}$	Complex variable
$\underline{q}$	Complex variable
$\underline{r}(z)$	Reflection coefficient at location z (referred to $\underline{Z}_0$)
$\underline{r}_{1\mathrm{t}}$	Reflection coefficient at the input of a T network (referred to $\underline{Z}_0$)
$\underline{r}_{1\mathrm{tp},\,50\,\Omega}$	Reflection coefficient at the input of a two-port referred to $50\,\Omega$
$\underline{r}_{1\pi}$	Reflection coefficient at the input of a π network (referred to $\underline{Z}_0$)
$\underline{r}_{\ell\mathrm{tp},\,50\,\Omega}$	Reflection coefficient of the load impedance of $\underline{Z}_\ell$ referred to $50\,\Omega$
$\underline{S}_{11\mathrm{tp},\,50\,\Omega}$	S-parameter S_{11} of a two-port referred to $50\,\Omega$
$\underline{S}_{12\mathrm{tp},\,50\,\Omega}$	S-parameter S_{12} of a two-port referred to $50\,\Omega$
$\underline{S}_{21\mathrm{tp},\,50\,\Omega}$	S-parameter S_{21} of a two-port referred to $50\,\Omega$
$\underline{S}_{22\mathrm{tp},\,50\,\Omega}$	S-parameter S_{22} of a two-port referred to $50\,\Omega$
$\underline{V}(z)$	Complex amplitude of the voltage along a transmission line at location z
$\underline{V}_1$	Complex amplitude of the voltage at the beginning of a transmission line (at its input)
$\underline{V}_1$	Complex amplitude of the voltage at a network's input
$\underline{V}_2$	Complex amplitude of the voltage at the end of a transmission line (at its load)
$\underline{V}_\mathrm{i}(z)$	Complex amplitude of the incident voltage at location z of a transmission line
$\underline{V}_\ell$	Complex amplitude of the voltage at the load impedance $\underline{Z}_\ell$
$\underline{V}_\mathrm{r}(z)$	Complex amplitude of the reflected voltage at location z of a transmission line
x	Real variable

X_i	Defined as $-\omega L_\mathrm{s}$ in Figure A.4 and subsequent calculations
X_i	Defined as $\frac{1}{\omega C_1}$ in Figure A.6 and subsequent calculations
X_ℓ	Load reactance (in series to load resistance R_ℓ)
$\underline{Y}_1$	Admittance at the beginning of a transmission line (at its input, $(\underline{Y}_1 = \frac{1}{\underline{Z}_1})$
$\underline{Y}_{1\pi}$	Input admittance of a π network
$\underline{Z}_{1\mathrm{t}}$	Input impedance of a T network

A.2 Active power delivered from a source to a load as a function of available power

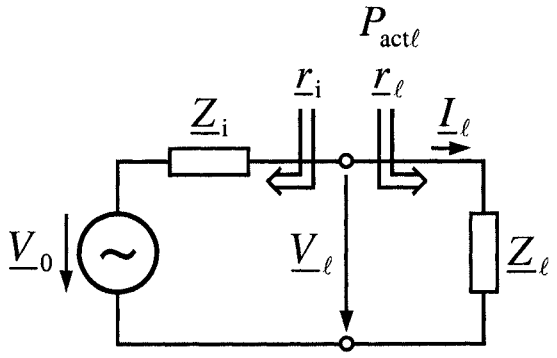

Figure A.1: Definitions and setup for $P_{\mathrm{act}\ell}$ derivation

If a voltage source of complex amplitude $\underline{V}_0$ and source impedance $\underline{Z}_\mathrm{i}$ is connected to a load impedance $\underline{Z}_\ell$, $P_{\mathrm{act}\ell}$ is the active power delivered to the load. It will be compared to the available power P_{actmaxi}, which equals the active power delivered to the load for a conjugate complex match $(\underline{Z}_\ell = \underline{Z}_\mathrm{i}^*)$.

The available power is defined by

$$P_{\mathrm{actmaxi}} = \frac{|\underline{V}_0|^2}{8\,\mathrm{Re}\{\underline{Z}_\mathrm{i}\}}. \tag{A.1}$$

For the setup shown in Figure A.1, the active power delivered to the load is

$$P_{\mathrm{act}\ell} = \frac{1}{2}\mathrm{Re}\{\underline{V}_\ell \underline{I}_\ell^*\} = \frac{1}{2}\mathrm{Re}\left\{\frac{\underline{Z}_\ell \underline{V}_0}{\underline{Z}_\mathrm{i}+\underline{Z}_\ell}\,\frac{\underline{Z}_\ell^* \underline{V}_0^*}{(\underline{Z}_\mathrm{i}^*+\underline{Z}_\ell^*)\,\underline{Z}_\ell^*}\right\}$$

$$P_{\mathrm{act}\ell} = \frac{|\underline{V}_0|^2}{2}\,\frac{\mathrm{Re}\{\underline{Z}_\ell\}}{(\mathrm{Re}\{\underline{Z}_\mathrm{i}\}+\mathrm{Re}\{\underline{Z}_\ell\})^2+(\mathrm{Im}\{\underline{Z}_\mathrm{i}\}+\mathrm{Im}\{\underline{Z}_\ell\})^2}.$$

Applying (A.1) yields

$$P_{\mathrm{act}\ell} = P_{\mathrm{actmaxi}}\,\frac{4\,\mathrm{Re}\{\underline{Z}_\mathrm{i}\}\,\mathrm{Re}\{\underline{Z}_\ell\}}{(\mathrm{Re}\{\underline{Z}_\mathrm{i}\}+\mathrm{Re}\{\underline{Z}_\ell\})^2+(\mathrm{Im}\{\underline{Z}_\mathrm{i}\}+\mathrm{Im}\{\underline{Z}_\ell\})^2}.$$

In the next step we will replace real and imaginary parts of source and load impedance with their reflection coefficient representations derived in (2.11) and (2.12).

Doing so gives

$$P_{\mathrm{act}\ell} = P_{\mathrm{actmaxi}} \frac{4\,\frac{R_0\,(1-|\underline{r}_\mathrm{i}|^2)-2X_0\,\mathrm{Im}\{\underline{r}_\mathrm{i}\}}{|1-\underline{r}_\mathrm{i}|^2}\,\frac{R_0\,(1-|\underline{r}_\ell|^2)-2X_0\,\mathrm{Im}\{\underline{r}_\ell\}}{|1-\underline{r}_\ell|^2}}{\left(\frac{R_0\,(1-|\underline{r}_\mathrm{i}|^2)-2X_0\,\mathrm{Im}\{\underline{r}_\mathrm{i}\}}{|1-\underline{r}_\mathrm{i}|^2}+\frac{R_0\,(1-|\underline{r}_\ell|^2)-2X_0\,\mathrm{Im}\{\underline{r}_\ell\}}{|1-\underline{r}_\ell|^2}\right)^2+\left(\frac{2R_0\,\mathrm{Im}\{\underline{r}_\mathrm{i}\}+X_0\,(1-|\underline{r}_\mathrm{i}|^2)}{|1-\underline{r}_\mathrm{i}|^2}+\frac{2R_0\,\mathrm{Im}\{\underline{r}_\ell\}+X_0\,(1-|\underline{r}_\ell|^2)}{|1-\underline{r}_\ell|^2}\right)^2}.$$

Putting

$$\frac{R_0\,(1-|\underline{r}_\mathrm{i}|^2)-2X_0\,\mathrm{Im}\{\underline{r}_\mathrm{i}\}}{|1-\underline{r}_\mathrm{i}|^2} = \frac{R_0\,(1-(\mathrm{Re}\{\underline{r}_\mathrm{i}\})^2-(\mathrm{Im}\{\underline{r}_\mathrm{i}\})^2)-2X_0\,\mathrm{Im}\{\underline{r}_\mathrm{i}\}}{(1-\mathrm{Re}\{\underline{r}_\mathrm{i}\})^2+(\mathrm{Im}\{\underline{r}_\mathrm{i}\})^2}, \qquad \frac{R_0\,(1-|\underline{r}_\ell|^2)-2X_0\,\mathrm{Im}\{\underline{r}_\ell\}}{|1-\underline{r}_\ell|^2} = \frac{R_0\,(1-(\mathrm{Re}\{\underline{r}_\ell\})^2-(\mathrm{Im}\{\underline{r}_\ell\})^2)-2X_0\,\mathrm{Im}\{\underline{r}_\ell\}}{(1-\mathrm{Re}\{\underline{r}_\ell\})^2+(\mathrm{Im}\{\underline{r}_\ell\})^2},$$

$$\frac{2R_0\,\mathrm{Im}\{\underline{r}_\mathrm{i}\}+X_0\,(1-|\underline{r}_\mathrm{i}|^2)}{|1-\underline{r}_\mathrm{i}|^2} = \frac{2R_0\,\mathrm{Im}\{\underline{r}_\mathrm{i}\}+X_0\,(1-(\mathrm{Re}\{\underline{r}_\mathrm{i}\})^2-(\mathrm{Im}\{\underline{r}_\mathrm{i}\})^2)}{(1-\mathrm{Re}\{\underline{r}_\mathrm{i}\})^2+(\mathrm{Im}\{\underline{r}_\mathrm{i}\})^2}, \text{ and } \frac{2R_0\,\mathrm{Im}\{\underline{r}_\ell\}+X_0\,(1-|\underline{r}_\ell|^2)}{|1-\underline{r}_\ell|^2} = \frac{2R_0\,\mathrm{Im}\{\underline{r}_\ell\}+X_0\,(1-(\mathrm{Re}\{\underline{r}_\ell\})^2-(\mathrm{Im}\{\underline{r}_\ell\})^2)}{(1-\mathrm{Re}\{\underline{r}_\ell\})^2+(\mathrm{Im}\{\underline{r}_\ell\})^2}$$

in the above equation followed by rearranging yields

$$P_{\mathrm{act}\ell} = P_{\mathrm{actmaxi}} \frac{[R_0\,(1-(\mathrm{Re}\{\underline{r}_\mathrm{i}\})^2-(\mathrm{Im}\{\underline{r}_\mathrm{i}\})^2)-2X_0\,\mathrm{Im}\{\underline{r}_\mathrm{i}\}]\,[R_0\,(1-(\mathrm{Re}\{\underline{r}_\ell\})^2-(\mathrm{Im}\{\underline{r}_\ell\})^2)-2X_0\,\mathrm{Im}\{\underline{r}_\ell\}]}{(R_0^2+X_0^2)\,[2\,\mathrm{Im}\{\underline{r}_\mathrm{i}\}\,\mathrm{Im}\{\underline{r}_\ell\}+(\mathrm{Im}\{\underline{r}_\mathrm{i}\})^2\,(\mathrm{Re}\{\underline{r}_\ell\})^2+(1-\mathrm{Re}\{\underline{r}_\mathrm{i}\}\,\mathrm{Re}\{\underline{r}_\ell\})^2+(\mathrm{Im}\{\underline{r}_\ell\})^2\,((\mathrm{Re}\{\underline{r}_\mathrm{i}\})^2+(\mathrm{Im}\{\underline{r}_\mathrm{i}\})^2)]}.$$

Further rearranging according to

$$\begin{aligned}
&2\,\mathrm{Im}\{\underline{r}_\mathrm{i}\}\,\mathrm{Im}\{\underline{r}_\ell\}+(\mathrm{Im}\{\underline{r}_\mathrm{i}\})^2\,(\mathrm{Re}\{\underline{r}_\ell\})^2+(1-\mathrm{Re}\{\underline{r}_\mathrm{i}\}\,\mathrm{Re}\{\underline{r}_\ell\})^2+(\mathrm{Im}\{\underline{r}_\ell\})^2\,((\mathrm{Re}\{\underline{r}_\mathrm{i}\})^2+(\mathrm{Im}\{\underline{r}_\mathrm{i}\})^2)\\
&= 1-2\,\mathrm{Re}\{\underline{r}_\mathrm{i}\}\,\mathrm{Re}\{\underline{r}_\ell\}+2\,\mathrm{Im}\{\underline{r}_\mathrm{i}\}\,\mathrm{Im}\{\underline{r}_\ell\}+((\mathrm{Re}\{\underline{r}_\mathrm{i}\})^2+(\mathrm{Im}\{\underline{r}_\mathrm{i}\})^2)\,((\mathrm{Re}\{\underline{r}_\ell\})^2+(\mathrm{Im}\{\underline{r}_\ell\})^2)\\
&= 1-\underline{r}_\mathrm{i}\,\underline{r}_\ell-\underline{r}_\mathrm{i}^*\,\underline{r}_\ell^*+|\underline{r}_\mathrm{i}|^2\,|\underline{r}_\ell|^2 = 1-2\,\mathrm{Re}\{\underline{r}_\mathrm{i}\,\underline{r}_\ell\}+|\underline{r}_\mathrm{i}\,\underline{r}_\ell|^2 = 1-2\,\mathrm{Re}\{\underline{r}_\mathrm{i}\,\underline{r}_\ell\}+(\mathrm{Re}\{\underline{r}_\mathrm{i}\,\underline{r}_\ell\})^2+(\mathrm{Im}\{\underline{r}_\mathrm{i}\,\underline{r}_\ell\})^2\\
&= (1-\mathrm{Re}\{\underline{r}_\mathrm{i}\,\underline{r}_\ell\})^2+(\mathrm{Im}\{\underline{r}_\mathrm{i}\,\underline{r}_\ell\})^2 = |1-\underline{r}_\mathrm{i}\,\underline{r}_\ell|^2
\end{aligned}$$

finally gives

$$P_{\mathrm{act}\ell} = P_{\mathrm{actmaxi}} \frac{[R_0\,(1-|\underline{r}_\mathrm{i}|^2)-2X_0\,\mathrm{Im}\{\underline{r}_\mathrm{i}\}]\,[R_0\,(1-|\underline{r}_\ell|^2)-2X_0\,\mathrm{Im}\{\underline{r}_\ell\}]}{|\underline{Z}_0|^2\,|1-\underline{r}_\mathrm{i}\,\underline{r}_\ell|^2}. \tag{A.2}$$

For a real characteristic impedance ($X_0 = 0$), (A.2) is equal to [72a].

A.3 Active power in a transmission line and its transducer and power gain

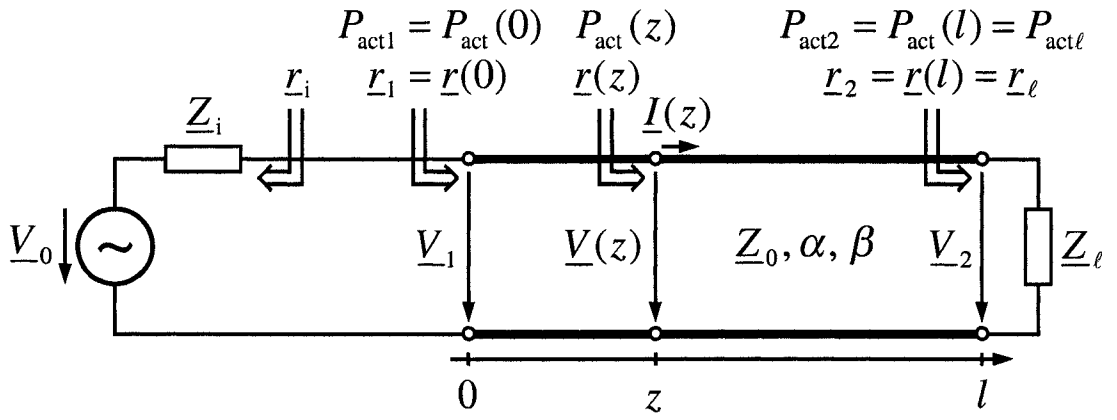

Figure A.2: Definitions and setup for $P_{act}(z)$ derivation

Consider a transmission line of length l in the setup depicted in Figure A.2. Its complex characteristic impedance is $\underline{Z}_0$, its attenuation constant α, and its phase constant β. The line is driven by a voltage source of complex amplitude $\underline{V}_0$ and source impedance $\underline{Z}_i$. it's terminated by a load impedance $\underline{Z}_\ell$.

$\underline{V}(z)$, the complex amplitude of the voltage along the line at location z, may be computed as the sum of the complex amplitude $\underline{V}_i(z)$ of the incident wave's voltage and the complex amplitude $\underline{V}_r(z)$ of the reflected wave's voltage.

Their ratio, as indicated in [26e], is the reflection coefficient $\underline{r}(z)$ at location z,

$$\underline{r}(z) := \frac{\underline{V}_r(z)}{\underline{V}_i(z)} = \underline{r}_2\, e^{-2\alpha(l-z)}\, e^{-j2\beta(l-z)} = \underline{r}_\ell\, e^{-2\alpha(l-z)}\, e^{-j2\beta(l-z)}. \tag{A.3}$$

By using this relationship in conjunction with [26d] (which derives the complex amplitude $\underline{V}(z)$ of the voltage or $\underline{I}(z)$ of the current along the transmission line at location z), we obtain

$$\underline{V}(z) = \underline{V}_i(0)\, e^{-\alpha z}\, e^{-j\beta z}\, (1 + \underline{r}(z)), \tag{A.4}$$

$$\underline{I}(z) = \frac{\underline{V}_i(0)\, e^{-\alpha z}\, e^{-j\beta z}\, (1 - \underline{r}(z))}{\underline{Z}_0}. \tag{A.5}$$

The complex amplitude $\underline{V}_1$ of the voltage at the line's input may be computed as a function of the reflection coefficients according to [73], yielding

$$\underline{V}_1 = \frac{\underline{V}_0}{2} \frac{(1 - \underline{r}_i)\,(1 + \underline{r}_1)}{1 - \underline{r}_i\, \underline{r}_1}, \tag{A.6}$$

where $\underline{r}_1 = \underline{r}(0)$.

Due to $\underline{V}_1 = \underline{V}(0)$, we obtain by comparison of (A.4) and (A.6) that

$$\underline{V}_\mathrm{i}(0) = \frac{\underline{V}_0}{2}\,\frac{1-\underline{r}_\mathrm{i}}{1-\underline{r}_\mathrm{i}\,\underline{r}_1}. \tag{A.7}$$

[26g] calculates the active power delivered to location z of the line,

$$P_\mathrm{act}(z) = \frac{1}{2}\,\mathrm{Re}\left\{\underline{V}(z)\,\underline{I}^*(z)\right\}. \tag{A.8}$$

Applying (A.4) and (A.5) yields

$$\begin{aligned} P_\mathrm{act}(z) &= \frac{1}{2}\,\mathrm{Re}\left\{\underline{V}_\mathrm{i}(0)\,\mathrm{e}^{-\alpha z}\,\mathrm{e}^{-\mathrm{j}\beta z}\,(1+\underline{r}(z))\,\frac{\underline{V}_\mathrm{i}^*(0)\,\mathrm{e}^{-\alpha z}\,\mathrm{e}^{\mathrm{j}\beta z}\,(1-\underline{r}^*(z))}{\underline{Z}_0^*}\right\} \\ &= \frac{1}{2}\,|\underline{V}_\mathrm{i}(0)|^2\,\mathrm{e}^{-2\alpha z}\,\mathrm{Re}\left\{\frac{1+\underline{r}(z)-\underline{r}^*(z)-|\underline{r}(z)|^2}{\underline{Z}_0^*}\right\}. \end{aligned}$$

$$P_\mathrm{act}(z) \overset{(A.7)}{=} \frac{|\underline{V}_0|^2}{8}\,\frac{\mathrm{e}^{-2\alpha z}\,|1-\underline{r}_\mathrm{i}|^2}{|1-\underline{r}_\mathrm{i}\,\underline{r}_1|^2}\,\mathrm{Re}\left\{\frac{(1-|\underline{r}(z)|^2+2\mathrm{j}\,\mathrm{Im}\{\underline{r}(z)\})\,(R_0+\mathrm{j}X_0)}{|\underline{Z}_0|^2}\right\}$$

$$P_\mathrm{act}(z) \overset{(A.1)}{=} P_\mathrm{actmaxi}\,\mathrm{Re}\{\underline{Z}_\mathrm{i}\}\,\frac{\mathrm{e}^{-2\alpha z}\,|1-\underline{r}_\mathrm{i}|^2}{|1-\underline{r}_\mathrm{i}\,\underline{r}_1|^2}\,\frac{R_0\,(1-|\underline{r}(z)|^2)-2X_0\,\mathrm{Im}\{\underline{r}(z)\}}{|\underline{Z}_0|^2}$$

$$P_\mathrm{act}(z) \overset{(2.11)}{=} P_\mathrm{actmaxi}\,\mathrm{e}^{-2\alpha z}\,\frac{[R_0\,(1-|\underline{r}_\mathrm{i}|^2)-2X_0\,\mathrm{Im}\{\underline{r}_\mathrm{i}\}]\,[R_0\,(1-|\underline{r}(z)|^2)-2X_0\,\mathrm{Im}\{\underline{r}(z)\}]}{|\underline{Z}_0|^2\,|1-\underline{r}_\mathrm{i}\,\underline{r}_1|^2}$$

$$P_\mathrm{act}(z) \overset{(A.3)}{=} P_\mathrm{actmaxi}\,\mathrm{e}^{-2\alpha z}\,\frac{[R_0\,(1-|\underline{r}_\mathrm{i}|^2)-2X_0\,\mathrm{Im}\{\underline{r}_\mathrm{i}\}]\,[R_0\,(1-|\underline{r}(z)|^2)-2X_0\,\mathrm{Im}\{\underline{r}(z)\}]}{|\underline{Z}_0|^2\,|1-\underline{r}_\mathrm{i}\,\underline{r}_\ell\,\mathrm{e}^{-2\alpha l}\,\mathrm{e}^{-\mathrm{j}2\beta l}|^2}. \tag{A.9}$$

This result is partially calculated in [26g]. However, [26g] does not take into account that the complex amplitude of the incident wave's voltage depends on the load impedance or its reflection coefficient $\underline{r}_\ell$, respectively.

The active power delivered to the load is $P_{\mathrm{act}\ell} = P_\mathrm{act}(l)$, hence the transducer power gain $g_{\mathrm{T,L}}$ of the line is

$$g_{\mathrm{T,L}} := \frac{P_{\mathrm{act}\ell}}{P_\mathrm{actmaxi}} = \mathrm{e}^{-2\alpha l}\,\frac{[R_0\,(1-|\underline{r}_\mathrm{i}|^2)-2X_0\,\mathrm{Im}\{\underline{r}_\mathrm{i}\}]\,[R_0\,(1-|\underline{r}_\ell|^2)-2X_0\,\mathrm{Im}\{\underline{r}_\ell\}]}{|\underline{Z}_0|^2\,|1-\underline{r}_\mathrm{i}\,\underline{r}_\ell\,\mathrm{e}^{-2\alpha l}\,\mathrm{e}^{-\mathrm{j}2\beta l}|^2}. \tag{A.10}$$

In the following sections we will additionally need the power gain g_L of the line or $P_{\mathrm{act}\ell}$, the active power delivered to the load, as a function of $P_\mathrm{act1} = P_\mathrm{act}(0)$, the active power delivered to the line's input at $z = 0$.

To derive it, we use (A.2), where $\underline{r}_\ell$ is replaced with $\underline{r}(0) = \underline{r}_1 = \underline{r}_\ell\,\mathrm{e}^{-2\alpha l}\,\mathrm{e}^{-\mathrm{j}2\beta l}$ (from (A.3)), in (A.10), yielding

$$g_\mathrm{L} := \frac{P_{\mathrm{act}\ell}}{P_\mathrm{act1}} = \mathrm{e}^{-2\alpha l}\,\frac{R_0\,(1-|\underline{r}_\ell|^2)-2X_0\,\mathrm{Im}\{\underline{r}_\ell\}}{R_0\,(1-|\underline{r}_\ell\,\mathrm{e}^{-2\alpha l}\,\mathrm{e}^{-\mathrm{j}2\beta l}|^2)-2X_0\,\mathrm{Im}\{\underline{r}_\ell\,\mathrm{e}^{-2\alpha l}\,\mathrm{e}^{-\mathrm{j}2\beta l}\}} \tag{A.11}$$

$$g_\mathrm{L} = \mathrm{e}^{-2\alpha l}\,\frac{R_0\,(1-|\underline{r}_\ell|^2)-2X_0\,\mathrm{Im}\{\underline{r}_\ell\}}{R_0\,(1-\mathrm{e}^{-4\alpha l}\,|\underline{r}_\ell|^2)-2X_0\,\mathrm{e}^{-2\alpha l}\,\mathrm{Im}\{\underline{r}_\ell\,\mathrm{e}^{-\mathrm{j}2\beta l}\}}. \tag{A.12}$$

A similar formula is derived in [28] and [29].

A.4 Input reflection coefficient and power gain of L, π, and T networks at a fixed operating frequency

A.4.1 Calculation using network elements' values

A.4.1.1 π network

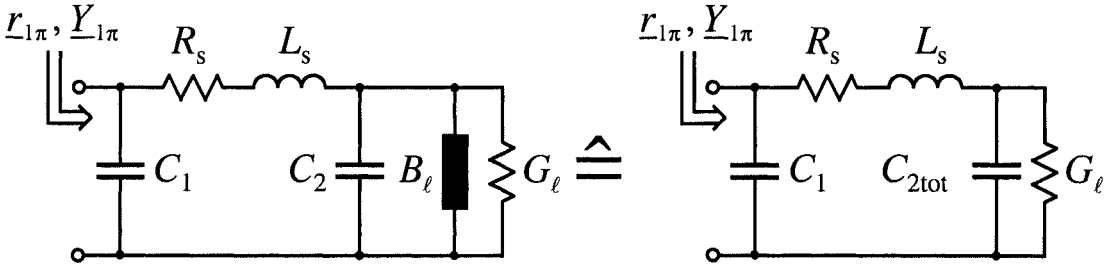

Figure A.3: Definitions for calculation of the π network's input reflection coefficient

Using the definitions of Figure A.3, the input admittance $\underline{Y}_{1\pi}$ is given by[1]

$$\left.\begin{aligned} \underline{Y}_{1\pi} &= \mathrm{j}\omega C_1 + \frac{1}{R_s + \mathrm{j}\omega L_s + \frac{1}{G_\ell + \mathrm{j}\omega C_{2tot}}} \\ \text{where} \quad G_\ell &= \mathrm{Re}\left\{\frac{1}{\underline{Z}_\ell}\right\}, \quad C_{2tot} = C_2 + \frac{1}{\omega}\,\mathrm{Im}\left\{\frac{1}{\underline{Z}_\ell}\right\}. \end{aligned}\right\} \tag{A.13}$$

Applying the preceding admittance and (2.9), we may compute the π network's input reflection coefficient $\underline{r}_{1\pi}$ referred to $\underline{Z}_0$, obtaining

$$\underline{r}_{1\pi} = \frac{1 - \underline{Y}_{1\pi}\underline{Z}_0}{1 + \underline{Y}_{1\pi}\underline{Z}_0}. \tag{A.14}$$

Since the π network's power gain g_π is independent of the driving source's impedance (e. g. according to (A.26)), we may simplify its derivation by choosing the source impedance to cancel all reactive components at the input of the π network.

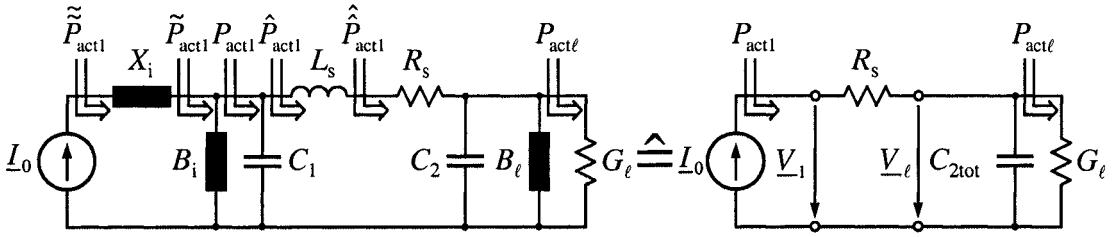

Figure A.4: Definitions for calculation of the π network's power gain and equivalent circuit for $X_i = -\omega L_s$, $B_i = -\omega C_1$

[1]There is no need to distinguish C_{2tot} and L_{2tot} depending on the sign of $C_2 + \frac{1}{\omega}\,\mathrm{Im}\left\{\frac{1}{\underline{Z}_\ell}\right\}$. The calculated $\underline{Y}_{1\pi}$, $\underline{r}_{1\pi}$, or g_π resemble proper values although a formally negative C_{2tot} might occur.

All reactive components in Figure A.4, namely X_i, $B_{\mathrm{i},\ell}$, $C_{1,2}$, and L_s, are lossless. Thus $\widetilde{\widetilde{P}}_{\mathrm{act1}} = \widetilde{P}_{\mathrm{act1}} = P_{\mathrm{act1}} = \widehat{P}_{\mathrm{act1}} = \widehat{\widehat{P}}_{\mathrm{act1}}$ holds, which equals the incident active power in the equivalent circuit (right half of Figure A.4).
Using the definitions of Figure A.4 yields

$$P_{\mathrm{act1}} = \frac{1}{2}\mathrm{Re}\{\underline{V}_1\,\underline{I}_0^*\} = \frac{1}{2}\mathrm{Re}\left\{|\underline{I}_0|^2\left(R_\mathrm{s} + \frac{1}{G_\ell + \mathrm{j}\omega C_{2\mathrm{tot}}}\right)\right\}$$

$$P_{\mathrm{act1}} = \frac{1}{2}|\underline{I}_0|^2\left(R_\mathrm{s} + \frac{G_\ell}{G_\ell^2 + \omega^2 C_{2\mathrm{tot}}^2}\right).$$

The active power delivered to the load is given by

$$P_{\mathrm{act}\ell} = \frac{1}{2}|\underline{V}_\ell|^2 G_\ell = \frac{1}{2}|\underline{I}_0|^2 \frac{G_\ell}{G_\ell^2 + \omega^2 C_{2\mathrm{tot}}^2}.$$

Thus the π network's power gain is

$$g_\pi = \frac{P_{\mathrm{act}\ell}}{P_{\mathrm{act1}}} = \frac{G_\ell}{R_\mathrm{s}\left(G_\ell^2 + \omega^2 C_{2\mathrm{tot}}^2\right) + G_\ell} = \frac{1}{1 + \frac{R_\mathrm{s}}{\frac{G_\ell}{G_\ell^2 + \omega^2 C_{2\mathrm{tot}}^2}}}\,^\dagger. \tag{A.15}$$

Two L networks, each for $C_1 = 0$ or $C_2 = 0$, may be viewed as limits of the π network. Their input impedances and power gains are computed by putting $C_1 = 0$ or $C_2 = 0$, respectively.

A.4.1.2 T network

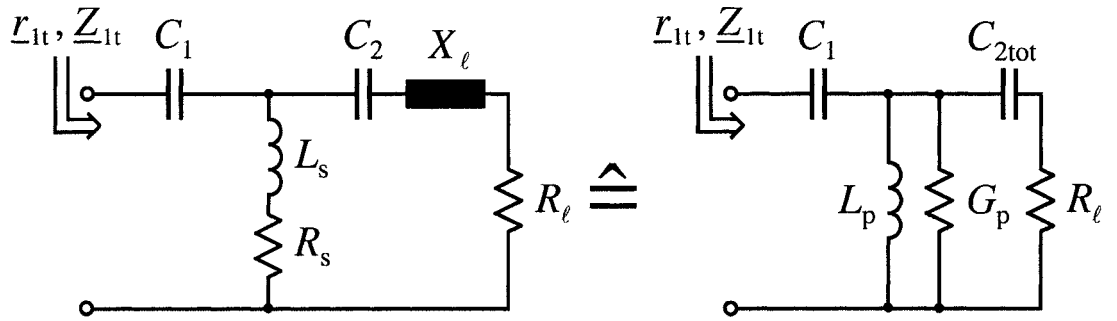

Figure A.5: Definitions for calculation of the T network's input reflection coefficient and its equivalent circuit after series-to-parallel transformation of R_s and L_s

Calculation of the T network's input reflection coefficient starts by series-to-parallel-transformation of R_s and L_s in G_p and L_p (right half of Figure A.5). [34c] computes the parallel components' values,

---

$^\dagger \frac{G_\ell}{G_\ell^2 + \omega^2 C_{2\mathrm{tot}}^2}$ is the series resistance after parallel-to-series transformation of G_ℓ and $C_{2\mathrm{tot}}$ (calculated using (A.19) after replacing G_p with G_ℓ and $\frac{1}{\omega L_\mathrm{p}}$ by $\omega C_{2\mathrm{tot}}$).

$$G_\mathrm{p} = \frac{R_\mathrm{s}}{R_\mathrm{s}^2 + \omega^2 L_\mathrm{s}^2}, \quad \text{(A.16)} \qquad L_\mathrm{p} = \frac{R_\mathrm{s}^2 + \omega^2 L_\mathrm{s}^2}{\omega^2 L_\mathrm{s}}. \quad \text{(A.17)}$$

Additionally, we need to examine the transformed network's element values in case R_s, L_s tend to zero or infinity. However, R_s and L_s are not independently of each other, but obey (3.1). If the limits of G_p and L_p are derived using (3.1), we obtain

(i) If $L_\mathrm{s} = 0$ then $R_\mathrm{s} = R_{\mathrm{s}0}$:
  a) $R_{\mathrm{s}0} = 0$:
    - $0 < b_1 < \frac{1}{2}$: $G_\mathrm{p} \to \infty$, $L_\mathrm{p} \to \infty$ or $\frac{1}{L_\mathrm{p}} = 0$
      (since $G_\mathrm{i} - G_\mathrm{m} - G_\mathrm{p} < 0$, matching is impossible, thus never part of a valid solution)
    - $b_1 = \frac{1}{2}$: $G_\mathrm{p} \to \infty$, $L_\mathrm{p} = \frac{a_1^2}{\omega}$ or $\frac{1}{L_\mathrm{p}} = \frac{\omega}{a_1^2}$
      (since $G_\mathrm{i} - G_\mathrm{m} - G_\mathrm{p} < 0$, matching is impossible, thus never part of a valid solution)
    - $\frac{1}{2} < b_1 < 2$: $G_\mathrm{p} \to \infty$, $L_\mathrm{p} = 0$ or $\frac{1}{L_\mathrm{p}} \to \infty$
      (since $G_\mathrm{i} - G_\mathrm{m} - G_\mathrm{p} < 0$, matching is impossible, thus never part of a valid solution)
    - $b_1 = 2$: $G_\mathrm{p} = a_1$, $L_\mathrm{p} = 0$ or $\frac{1}{L_\mathrm{p}} \to \infty$
      ($b_1 = b_N = 2$ if $b_N \leq 2$)
    - $b_1 > 2$: $G_\mathrm{p} = 0$, $L_\mathrm{p} = 0$ or $\frac{1}{L_\mathrm{p}} \to \infty$
      (impossible if $b_N \leq 2$)
  b) $R_{\mathrm{s}0} > 0$: $G_\mathrm{p} = \frac{1}{R_{\mathrm{s}0}}$, $L_\mathrm{p} \to \infty$ or $\frac{1}{L_\mathrm{p}} = 0$.

(ii) If $L_\mathrm{s} \to \infty$ then $R_\mathrm{s} \to \infty$ (except $R_\mathrm{s} = R_{\mathrm{s}0}$ if $R_\mathrm{s} = \text{const.}$), $G_\mathrm{p} = 0$, and $L_\mathrm{p} \to \infty$ or $\frac{1}{L_\mathrm{p}} = 0$. (A.18)

The inverse parallel-to-series transformation is given by

$$R_\mathrm{s} = \frac{G_\mathrm{p}}{G_\mathrm{p}^2 + \frac{1}{\omega^2 L_\mathrm{p}^2}}, \quad \text{(A.19)} \qquad L_\mathrm{s} = \frac{\frac{1}{\omega^2 L_\mathrm{p}}}{G_\mathrm{p}^2 + \frac{1}{\omega^2 L_\mathrm{p}^2}}. \quad \text{(A.20)}$$

Using the definitions in Figure A.5 yields the input impedance $\underline{Z}_{1t}$ of the series-to-parallel transformed equivalent circuit[2],

$$\underline{Z}_{1\mathrm{t}} = \frac{1}{\mathrm{j}\omega C_1} + \frac{1}{G_\mathrm{p} + \frac{1}{\mathrm{j}\omega L_\mathrm{p}} + \frac{1}{R_\ell + \frac{1}{\mathrm{j}\omega C_{2\mathrm{tot}}}}}$$

$$\text{where} \quad R_\ell = \mathrm{Re}\{\underline{Z}_\ell\}, \quad C_{2\mathrm{tot}} = \frac{1}{\frac{1}{C_2} - \omega \mathrm{Im}\{\underline{Z}_\ell\}}. \qquad \text{(A.21)}$$

[2]There is no need to distinguish $C_{2\mathrm{tot}}$ and $L_{2\mathrm{tot}}$ depending on the sign of $\frac{1}{C_2} - \omega \mathrm{Im}\{\underline{Z}_\ell\}$. The calculated $\underline{Z}_{1t}$, $\underline{r}_{1t}$, or g_t resemble proper values although a formally negative $C_{2\mathrm{tot}}$ might occur.

Applying the preceding impedance and (2.9), we may compute the T network's input reflection coefficient $\underline{r}_{1t}$ referred to $\underline{Z}_0$, obtaining

$$\underline{r}_{1t} = \frac{\underline{Z}_{1t} - \underline{Z}_0}{\underline{Z}_{1t} + \underline{Z}_0}. \tag{A.22}$$

Since the T network's power gain g_t is independent of the driving source's impedance (e. g. according to (A.26)), we may simplify its derivation by choosing the source impedance to cancel all reactive components at the input of the T network.

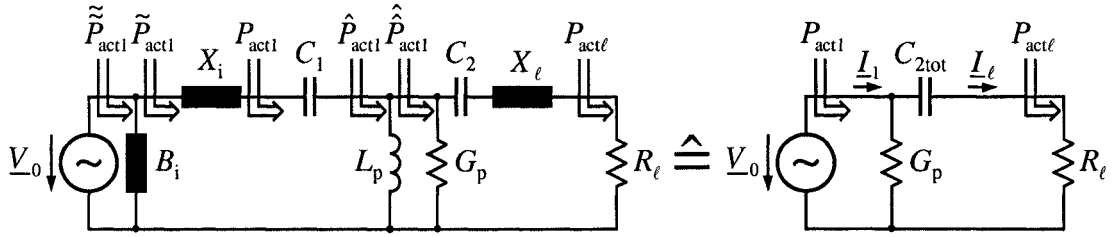

Figure A.6: Definitions for calculation of the T network's power gain and equivalent circuit for $B_i = \frac{1}{\omega L_p}$, $X_i = \frac{1}{\omega C_1}$

All reactive components in Figure A.6, namely B_i, $X_{i,\ell}$, $C_{1,2}$, and L_p, are lossless. Thus $\tilde{\tilde{P}}_{act1} = \tilde{P}_{act1} = P_{act1} = \hat{P}_{act1} = \hat{\hat{P}}_{act1}$ holds, which equals the incident active power in the equivalent circuit (right half of Figure A.6).
Using the definitions of Figure A.6 yields

$$P_{act1} = \frac{1}{2}\mathrm{Re}\{\underline{V}_0 \underline{I}_1^*\} = \frac{1}{2}\mathrm{Re}\left\{|\underline{V}_0|^2 \left(G_p + \frac{1}{R_\ell - \frac{1}{j\omega C_{2tot}}}\right)\right\}$$

$$P_{act1} = \frac{1}{2}|\underline{V}_0|^2 \left(G_p + \frac{R_\ell}{R_\ell^2 + \frac{1}{\omega^2 C_{2tot}^2}}\right).$$

The active power delivered to the load is given by

$$P_{act\ell} = \frac{1}{2}|\underline{I}_\ell|^2 R_\ell = \frac{1}{2}|\underline{V}_0|^2 \frac{R_\ell}{R_\ell^2 + \frac{1}{\omega^2 C_{2tot}^2}}.$$

Thus the T network's power gain is

$$g_t = \frac{P_{act\ell}}{P_{act1}} = \frac{R_\ell}{G_p\left(R_\ell^2 + \frac{1}{\omega^2 C_{2tot}^2}\right) + R_\ell} = \frac{1}{1 + \frac{G_p}{\frac{R_\ell}{R_\ell^2 + \frac{1}{\omega^2 C_{2tot}^2}}}} \ddagger. \tag{A.23}$$

Two L networks, each for $C_1 \to \infty$ or $C_2 \to \infty$, may be viewed as limits of the T network. Their input impedances and power gains are computed by putting $C_1 \to \infty$ or $C_2 \to \infty$, respectively.

---

‡ $\frac{R_\ell}{R_\ell^2 + \frac{1}{\omega^2 C_{2tot}^2}}$ is the parallel conductance after series-to-parallel transformation of R_ℓ and C_{2tot} (calculated using (A.16) after replacing R_s with R_ℓ and ωL_s with $\frac{1}{\omega C_{2tot}}$).

A.4.2 Calculation using (measured) S-parameters

The following formulae for the calculation of a two port's input impedance and power gain using (measured) S-parameters applies to any two-port, thus there is no difference in the calculations for the L , π , or T network.

Since common network analysers measure S-parameters referred to a characteristic impedance of $50\,\Omega$ for both ports, it will also be the characteristic impedance all reflection coefficients are referred to in the following formulae.

[74a] computes the input reflection coefficient of a two-port tp as a function of its load,

$$\underline{r}_{1\mathrm{tp},\,50\,\Omega} = \underline{S}_{11\mathrm{tp},\,50\,\Omega} + \frac{\underline{S}_{21\mathrm{tp},\,50\,\Omega}\,\underline{S}_{12\mathrm{tp},\,50\,\Omega}\,\underline{r}_{\ell\mathrm{tp},\,50\,\Omega}}{1 - \underline{S}_{22\mathrm{tp},\,50\,\Omega}\,\underline{r}_{\ell\mathrm{tp},\,50\,\Omega}}. \tag{A.24}$$

The two-port's power gain may be calculated from [74b] or by applying (A.2) and (A.24) to [72b], yielding

$$g_{\mathrm{tp}}(\underline{r}_{\ell\mathrm{tp},\,50\,\Omega}) = \frac{|\underline{S}_{21\mathrm{tp},\,50\,\Omega}|^2\,(1 - |\underline{r}_{\ell\mathrm{tp},\,50\,\Omega}|^2)}{|1 - \underline{S}_{22\mathrm{tp},\,50\,\Omega}\,\underline{r}_{\ell\mathrm{tp},\,50\,\Omega}|^2\,(1 - |\underline{r}_{1\mathrm{tp},\,50\,\Omega}|^2)}. \tag{A.25}$$

Using (A.24) and the relationship $|\underline{p}|^2\,|\underline{q}|^2 = |\underline{p}\,\underline{q}|^2$ gives

$$g_{\mathrm{tp}}(\underline{r}_{\ell\mathrm{tp},\,50\,\Omega}) = \frac{|\underline{S}_{21\mathrm{tp},\,50\,\Omega}|^2\,(1 - |\underline{r}_{\ell\mathrm{tp},\,50\,\Omega}|^2)}{|1 - \underline{S}_{22\mathrm{tp},\,50\,\Omega}\,\underline{r}_{\ell\mathrm{tp},\,50\,\Omega}|^2 - |(1 - \underline{S}_{22\mathrm{tp},\,50\,\Omega}\,\underline{r}_{\ell\mathrm{tp},\,50\,\Omega})\,\underline{S}_{11\mathrm{tp},\,50\,\Omega} + \underline{S}_{21\mathrm{tp},\,50\,\Omega}\,\underline{S}_{12\mathrm{tp},\,50\,\Omega}\,\underline{r}_{\ell\mathrm{tp},\,50\,\Omega}|^2}. \tag{A.26}$$

The L, π, and T networks considered are reciprocal networks ([75]). Then, according to [26i] the following equality holds,

$$\underline{S}_{21\mathrm{tp},\,50\,\Omega} = \underline{S}_{12\mathrm{tp},\,50\,\Omega}. \tag{A.27}$$

If the networks would additionally be lossless ($R_{\mathrm{s}} = 0$ or $G_{\mathrm{p}} = 0$), they would consume no active power, thus

$$g_{\mathrm{tp}}(\underline{r}_{\ell\mathrm{tp},\,50\,\Omega}) = 1. \tag{A.28}$$

Appendix B

Lossy L, π, and T Matching Networks

B.1 Definitions/notations

From this chapter on, the following definitions/notations will be used:

Latin letters

$C_{1(\mathrm{p})}$	Lossy capacitance C_1 of a π network, index p indicates usage of parallel loss model
$C_{1(\mathrm{s})}$	Lossy capacitance C_1 of a T network, index s indicates usage of series loss model
$C_{2(\mathrm{p})}$	Lossy capacitance C_2 of a π network, index p indicates usage of parallel loss model
$C_{2(\mathrm{s})}$	Lossy capacitance C_2 of a T network, index s indicates usage of series loss model
$g_{\mathrm{t,\,llcapdes}}$	Power gain of a T network including losses of all elements designed as if its capacitors would be lossless
$g_{\mathrm{t,lldes}}$	Power gain of a T network designed as if it would be lossless
$g_{\mathrm{t,outma}}$	Power gain of a T network which is (exactly) matched at its output
$g_{\pi,\,\mathrm{llcapdes}}$	Power gain of a π network including losses of all elements designed as if its capacitors would be lossless
$g_{\pi,\mathrm{outma}}$	Power gain of a π network which is (exactly) matched at its output
G_{irest}	Resulting total source conductance of the "inner" T network as defined in Appendix B.3.3
$G_{\ell\mathrm{rest}}$	Resulting total load conductance of the "inner" T network as defined in Appendix B.3.3
$G_{\mathrm{s}C_1}$	Series loss conductance of capacitance $C_{1(\mathrm{s})}$ of a T network ($G_{\mathrm{s}C_1} = \frac{1}{R_{\mathrm{s}C_1}}$)
$G_{\mathrm{s}C_2}$	Series loss conductance of capacitance $C_{2(\mathrm{s})}$ of a T network ($G_{\mathrm{s}C_2} = \frac{1}{R_{\mathrm{s}C_2}}$)
$\underline{I}_{\mathrm{st}}$	Complex amplitude of a current flowing through R_ℓ (and thus through $R_{\ell\mathrm{rest}}$) of the T network in Appendix B.3.3
$\underline{I}_{\mathrm{s}\pi}$	Complex amplitude of a current flowing through R_s of the π network in Appendix B.3.2
P_{act1}	Active power transferred to the input of a network
P_{act2}	Active power transferred to a particular part of a network
P_{act3}	Active power transferred to a particular part of a network
Q_1	Q factor of capacitor C_1 of a π or T network
Q_2	Q factor of capacitor C_2 of a π or T network
$\underline{r}_{\mathrm{1t,\,lldes,\,Z_{0ll}}}$	Reflection coefficient at the input of a T network designed as if it would be lossless (referred to $Z_{0\mathrm{ll}}$)
$\underline{r}_{\mathrm{1}\pi,\,\mathrm{lldes,\,Z_{0ll}}}$	Reflection coefficient at the input of a π network designed as if it would be lossless referred to $Z_{0\mathrm{ll}}$

R_{irest}	Resulting total source resistance of the "inner" T network as defined in Appendix B.3.3 ($R_{\mathrm{irest}} = \frac{1}{G_{\mathrm{irest}}}$)
$R_{\mathrm{ires}\pi}$	Resulting total source resistance of the "inner" π network as defined in Appendix B.3.2
$R_{\ell\mathrm{rest}}$	Resulting total load resistance of the "inner" T network as defined in Appendix B.3.3 ($R_{\ell\mathrm{rest}} = \frac{1}{G_{\ell\mathrm{rest}}}$)
$R_{\ell\mathrm{res}\pi}$	Resulting total load resistance of the "inner" π network as defined in Appendix B.3.2
$R_{\mathrm{p}C_1}$	Parallel loss resistance of capacitance $C_{1(\mathrm{p})}$ of a π network
$R_{\mathrm{p}C_2}$	Parallel loss resistance of capacitance $C_{2(\mathrm{p})}$ of a π network
$R_{\mathrm{s}C_1}$	Series loss resistance of capacitance $C_{1(\mathrm{s})}$ of a T network
$R_{\mathrm{s}C_2}$	Series loss resistance of capacitance $C_{2(\mathrm{s})}$ of a T network
$\widetilde{\widetilde{S}}_{\mathrm{t}}$	Abbreviation for a sum in Appendix B.2.2.2
$\underline{V}_{\mathrm{pt}}$	Complex amplitude of the voltage at G_{p} of the T network in Appendix B.3.3
$\underline{V}_{\mathrm{p}\pi}$	Complex amplitude of the voltage at the load R_ℓ (and thus at $R_{\ell\mathrm{res}\pi}$) of the π network in Appendix B.3.2

B.2 Matching of a resistive load to a resistive source (matching at the network's input)

B.2.1 π network

B.2.1.1 Optimum value of parameter R_{m} for maximum power gain

As indicated in the overview of the proof given in Section 3.5.2.2, we begin the actual proof by assuming all $a_n = 0$, thus $R_{\mathrm{s}} = R_{\mathrm{s0}}$ throughout the valid range of R_{m}. We then obtain from (3.26)

$$\left(\frac{R_{\mathrm{s}}}{R_{\mathrm{m}}} - \frac{\mathrm{d}R_{\mathrm{s}}}{\mathrm{d}R_{\mathrm{m}}}\right)\Bigg|_{a_n=0\,\forall n} = \frac{R_{\mathrm{s0}}}{R_{\mathrm{m}}}.$$

Since R_{s0}, $R_{\mathrm{m}} \geq 0$, numerator and denominator of $\left(\frac{R_{\mathrm{s}}}{R_{\mathrm{m}}} - \frac{\mathrm{d}R_{\mathrm{s}}}{\mathrm{d}R_{\mathrm{m}}}\right)\Big|_{a_n=0\,\forall n}$ are always ≥ 0.

If at least one $a_n > 0$, we check numerator and denominator of (3.26) separately:

1. Since ωL_{s}, R_{m}, R_{s}, a_n are ≥ 0, and $b_n > 0$, the numerator will always be ≥ 0 for $R_{\mathrm{s}}\frac{\partial(\omega L_{\mathrm{s}})}{\partial R_{\mathrm{s}}} + R_{\mathrm{m}}\frac{\partial(\omega L_{\mathrm{s}})}{\partial R_{\mathrm{m}}} \leq 0$.

   Conversely, if $R_{\mathrm{s}}\frac{\partial(\omega L_{\mathrm{s}})}{\partial R_{\mathrm{s}}} + R_{\mathrm{m}}\frac{\partial(\omega L_{\mathrm{s}})}{\partial R_{\mathrm{m}}} > 0$,

   $$b_N\left(R_{\mathrm{s}}\frac{\partial(\omega L_{\mathrm{s}})}{\partial R_{\mathrm{s}}} + R_{\mathrm{m}}\frac{\partial(\omega L_{\mathrm{s}})}{\partial R_{\mathrm{m}}}\right) \geq b_n\left(R_{\mathrm{s}}\frac{\partial(\omega L_{\mathrm{s}})}{\partial R_{\mathrm{s}}} + R_{\mathrm{m}}\frac{\partial(\omega L_{\mathrm{s}})}{\partial R_{\mathrm{m}}}\right)$$

   holds due to $b_N > b_{N-1} > \ldots > b_1 > 0$.

From (3.1) we get $R_\mathrm{s} \geq \sum_{n=1}^{N} a_n \left(\omega L_\mathrm{s}\right)^{b_n}$, thus obtaining

$$\begin{aligned} & R_\mathrm{s}\,\omega L_\mathrm{s} - \sum_{n=1}^{N} a_n b_n \left(\omega L_\mathrm{s}\right)^{b_n} \left(R_\mathrm{s} \frac{\partial(\omega L_\mathrm{s})}{\partial R_\mathrm{s}} + R_\mathrm{m} \frac{\partial(\omega L_\mathrm{s})}{\partial R_\mathrm{m}} \right) \\ \geq\ & R_\mathrm{s}\,\omega L_\mathrm{s} - b_N\, R_\mathrm{s} \left(R_\mathrm{s} \frac{\partial(\omega L_\mathrm{s})}{\partial R_\mathrm{s}} + R_\mathrm{m} \frac{\partial(\omega L_\mathrm{s})}{\partial R_\mathrm{m}} \right). \end{aligned}$$

After applying (3.27), (3.28), and $R_\mathrm{s} \geq 0$, we finally have to check

$$\begin{aligned} & \omega L_\mathrm{s} - b_N \left(R_\mathrm{s} \frac{\partial(\omega L_\mathrm{s})}{\partial R_\mathrm{s}} + R_\mathrm{m} \frac{\partial(\omega L_\mathrm{s})}{\partial R_\mathrm{m}} \right) \\ =\ & \frac{(R_\mathrm{m}+R_\mathrm{s})\left((2-b_N)\left(R_\mathrm{i}-R_\mathrm{m}-R_\mathrm{s}\right)+b_N\left(R_\mathrm{m}+R_\mathrm{s}\right)\right)}{2\sqrt{\left(R_\mathrm{m}+R_\mathrm{s}\right)\left(R_\mathrm{i}-R_\mathrm{m}-R_\mathrm{s}\right)}} \\ & + \frac{R_\mathrm{m}\left((2-b_N)\left(R_\ell-R_\mathrm{m}\right)+b_N\,R_\mathrm{m}\right)}{2\sqrt{R_\mathrm{m}\left(R_\ell-R_\mathrm{m}\right)}}, \end{aligned}$$

which is always ≥ 0 throughout the (utmost) valid range of R_m indicated in (3.20) if $0 < b_N \leq 2$ holds[1].

2. Since ωL_s, R_m, a_n are ≥ 0, and $b_n > 0$, the denominator will always be ≥ 0 for $\frac{\partial(\omega L_\mathrm{s})}{\partial R_\mathrm{s}} \leq 0$.

   Conversely, if $\frac{\partial(\omega L_\mathrm{s})}{\partial R_\mathrm{s}} > 0$,

$$a_n b_N \left(\omega L_\mathrm{s}\right)^{b_n} \frac{\partial(\omega L_\mathrm{s})}{\partial R_\mathrm{s}} \geq a_n b_n \left(\omega L_\mathrm{s}\right)^{b_n} \frac{\partial(\omega L_\mathrm{s})}{\partial R_\mathrm{s}}$$

   holds due to $b_N > b_{N-1} > \ldots > b_1 > 0$.

   From (3.1) we get $R_\mathrm{s} \geq \sum_{n=1}^{N} a_n \left(\omega L_\mathrm{s}\right)^{b_n}$, thus obtaining

$$\omega L_\mathrm{s} - \sum_{n=1}^{N} a_n b_n \left(\omega L_\mathrm{s}\right)^{b_n} \frac{\partial(\omega L_\mathrm{s})}{\partial R_\mathrm{s}} \geq \omega L_\mathrm{s} - b_N\, R_\mathrm{s} \frac{\partial(\omega L_\mathrm{s})}{\partial R_\mathrm{s}}.$$

   After applying (3.28), we finally have to check

$$\begin{aligned} & \omega L_\mathrm{s} - b_N\, R_\mathrm{s} \frac{\partial(\omega L_\mathrm{s})}{\partial R_\mathrm{s}} \\ =\ & \frac{(2-b_N)\left(R_\mathrm{m}+R_\mathrm{s}\right)\left(R_\mathrm{i}-R_\mathrm{m}-R_\mathrm{s}\right)+b_N\left(R_\mathrm{m}\left(R_\mathrm{i}-R_\mathrm{m}\right)+R_\mathrm{s}^2\right)}{2\sqrt{\left(R_\mathrm{m}+R_\mathrm{s}\right)\left(R_\mathrm{i}-R_\mathrm{m}-R_\mathrm{s}\right)}} \\ & + \sqrt{R_\mathrm{m}\left(R_\ell-R_\mathrm{m}\right)}, \end{aligned}$$

   which is always ≥ 0 throughout the (utmost) valid range of R_m indicated in (3.20) if $0 < b_N \leq 2$ holds[1].

---

[1] The proof would still be valid if we would put $b_N = 0$, but its initial definition in (3.1) was $b_N > b_{N-1} > \ldots > b_1 > 0$.

Combining all preceding parts of the proof, we may conclude that (at least) for $0 < b_N \leq 2$ numerator and denominator of $\frac{R_s}{R_m} - \frac{dR_s}{dR_m}$ in (3.26) and thus $\frac{dg_{\pi,\,inma}}{dR_m}$ itself remains ≥ 0 throughout the (utmost) valid range of R_m indicated in (3.20).

B.2.1.2 Optimum value of load resistance R_ℓ for maximum power gain

In Section 3.5.2.2 the parameter R_m was optimised for maximum $g_{\pi,\,inma}$. However, the maximum $g_{\pi,\,inma}$ still depends on R_ℓ (for the intended aplication, R_i is fixed and known).

Thus it's necessary to investigate which R_ℓ yields the maximum $g_{\pi,\,inma}$ if R_m is chosen for optimum $g_{\pi,\,inma}$ according to Section 3.5.2.2.

Which R_ℓ is likely to yield the maximum $g_{\pi,\,inma}$?

As indicated in Section 3.5.2.1, $L_s = 0$ for $R_\ell = R_i - R_{s0}$, the limit which separates the two possible (utmost) upper limits of R_m. Then the lowest R_s occurs ($R_s = R_{s0}$).

Supposing that the highest $g_{\pi,\,inma}$ coincides with the lowest R_s requires proving of $\frac{dg_{\pi,\,inma}(R_m=R_\ell)}{dR_\ell} \geq 0$ if $R_\ell \leq R_i - R_{s0}$ or $\frac{dg_{\pi,\,inma}(R_m=R_{mlim})}{dR_\ell} \leq 0$ if $R_\ell > R_i - R_{s0}$, respectively, thereby obtaining that $g_{\pi,\,inma}$ at $R_m = R_\ell = R_i - R_{s0}$ is greater (or equal) than any other $g_{\pi,\,inma}$.

According to Section 3.5.2.2, the proof has to be split in two parts:

(i) $R_\ell \leq R_i - R_{s0}$, hence $0 \leq R_m \leq R_\ell$

The highest $g_{\pi,\,inma}$ is obtained if $R_m = R_\ell$. $g_{\pi,\,inma}$ is given by (3.24),

$$g_{\pi,\,inma}(R_m = R_\ell) = \frac{R_\ell}{R_\ell + R_s(R_m = R_\ell)}.$$

Its derivative with respect to R_ℓ is

$$\frac{dg_{\pi,\,inma}(R_m=R_\ell)}{dR_\ell} = \frac{R_\ell}{(R_\ell+R_s(R_m=R_\ell))^2}\left(\frac{R_s(R_m=R_\ell)}{R_\ell} - \frac{dR_s(R_m=R_\ell)}{dR_\ell}\right).$$

Since R_ℓ, $R_s(R_m = R_\ell) \geq 0$, it suffices to check $\frac{R_s(R_m=R_\ell)}{R_\ell} - \frac{dR_s(R_m=R_\ell)}{dR_\ell}$.

Using (3.1), we define an implicit function for $R_s(R_m = R_\ell)$,

$$\widetilde{\psi}_\pi := R_{s0} + \left(\sum_{n=1}^{N} a_n \left(\omega L_s(R_m = R_\ell)\right)^{b_n}\right) - R_s(R_m = R_\ell) \equiv 0.$$

Comparing the implicit function and the factor to check to those of Section 3.5.2.2, it's quite obvious that the proofs are similar if R_s is replaced with $R_s(R_m = R_\ell)$ and R_m with R_ℓ. Regarding the derivatives, those with respect to R_s or R_m are replaced with derivatives with respect to $R_s(R_m = R_\ell)$ or R_ℓ.

Then $\frac{R_s(R_m=R_\ell)}{R_\ell} - \frac{dR_s(R_m=R_\ell)}{dR_\ell}$ is given by (3.26) if the indicated replacements are applied.

To prove that $\frac{R_s(R_m=R_\ell)}{R_\ell} - \frac{dR_s(R_m=R_\ell)}{dR_\ell} \geq 0$ the proof of Section 3.5.2.2 may be adapted accordingly. All estimations are valid if the indicated replacements are made, hence prior to the usage of ωL_s and its partial derivatives the terms to check are similar. However, ωL_s and its partial derivatives have changed compared to those of Section 3.5.2.2 and are given by

$$\omega L_s(R_m = R_\ell) = \sqrt{(R_\ell + R_s(R_m = R_\ell))\,(R_i - R_\ell - R_s(R_m = R_\ell))},$$

$$\frac{\partial(\omega L_s(R_m = R_\ell))}{\partial R_\ell} = \frac{R_i - 2\,(R_\ell + R_s(R_m = R_\ell))}{2\sqrt{(R_\ell + R_s(R_m = R_\ell))\,(R_i - R_\ell - R_s(R_m = R_\ell))}},$$

$$\frac{\partial(\omega L_s(R_m = R_\ell))}{\partial R_s(R_m = R_\ell)} = \frac{R_i - 2\,(R_\ell + R_s(R_m = R_\ell))}{2\sqrt{(R_\ell + R_s(R_m = R_\ell))\,(R_i - R_\ell - R_s(R_m = R_\ell))}}.$$

($L_s(R_m = R_\ell)$ is obtained by putting $R_m = R_\ell$ in (3.19)).

Similar to Section 3.5.2.2, we begin the proof by assuming all $a_n = 0$, thus $R_s = R_{s0}$ throughout the valid range of R_m. We then obtain

$$\left(\frac{R_s(R_m = R_\ell)}{R_\ell} - \frac{dR_s(R_m = R_\ell)}{dR_\ell}\right)\Bigg|_{a_n=0\,\forall n} = \frac{R_{s0}}{R_\ell}.$$

Numerator and denominator of $\left(\frac{R_s(R_m=R_\ell)}{R_\ell} - \frac{dR_s(R_m=R_\ell)}{dR_\ell}\right)\Big|_{a_n=0\,\forall n}$ are always ≥ 0 because R_{s0}, $R_\ell \geq 0$.

If at least one $a_n > 0$, numerator and denominator of $\left(\frac{R_s(R_m=R_\ell)}{R_\ell} - \frac{dR_s(R_m=R_\ell)}{dR_\ell}\right)$ are checked separately similar to Section 3.5.2.2, yielding the following terms which have to be proved to be ≥ 0:

1. In case of the numerator $R_s(R_\ell) \geq 0$, $\omega L_s(R_m = R_\ell)$, $\frac{\partial(\omega L_s(R_m=R_\ell))}{\partial R_\ell}$, and $\frac{\partial(\omega L_s(R_m=R_\ell))}{\partial R_s(R_m=R_\ell)}$ are applied, yielding

$$\omega L_s(R_m = R_\ell) - b_N\left(R_s(R_m = R_\ell)\,\frac{\partial(\omega L_s(R_m=R_\ell))}{\partial R_s(R_m=R_\ell)} + R_\ell\,\frac{\partial(\omega L_s(R_m=R_\ell))}{\partial R_\ell}\right)$$
$$= \frac{(R_\ell+R_s(R_m=R_\ell))\,((2-b_N)\,(R_i-R_\ell-R_s(R_m=R_\ell))+b_N\,(R_\ell+R_s(R_m=R_\ell)))}{2\sqrt{(R_\ell+R_s(R_m=R_\ell))\,(R_i-R_\ell-R_s(R_m=R_\ell))}},$$

   which is always ≥ 0 if $0 < b_N \leq 2$ holds[2], because (3.20) still holds if $R_m = R_\ell$.

2. In case of the denominator $\omega L_s(R_m = R_\ell)$ and $\frac{\partial(\omega L_s(R_m=R_\ell))}{\partial R_s(R_m=R_\ell)}$ are applied, yielding

$$\omega L_s(R_m = R_\ell) - b_N\,R_s(R_m = R_\ell)\,\frac{\partial(\omega L_s(R_m=R_\ell))}{\partial R_s(R_m=R_\ell)}$$
$$= \frac{(2-b_N)\,(R_\ell+R_s(R_m=R_\ell))\,(R_i-R_\ell-R_s(R_m=R_\ell))+b_N\,(R_\ell\,(R_i-R_\ell)+R_s^2(R_m=R_\ell))}{2\sqrt{(R_\ell+R_s(R_m=R_\ell))\,(R_i-R_\ell-R_s(R_m=R_\ell))}},$$

[2] The proof would still be valid if we would put $b_N = 0$, but its initial definition in (3.1) was $b_N > b_{N-1} > \ldots > b_1 > 0$.

which is always ≥ 0 if $0 < b_N \leq 2$ holds[2], because (3.20) still holds if $R_\mathrm{m} = R_\ell$.

Combining all preceding parts of the proof, we may conclude that (at least) for $0 < b_N \leq 2$ numerator and denominator of $\frac{R_\mathrm{s}(R_\mathrm{m}=R_\ell)}{R_\ell} - \frac{\mathrm{d}R_\mathrm{s}(R_\mathrm{m}=R_\ell)}{\mathrm{d}R_\ell}$ and thus $\frac{R_\mathrm{s}(R_\mathrm{m}=R_\ell)}{R_\ell} - \frac{\mathrm{d}R_\mathrm{s}(R_\mathrm{m}=R_\ell)}{\mathrm{d}R_\ell}$ itself remains ≥ 0 if $R_\ell \leq R_\mathrm{i} - R_\mathrm{s0}$.

(ii) $R_\ell > R_\mathrm{i} - R_\mathrm{s0}$, hence $0 \leq R_\mathrm{m} \leq R_\mathrm{mlim}$

The highest $g_{\pi,\,\mathrm{inma}}$ is obtained if $R_\mathrm{m} = R_\mathrm{mlim} = R_\mathrm{i} - R_\mathrm{s}(R_\mathrm{m} = R_\mathrm{mlim})$. $g_{\pi,\,\mathrm{inma}}$ is given by (3.24),

$$g_{\pi,\,\mathrm{inma}}(R_\mathrm{m} = R_\mathrm{mlim}) = \frac{R_\mathrm{mlim}}{R_\mathrm{i}}.$$

Its derivative with respect to R_ℓ is

$$\frac{\mathrm{d}g_{\pi,\,\mathrm{inma}}(R_\mathrm{m} = R_\mathrm{mlim})}{\mathrm{d}R_\ell} = \frac{1}{R_\mathrm{i}} \frac{\mathrm{d}R_\mathrm{mlim}}{\mathrm{d}R_\ell}.$$

Since $R_\mathrm{i} \geq 0$, it suffices to check $\frac{\mathrm{d}R_\mathrm{mlim}}{\mathrm{d}R_\ell}$.

As $R_\mathrm{s}(R_\mathrm{m} = R_\mathrm{mlim})$ is a function of $L_\mathrm{s}(R_\mathrm{m} = R_\mathrm{mlim})$, which itself is a function of R_ℓ and implicitly[3] of R_s according to (3.19), we define the implicit function $\widetilde{\widetilde{\psi}}_\pi \equiv 0$ from (3.21), (3.1), and (3.19),

$$\widetilde{\widetilde{\psi}}_\pi := R_\mathrm{s0} + \left(\sum_{n=1}^{N} a_n \left(\sqrt{R_\mathrm{mlim}\,(R_\ell - R_\mathrm{mlim})} \right)^{b_n} \right) - R_\mathrm{i} + R_\mathrm{mlim} \equiv 0.$$

Then we compute the implicit function's partial derivatives with respect to R_ℓ and R_mlim,

$$\begin{aligned}
\frac{\partial \widetilde{\widetilde{\psi}}_\pi}{\partial R_\ell} &= \frac{\sum_{n=1}^{N} a_n b_n \left(\sqrt{R_\mathrm{mlim}\,(R_\ell - R_\mathrm{mlim})} \right)^{b_n - 1} R_\mathrm{mlim}}{2\sqrt{R_\mathrm{mlim}\,(R_\ell - R_\mathrm{mlim})}}, \\
\frac{\partial \widetilde{\widetilde{\psi}}_\pi}{\partial R_\mathrm{mlim}} &= \frac{\sum_{n=1}^{N} a_n b_n \left(\sqrt{R_\mathrm{mlim}\,(R_\ell - R_\mathrm{mlim})} \right)^{b_n - 1} (R_\ell - 2\,R_\mathrm{mlim})}{2\sqrt{R_\mathrm{mlim}\,(R_\ell - R_\mathrm{mlim})}} + 1.
\end{aligned}$$

Applying the implicit function theorem [64] and multiplying numerator and denominator of the resulting fraction by $\sqrt{R_\mathrm{mlim}\,(R_\ell - R_\mathrm{mlim})}$ gives

$$\frac{\mathrm{d}R_\mathrm{mlim}}{\mathrm{d}R_\ell} = -\frac{\sum_{n=1}^{N} a_n b_n \left(\sqrt{R_\mathrm{mlim}\,(R_\ell - R_\mathrm{mlim})} \right)^{b_n} R_\mathrm{mlim}}{2\,R_\mathrm{mlim}\,(R_\ell - R_\mathrm{mlim}) + \sum_{n=1}^{N} a_n b_n \left(\sqrt{R_\mathrm{mlim}\,(R_\ell - R_\mathrm{mlim})} \right)^{b_n} (R_\ell - 2\,R_\mathrm{mlim})}.$$

As indicated above, supposed the maximum $g_{\pi,\,\mathrm{inma}}$ occurs at $R_\ell = R_\mathrm{i} - R_\mathrm{s0}$, we have to prove that $\frac{\mathrm{d}R_\mathrm{mlim}}{\mathrm{d}R_\ell} \leq 0$ if $R_\ell > R_\mathrm{i} - R_\mathrm{s0}$.

---

[3] In particular, $R_\mathrm{s}(R_\mathrm{m} = R_\mathrm{mlim})$ and $L_\mathrm{s}(R_\mathrm{m} = R_\mathrm{mlim})$ are both functions of R_ℓ only. However, we usually may not be able to solve for $R_\mathrm{s}(R_\mathrm{m} = R_\mathrm{mlim})$ explicitly after applying (3.19) to (3.1).

For ease of understanding, an overview of the following proof is given below.

To prove that numerator and denominator are ≤ 0 for certain b_N, we firstly assume all $a_n = 0$ or $R_\mathrm{s} = R_\mathrm{s0}$ and calculate $\frac{\mathrm{d}R_\mathrm{mlim}}{\mathrm{d}R_\ell}$, which will equal zero for any $R_\ell > R_\mathrm{i} - R_\mathrm{s0}$.

Secondly, we assume that at least one $a_n > 0$, hence $R_\mathrm{s} > R_\mathrm{s0}$ (according to (3.1)). Then the numerator of $\frac{\mathrm{d}R_\mathrm{mlim}}{\mathrm{d}R_\ell}$ is always ≥ 0 and all terms of the denominator are ≥ 0 except $R_\ell - 2R_\mathrm{mlim}$. Thus, if $R_\ell \geq 2R_\mathrm{mlim}$, the denominator is always ≥ 0. If $R_\ell < 2R_\mathrm{mlim}$, we have to use certain inequalities to prove that (at least) for $b_N \leq 2$ the numerator will be ≥ 0. However, since b_N was restricted to $b_N \leq 2$ in Section 3.5.2.2, it suffices to check the minimum estimated value of the denominator at $b_N = 2$. The positive (or zero) numerator and denominator yield a $\frac{\mathrm{d}R_\mathrm{mlim}}{\mathrm{d}R_\ell} \leq 0$.

We then know that for all possible values of R_s0, a_n, and b_n according to (3.1), $\frac{\mathrm{d}g_{\pi,\,\mathrm{inma}}(R_\mathrm{m}=R_\mathrm{mlim})}{\mathrm{d}R_\ell} \leq 0$ if $R_\ell > R_\mathrm{i} - R_\mathrm{s0}$ and (at least) $b_N \leq 2$.

As indicated above, we begin the actual proof by assuming all $a_n = 0$, thus $R_\mathrm{s} = R_\mathrm{s0}$. We then obtain

$$\left.\frac{\mathrm{d}R_\mathrm{mlim}}{\mathrm{d}R_\ell}\right|_{a_n=0\,\forall n} = 0.$$

Then $R_\mathrm{mlim} = R_\mathrm{i} - R_\mathrm{s0}$ for any $R_\ell > R_\mathrm{i} - R_\mathrm{s0}$ independently of R_ℓ.

If at least one $a_n > 0$, the numerator of $\frac{\mathrm{d}R_\mathrm{mlim}}{\mathrm{d}R_\ell}$ is always ≥ 0 and all terms of the denominator are ≥ 0 except $R_\ell - 2R_\mathrm{mlim}$.

Thus, if $R_\ell \geq 2R_\mathrm{mlim}$, the denominator is always ≥ 0, too.

Conversely, if $R_\ell < 2R_\mathrm{mlim}$, we obtain from (3.21), (3.1) and (3.19) that $R_\mathrm{s}(R_\mathrm{mlim}) - R_\mathrm{s0} = R_\mathrm{i} - R_\mathrm{mlim} - R_\mathrm{s0} = \sum_{n=1}^{N} a_n \left(\sqrt{R_\mathrm{mlim}\,(R_\ell - R_\mathrm{mlim})}\right)^{b_n}$. Hence,

$$\begin{aligned}
&2\,R_\mathrm{mlim}\,(R_\ell - R_\mathrm{mlim}) \\
&+ \sum_{n=1}^{N} a_n b_n \left(\sqrt{R_\mathrm{mlim}\,(R_\ell - R_\mathrm{mlim})}\right)^{b_n} (R_\ell - 2\,R_\mathrm{mlim}) \\
&\geq\ 2\,R_\mathrm{mlim}\,(R_\ell - R_\mathrm{mlim}) + b_N\,(R_\mathrm{i} - R_\mathrm{mlim} - R_\mathrm{s0})\,(R_\ell - 2\,R_\mathrm{mlim})
\end{aligned}$$

holds due to $b_N > b_{N-1} > \ldots > b_1 > 0$.

Since b_N was restricted to $b_N \leq 2$ in Section 3.5.2.2, it suffices to check if the minimum estimated value is ≥ 0. Its minimum occurs at $b_N = 2$, yielding

$$\begin{aligned}
&2\,R_\mathrm{mlim}\,(R_\ell - R_\mathrm{mlim}) + 2\,(R_\mathrm{i} - R_\mathrm{mlim} - R_\mathrm{s0})\,(R_\ell - 2\,R_\mathrm{mlim}) \\
&=\ 2\left((R_\mathrm{i} - R_\mathrm{s0})\,(R_\ell - (R_\mathrm{i} - R_\mathrm{s0})) + (R_\mathrm{i} - R_\mathrm{mlim} - R_\mathrm{s0})^2\right),
\end{aligned}$$

which is always ≥ 0 if $R_\ell > R_\mathrm{i} - R_\mathrm{s0}$.

Combining all preceding parts of the proof, we may conclude that numerator and denominator of $\frac{\mathrm{d}R_\mathrm{mlim}}{\mathrm{d}R_\ell}$ are ≥ 0 and thus $\frac{\mathrm{d}R_\mathrm{mlim}}{\mathrm{d}R_\ell}$ and $\frac{\mathrm{d}g_{\pi,\,\mathrm{inma}}(R_\mathrm{m}=R_\mathrm{mlim})}{\mathrm{d}R_\ell}$ remain ≤ 0 if $R_\ell > R_\mathrm{i} - R_\mathrm{s0}$ and (at least) $b_N \leq 2$.

Summarising both proofs yields a maximum $g_{\pi,\,\mathrm{inma}}$ at $R_\ell = R_\mathrm{i} - R_{\mathrm{s}0}$ if $0 < b_N \leq 2$ and if R_m was chosen according to Section 3.5.2.2. If R_ℓ is lower or higher, $g_{\pi,\,\mathrm{inma}}$ decreases except for $R_\mathrm{s} = R_{\mathrm{s}0}$, where it stays constant at its maximum value if R_ℓ increases further.

B.2.2 T network

B.2.2.1 Optimum value of parameter G_m for maximum power gain

As indicated in the overview of the proof given in Section 3.5.3.2, we begin the actual proof by assuming all $a_n = 0$, thus $R_\mathrm{s} = R_{\mathrm{s}0}$ throughout the valid range of G_m. We then obtain from (3.39)

$$\left(\frac{G_\mathrm{p}}{G_\mathrm{m}} - \frac{\mathrm{d}G_\mathrm{p}}{\mathrm{d}G_\mathrm{m}}\right)\Bigg|_{a_n=0\,\forall n} = \frac{G_\mathrm{p}\left(\frac{1}{\omega^2 L_\mathrm{p}^2} - G_\mathrm{p}^2 - 2\,\frac{1}{\omega L_\mathrm{p}}\left(G_\mathrm{p}\,\frac{\partial(\frac{1}{\omega L_\mathrm{p}})}{\partial G_\mathrm{p}} + G_\mathrm{m}\,\frac{\partial(\frac{1}{\omega L_\mathrm{p}})}{\partial G_\mathrm{m}}\right)\right)}{G_\mathrm{m}\left(\frac{1}{\omega^2 L_\mathrm{p}^2} - G_\mathrm{p}^2 - 2\,\frac{1}{\omega L_\mathrm{p}}\,G_\mathrm{p}\,\frac{\partial(\frac{1}{\omega L_\mathrm{p}})}{\partial G_\mathrm{p}}\right)}.$$

Applying (3.32), (3.40), and (3.41) yields

$$\left(\frac{G_\mathrm{p}}{G_\mathrm{m}} - \frac{\mathrm{d}G_\mathrm{p}}{\mathrm{d}G_\mathrm{m}}\right)\Bigg|_{a_n=0\,\forall n} = \frac{G_\mathrm{p}\,(G_\mathrm{m}+G_\mathrm{p})}{\sqrt{G_\mathrm{m}\,(G_\ell - G_\mathrm{m})}} \cdot \frac{2\sqrt{G_\mathrm{m}\,(G_\ell - G_\mathrm{m})}\,\sqrt{(G_\mathrm{m}+G_\mathrm{p})\,(G_\mathrm{i}-G_\mathrm{m}-G_\mathrm{p})} + G_\mathrm{m}\,(G_\mathrm{i}-G_\mathrm{m}-G_\mathrm{p}+G_\ell-G_\mathrm{m}) + G_\mathrm{p}\,(G_\ell - G_\mathrm{m})}{G_\mathrm{m}\,(G_\mathrm{i}-G_\mathrm{m}+G_\ell-G_\mathrm{m})\,\sqrt{(G_\mathrm{m}+G_\mathrm{p})\,(G_\mathrm{i}-G_\mathrm{m}-G_\mathrm{p})} + (G_\mathrm{i}\,G_\mathrm{p} + 2\,G_\mathrm{m}\,(G_\mathrm{i}-G_\mathrm{m}-G_\mathrm{p}))\,\sqrt{G_\mathrm{m}\,(G_\ell - G_\mathrm{m})}}$$

Since G_i, G_ℓ, G_m, $G_\mathrm{p} \geq 0$, and (3.33) applies, numerator and denominator of $\left(\frac{G_\mathrm{p}}{G_\mathrm{m}} - \frac{\mathrm{d}G_\mathrm{p}}{\mathrm{d}G_\mathrm{m}}\right)\Big|_{a_n=0\,\forall n}$ are always ≥ 0.

If at least one $a_n > 0$, we begin by deriving some inequalities which we will use to check numerator and denominator of (3.39) separately.

By thoroughly reviewing numerator and denominator, we identify two common terms. For the second one we can prove that

$$2\,G_\mathrm{p}\,\frac{1}{\omega L_\mathrm{p}} - \left(\frac{1}{\omega^2 L_\mathrm{p}^2} - G_\mathrm{p}^2\right)\sum_{n=1}^{N} a_n b_n\,\Lambda^{b_n-1} \geq 0$$

holds if $0 < b_N \leq 2$.

The proof has to be split in two cases.

If $G_\mathrm{p} \geq \frac{1}{\omega L_\mathrm{p}}$ and G_p, ωL_p, $a_n \geq 0$, and $b_n > 0$, the above estimate is valid for any b_N.

However, if $G_\mathrm{p} < \frac{1}{\omega L_\mathrm{p}}$, several estimates are needed. Since $b_N > b_{N-1} > \ldots > b_1 > 0$ and $R_\mathrm{s} \geq \sum_{n=1}^{N} a_n \, (\omega L_\mathrm{s})^{b_n}$ (from (3.1)), we obtain after applying (A.16) and (A.17)

$$
\begin{aligned}
& 2\,G_\mathrm{p}\,\frac{1}{\omega L_\mathrm{p}} - \left(\frac{1}{\omega^2 L_\mathrm{p}^2} - G_\mathrm{p}^2\right) \sum_{n=1}^{N} a_n b_n \, \Lambda^{b_n - 1} \\
& \geq \; 2\,G_\mathrm{p}\,\frac{1}{\omega L_\mathrm{p}} - \left(\frac{1}{\omega^2 L_\mathrm{p}^2} - G_\mathrm{p}^2\right) b_N \, \frac{\sum_{n=1}^{N} a_n \, \Lambda^{b_n}}{\Lambda} \\
& \geq \; 2\,G_\mathrm{p}\,\frac{1}{\omega L_\mathrm{p}} - \left(\frac{1}{\omega^2 L_\mathrm{p}^2} - G_\mathrm{p}^2\right) b_N \, \frac{\frac{G_\mathrm{p}}{G_\mathrm{p}^2 + \frac{1}{\omega^2 L_\mathrm{p}^2}}}{\Lambda} = \frac{G_\mathrm{p}\left((2 - b_N)\,\frac{1}{\omega^2 L_\mathrm{p}^2} + b_N\,G_\mathrm{p}^2\right)}{\frac{1}{\omega L_\mathrm{p}}},
\end{aligned}
$$

which is always ≥ 0 if $0 < b_N \leq 2$ holds[4].

From now on we limit the inductor's Q factor to $Q \geq 1$, which just indicates that $\omega L_\mathrm{s} \geq R_\mathrm{s}$ or $\frac{1}{\omega L_\mathrm{p}} \geq G_\mathrm{p}$ (from (A.17) and (A.16)) and is likely to assume for a useful variable inductor.

Combined with the preceding estimate, we finally obtain

$$
2\,G_\mathrm{p}\,\frac{1}{\omega L_\mathrm{p}} \geq 2\,G_\mathrm{p}\,\frac{1}{\omega L_\mathrm{p}} - \left(\frac{1}{\omega^2 L_\mathrm{p}^2} - G_\mathrm{p}^2\right) \sum_{n=1}^{N} a_n b_n \, \Lambda^{b_n - 1} \geq 0,
$$

which we will use in the following proof.

After deriving all necessary estimates, we check numerator and denominator of (3.39) separately:

1. Since ωL_p, G_m, G_p, a_n are ≥ 0, $b_n > 0$, and the preceding estimates apply, the numerator will always be ≥ 0 for $G_\mathrm{p}\,\frac{\partial(\frac{1}{\omega L_\mathrm{p}})}{\partial G_\mathrm{p}} + G_\mathrm{m}\,\frac{\partial(\frac{1}{\omega L_\mathrm{p}})}{\partial G_\mathrm{m}} \leq 0$.

   Conversely, if $G_\mathrm{p}\,\frac{\partial(\frac{1}{\omega L_\mathrm{p}})}{\partial G_\mathrm{p}} + G_\mathrm{m}\,\frac{\partial(\frac{1}{\omega L_\mathrm{p}})}{\partial G_\mathrm{m}} > 0$, the preceding estimates apply and

$$
\begin{aligned}
& G_\mathrm{p}\left(\tfrac{1}{\omega^2 L_\mathrm{p}^2} - G_\mathrm{p}^2 + 2\,G_\mathrm{p}\,\tfrac{1}{\omega L_\mathrm{p}} \sum_{n=1}^{N} a_n b_n \, \Lambda^{b_n - 1}\right) \\
& - \left(2\,G_\mathrm{p}\,\tfrac{1}{\omega L_\mathrm{p}} - \left(\tfrac{1}{\omega^2 L_\mathrm{p}^2} - G_\mathrm{p}^2\right) \sum_{n=1}^{N} a_n b_n \, \Lambda^{b_n - 1}\right) \\
& \quad \cdot \left(G_\mathrm{p}\,\tfrac{\partial(\frac{1}{\omega L_\mathrm{p}})}{\partial G_\mathrm{p}} + G_\mathrm{m}\,\tfrac{\partial(\frac{1}{\omega L_\mathrm{p}})}{\partial G_\mathrm{m}}\right) \\
& \geq \; G_\mathrm{p}\left(\tfrac{1}{\omega^2 L_\mathrm{p}^2} - G_\mathrm{p}^2\right) - 2\,G_\mathrm{p}\,\tfrac{1}{\omega L_\mathrm{p}}\left(G_\mathrm{p}\,\tfrac{\partial(\frac{1}{\omega L_\mathrm{p}})}{\partial G_\mathrm{p}} + G_\mathrm{m}\,\tfrac{\partial(\frac{1}{\omega L_\mathrm{p}})}{\partial G_\mathrm{m}}\right)
\end{aligned}
$$

[4]The proof would still be valid if we would put $b_N = 0$, but its initial definition in (3.1) was $b_N > b_{N-1} > \ldots > b_1 > 0$.

holds.

After applying (3.32), (3.40), (3.41), and $G_\mathrm{m} \geq 0$, we finally have to check

$$\begin{aligned} &\tfrac{1}{\omega^2 L_\mathrm{p}^2} - G_\mathrm{p}^2 - 2\,\tfrac{1}{\omega L_\mathrm{p}} \left(G_\mathrm{p}\, \tfrac{\partial(\frac{1}{\omega L_\mathrm{p}})}{\partial G_\mathrm{p}} + G_\mathrm{m}\, \tfrac{\partial(\frac{1}{\omega L_\mathrm{p}})}{\partial G_\mathrm{m}} \right) \\ &\quad = G_\mathrm{m}\,(G_\mathrm{m} + G_\mathrm{p}) \left(2 + \tfrac{G_\mathrm{m}\,(G_\mathrm{i} - G_\mathrm{m} - G_\mathrm{p} + G_\ell - G_\mathrm{m}) + G_\mathrm{p}\,(G_\ell - G_\mathrm{m})}{\sqrt{G_\mathrm{m}\,(G_\ell - G_\mathrm{m})}\,\sqrt{(G_\mathrm{m} + G_\mathrm{p})\,(G_\mathrm{i} - G_\mathrm{m} - G_\mathrm{p})}} \right), \end{aligned}$$

which is always ≥ 0 throughout the (utmost) valid range of G_m indicated in (3.33).

2. Since ωL_p, G_m, G_p, a_n are ≥ 0, $b_n > 0$, and the preceding estimates apply, the denominator will always be ≥ 0 for $\frac{\partial(\frac{1}{\omega L_\mathrm{p}})}{\partial G_\mathrm{p}} \leq 0$.

Conversely, if $\frac{\partial(\frac{1}{\omega L_\mathrm{p}})}{\partial G_\mathrm{p}} > 0$, the preceding estimates apply and

$$\begin{aligned} &G_\mathrm{m} \left(\tfrac{1}{\omega^2 L_\mathrm{p}^2} - G_\mathrm{p}^2 + 2\,G_\mathrm{p}\, \tfrac{1}{\omega L_\mathrm{p}} \left(\sum_{n=1}^{N} a_n b_n\, \Lambda^{b_n - 1} \right) \right. \\ &\qquad \left. - \left(2\,G_\mathrm{p}\, \tfrac{1}{\omega L_\mathrm{p}} - \left(\tfrac{1}{\omega^2 L_\mathrm{p}^2} - G_\mathrm{p}^2 \right) \sum_{n=1}^{N} a_n b_n\, \Lambda^{b_n - 1} \right) \tfrac{\partial(\frac{1}{\omega L_\mathrm{p}})}{\partial G_\mathrm{p}} \right) \\ &\geq G_\mathrm{m} \left(\tfrac{1}{\omega^2 L_\mathrm{p}^2} - G_\mathrm{p}^2 - 2\,\tfrac{1}{\omega L_\mathrm{p}}\, G_\mathrm{p}\, \tfrac{\partial(\frac{1}{\omega L_\mathrm{p}})}{\partial G_\mathrm{p}} \right) \end{aligned}$$

holds.

After applying (3.32), (3.41), and $G_\mathrm{m} \geq 0$, we finally have to check

$$\begin{aligned} &\tfrac{1}{\omega^2 L_\mathrm{p}^2} - G_\mathrm{p}^2 - 2\,\tfrac{1}{\omega L_\mathrm{p}}\, G_\mathrm{p}\, \tfrac{\partial(\frac{1}{\omega L_\mathrm{p}})}{\partial G_\mathrm{p}} \\ &\quad = G_\mathrm{m}\,(G_\mathrm{i} - G_\mathrm{m} + G_\ell - G_\mathrm{m}) + \tfrac{(G_\mathrm{i}\,G_\mathrm{p} + 2\,G_\mathrm{m}\,(G_\mathrm{i} - G_\mathrm{m} - G_\mathrm{p}))\,\sqrt{G_\mathrm{m}\,(G_\ell - G_\mathrm{m})}}{\sqrt{(G_\mathrm{m} + G_\mathrm{p})\,(G_\mathrm{i} - G_\mathrm{m} - G_\mathrm{p})}}, \end{aligned}$$

which is always ≥ 0 throughout the (utmost) valid range of G_m indicated in (3.33).

Combining all preceding parts of the proof, we may conclude that (at least) for $0 < b_N \leq 2$ and $Q \geq 1$ (hence $\omega L_\mathrm{s} \geq R_\mathrm{s}$ or $\frac{1}{\omega L_\mathrm{p}} \geq G_\mathrm{p}$), numerator and denominator of $\frac{G_\mathrm{p}}{G_\mathrm{m}} - \frac{\mathrm{d}G_\mathrm{p}}{\mathrm{d}G_\mathrm{m}}$ in (3.39) and thus $\frac{\mathrm{d}g_{\mathrm{t,\,inma}}}{\mathrm{d}G_\mathrm{m}}$ itself remains ≥ 0 throughout the (utmost) valid range of G_m indicated in (3.33).

B.2.2.2 Optimum value of load conductance G_ℓ for maximum power gain

In Section 3.5.3.2 the parameter G_m was optimised for maximum $g_{\mathrm{t,\,inma}}$. However, the maximum $g_{\mathrm{t,\,inma}}$ still depends on G_ℓ (for the intended aplication, G_i is fixed and known).

Thus it's necessary to investigate which G_ℓ yields the maximum $g_{\mathrm{t,\,inma}}$ if G_m is chosen for optimum $g_{\mathrm{t,\,inma}}$ according to Section 3.5.3.2.

Which G_ℓ is likely to yield the maximum $g_{\mathrm{t,\,inma}}$?

As indicated in Section 3.5.3.1, $L_{\mathrm{s,p}} \to \infty$ for $G_\ell = G_\mathrm{i}$, the limit which separates the two possible (utmost) upper limits of G_m. Then, according to case (ii) in (A.18), the lowest G_p occurs ($G_\mathrm{p} = 0$).

Supposing that the highest $g_{\mathrm{t,\,inma}}$ coincides with the lowest G_p requires proving of $\frac{\mathrm{d}g_{\mathrm{t,\,inma}}(G_\mathrm{m}=G_\ell)}{\mathrm{d}G_\ell} \geq 0$ if $G_\ell \leq G_\mathrm{i}$ or $\frac{\mathrm{d}g_{\mathrm{t,\,inma}}(G_\mathrm{m}=G_{\mathrm{mlim}})}{\mathrm{d}G_\ell} \leq 0$ if $G_\ell > G_\mathrm{i}$, respectively, thereby obtaining that $g_{\mathrm{t,\,inma}}$ at $G_\mathrm{m} = G_\ell = G_\mathrm{i}$ is greater (or equal) than any other $g_{\mathrm{t,\,inma}}$.

According to Section 3.5.3.2, the proof has to be split in two parts:

(i) $G_\ell \leq G_\mathrm{i}$, hence $0 \leq G_\mathrm{m} \leq G_\ell$

The highest $g_{\mathrm{t,\,inma}}$ is obtained if $G_\mathrm{m} = G_\ell$. $g_{\mathrm{t,\,inma}}$ is given by (3.37),

$$g_{\mathrm{t,\,inma}}(G_\mathrm{m} = G_\ell) = \frac{G_\ell}{G_\ell + G_\mathrm{p}(G_\mathrm{m} = G_\ell)}.$$

Its derivative with respect to G_ℓ is

$$\frac{\mathrm{d}g_{\mathrm{t,\,inma}}(G_\mathrm{m}=G_\ell)}{\mathrm{d}G_\ell} = \frac{G_\ell}{(G_\ell+G_\mathrm{p}(G_\mathrm{m}=G_\ell))^2}\left(\frac{G_\mathrm{p}(G_\mathrm{m}=G_\ell)}{G_\ell} - \frac{\mathrm{d}G_\mathrm{p}(G_\mathrm{m}=G_\ell)}{\mathrm{d}G_\ell}\right).$$

Since G_ℓ, $G_\mathrm{p}(G_\mathrm{m} = G_\ell) \geq 0$, it suffices to check $\frac{G_\mathrm{p}(G_\mathrm{m}=G_\ell)}{G_\ell} - \frac{\mathrm{d}G_\mathrm{p}(G_\mathrm{m}=G_\ell)}{\mathrm{d}G_\ell}$.

Using (3.1) and (A.19), we define an implicit function for $R_\mathrm{s}(G_\mathrm{m} = G_\ell)$,

$$\widetilde{\psi}_\mathrm{t} := R_{\mathrm{s}0} + \left(\sum_{n=1}^{N} a_n \left(\frac{\frac{1}{\omega L_\mathrm{p}(G_\mathrm{m}=G_\ell)}}{G_\mathrm{p}^2(G_\mathrm{m}=G_\ell)+\frac{1}{\omega^2 L_\mathrm{p}^2(G_\mathrm{m}=G_\ell)}}\right)^{b_n}\right) - \frac{G_\mathrm{p}(G_\mathrm{m}=G_\ell)}{G_\mathrm{p}^2(G_\mathrm{m}=G_\ell)+\frac{1}{\omega^2 L_\mathrm{p}^2(G_\mathrm{m}=G_\ell)}} \equiv 0.$$

Comparing the implicit function and the factor to check to those of Section 3.5.3.2, it's quite obvious that the proofs are similar if G_p is replaced with $G_\mathrm{p}(G_\mathrm{m} = G_\ell)$ and G_m with G_ℓ. Regarding the derivatives, those with respect to G_p or G_m are replaced with derivatives with respect to $G_\mathrm{p}(G_\mathrm{m} = G_\ell)$ or G_ℓ.

Then $\frac{G_\mathrm{p}(G_\mathrm{m}=G_\ell)}{G_\ell} - \frac{\mathrm{d}G_\mathrm{p}(G_\mathrm{m}=G_\ell)}{\mathrm{d}G_\ell}$ is given by (3.39) if the indicated replacements are applied.

To prove that $\frac{G_\mathrm{p}(G_\mathrm{m}=G_\ell)}{G_\ell} - \frac{\mathrm{d}G_\mathrm{p}(G_\mathrm{m}=G_\ell)}{\mathrm{d}G_\ell} \geq 0$ the proof of Section 3.5.3.2 may be adapted accordingly. All estimations are valid if the indicated replacements are made, hence prior to the usage of $\frac{1}{\omega L_\mathrm{p}}$ and its partial derivatives the terms to check are similar. However, $\frac{1}{\omega L_\mathrm{p}}$ and its partial derivatives have changed compared to those of Section 3.5.3.2 and are given by

$$\begin{aligned}
\frac{1}{\omega L_\mathrm{p}(G_\mathrm{m}=G_\ell)} &= \sqrt{(G_\ell + G_\mathrm{p}(G_\mathrm{m} = G_\ell))\,(G_\mathrm{i} - G_\ell - G_\mathrm{p}(G_\mathrm{m} = G_\ell))}\,, \\
\frac{\partial(\frac{1}{\omega L_\mathrm{p}(G_\mathrm{m}=G_\ell)})}{\partial G_\ell} &= \frac{G_\mathrm{i} - 2\,(G_\ell + G_\mathrm{p}(G_\mathrm{m}=G_\ell))}{2\sqrt{(G_\ell+G_\mathrm{p}(G_\mathrm{m}=G_\ell))\,(G_\mathrm{i}-G_\ell-G_\mathrm{p}(G_\mathrm{m}=G_\ell))}}, \\
\frac{\partial(\frac{1}{\omega L_\mathrm{p}(G_\mathrm{m}=G_\ell)})}{\partial G_\mathrm{p}(G_\mathrm{m}=G_\ell)} &= \frac{G_\mathrm{i} - 2\,(G_\ell + G_\mathrm{p}(G_\mathrm{m}=G_\ell))}{2\sqrt{(G_\ell+G_\mathrm{p}(G_\mathrm{m}=G_\ell))\,(G_\mathrm{i}-G_\ell-G_\mathrm{p}(G_\mathrm{m}=G_\ell))}}.
\end{aligned}$$

($L_\mathrm{p}(G_\mathrm{m} = G_\ell)$ is obtained by putting $G_\mathrm{m} = G_\ell$ in (3.32)).

Similar to Section 3.5.3.2, we begin the proof by assuming all $a_n = 0$, thus $R_\mathrm{s} = R_\mathrm{s0}$ throughout the valid range of G_m. We then obtain

$$\left(\frac{G_\mathrm{p}(G_\mathrm{m}=G_\ell)}{G_\ell} - \frac{\mathrm{d}G_\mathrm{p}(G_\mathrm{m}=G_\ell)}{\mathrm{d}G_\ell}\right)\Bigg|_{a_n=0\,\forall n} = \frac{G_\mathrm{p}(G_\mathrm{m}=G_\ell)}{G_\ell}$$
$$\cdot \frac{\frac{1}{\omega^2 L_\mathrm{p}^2(G_\mathrm{m}=G_\ell)} - G_\mathrm{p}^2(G_\mathrm{m}=G_\ell) - 2\,\frac{1}{\omega L_\mathrm{p}(G_\mathrm{m}=G_\ell)}\left(G_\mathrm{p}(G_\mathrm{m}=G_\ell)\,\frac{\partial(\frac{1}{\omega L_\mathrm{p}(G_\mathrm{m}=G_\ell)})}{\partial G_\mathrm{p}(G_\mathrm{m}=G_\ell)} + G_\ell\,\frac{\partial(\frac{1}{\omega L_\mathrm{p}(G_\mathrm{m}=G_\ell)})}{\partial G_\ell}\right)}{\frac{1}{\omega^2 L_\mathrm{p}^2(G_\mathrm{m}=G_\ell)} - G_\mathrm{p}^2(G_\mathrm{m}=G_\ell) - 2\,\frac{1}{\omega L_\mathrm{p}(G_\mathrm{m}=G_\ell)}\,G_\mathrm{p}(G_\mathrm{m}=G_\ell)\,\frac{\partial(\frac{1}{\omega L_\mathrm{p}(G_\mathrm{m}=G_\ell)})}{\partial G_\mathrm{p}(G_\mathrm{m}=G_\ell)}}.$$

Applying $\frac{1}{\omega L_\mathrm{p}(G_\mathrm{m}=G_\ell)}$ and its partial derivatives gives

$$\left(\frac{G_\mathrm{p}(G_\mathrm{m}=G_\ell)}{G_\ell} - \frac{\mathrm{d}G_\mathrm{p}(G_\mathrm{m}=G_\ell)}{\mathrm{d}G_\ell}\right)\Bigg|_{a_n=0\,\forall n} = \frac{G_\mathrm{p}(G_\mathrm{m}=G_\ell)\,(G_\ell + 2\,G_\mathrm{p}(G_\mathrm{m}=G_\ell))}{G_\ell\,(G_\mathrm{i}-G_\ell)},$$

which is always ≥ 0 if $G_\ell \leq G_\mathrm{i}$.

If at least one $a_n > 0$, numerator and denominator of $\frac{G_\mathrm{p}(G_\mathrm{m}=G_\ell)}{G_\ell} - \frac{\mathrm{d}G_\mathrm{p}(G_\mathrm{m}=G_\ell)}{\mathrm{d}G_\ell}$ are checked separately similar to Section 3.5.3.2, yielding the following terms which have to be proved to be ≥ 0 if $\omega L_\mathrm{s}(G_\mathrm{m} = G_\ell) \geq R_\mathrm{s}(G_\mathrm{m} = G_\ell)$ or $\frac{1}{\omega L_\mathrm{p}(G_\mathrm{m}=G_\ell)} \geq G_\mathrm{p}(G_\mathrm{m} = G_\ell)$ and $0 < b_N \leq 2$ holds:

1. In case of the numerator $G_\mathrm{p}(G_\mathrm{m} = G_\ell) \geq 0$, $\frac{1}{\omega L_\mathrm{p}(G_\mathrm{m}=G_\ell)}$, $\frac{\partial(\frac{1}{\omega L_\mathrm{p}(G_\mathrm{m}=G_\ell)})}{\partial G_\ell}$, and $\frac{\partial(\frac{1}{\omega L_\mathrm{p}(G_\mathrm{m}=G_\ell)})}{\partial G_\mathrm{p}(G_\mathrm{m}=G_\ell)}$ are applied, yielding

$$\begin{aligned}&\tfrac{1}{\omega^2 L_\mathrm{p}^2(G_\mathrm{m}=G_\ell)} - G_\mathrm{p}^2(G_\mathrm{m} = G_\ell)\\ &- 2\,\tfrac{1}{\omega L_\mathrm{p}(G_\mathrm{m}=G_\ell)}\left(G_\mathrm{p}(G_\mathrm{m} = G_\ell)\,\tfrac{\partial(\frac{1}{\omega L_\mathrm{p}(G_\mathrm{m}=G_\ell)})}{\partial G_\mathrm{p}(G_\mathrm{m}=G_\ell)} + G_\ell\,\tfrac{\partial(\frac{1}{\omega L_\mathrm{p}(G_\mathrm{m}=G_\ell)})}{\partial G_\ell}\right)\\ &= G_\ell\,(G_\ell + 2\,G_\mathrm{p}(G_\mathrm{m} = G_\ell)),\end{aligned}$$

which is always ≥ 0.

2. In case of the denominator $G_\ell \geq 0$, $\frac{1}{\omega L_\mathrm{p}(G_\mathrm{m}=G_\ell)}$, and $\frac{\partial(\frac{1}{\omega L_\mathrm{p}(G_\mathrm{m}=G_\ell)})}{\partial G_\mathrm{p}(G_\mathrm{m}=G_\ell)}$ are applied, yielding

$$\begin{aligned}&\tfrac{1}{\omega^2 L_\mathrm{p}^2(G_\mathrm{m}=G_\ell)} - G_\mathrm{p}^2(G_\mathrm{m} = G_\ell) - 2\,\tfrac{1}{\omega L_\mathrm{p}(G_\mathrm{m}=G_\ell)}\,G_\mathrm{p}(G_\mathrm{m} = G_\ell)\,\tfrac{\partial(\frac{1}{\omega L_\mathrm{p}(G_\mathrm{m}=G_\ell)})}{\partial G_\mathrm{p}(G_\mathrm{m}=G_\ell)}\\ &= G_\ell\,(G_\mathrm{i} - G_\ell),\end{aligned}$$

which is always ≥ 0 if $G_\ell \leq G_\mathrm{i}$.

Combining all preceding parts of the proof, we may conclude that (at least) for $0 < b_N \leq 2$ and $Q \geq 1$ (hence $\omega L_\mathrm{s} \geq R_\mathrm{s}$ or $\frac{1}{\omega L_\mathrm{p}} \geq G_\mathrm{p}$), numerator and denominator of $\frac{G_\mathrm{p}(G_\mathrm{m}=G_\ell)}{G_\ell} - \frac{\mathrm{d}G_\mathrm{p}(G_\mathrm{m}=G_\ell)}{\mathrm{d}G_\ell}$ and thus $\frac{\mathrm{d}g_{\mathrm{t,\,inma}}(G_\mathrm{m}=G_\ell)}{\mathrm{d}G_\ell}$ itself remains ≥ 0 if $G_\ell \leq G_\mathrm{i}$.

(ii) $G_\ell > G_\mathrm{i}$, hence $0 \leq G_\mathrm{m} \leq G_\mathrm{mlim}$

The highest $g_{\mathrm{t,\,inma}}$ is obtained if $G_\mathrm{m} = G_\mathrm{mlim} = G_\mathrm{i} - G_\mathrm{p}(G_\mathrm{m} = G_\mathrm{mlim})$. $g_{\mathrm{t,\,inma}}$ is given by (3.37),

$$g_{\mathrm{t,\,inma}}(G_\mathrm{m} = G_\mathrm{mlim}) = \frac{G_\mathrm{mlim}}{G_\mathrm{i}}$$

Its derivative with respect to G_ℓ is

$$\frac{\mathrm{d}g_{\mathrm{t,\,inma}}(G_\mathrm{m} = G_\mathrm{mlim})}{\mathrm{d}G_\ell} = \frac{1}{G_\mathrm{i}}\,\frac{\mathrm{d}G_\mathrm{mlim}}{\mathrm{d}G_\ell}.$$

Since $G_\mathrm{i} \geq 0$, it suffices to check $\frac{\mathrm{d}G_\mathrm{mlim}}{\mathrm{d}G_\ell}$.

As $R_{\mathrm{s}}(G_{\mathrm{m}} = G_{\mathrm{mlim}})$ is a function of $L_{\mathrm{s}}(G_{\mathrm{m}} = G_{\mathrm{mlim}})$, and both are functions of $G_{\mathrm{p}}(G_{\mathrm{m}} = G_{\mathrm{mlim}})$ and $L_{\mathrm{p}}(G_{\mathrm{m}} = G_{\mathrm{mlim}})$ according to (A.19), (A.20), and G_ℓ according to (3.32), where $G_{\mathrm{p}}(G_{\mathrm{m}} = G_{\mathrm{mlim}})$ itself is a function of G_ℓ and implicitly[5] of $G_{\mathrm{p}}(G_{\mathrm{m}} = G_{\mathrm{mlim}})$, we define the implicit function $\widetilde{\widetilde{\psi}}_{\mathrm{t}} \equiv 0$ from (3.1), (A.19), (A.20), (3.32), and (3.34),

$$\widetilde{\widetilde{\psi}}_{\mathrm{t}} := R_{\mathrm{s0}} + \left(\sum_{n=1}^{N} a_n \left(\frac{\sqrt{G_{\mathrm{mlim}}\,(G_\ell - G_{\mathrm{mlim}})}}{(G_{\mathrm{i}} - G_{\mathrm{mlim}})^2 + G_{\mathrm{mlim}}\,(G_\ell - G_{\mathrm{mlim}})} \right)^{b_n} \right) - \frac{G_{\mathrm{i}} - G_{\mathrm{mlim}}}{(G_{\mathrm{i}} - G_{\mathrm{mlim}})^2 + G_{\mathrm{mlim}}\,(G_\ell - G_{\mathrm{mlim}})} \equiv 0.$$

Then we compute the implicit function's partial derivatives with respect to G_ℓ and G_{mlim},

$$\begin{aligned}
\frac{\partial \widetilde{\widetilde{\psi}}_{\mathrm{t}}}{\partial G_\ell} &= \left(\sum_{n=1}^{N} a_n b_n \left(\frac{\sqrt{G_{\mathrm{mlim}}\,(G_\ell - G_{\mathrm{mlim}})}}{(G_{\mathrm{i}} - G_{\mathrm{mlim}})^2 + G_{\mathrm{mlim}}\,(G_\ell - G_{\mathrm{mlim}})} \right)^{b_n - 1} \frac{G_{\mathrm{mlim}}\,((G_{\mathrm{i}} - G_{\mathrm{mlim}})^2 - G_{\mathrm{mlim}}\,(G_\ell - G_{\mathrm{mlim}}))}{2\sqrt{G_{\mathrm{mlim}}\,(G_\ell - G_{\mathrm{mlim}})}\,((G_{\mathrm{i}} - G_{\mathrm{mlim}})^2 + G_{\mathrm{mlim}}\,(G_\ell - G_{\mathrm{mlim}}))^2} \right) \\
&\quad + \frac{G_{\mathrm{mlim}}\,(G_{\mathrm{i}} - G_{\mathrm{mlim}})}{((G_{\mathrm{i}} - G_{\mathrm{mlim}})^2 + G_{\mathrm{mlim}}\,(G_\ell - G_{\mathrm{mlim}}))^2}, \\
\frac{\partial \widetilde{\widetilde{\psi}}_{\mathrm{t}}}{\partial G_{\mathrm{mlim}}} &= \left(\sum_{n=1}^{N} a_n b_n \left(\frac{\sqrt{G_{\mathrm{mlim}}\,(G_\ell - G_{\mathrm{mlim}})}}{(G_{\mathrm{i}} - G_{\mathrm{mlim}})^2 + G_{\mathrm{mlim}}\,(G_\ell - G_{\mathrm{mlim}})} \right)^{b_n - 1} \frac{G_\ell\,(G_{\mathrm{i}}^2 - G_\ell\,G_{\mathrm{mlim}}) + 2\,G_{\mathrm{mlim}}\,G_{\mathrm{i}}\,(G_\ell - G_{\mathrm{i}})}{2\sqrt{G_{\mathrm{mlim}}\,(G_\ell - G_{\mathrm{mlim}})}\,((G_{\mathrm{i}} - G_{\mathrm{mlim}})^2 + G_{\mathrm{mlim}}\,(G_\ell - G_{\mathrm{mlim}}))^2} \right) \\
&\quad + \frac{G_{\mathrm{i}}\,(G_\ell - G_{\mathrm{i}})}{((G_{\mathrm{i}} - G_{\mathrm{mlim}})^2 + G_{\mathrm{mlim}}\,(G_\ell - G_{\mathrm{mlim}}))^2}.
\end{aligned}$$

Applying the implicit function theorem [64] gives

$$\frac{\mathrm{d}G_{\mathrm{mlim}}}{\mathrm{d}G_\ell} = -\frac{G_{\mathrm{mlim}} \left(2\,(G_{\mathrm{i}} - G_{\mathrm{mlim}})\sqrt{G_{\mathrm{mlim}}\,(G_\ell - G_{\mathrm{mlim}})} + \left((G_{\mathrm{i}} - G_{\mathrm{mlim}})^2 - G_{\mathrm{mlim}}\,(G_\ell - G_{\mathrm{mlim}}) \right) \sum_{n=1}^{N} a_n b_n \left(\frac{\sqrt{G_{\mathrm{mlim}}\,(G_\ell - G_{\mathrm{mlim}})}}{(G_{\mathrm{i}} - G_{\mathrm{mlim}})^2 + G_{\mathrm{mlim}}\,(G_\ell - G_{\mathrm{mlim}})} \right)^{b_n - 1} \right)}{2\,G_{\mathrm{i}}\,(G_\ell - G_{\mathrm{i}})\sqrt{G_{\mathrm{mlim}}\,(G_\ell - G_{\mathrm{mlim}})} + \left(G_\ell\,(G_{\mathrm{i}}^2 - G_\ell\,G_{\mathrm{mlim}}) + 2\,G_{\mathrm{mlim}}\,G_{\mathrm{i}}\,(G_\ell - G_{\mathrm{i}}) \right) \sum_{n=1}^{N} a_n b_n \left(\frac{\sqrt{G_{\mathrm{mlim}}\,(G_\ell - G_{\mathrm{mlim}})}}{(G_{\mathrm{i}} - G_{\mathrm{mlim}})^2 + G_{\mathrm{mlim}}\,(G_\ell - G_{\mathrm{mlim}})} \right)^{b_n - 1}}.$$

[5] In particular, $R_{\mathrm{s}}(G_{\mathrm{m}} = G_{\mathrm{mlim}})$, $L_{\mathrm{s}}(G_{\mathrm{m}} = G_{\mathrm{mlim}})$, $G_{\mathrm{p}}(G_{\mathrm{m}} = G_{\mathrm{mlim}})$, and $L_{\mathrm{p}}(G_{\mathrm{m}} = G_{\mathrm{mlim}})$ are all functions of G_ℓ only. However, we usually may not be able to solve for $G_{\mathrm{p}}(G_{\mathrm{m}} = G_{\mathrm{mlim}})$ explicitly after applying (A.19), (A.20), and (3.32) to (3.1).

As indicated above, supposed the maximum $g_{\mathrm{t,\,inma}}$ occurs at $G_\ell = G_\mathrm{i}$, we have to prove that $\frac{\mathrm{d}G_\mathrm{mlim}}{\mathrm{d}G_\ell} \leq 0$ if $G_\ell > G_\mathrm{i}$.

For ease of understanding, an overview of the following proof is given below.

To prove that numerator and denominator are ≤ 0 for certain b_N, we abbreviate $\widetilde{\widetilde{S}}_\mathrm{t} = \sum_{n=1}^{N} a_n b_n \left(\frac{\sqrt{G_\mathrm{mlim}\,(G_\ell - G_\mathrm{mlim})}}{(G_\mathrm{i}-G_\mathrm{mlim})^2 + G_\mathrm{mlim}\,(G_\ell - G_\mathrm{mlim})} \right)^{b_n - 1}$ and obtain

$$\frac{\mathrm{d}G_\mathrm{mlim}}{\mathrm{d}G_\ell} = -\frac{G_\mathrm{mlim}\left(2\,(G_\mathrm{i}-G_\mathrm{mlim})\,\sqrt{G_\mathrm{mlim}\,(G_\ell-G_\mathrm{mlim})} + \left((G_\mathrm{i}-G_\mathrm{mlim})^2 - G_\mathrm{mlim}\,(G_\ell-G_\mathrm{mlim})\right)\widetilde{\widetilde{S}}_\mathrm{t}\right)}{2\,G_\mathrm{i}\,(G_\ell-G_\mathrm{i})\,\sqrt{G_\mathrm{mlim}\,(G_\ell-G_\mathrm{mlim})} + \left(G_\ell\,(G_\mathrm{i}^2 - G_\ell\,G_\mathrm{mlim}) + 2\,G_\mathrm{mlim}\,G_\mathrm{i}\,(G_\ell-G_\mathrm{i})\right)\widetilde{\widetilde{S}}_\mathrm{t}}.$$

We firstly assume all $a_n = 0$ or $R_\mathrm{s} = R_\mathrm{s0}$, hence $\widetilde{\widetilde{S}}_\mathrm{t} = 0$ and calculate $\frac{\mathrm{d}G_\mathrm{mlim}}{\mathrm{d}G_\ell}$, which will be ≤ 0 for any $G_\ell > G_\mathrm{i}$.

Secondly, we assume that at least one $a_n > 0$, hence $R_\mathrm{s} > R_\mathrm{s0}$ (according to (3.1)) or $\widetilde{\widetilde{S}}_\mathrm{t} > 0$. We then prove that $b_N \frac{G_\mathrm{i}-G_\mathrm{mlim}}{\sqrt{G_\mathrm{mlim}\,(G_\ell-G_\mathrm{mlim})}} \geq \widetilde{\widetilde{S}}_\mathrm{t}$ and check numerator and denominator separately:

1. If $(G_\mathrm{i} - G_\mathrm{mlim})^2 - G_\mathrm{mlim}\,(G_\ell - G_\mathrm{mlim}) \geq 0$, the numerator is always ≥ 0. Conversely, if $(G_\mathrm{i} - G_\mathrm{mlim})^2 - G_\mathrm{mlim}\,(G_\ell - G_\mathrm{mlim}) < 0$, we have to use the preceding estimate. Since b_N was restricted to $b_N \leq 2$ in Section 3.5.3.2, it suffices to check the minimum estimated value of the numerator at $b_N = 2$, which will be ≥ 0.
2. If $G_\ell\,(G_\mathrm{i}^2 - G_\ell\,G_\mathrm{mlim}) + 2\,G_\mathrm{mlim}\,G_\mathrm{i}\,(G_\ell - G_\mathrm{i}) \geq 0$, hence $G_\mathrm{mlim} \leq \frac{G_\ell\,G_\mathrm{i}^2}{(G_\ell-G_\mathrm{i})^2+G_\mathrm{i}^2}$, the denominator is always ≥ 0. Conversely, if $G_\mathrm{mlim} > \frac{G_\ell\,G_\mathrm{i}^2}{(G_\ell-G_\mathrm{i})^2+G_\mathrm{i}^2}$, we have to use the preceding estimate. Since b_N was restricted to $b_N \leq 2$ in Section 3.5.3.2, it suffices to check the minimum estimated value of the denominator at $b_N = 2$. To prove that this value is ≥ 0, we consider $0 \leq G_\mathrm{mlim} \leq G_\mathrm{i} < G_\ell$ yielding $G_\ell \geq 2G_\mathrm{i}$ if $G_\mathrm{mlim} > \frac{G_\ell\,G_\mathrm{i}^2}{(G_\ell-G_\mathrm{i})^2+G_\mathrm{i}^2}$.

We then know that for all possible values of R_s0, a_n, and b_n according to (3.1), $\frac{\mathrm{d}G_\mathrm{mlim}}{\mathrm{d}G_\ell}$ and thus $\frac{\mathrm{d}g_{\mathrm{t,\,inma}}(G_\mathrm{m}=G_\mathrm{mlim})}{\mathrm{d}G_\ell}$ itself is always ≤ 0 if $G_\ell > G_\mathrm{i}$ and (at least) $b_N \leq 2$.

As indicated above, we begin the actual proof by assuming all $a_n = 0$, thus $R_\mathrm{s} = R_\mathrm{s0}$ for any valid G_m. We then obtain

$$\left.\frac{\mathrm{d}G_\mathrm{mlim}}{\mathrm{d}G_\ell}\right|_{a_n=0\,\forall n} = -\frac{G_\mathrm{mlim}\left(2\,(G_\mathrm{i} - G_\mathrm{mlim})\,\sqrt{G_\mathrm{mlim}\,(G_\ell - G_\mathrm{mlim})}\right)}{2\,G_\mathrm{i}\,(G_\ell - G_\mathrm{i})\,\sqrt{G_\mathrm{mlim}\,(G_\ell - G_\mathrm{mlim})}}.$$

Numerator and denominator of this fraction are always ≥ 0 if $G_\ell > G_\mathrm{i}$, hence $\left.\frac{\mathrm{d}G_\mathrm{mlim}}{\mathrm{d}G_\ell}\right|_{a_n=0\,\forall n}$ is always ≤ 0.

If at least one $a_n > 0$, we begin by deriving an inequality which we will use to check numerator and denominator separately.

Since $b_N > b_{N-1} > ... > b_1 > 0$,

$$\sum_{n=1}^{N} a_n b_N \left(\frac{\sqrt{G_{\mathrm{mlim}}\,(G_\ell - G_{\mathrm{mlim}})}}{(G_\mathrm{i} - G_{\mathrm{mlim}})^2 + G_{\mathrm{mlim}}\,(G_\ell - G_{\mathrm{mlim}})} \right)^{b_n - 1}$$
$$\geq \sum_{n=1}^{N} a_n b_n \left(\frac{\sqrt{G_{\mathrm{mlim}}\,(G_\ell - G_{\mathrm{mlim}})}}{(G_\mathrm{i} - G_{\mathrm{mlim}})^2 + G_{\mathrm{mlim}}\,(G_\ell - G_{\mathrm{mlim}})} \right)^{b_n - 1}.$$

holds.

Furthermore, from the definition of the implicit function we obtain $\frac{G_\mathrm{i} - G_{\mathrm{mlim}}}{(G_\mathrm{i} - G_{\mathrm{mlim}})^2 + G_{\mathrm{mlim}}\,(G_\ell - G_{\mathrm{mlim}})} \geq \sum_{n=1}^{N} a_n \left(\frac{\sqrt{G_{\mathrm{mlim}}\,(G_\ell - G_{\mathrm{mlim}})}}{(G_\mathrm{i} - G_{\mathrm{mlim}})^2 + G_{\mathrm{mlim}}\,(G_\ell - G_{\mathrm{mlim}})} \right)^{b_n}$ or $\frac{G_\mathrm{i} - G_{\mathrm{mlim}}}{\sqrt{G_{\mathrm{mlim}}\,(G_\ell - G_{\mathrm{mlim}})}} \geq \sum_{n=1}^{N} a_n \left(\frac{\sqrt{G_{\mathrm{mlim}}\,(G_\ell - G_{\mathrm{mlim}})}}{(G_\mathrm{i} - G_{\mathrm{mlim}})^2 + G_{\mathrm{mlim}}\,(G_\ell - G_{\mathrm{mlim}})} \right)^{b_n - 1}$.

Combining both estimates yields

$$b_N \frac{G_\mathrm{i} - G_{\mathrm{mlim}}}{\sqrt{G_{\mathrm{mlim}}\,(G_\ell - G_{\mathrm{mlim}})}}$$
$$\geq \sum_{n=1}^{N} a_n b_n \left(\frac{\sqrt{G_{\mathrm{mlim}}\,(G_\ell - G_{\mathrm{mlim}})}}{(G_\mathrm{i} - G_{\mathrm{mlim}})^2 + G_{\mathrm{mlim}}\,(G_\ell - G_{\mathrm{mlim}})} \right)^{b_n - 1}.$$

After deriving the required estimate, we check numerator and denominator of $\frac{\mathrm{d}G_{\mathrm{mlim}}}{\mathrm{d}G_\ell}$ separately:

1. If $(G_\mathrm{i} - G_{\mathrm{mlim}})^2 - G_{\mathrm{mlim}}\,(G_\ell - G_{\mathrm{mlim}}) \geq 0$, the numerator of $\frac{\mathrm{d}G_{\mathrm{mlim}}}{\mathrm{d}G_\ell}$ is always ≥ 0.

   Conversely, if $(G_\mathrm{i} - G_{\mathrm{mlim}})^2 - G_{\mathrm{mlim}}\,(G_\ell - G_{\mathrm{mlim}}) < 0$, the preceding estimate applies and

$$G_{\mathrm{mlim}} \Bigg(2\,(G_\mathrm{i} - G_{\mathrm{mlim}}) \sqrt{G_{\mathrm{mlim}}\,(G_\ell - G_{\mathrm{mlim}})}$$
$$+ ((G_\mathrm{i} - G_{\mathrm{mlim}})^2 - G_{\mathrm{mlim}}\,(G_\ell - G_{\mathrm{mlim}}))$$
$$\cdot \sum_{n=1}^{N} a_n b_n \left(\frac{\sqrt{G_{\mathrm{mlim}}\,(G_\ell - G_{\mathrm{mlim}})}}{(G_\mathrm{i} - G_{\mathrm{mlim}})^2 + G_{\mathrm{mlim}}\,(G_\ell - G_{\mathrm{mlim}})} \right)^{b_n - 1} \Bigg)$$
$$\geq G_{\mathrm{mlim}} \Bigg(\frac{2\,(G_\mathrm{i} - G_{\mathrm{mlim}})\, G_{\mathrm{mlim}}\,(G_\ell - G_{\mathrm{mlim}})}{\sqrt{G_{\mathrm{mlim}}\,(G_\ell - G_{\mathrm{mlim}})}}$$
$$+ \frac{\left((G_\mathrm{i} - G_{\mathrm{mlim}})^2 - G_{\mathrm{mlim}}\,(G_\ell - G_{\mathrm{mlim}})\right) b_N\,(G_\mathrm{i} - G_{\mathrm{mlim}})}{\sqrt{G_{\mathrm{mlim}}\,(G_\ell - G_{\mathrm{mlim}})}} \Bigg).$$

As $0 \leq G_{\text{mlim}} \leq G_{\text{i}} < G_\ell$, G_{mlim}, $G_{\text{i}} - G_{\text{mlim}}$, and the denominator of the fractions are ≥ 0. Since b_N was restricted to $b_N \leq 2$ in Section 3.5.3.2, it suffices to check if the minimum estimated value is ≥ 0. Its minimum occurs at $b_N = 2$, yielding

$$\begin{aligned} & 2\,G_{\text{mlim}}\,(G_\ell - G_{\text{mlim}}) + \left((G_{\text{i}} - G_{\text{mlim}})^2 - G_{\text{mlim}}\,(G_\ell - G_{\text{mlim}})\right) 2 \\ &= \; 2\,(G_{\text{i}} - G_{\text{mlim}})^2, \end{aligned}$$

which is always ≥ 0 according to (3.33).

Hence the numerator of $\frac{\mathrm{d}G_{\text{mlim}}}{\mathrm{d}G_\ell}$ is always ≥ 0 if $G_\ell > G_{\text{i}}$ and (at least) $b_N \leq 2$.

2. The denominator of $\frac{\mathrm{d}G_{\text{mlim}}}{\mathrm{d}G_\ell}$ is always ≥ 0 if

$$\begin{aligned} & G_\ell\,(G_{\text{i}}^2 - G_\ell\,G_{\text{mlim}}) + 2\,G_{\text{mlim}}\,G_{\text{i}}\,(G_\ell - G_{\text{i}}) \\ &= \; -\left((G_\ell - G_{\text{i}})^2 + G_{\text{i}}^2\right)\left(G_{\text{mlim}} - \frac{G_\ell\,G_{\text{i}}^2}{(G_\ell - G_{\text{i}})^2 + G_{\text{i}}^2}\right) \end{aligned}$$

is ≥ 0, which is equivalent to $G_{\text{mlim}} \leq \frac{G_\ell\,G_{\text{i}}^2}{(G_\ell - G_{\text{i}})^2 + G_{\text{i}}^2}$.

Conversely, if $G_\ell\,(G_{\text{i}}^2 - G_\ell\,G_{\text{mlim}}) + 2\,G_{\text{mlim}}\,G_{\text{i}}\,(G_\ell - G_{\text{i}}) < 0$ or $G_{\text{mlim}} > \frac{G_\ell\,G_{\text{i}}^2}{(G_\ell - G_{\text{i}})^2 + G_{\text{i}}^2}$, the preceding estimate applies and

$$\begin{aligned} & 2\,G_{\text{i}}\,(G_\ell - G_{\text{i}})\,\sqrt{G_{\text{mlim}}\,(G_\ell - G_{\text{mlim}})} \\ & + \left(G_\ell\,(G_{\text{i}}^2 - G_\ell\,G_{\text{mlim}}) + 2\,G_{\text{mlim}}\,G_{\text{i}}\,(G_\ell - G_{\text{i}})\right) \\ & \quad \cdot \sum_{n=1}^{N} a_n b_n \left(\frac{\sqrt{G_{\text{mlim}}\,(G_\ell - G_{\text{mlim}})}}{(G_{\text{i}} - G_{\text{mlim}})^2 + G_{\text{mlim}}\,(G_\ell - G_{\text{mlim}})}\right)^{b_n - 1} \\ \geq \; & \frac{2\,G_{\text{i}}\,(G_\ell - G_{\text{i}})\,G_{\text{mlim}}\,(G_\ell - G_{\text{mlim}})}{\sqrt{G_{\text{mlim}}\,(G_\ell - G_{\text{mlim}})}} \\ & + \frac{\left(G_\ell\,(G_{\text{i}}^2 - G_\ell\,G_{\text{mlim}}) + 2\,G_{\text{mlim}}\,G_{\text{i}}\,(G_\ell - G_{\text{i}})\right) b_N\,(G_{\text{i}} - G_{\text{mlim}})}{\sqrt{G_{\text{mlim}}\,(G_\ell - G_{\text{mlim}})}}. \end{aligned}$$

The denominator of the fractions is ≥ 0. Since b_N was restricted to $b_N \leq 2$ in Section 3.5.3.2, it suffices to check if the minimum estimated value is ≥ 0. Its minimum occurs at $b_N = 2$, yielding

$$\begin{aligned} & 2\,G_{\text{i}}\,(G_\ell - G_{\text{i}})\,G_{\text{mlim}}\,(G_\ell - G_{\text{mlim}}) \\ & + \left(G_\ell\,(G_{\text{i}}^2 - G_\ell\,G_{\text{mlim}}) + 2\,G_{\text{mlim}}\,G_{\text{i}}\,(G_\ell - G_{\text{i}})\right) 2\,(G_{\text{i}} - G_{\text{mlim}}) \\ & = \; 2\,G_{\text{i}}^2\left(G_{\text{i}}^2 + (G_{\text{i}} - G_{\text{mlim}})^2\right) + 2\left(G_{\text{i}}^3 + G_{\text{mlim}}^2\,(G_\ell - G_{\text{i}})\right)(G_\ell - 2\,G_{\text{i}}), \end{aligned}$$

which is always ≥ 0 if $G_\ell > 2G_{\text{i}}$. The latter can be proved if $G_{\text{mlim}} > \frac{G_\ell\,G_{\text{i}}^2}{(G_\ell - G_{\text{i}})^2 + G_{\text{i}}^2}$ and $0 \leq G_{\text{mlim}} \leq G_{\text{i}} < G_\ell$ are considered, hence

$$0 \;<\; G_\ell - G_{\text{mlim}} \;<\; G_\ell - \frac{G_\ell\,G_{\text{i}}^2}{(G_\ell - G_{\text{i}})^2 + G_{\text{i}}^2} \;=\; \frac{G_\ell\,(G_\ell - G_{\text{i}})^2}{(G_\ell - G_{\text{i}})^2 + G_{\text{i}}^2},$$

$$0 \;\leq\; G_{\text{i}} - G_{\text{mlim}} \;<\; G_{\text{i}} - \frac{G_\ell\,G_{\text{i}}^2}{(G_\ell - G_{\text{i}})^2 + G_{\text{i}}^2} \;=\; \frac{G_{\text{i}}\,(G_\ell - G_{\text{i}})\,(G_\ell - 2\,G_{\text{i}})}{(G_\ell - G_{\text{i}})^2 + G_{\text{i}}^2}.$$

Since $\frac{G_\ell G_i^2}{(G_\ell - G_i)^2 + G_i^2}$ is always $\leq G_\ell$, but is $\leq G_i$ only if $G_\ell \geq 2\,G_i$, a valid $G_{mlim} > \frac{G_\ell G_i^2}{(G_\ell - G_i)^2 + G_i^2}$ may exist[6] only if $G_\ell \geq 2\,G_i$.

Hence the denominator of $\frac{dG_{mlim}}{dG_\ell}$ is always ≥ 0 if $G_\ell > G_i$ and (at least) $b_N \leq 2$.

Combining all preceding parts of the proof, we may conclude that numerator and denominator of $\frac{dG_{mlim}}{dG_\ell}$ are ≥ 0 and thus $\frac{dG_{mlim}}{dG_\ell}$ and $\frac{dg_{t,\,inma}(G_m = G_{mlim})}{dG_\ell}$ remain ≤ 0 if $G_\ell > G_i$, and (at least) $b_N \leq 2$.

Summarising both proofs yields a maximum $g_{t,\,inma}$ at $G_\ell = G_i$ if the inductor's Q factor is limited to $Q \geq 1$ (hence $\omega L_s \geq R_s$ or $\frac{1}{\omega L_p} \geq G_p$), $0 < b_N \leq 2$ and if G_m was chosen according to Section 3.5.3.2. If G_ℓ is lower or higher, $g_{t,\,inma}$ decreases.

B.3 Matching of a resistive load to a resistive source (matching at the network's input) including the losses of all network elements

B.3.1 Introduction

As indicated in Section 3.5.1, the power gain of π or T networks may be derived in a simpler manner than that used in Sections 3.5.2.1 and 3.5.3.1. This simpler approach is e. g. applied by [51b] and based on taking into account that active power may be transferred to resistive circuit elements only. Due to its simplicity, it's ideally suited to include the losses of all network elements.

To illustrate the method, it's applied to π and T networks which are designed to match a resistive load to a resistive source at the network's input.

B.3.2 π network

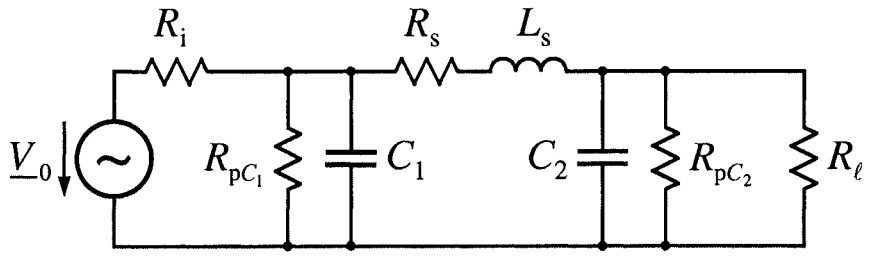

Figure B.1: π network's equivalent circuit including losses of all network elements

Consider the π network of Figure B.1 which takes into account the losses of all network elements. Comparison to the network designed in Section 3.5.2.1 yields

[6] It should be noted that depending on the given values of R_s, G_ℓ, and G_i, $G_{mlim} \leq \frac{G_\ell G_i^2}{(G_\ell - G_i)^2 + G_i^2}$ may also occur if $G_\ell \geq 2\,G_i$.

that it is still applicable for the "inner" π network consisting of C_1, R_s, L_s, and C_2, which transforms the load $R_{\ell\text{res}\pi} = \frac{1}{\frac{1}{R_{pC_2}}+\frac{1}{R_\ell}}$ to $R_{i\text{res}\pi} = \frac{1}{\frac{1}{R_i}-\frac{1}{R_{pC_1}}}$ at the network's input.

The resulting input resistance $R_{i\text{res}\pi}$ the "inner" π network is matched to is chosen to obtain the required input resistance R_i of the total network whose input resistance at matching frequency is equal to $R_{i\text{res}\pi}$ in parallel to R_{pC_1}.

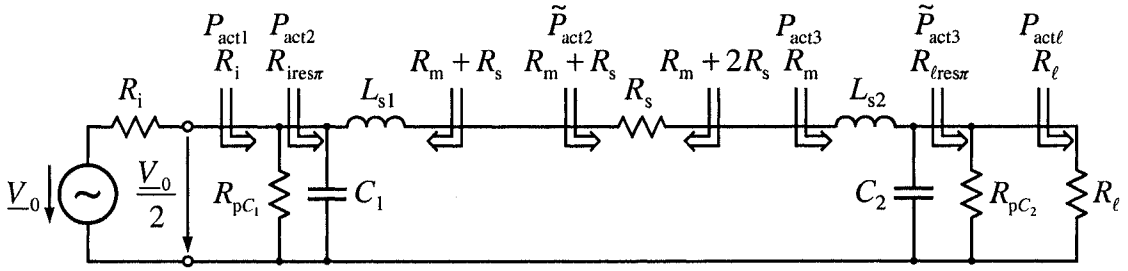

Figure B.2: Definitions and setup for power gain derivation of the π network including losses of all network elements

Thus the π network transforms its load R_ℓ to R_i at the network's input if its elements are set according to the design formulae derived in Section 3.5.2.1 where R_i is replaced with $R_{i\text{res}\pi}$ and R_ℓ with $R_{\ell\text{res}\pi}$. Then, at matching frequency, the π network's resulting equivalent circuit is given by Figure B.2. Similar to Section 3.5.2.1, L_s is split in $L_{s1,2}$ to illustrate reactive cancellation in each of the two L networks building the π network.

If the π network's input is matched to R_i, the voltage at its input is equal to $\frac{\underline{V}_0}{2}$. Hence the active power delivered to its input is given by

$$P_{act1} = \frac{1}{2}\frac{\frac{|\underline{V}_0|^2}{4}}{R_i} = \frac{1}{8}\frac{\underline{V}_0^2}{R_i} \overset{(2.22)}{=} P_{actmaxi}.$$

P_{act2}, the active power transferred to the "inner" π network, is equal to P_{act1} diminished by the active power R_{pC_1} consumes, thus

$$P_{act2} = P_{act1} - \frac{1}{2}\frac{\frac{|\underline{V}_0|^2}{4}}{R_{pC_1}} = P_{actmaxi}\left(1 - \frac{R_i}{R_{pC_1}}\right).$$

Since C_1 and L_{s1} are purely reactive, they do not consume any active power, and $\tilde{P}_{act2} = P_{act2}$.

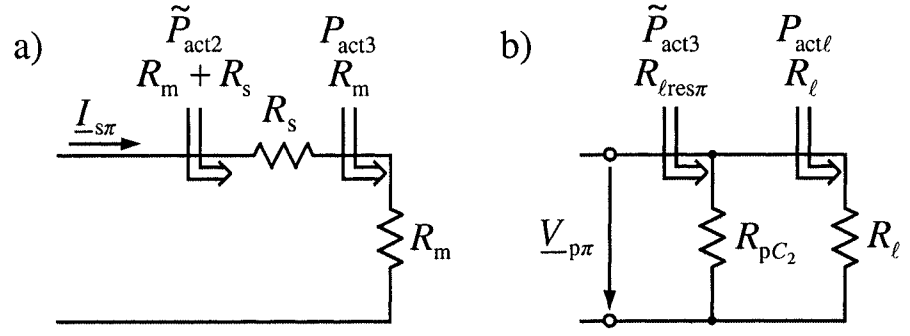

Figure B.3: Equivalent circuit to derive P_{act3} and $P_{act\ell}$ according to [51b]

For our chosen parametrisation, R_m is the input resistance of the partial network to the right of R_s. Then, as indicated in Figure B.3 a), the same current $\underline{I}_{\mathrm{s}\pi}$ flows through R_s and R_m. Thus we obtain $\widetilde{P}_\mathrm{act2} = \frac{1}{2}(R_\mathrm{m} + R_\mathrm{s})\,|\underline{I}_{\mathrm{s}\pi}|^2$ and $P_\mathrm{act3} = \frac{1}{2} R_\mathrm{m}\,|\underline{I}_{\mathrm{s}\pi}|^2$, or

$$P_\mathrm{act3} = \frac{R_\mathrm{m}}{R_\mathrm{m} + R_\mathrm{s}}\,\widetilde{P}_\mathrm{act2} = P_\mathrm{actmaxi}\,\frac{1}{1 + \frac{R_\mathrm{s}}{R_\mathrm{m}}}\left(1 - \frac{R_\mathrm{i}}{R_{\mathrm{p}C_1}}\right).$$

Again L_s2 and C_2 are purely reactive, do not consume any active power, and $\widetilde{P}_\mathrm{act3} = P_\mathrm{act3}$.

Then, as shown in Figure B.3 b), the same voltage $\underline{V}_{\mathrm{p}\pi}$ is applied to $R_{\mathrm{p}C_2}$ and R_ℓ. Thus $\widetilde{P}_\mathrm{act3} = \frac{1}{2}\,|\underline{V}_{\mathrm{p}\pi}|^2 \left(\frac{1}{R_{\mathrm{p}C_2}} + \frac{1}{R_\ell}\right)$ and $P_{\mathrm{act}\ell} = \frac{1}{2}\,|\underline{V}_{\mathrm{p}\pi}|^2\,\frac{1}{R_\ell}$, or

$$P_{\mathrm{act}\ell} = \frac{\widetilde{P}_\mathrm{act3}}{1 + \frac{R_\ell}{R_{\mathrm{p}C_2}}} = P_\mathrm{actmaxi}\,\frac{1}{1 + \frac{R_\mathrm{s}}{R_\mathrm{m}}}\,\frac{1 - \frac{R_\mathrm{i}}{R_{\mathrm{p}C_1}}}{1 + \frac{R_\ell}{R_{\mathrm{p}C_2}}}.$$

Summarising the preceding considerations yields the power gain of the π network including losses of all network elements,

$$g_{\pi,\,\mathrm{inma}} = \frac{1}{1 + \frac{R_\mathrm{s}}{R_\mathrm{m}}}\,\frac{1 - \frac{R_\mathrm{i}}{R_{\mathrm{p}C_1}}}{1 + \frac{R_\ell}{R_{\mathrm{p}C_2}}}. \tag{B.1}$$

Despite its apparent simplicity, the formula is quite complicated because usually $R_{\mathrm{p}C_{1,2}}$ and R_s are functions of the parameter R_m.

Even for the "simple" case of constant Q factors of all network elements, hence $R_{\mathrm{p}C_1} = \frac{Q_1}{\omega C_{1(\mathrm{p})}}$, $R_\mathrm{s} = \frac{1}{Q}\,\omega L_\mathrm{s}$, and $R_{\mathrm{p}C_2} = \frac{Q_2}{\omega C_{2(\mathrm{p})}}$, explicit derivation of those functions is somewhat difficult.

One approach is to put $\frac{Q_2}{\omega C_2}$ and the design formula of C_2 (given by (3.18) if R_ℓ is replaced with $R_{\ell\mathrm{res}\pi}$) in $R_{\ell\mathrm{res}\pi} = \frac{1}{\frac{1}{R_{\mathrm{p}C_2}} + \frac{1}{R_\ell}}$ and solve the resulting equation for $R_{\ell\mathrm{res}\pi}$ — the solution has to be real, positive, and $< R_\ell$.

Then we perform similar calculations for $R_{\mathrm{p}C_1}$ and $R_{\mathrm{ires}\pi}$, put the solutions in $R_\mathrm{s} = \frac{1}{Q}\,\omega L_\mathrm{s}$, where L_s is given by (3.19) if R_i is replaced with $R_{\mathrm{ires}\pi}$ and R_ℓ with $R_{\ell\mathrm{res}\pi}$, and solve for R_s. However, more than one solution is obtained. Thus we additionally need to derive which solution is real and applies in which range of R_m.

Since the derivations sketched are quite lengthy, time consuming, and not needed within this work, they are not included herein.

B.3.3 T network

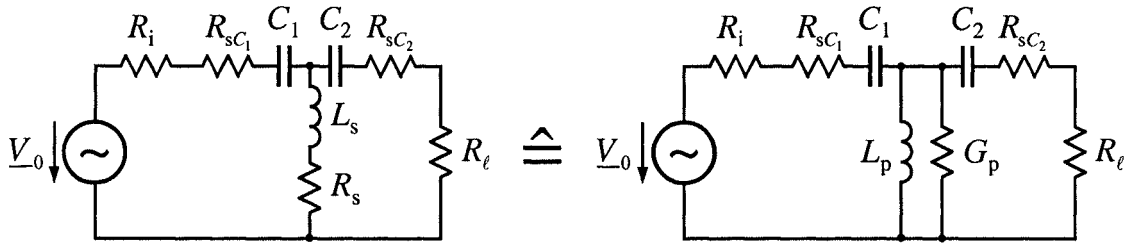

Figure B.4: (Transformed) T network's equivalent circuit including losses of all network elements

Consider the T network of Figure B.4 which takes into account the losses of all network elements. Comparison to the network designed in Section 3.5.3.1 yields that it is still applicable for the "inner" T network consisting of C_1, G_p, L_p, and C_2, which transforms the load $G_{\ell\mathrm{rest}} = \frac{1}{R_{\ell\mathrm{rest}}} = \frac{1}{R_{\mathrm{s}C_2}+R_\ell} = \frac{1}{\frac{1}{G_{\mathrm{s}C_2}}+\frac{1}{G_\ell}}$ to $G_\mathrm{irest} = \frac{1}{R_\mathrm{irest}} = \frac{1}{R_\mathrm{i}-R_{\mathrm{s}C_1}} = \frac{1}{\frac{1}{G_\mathrm{i}}-\frac{1}{G_{\mathrm{s}C_1}}}$ at the network's input (in the formulae, the definitions $G_\mathrm{i} = \frac{1}{R_\mathrm{i}}$, $G_\ell = \frac{1}{R_\ell}$, and $G_{\mathrm{s}C_{1,2}} = \frac{1}{R_{\mathrm{s}C_{1,2}}}$ were used).

The resulting input conductance G_irest the "inner" T network is matched to is chosen to obtain the required input conductance $G_\mathrm{i} = \frac{1}{R_\mathrm{i}}$ of the total network whose input conductance at matching frequency is equal to G_irest in series to $G_{\mathrm{s}C_1}$.

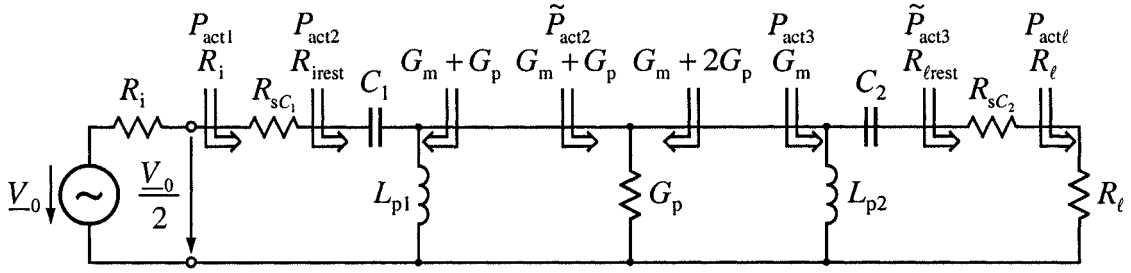

Figure B.5: Definitions and setup for power gain derivation of the T network including losses of all network elements

Thus the T network transforms its load $G_\ell = \frac{1}{R_\ell}$ to $G_\mathrm{i} = \frac{1}{R_\mathrm{i}}$ at the network's input if its elements are set according to the design formulae derived in Section 3.5.3.1 where G_i is replaced with G_irest and G_ℓ with $G_{\ell\mathrm{rest}}$. Then, at matching frequency, the T network's resulting equivalent circuit is given by Figure B.5. Similar to Section 3.5.3.1, L_p is split in $L_{\mathrm{p}1,2}$ to illustrate susceptive cancellation in each of the two L networks building the T network.

If the T network's input is matched to $R_\mathrm{i} = \frac{1}{G_\mathrm{i}}$, the voltage at its input is equal to $\frac{\underline{V}_0}{2}$. Hence the active power delivered to its input is given by

$$P_\mathrm{act1} = \frac{1}{2}\frac{\frac{|\underline{V}_0|^2}{4}}{R_\mathrm{i}} = \frac{1}{8}\frac{\underline{V}_0^2}{R_\mathrm{i}} \overset{(2.22)}{=} P_\mathrm{actmaxi}$$

and the current flowing into the "inner" T network is equal to $\frac{\underline{V}_0}{2R_\mathrm{i}}$.

P_{act2}, the active power transferred to the "inner" T network, is equal to P_{act1} diminished by the active power $R_{\text{s}C_1}$ consumes, thus

$$P_{\text{act2}} = P_{\text{act1}} - \frac{1}{2} R_{\text{s}C_1} \frac{|\underline{V}_0|^2}{4R_{\text{i}}^2} = P_{\text{actmaxi}} \left(1 - \frac{R_{\text{s}C_1}}{R_{\text{i}}}\right).$$

Since C_1 and L_{s1} are purely reactive, they do not consume any active power, and $\widetilde{P}_{\text{act2}} = P_{\text{act2}}$.

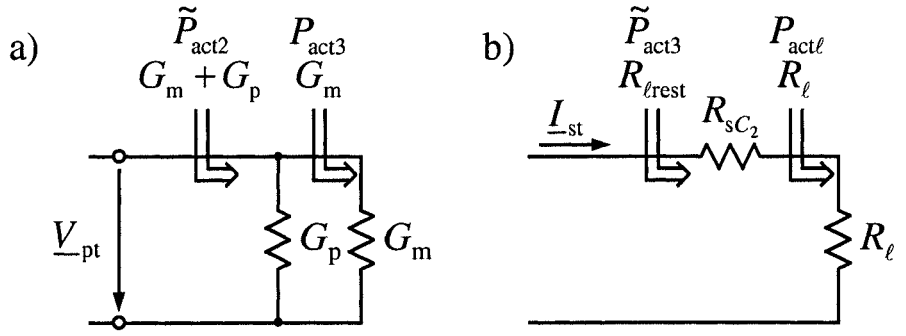

Figure B.6: Equivalent circuit to derive P_{act3} and $P_{\text{act}\ell}$ according to [51b]

For our chosen parametrisation, G_{m} is the input conductance of the partial network to the right of G_{p}. Then, as indicated in Figure B.6 a), the same voltage $\underline{V}_{\text{pt}}$ is applied to G_{p} and G_{m}. Thus we obtain $\widetilde{P}_{\text{act2}} = \frac{1}{2} |\underline{V}_{\text{pt}}|^2 (G_{\text{m}} + G_{\text{p}})$ and $P_{\text{act3}} = \frac{1}{2} |\underline{V}_{\text{pt}}|^2 G_{\text{m}}$, or

$$P_{\text{act3}} = \frac{G_{\text{m}}}{G_{\text{m}} + G_{\text{p}}} \widetilde{P}_{\text{act2}} = P_{\text{actmaxi}} \frac{1}{1 + \frac{G_{\text{p}}}{G_{\text{m}}}} \left(1 - \frac{R_{\text{s}C_1}}{R_{\text{i}}}\right).$$

Again L_{p2} and C_2 are purely reactive, do not consume any active power, and $\widetilde{P}_{\text{act3}} = P_{\text{act3}}$.

Then, as shown in Figure B.6 b), the same current $\underline{I}_{\text{st}}$ flows through $R_{\text{s}C_2}$ and R_{ℓ}. Thus $\widetilde{P}_{\text{act3}} = \frac{1}{2} (R_{\text{s}C_2} + R_{\ell}) |\underline{I}_{\text{st}}|^2$ and $P_{\text{act}\ell} = \frac{1}{2} R_{\ell} |\underline{I}_{\text{st}}|^2$, or

$$P_{\text{act}\ell} = \frac{\widetilde{P}_{\text{act3}}}{1 + \frac{R_{\text{s}C_2}}{R_{\ell}}} = P_{\text{actmaxi}} \frac{1}{1 + \frac{G_{\text{p}}}{G_{\text{m}}}} \frac{1 - \frac{R_{\text{s}C_1}}{R_{\text{i}}}}{1 + \frac{R_{\text{s}C_2}}{R_{\ell}}}.$$

Summarising the preceding considerations yields the power gain of the T network including losses of all network elements,

$$g_{\text{t, inma}} = \frac{1}{1 + \frac{G_{\text{p}}}{G_{\text{m}}}} \frac{1 - \frac{G_{\text{i}}}{G_{\text{s}C_1}}}{1 + \frac{G_{\ell}}{G_{\text{s}C_2}}}. \tag{B.2}$$

Despite its apparent simplicity, the formula is quite complicated because usually $R_{\text{s}C_{1,2}}$ and G_{p} are functions of the parameter G_{m}.

Even for the "simple" case of constant Q factors of all network elements, hence $G_{sC_1} = Q_1 \omega C_{1(s)}$, $G_p = \frac{1}{Q \omega L_p}$, and $G_{sC_2} = Q_2 \omega C_{2(s)}$, explicit derivation of those functions is somewhat difficult.

One approach is to put $Q_2 \omega C_2$ and the design formula of C_2 (given by (3.31) if G_ℓ is replaced with $G_{\ell rest}$) in $G_{\ell rest} = \frac{1}{\frac{1}{G_{sC_2}} + \frac{1}{G_\ell}}$ and solve the resulting equation for $G_{\ell rest}$ — the solution has to be real, positive, and $< G_\ell$.

Then we perform similar calculations for G_{sC_1} and G_{irest}, put the solutions in $G_p = \frac{1}{Q \omega L_p}$, where L_p is given by (3.32) if G_i is replaced with G_{irest} and G_ℓ with $G_{\ell rest}$, and solve for G_p. However, more than one solution is obtained. Thus we additionally need to derive which solution is real and applies in which range of G_m.

Since the derivations sketched are quite lengthy, time consuming, and not needed within this work, they are not included herein.

B.4 Matching of a resistive source to a resistive load (matching at the network's output)

B.4.1 π network

To derive the elements' values for matching of a (real) source conductance $G_i = \frac{1}{R_i}$ to a (real) load conductance $G_\ell = \frac{1}{R_\ell}$ if a π network with a lossy "central" inductor is used, calculations are based on the (transformed) π network's equivalent circuit in Figure 3.14.

As in Section 3.5.2.1, an approach similar to [13] (derivation for a lossless π network) is used, where reactive cancellation is applied to each of the two L networks — C_{m1} cancels L_{s1} and C_{m2} cancels L_{s2}.

Additionally, the remaining resistances have to be equal. To match the source to the load, we may choose $R_{m1} = R_m$. At matching frequency, $\underline{Z}_{1i} = R_m$ holds and thus $\underline{Z}_{2i} = \underline{Z}_{1i} + R_s = R_m + R_s$. To achieve a (conjugate complex) match of the source to the load, $\underline{Z}_{2i}$ must be equal to R_{m2}, hence $R_{m2} = R_m + R_s$. Conversely, $\underline{Z}_{2\ell} = R_{m2} = R_m + R_s$ and $\underline{Z}_{1\ell} = \underline{Z}_{2\ell} + R_s = R_m + 2R_s$ at matching frequency, which is not equal to $R_{m1} = R_m$ as it would be for a conjugate complex match of the load to the source.

Different choices of $R_{m1,2}$ are also possible, but those shown above are ideally suited for the extension to complex sources.

Using the preceding choice for $R_{m1,2}$, we would obtain $C_{1,2}$ (and $C_{m1,2}$) from parallel-to-series transformation equations for $R_{m1,2}$. Applying reactive cancellation would then yield $L_{s1,2}$ (and L_s). The calculations are not shown here because we alternatively may use the formulae from [13] if they are rewritten in our resistance notation and if we use $R_{m1} = R_m$ for the left L network and $R_{m2} = R_m + R_s$ for the right L network ([13] derives the lossless case, where $R_{m1} = R_{m2} = R_m$).

Since $R_{m1,2}$ was obtained from parallel-to-series transformation of passive components (source resistance $R_i > 0$ and load resistance $R_\ell > 0$), $R_{m1,2} \geq 0$ holds. Then the calculations described above yield the capacitances $C_{1,2}$ and the inductance L_s of the **original** π network in Figure 3.13 a), where

$$C_1 = \overset{+}{(-)} \frac{1}{\omega R_i} \sqrt{\frac{R_i - R_m}{R_m}}, \quad \text{(B.3)} \qquad C_2 = \overset{+}{[-]} \frac{1}{\omega R_\ell} \sqrt{\frac{R_\ell - R_m - R_s}{R_m + R_s}}, \quad \text{(B.4)}$$

$$L_s = \frac{\overset{+}{(-)}\sqrt{R_m\,(R_i - R_m)}\ \overset{+}{[-]}\sqrt{(R_m + R_s)\,(R_\ell - R_m - R_s)}}{\omega}. \quad \text{(B.5)}$$

(The negative signs in parentheses/square brackets would apply if we would use (lossless) variable inductors $L_{1,2} = -\frac{1}{\omega^2 C_{1,2}}$. Then a negative L_s might occur, which would be just equal to a variable capacitor $C_s = -\frac{1}{\omega^2 L_s}$. As indicated by using parentheses/square brackets, reactive cancellation causes a negative sign of the first square root in L_s, if L_1 is used instead of C_1, or a negative sign of the second square root in L_s, if L_2 is used instead of C_2, respectively. We will need these changes during the extension to inductive sources.)

Comparing the formulae to those of Section 3.5.2.1 yields that they are similar except that R_i, R_ℓ, and the indices of the capacitances are exchanged. Thus the conditions to R_m are changed accordingly. Hence, for valid R_m the designability conditions are

$$0 \leq R_m \leq R_i \text{ and } 0 \leq R_m + R_s \leq R_\ell. \quad \text{(B.6)}$$

As $R_s \geq R_{s0}$ (from (3.1)), we immediately obtain that R_{s0} is limited by $R_{s0} \leq R_\ell$. If R_{s0} would be higher, the π network would not be able to match any source.

Similar to Section 3.5.2.1, there is an upper limit of R_m which is given by R_i if $R_i \leq R_\ell - R_{s0}$ or by R_{mlim} if $R_i > R_\ell - R_{s0}$, respectively. R_{mlim} is the highest parameter R_m which solves

$$R_{mlim} = R_\ell - R_s(R_{mlim}) \quad \text{(B.7)}$$

for $0 \leq R_{mlim} < R_i$ and involves valid network elements. The change in the upper limit occurs at $R_i = R_\ell - R_{s0}$, where, as before, a match would not need any additional components ($L_s = 0$ and $C_{1,2} = 0$ would match). It's interesting to note that (for a resistive load) there is no other solution where $L_s = 0$ [†].

Depending on the particular R_s used (given as a function of ωL_s or R_m), additional restrictions to R_m might apply, limiting R_m even further or involving intervals within the limits derived above where matching is impossible. However, (B.6) holds throughout the valid range of R_m.

[†]Theoretically $L_s = 0$ might additionally occur for $R_m = 0$ if $R_s(R_m = 0) = 0$, which would be possible for $R_{s0} = 0$. However, since $L_s = 0$, the source resistor would not be transformed. Hence matching would be impossible unless $R_i = R_\ell - R_{s0} = R_\ell = R_m = 0$ — this solution is already described by (a limit of) R_{mlim}.

Additionally, the upper limits in (B.6) separate π and L networks — $C_1 = 0$ if $R_\mathrm{m} = R_\mathrm{i}$ or $C_2 = 0$ if $R_\mathrm{m} = R_\mathrm{mlim}$, respectively.

After designing the π network's output impedance to match the load resistance R_ℓ, we compute the active power $P_{\mathrm{act}\ell}$ delivered to its load resistance R_ℓ. Since the capacitive and inductive reactances in Figure 3.14 cancel at matching frequency, we obtain

$$\begin{aligned} P_{\mathrm{act}\ell} &= \frac{1}{2} R_\mathrm{m2} \frac{|\widetilde{\underline{V}}_0|^2}{(R_\mathrm{m1} + R_\mathrm{s} + R_\mathrm{m2})^2} \overset{(3.16)}{=} \frac{1}{2} (R_\mathrm{m} + R_\mathrm{s}) \frac{\frac{|\underline{V}_0|^2}{1+\omega^2 R_\mathrm{i}^2 C_1^2}}{4\,(R_\mathrm{m} + R_\mathrm{s})^2} \\ P_{\mathrm{act}\ell} &\overset{(B.3)}{=} \frac{|\underline{V}_0|^2}{8\,R_\mathrm{i}} \frac{R_\mathrm{m}}{R_\mathrm{m} + R_\mathrm{s}} \overset{(2.22)}{=} P_\mathrm{actmaxi} \frac{1}{1 + \frac{R_\mathrm{s}}{R_\mathrm{m}}}. \end{aligned} \tag{B.8}$$

For a given R_m, the network elements' values $C_{1,2}$ and L_s differ from those matching the load to the source in Section 3.5.2.1. Since $R_\mathrm{s} \neq 0$ prevents matching of the load to the source if the network is designed for matching the source to the load, the active power P_acts delivered to R_s is also not equal to that derived in Section 3.5.2.1. However, the same current flows through R_s and $R_\mathrm{m2} = R_\mathrm{m} + R_\mathrm{s}$, hence it's given by

$$P_\mathrm{acts} = P_{\mathrm{act}\ell} \frac{R_\mathrm{s}}{R_\mathrm{m} + R_\mathrm{s}} \overset{(B.8)}{=} P_\mathrm{actmaxi} \frac{\frac{R_\mathrm{m}}{R_\mathrm{s}}}{\left(1 + \frac{R_\mathrm{m}}{R_\mathrm{s}}\right)^2}. \tag{B.9}$$

For optimisation, we will need the power gain $g_{\pi,\,\mathrm{outma}}$ of the matched π network. The active power delivered to the network's input is $P_\mathrm{act1} = P_\mathrm{acts} + P_{\mathrm{act}\ell}$ (refer to Figure A.4). Thus we obtain

$$g_{\pi,\,\mathrm{outma}} = \frac{P_{\mathrm{act}\ell}}{P_\mathrm{act1}} = \frac{P_{\mathrm{act}\ell}}{P_\mathrm{acts} + P_{\mathrm{act}\ell}} \overset{(B.8),(B.9)}{=} \frac{R_\mathrm{m} + R_\mathrm{s}}{R_\mathrm{m} + 2R_\mathrm{s}} = \frac{1 + \frac{R_\mathrm{s}}{R_\mathrm{m}}}{1 + 2\,\frac{R_\mathrm{s}}{R_\mathrm{m}}}. \tag{B.10}$$

(Alternatively we could derive $g_{\pi,\,\mathrm{outma}}$ from (A.15) if we put $C_\mathrm{2tot} = C_2$. However, we gain more insight in the circuit's behaviour if it is computed as shown above.)

Comparing the preceding results to those of Section 3.5.2.1 yields that in the formulae of L_s, R_mlim and the limits of R_m, R_i, and R_ℓ are exchanged, whereas for $C_{1,2}$ additionally the indices have to be exchanged.

Since

$$\frac{\mathrm{d}g_{\pi,\,\mathrm{outma}}}{\mathrm{d}R_\mathrm{m}} \overset{(B.10)}{=} \frac{R_\mathrm{m}}{(R_\mathrm{m} + 2R_\mathrm{s})^2} \left(\frac{R_\mathrm{s}}{R_\mathrm{m}} - \frac{\mathrm{d}R_\mathrm{s}}{\mathrm{d}R_\mathrm{m}} \right), \tag{B.11}$$

deriving of the optimum R_m requires simply checking of the sign of $\frac{R_\mathrm{s}}{R_\mathrm{m}} - \frac{\mathrm{d}R_\mathrm{s}}{\mathrm{d}R_\mathrm{m}}$ similar to Section 3.5.2.2.

Conversely, deriving the optimum source resistance R_i if R_m is chosen for maximum $g_{\pi,\,\mathrm{outma}}$ involves

$$g_{\pi,\,\mathrm{outma}}(R_\mathrm{m} = R_\mathrm{i}) = \frac{R_\mathrm{i} + R_\mathrm{s}(R_\mathrm{m} = R_\mathrm{i})}{R_\mathrm{i} + 2\,R_\mathrm{s}(R_\mathrm{m} = R_\mathrm{i})}$$

and

$$\frac{\mathrm{d}g_{\pi,\mathrm{outma}}(R_\mathrm{m}=R_\mathrm{i})}{\mathrm{d}R_\mathrm{i}} = \frac{R_\mathrm{i}}{(R_\mathrm{i}+2\,R_\mathrm{s}(R_\mathrm{m}=R_\mathrm{i}))^2}\left(\frac{R_\mathrm{s}(R_\mathrm{m}=R_\mathrm{i})}{R_\mathrm{i}} - \frac{\mathrm{d}\,(R_\mathrm{s}(R_\mathrm{m}=R_\mathrm{i}))}{\mathrm{d}R_\mathrm{i}}\right)$$

if R_i is the upper limit of R_m or

$$g_{\pi,\mathrm{outma}}(R_\mathrm{m}=R_\mathrm{mlim}) = \frac{R_\ell}{2\,R_\ell - R_\mathrm{mlim}}$$

and

$$\frac{\mathrm{d}g_{\pi,\mathrm{outma}}(R_\mathrm{m}=R_\mathrm{mlim})}{\mathrm{d}R_\mathrm{i}} = \frac{R_\ell}{(2\,R_\ell - R_\mathrm{mlim})^2}\,\frac{\mathrm{d}R_\mathrm{mlim}}{\mathrm{d}R_\mathrm{i}}$$

if R_mlim is the upper limit of R_m.

Thus, similar to Section 3.5.2.3 and Appendix B.2.1.2, the optimisation with respect to R_i requires simply checking of the sign of $\frac{R_\mathrm{s}(R_\mathrm{m}=R_\mathrm{i})}{R_\mathrm{i}} - \frac{\mathrm{d}(R_\mathrm{s}(R_\mathrm{m}=R_\mathrm{i}))}{\mathrm{d}R_\mathrm{i}}$ or $\frac{\mathrm{d}R_\mathrm{mlim}}{\mathrm{d}R_\mathrm{i}}$. Hence the proofs of Sections 3.5.2.2, 3.5.2.3 and Appendices B.2.1.1, B.2.1.2 apply if R_i and R_ℓ are exchanged.

Furthermore, the extension to complex sources can be performed in a similar manner as the extension to complex loads, in particular because in addition to R_i, R_ℓ, the indices of $C_{1,2}$ are exchanged compared to the case of matching the load to the source.

B.4.2 T network

To derive the elements' values for matching of a (real) source resistance $R_\mathrm{i} = \frac{1}{G_\mathrm{i}}$ to a (real) load resistance $R_\ell = \frac{1}{G_\ell}$ if a T network with a lossy "central" inductor is used, calculations are based on the (transformed) T network's equivalent circuit in Figure 3.15.

As in Section 3.5.3.1, an approach similar to [13] (derivation for a lossless T network) is used, where susceptive cancellation is applied to each of the two L networks — C_m1 cancels L_p1 and C_m2 cancels L_p2.

Additionally, the remaining conductances have to be equal. To match the source to the load, we may choose $G_\mathrm{m1} = G_\mathrm{m}$. At matching frequency, $\underline{Y}_\mathrm{1i} = G_\mathrm{m}$ holds and thus $\underline{Y}_\mathrm{2i} = \underline{Y}_\mathrm{1i} + G_\mathrm{p} = G_\mathrm{m} + G_\mathrm{p}$. To achieve a (conjugate complex) match of the source to the load, $\underline{Y}_\mathrm{2i}$ must be equal to G_m2, hence $G_\mathrm{m2} = G_\mathrm{m} + G_\mathrm{p}$. Conversely, $\underline{Y}_{2\ell} = G_\mathrm{m2} = G_\mathrm{m} + G_\mathrm{p}$ and $\underline{Y}_{1\ell} = \underline{Y}_{2\ell} + G_\mathrm{p} = G_\mathrm{m} + 2G_\mathrm{p}$ at matching frequency, which is not equal to $G_\mathrm{m1} = G_\mathrm{m}$ as it would be for a conjugate complex match of the load to the source.

Different choices of $G_{\mathrm{m1},2}$ are also possible, but those shown above are ideally suited for the extension to complex sources.

Using the preceding choice for $G_{\mathrm{m1,2}}$, we would obtain $C_{1,2}$ (and $C_{\mathrm{m1,2}}$) from series-to-parallel transformation equations for $G_{\mathrm{m1,2}}$. Applying susceptive cancellation would then yield $L_{\mathrm{p1,2}}$ (and L_p). The calculations are not shown here because we

alternatively may use the formulae from [13] if they are rewritten in our conductance notation and if we use $G_{\mathrm{m1}} = G_{\mathrm{m}}$ for the left L network and $G_{\mathrm{m2}} = G_{\mathrm{m}} + G_{\mathrm{p}}$ for the right L network ([13] derives the lossless case in resistive notation, where $G_{\mathrm{m1}} = G_{\mathrm{m2}} = G_{\mathrm{m}}$).

Since $G_{\mathrm{m1,2}}$ was obtained from series-to-parallel transformation of passive components (source conductance $G_{\mathrm{i}} > 0$ and load conductance $G_\ell > 0$), $G_{\mathrm{m1,2}} \geq 0$ holds. Then the calculations described above yield the capacitances $C_{1,2}$ and the inductance L_{p} of the **original** T network in Figure 3.13 b), where

$$C_1 = \overset{+}{(-)} \frac{G_{\mathrm{i}}}{\omega} \sqrt{\frac{G_{\mathrm{m}}}{G_{\mathrm{i}} - G_{\mathrm{m}}}}, \quad \text{(B.12)} \qquad C_2 = \overset{+}{[-]} \frac{G_\ell}{\omega} \sqrt{\frac{G_{\mathrm{m}} + G_{\mathrm{p}}}{G_\ell - G_{\mathrm{m}} - G_{\mathrm{p}}}}, \quad \text{(B.13)}$$

$$L_{\mathrm{p}} = \frac{1}{\omega \left(\overset{+}{(-)} \sqrt{G_{\mathrm{m}} \left(G_{\mathrm{i}} - G_{\mathrm{m}}\right)} \overset{+}{[-]} \sqrt{\left(G_{\mathrm{m}} + G_{\mathrm{p}}\right) \left(G_\ell - G_{\mathrm{m}} - G_{\mathrm{p}}\right)} \right)}. \quad \text{(B.14)}$$

(The negative signs in parentheses/square brackets would apply if we would use (lossless) variable inductors $L_{1,2} = -\frac{1}{\omega^2 C_{1,2}}$. Then a negative L_{p} might occur, which would be just equal to a variable capacitor $C_{\mathrm{p}} = -\frac{1}{\omega^2 L_{\mathrm{p}}}$. As indicated by using parentheses/square brackets, susceptive cancellation causes a negative sign of the first square root in L_{p}, if L_1 is used instead of C_1, or a negative sign of the second square root in L_{p}, if L_2 is used instead of C_2, respectively. We would need these changes during the extension to inductive sources.)

Comparing the formulae to those of Section 3.5.3.1 yields that they are similar except that G_{i}, G_ℓ, and the indices of the capacitances are exchanged. Thus the conditions to G_{m} are changed accordingly. Hence, for valid G_{m} the designability conditions are

$$0 \leq G_{\mathrm{m}} \leq G_{\mathrm{i}} \text{ and } 0 \leq G_{\mathrm{m}} + G_{\mathrm{p}} \leq G_\ell. \quad \text{(B.15)}$$

Similar to Section 3.5.3.1, there is an upper limit of G_{m} which is given by G_{i} if $G_{\mathrm{i}} \leq G_\ell$ or by G_{mlim} if $G_{\mathrm{i}} > G_\ell$, respectively. G_{mlim} is the highest parameter G_{m} which solves

$$G_{\mathrm{mlim}} = G_\ell - G_{\mathrm{p}}(G_{\mathrm{mlim}}) \quad \text{(B.16)}$$

for $0 \leq G_{\mathrm{mlim}} < G_{\mathrm{i}}$ and involves valid network elements. The change in the upper limit occurs at $G_{\mathrm{i}} = G_\ell$, where, as before, a match would not need any additional components ($L_{\mathrm{s}} \to \infty$, hence $L_{\mathrm{p}} \to \infty$, and $C_{1,2} \to \infty$ would match). It's interesting to note that (for a resistive load) there is no other solution where $L_{\mathrm{s,p}} \to \infty$ or $\frac{1}{L_{\mathrm{p}}} = 0$[‡].

[‡]Theoretically $\frac{1}{L_{\mathrm{p}}} = 0$ might additionally occur for $G_{\mathrm{m}} = 0$ if $G_{\mathrm{p}}(G_{\mathrm{m}} = 0) = 0$. However, since $L_{\mathrm{s,p}} \to \infty$ ($\frac{1}{L_{\mathrm{p}}} = 0$ and $G_{\mathrm{p}} = 0$ is case (ii) in (A.18)), the load conductor would not be transformed. Hence matching would be impossible unless $G_{\mathrm{i}} = G_\ell = G_{\mathrm{m}} = 0$ — this solution is

Depending on the particular R_s used, hence the particular G_p used (given as a function of ωL_p or G_m), additional restrictions to G_m might apply, limiting G_m even further or involving intervals within the limits derived above where matching is impossible. However, (3.33) holds throughout the valid range of G_m.

Additionally, the upper limits in (B.15) separate T and L networks — $C_1 \to \infty$ if $G_m = G_i$ or $C_2 \to \infty$ if $G_m = G_{mlim}$, respectively.

After designing the T network's output impedance to match the load conductance G_ℓ, we compute the active power $P_{act\ell}$ delivered to its load conductance G_ℓ. Since the capacitive and inductive susceptances in Figure 3.15 cancel at matching frequency, we obtain

$$P_{act\ell} = \frac{1}{2} G_{m2} \frac{|\underline{\widetilde{I}}_0|^2}{(G_{m1} + G_p + G_{m2})^2} \overset{(3.29)}{=} \frac{1}{2} (G_m + G_p) \frac{|\underline{V}_0|^2 \frac{\omega^2 G_i^2 C_1^2}{G_i^2 + \omega^2 C_1^2}}{4 (G_m + G_p)^2}$$

$$P_{act\ell} \overset{(B.12)}{=} \frac{|\underline{V}_0|^2}{8 R_i} \frac{G_m}{G_m + G_p} \overset{(2.22)}{=} P_{actmaxi} \frac{1}{1 + \frac{G_p}{G_m}}. \tag{B.17}$$

For a given G_m, the network elements' values $C_{1,2}$ and L_p differ from those matching the load to the source in Section 3.5.3.1. Since $G_p \neq 0$, thus $R_s \neq 0$, prevents matching of the load to the source if the network is designed for matching the source to the load, the active power $P_{actp} = P_{acts}$ delivered to G_p or R_s is also not equal to that derived in Section 3.5.3.1. However, the same voltage is applied to G_p and $G_{m2} = G_m + G_s$, hence it's given by

$$P_{actp} = P_{act\ell} \frac{G_p}{G_m + G_p} \overset{(B.17)}{=} P_{actmaxi} \frac{\frac{G_m}{G_p}}{\left(1 + \frac{G_m}{G_p}\right)^2}. \tag{B.18}$$

For optimisation, we will need the power gain $g_{t,\,outma}$ of the matched T network. The active power delivered to the network's input is $P_{act1} = P_{actp} + P_{act\ell}$ (refer to Figure A.6). Thus we obtain

$$g_{t,\,outma} = \frac{P_{act\ell}}{P_{act1}} = \frac{P_{act\ell}}{P_{actp} + P_{act\ell}} \overset{(B.17),(B.18)}{=} \frac{G_m + G_p}{G_m + 2G_p} = \frac{1 + \frac{G_p}{G_m}}{1 + 2\frac{G_p}{G_m}}. \tag{B.19}$$

(Alternatively we could derive $g_{t,\,outma}$ from (A.23) if we put $C_{2tot} = C_2$. However, we gain more insight in the circuit's behaviour if it is computed as shown above.)

Comparing the preceding results to those of Section 3.5.3.1 yields that in the formulae of L_p, G_{mlim} and the limits of G_m, G_i, and G_ℓ are exchanged, whereas for $C_{1,2}$ additionally the indices have to be exchanged.

---

already described by (a limit of) G_{mlim}.
Unique to the T network, case (i) b) in (A.18) describes a second point where $\frac{1}{L_p} = 0$ or $L_p \to \infty$, but $L_s = 0$, if $G_\ell \geq \frac{1}{R_{s0}}$ for $R_{s0} > 0$ and $G_m = G_{mlim} = G_\ell - \frac{1}{R_{s0}} = G_i$, hence $G_p = \frac{1}{R_{s0}}$ and $C_{1,2} \to \infty$. Compared to $L_s \to \infty$, which was lossless, $L_s = 0$ involves losses in R_{s0}.

Since

$$\frac{\mathrm{d}g_{\mathrm{t,\,outma}}}{\mathrm{d}G_{\mathrm{m}}} \overset{(B.19)}{=} \frac{G_{\mathrm{m}}}{(G_{\mathrm{m}}+2G_{\mathrm{p}})^2}\left(\frac{G_{\mathrm{p}}}{G_{\mathrm{m}}}-\frac{\mathrm{d}G_{\mathrm{p}}}{\mathrm{d}G_{\mathrm{m}}}\right), \tag{B.20}$$

deriving of the optimum R_{m} requires simply checking of the sign of $\frac{G_{\mathrm{p}}}{G_{\mathrm{m}}}-\frac{\mathrm{d}G_{\mathrm{p}}}{\mathrm{d}G_{\mathrm{m}}}$ similar to Section 3.5.3.2.

Conversely, deriving the optimum source conductance G_{i} if G_{m} is chosen for maximum $g_{\mathrm{t,\,outma}}$ involves

$$g_{\mathrm{t,\,outma}}(G_{\mathrm{m}}=G_{\mathrm{i}}) = \frac{G_{\mathrm{i}}+G_{\mathrm{p}}(G_{\mathrm{m}}=G_{\mathrm{i}})}{G_{\mathrm{i}}+2\,G_{\mathrm{p}}(G_{\mathrm{m}}=G_{\mathrm{i}})}$$

and

$$\frac{\mathrm{d}g_{\mathrm{t,\,outma}}(G_{\mathrm{m}}=G_{\mathrm{i}})}{\mathrm{d}G_{\mathrm{i}}} = \frac{G_{\mathrm{i}}}{(G_{\mathrm{i}}+2\,G_{\mathrm{p}}(G_{\mathrm{m}}=G_{\mathrm{i}}))^2}\left(\frac{G_{\mathrm{p}}(G_{\mathrm{m}}=G_{\mathrm{i}})}{G_{\mathrm{i}}}-\frac{\mathrm{d}\left(G_{\mathrm{p}}(G_{\mathrm{m}}=G_{\mathrm{i}})\right)}{\mathrm{d}G_{\mathrm{i}}}\right)$$

if G_{i} is the upper limit of G_{m} or

$$g_{\mathrm{t,\,outma}}(G_{\mathrm{m}}=G_{\mathrm{mlim}}) = \frac{G_{\ell}}{2\,G_{\ell}-G_{\mathrm{mlim}}}$$

and

$$\frac{\mathrm{d}g_{\mathrm{t,\,outma}}(G_{\mathrm{m}}=G_{\mathrm{mlim}})}{\mathrm{d}G_{\mathrm{i}}} = \frac{G_{\ell}}{(2\,G_{\ell}-G_{\mathrm{mlim}})^2}\frac{\mathrm{d}G_{\mathrm{mlim}}}{\mathrm{d}G_{\mathrm{i}}}$$

if G_{mlim} is the upper limit of G_{m}.

Thus, similar to Section 3.5.3.3 and Appendix B.2.2.2, the optimisation with respect to G_{i} requires simply checking of the sign of $\frac{G_{\mathrm{p}}(G_{\mathrm{m}}=G_{\mathrm{i}})}{G_{\mathrm{i}}}-\frac{\mathrm{d}(G_{\mathrm{p}}(G_{\mathrm{m}}=G_{\mathrm{i}}))}{\mathrm{d}G_{\mathrm{i}}}$ or $\frac{\mathrm{d}G_{\mathrm{mlim}}}{\mathrm{d}G_{\mathrm{i}}}$. Hence the proofs of Sections 3.5.3.2, 3.5.3.3 and Appendices B.2.2.1, B.2.2.2 apply if G_{i} and G_{ℓ} are exchanged.

Furthermore, the extension to complex sources can be performed in a similar manner as the extension to complex loads, in particular because in addition to G_{i}, G_{ℓ}, the indices of $C_{1,2}$ are exchanged compared to the case of matching the load to the source.

B.5 Approximate matching of a resistive load to a resistive source (approximate matching at the network's input), network with losses in all elements designed as if capacitors were lossless

B.5.1 π network

If the π network of Figure B.1 (which takes into account the losses of all network elements) is designed as if the capacitors were lossless (network elements given by

(3.17), (3.18), and (3.19)), its input is not exactly matched, but its power gain $g_{\pi,\,\mathrm{llcapdes}}$ may be calculated exactly by applying the method used in Appendix B.3.2 (and [51b]), yielding

$$\left(1+\frac{\left(R_{\mathrm{s}}+\frac{R_{\mathrm{m}}\left(1+\frac{R_\ell}{R_{\mathrm{p}C_2}}\right)}{1+\left(2+\frac{R_\ell}{R_{\mathrm{p}C_2}}\right)\frac{R_{\mathrm{m}}}{R_{\mathrm{p}C_2}}}\right)^2+\left(\sqrt{(R_{\mathrm{m}}+R_{\mathrm{s}})(R_{\mathrm{i}}-R_{\mathrm{m}}-R_{\mathrm{s}})}\,[-]\,\frac{\left(2+\frac{R_\ell}{R_{\mathrm{p}C_2}}\right)\frac{R_{\mathrm{m}}}{R_{\mathrm{p}C_2}}}{1+\left(2+\frac{R_\ell}{R_{\mathrm{p}C_2}}\right)\frac{R_{\mathrm{m}}}{R_{\mathrm{p}C_2}}}\sqrt{R_{\mathrm{m}}(R_\ell-R_{\mathrm{m}})}\right)^2}{R_{\mathrm{p}C_1}\left(R_{\mathrm{s}}+\frac{R_{\mathrm{m}}\left(1+\frac{R_\ell}{R_{\mathrm{p}C_2}}\right)}{1+\left(2+\frac{R_\ell}{R_{\mathrm{p}C_2}}\right)\frac{R_{\mathrm{m}}}{R_{\mathrm{p}C_2}}}\right)}\right)\cdot\left(1+\frac{R_\ell}{R_{\mathrm{p}C_2}}\right)\cdot\left(1+\frac{\left(1+\left(2+\frac{R_\ell}{R_{\mathrm{p}C_2}}\right)\frac{R_{\mathrm{m}}}{R_{\mathrm{p}C_2}}\right)R_{\mathrm{s}}}{\left(1+\frac{R_\ell}{R_{\mathrm{p}C_2}}\right)R_{\mathrm{m}}}\right)=\frac{1}{g_{\pi,\,\mathrm{llcapdes}}}. \tag{B.21}$$

(The negative sign in square brackets would apply for an extension to inductive loads if the case of undercompensation would be considered.)

Of course it's also possible to derive the π network's nonzero input reflection coefficient exactly. However, the resulting formula is quite lengthy and thus not given herein.

B.5.2 T network

If the T network of Figure B.4 (which takes into account the losses of all network elements) is designed as if the capacitors were lossless (network elements given by (3.30), (3.31), and (3.32)), its input is not exactly matched, but its power gain $g_{\mathrm{t},\,\mathrm{llcapdes}}$ may be calculated exactly by applying the method used in Appendix B.3.3 (and [51b]), yielding

$$\left(1+\frac{\left(G_{\mathrm{p}}+\frac{G_{\mathrm{m}}\left(1+\frac{G_\ell}{G_{\mathrm{s}C_2}}\right)}{1+\left(2+\frac{G_\ell}{G_{\mathrm{s}C_2}}\right)\frac{G_{\mathrm{m}}}{G_{\mathrm{s}C_2}}}\right)^2+\left(\sqrt{(G_{\mathrm{m}}+G_{\mathrm{p}})(G_{\mathrm{i}}-G_{\mathrm{m}}-G_{\mathrm{p}})}\,[-]\,\frac{\left(2+\frac{G_\ell}{G_{\mathrm{s}C_2}}\right)\frac{G_{\mathrm{m}}}{G_{\mathrm{s}C_2}}}{1+\left(2+\frac{G_\ell}{G_{\mathrm{s}C_2}}\right)\frac{G_{\mathrm{m}}}{G_{\mathrm{s}C_2}}}\sqrt{G_{\mathrm{m}}(G_\ell-G_{\mathrm{m}})}\right)^2}{G_{\mathrm{s}C_1}\left(G_{\mathrm{p}}+\frac{G_{\mathrm{m}}\left(1+\frac{G_\ell}{G_{\mathrm{s}C_2}}\right)}{1+\left(2+\frac{G_\ell}{G_{\mathrm{s}C_2}}\right)\frac{G_{\mathrm{m}}}{G_{\mathrm{s}C_2}}}\right)}\right)\cdot\left(1+\frac{G_\ell}{G_{\mathrm{s}C_2}}\right)\cdot\left(1+\frac{\left(1+\left(2+\frac{G_\ell}{G_{\mathrm{s}C_2}}\right)\frac{G_{\mathrm{m}}}{G_{\mathrm{s}C_2}}\right)G_{\mathrm{p}}}{\left(1+\frac{G_\ell}{G_{\mathrm{s}C_2}}\right)G_{\mathrm{m}}}\right)=\frac{1}{g_{\mathrm{t},\,\mathrm{llcapdes}}}. \tag{B.22}$$

(The negative sign in square brackets would apply for an extension to inductive loads if the case of undercompensation would be considered.)

Of course it's also possible to derive the T network's nonzero input reflection coefficient exactly. However, the resulting formula is quite lengthy and thus not given herein.

Appendix C

Extension of the Method to Complex Loads

C.1 Matching of a complex load to a resistive source (matching at the network's input)

C.1.1 Complex load exhibiting an inductive imaginary part

C.1.1.1 π network

For complex loads exhibiting an inductive imaginary part, the formula of the inductance L_s differs from that of complex loads exhibiting a capacitive imaginary part. In particular, the second square root is subtracted instead of added, introducing additional zeros of L_s which will be derived in the following section.

From (3.1), the definition of R_s, we obtain

$$R_\mathrm{s}(L_\mathrm{s} = 0) = R_\mathrm{s0}. \tag{C.1}$$

Putting this result in (4.13) yields

$$0 = \frac{\sqrt{(R_\mathrm{m} + R_\mathrm{s0})\,(R_\mathrm{i} - R_\mathrm{m} - R_\mathrm{s0})} - \sqrt{R_\mathrm{m}\,(R_\ell - R_\mathrm{m})}}{\omega}.$$

In our frequency range of interest, the angular frequency ω stays finite. Thus L_s can only be zero if both square roots are equal. In particular, both square roots may be zero (similar to the capacitive case) or may have the same positive value.

Solving the former for R_m yields R_mlim as defined in (3.21) if $R_\ell = R_\mathrm{i} - R_\mathrm{s0}$. If $R_\ell \neq R_\mathrm{i} - R_\mathrm{s0}$, both square roots cannot be zero simultaneously[1,2].

Solving the latter in case of $R_\mathrm{s0} = 0$ requires $R_\mathrm{i} = R_\ell$ to hold and yields all $0 \leq R_\mathrm{m} \leq R_\mathrm{i} = R_\ell$ (C_1 and L_2tot in parallel resonance), introducing no additional limits compared to (3.20).

Conversely, solving the latter in case of $R_\mathrm{s0} > 0$ requires

$$(R_{\mathrm{m}L_\mathrm{s}0} + R_\mathrm{s0})\,(R_\mathrm{i} - R_{\mathrm{m}L_\mathrm{s}0} - R_\mathrm{s0}) = R_{\mathrm{m}L_\mathrm{s}0}\,(R_\ell - R_{\mathrm{m}L_\mathrm{s}0})$$

to be solved for R_m, yielding

$$R_{\mathrm{m}L_\mathrm{s}0} = R_\mathrm{s0}\,\frac{R_\mathrm{i} - R_\mathrm{s0}}{R_\ell - R_\mathrm{i} + 2R_\mathrm{s0}}. \tag{C.2}$$

If $R_\ell = R_\mathrm{i} - 2R_\mathrm{s0}$, there is no $R_{\mathrm{m}L_\mathrm{s}0}$ which solves the equation unless $R_\mathrm{s0} = R_\mathrm{i}$. But, since then $R_\ell = -R_\mathrm{s0}$, it would have to be ≤ 0 which would be out of the load's valid range.

Additionally, $R_{\mathrm{m}L_\mathrm{s}0}$ has to be > 0 and $< \mathrm{Min}\{R_\ell,\, R_\mathrm{mlim}\}$ to introduce a new limit within the (utmost) valid range of R_m.

The numerator of $R_{\mathrm{m}L_\mathrm{s}0}$ is ≥ 0 because $0 \leq R_\mathrm{s0} \leq R_\mathrm{i}$ as derived in Section 3.5.2.1.

If $R_\ell - R_\mathrm{i} + 2R_\mathrm{s0} < 0$, hence $0 \leq R_\ell < R_\mathrm{i} - 2R_\mathrm{s0}$ if $0 < R_\mathrm{s0} < \frac{R_\mathrm{i}}{2}$, the denominator of $R_{\mathrm{m}L_\mathrm{s}0}$ is < 0 and thus $R_{\mathrm{m}L_\mathrm{s}0} < 0$, introducing no additional limit of R_m.

If $R_\ell - R_\mathrm{i} + 2R_\mathrm{s0} > 0$, hence $R_\ell > R_\mathrm{i} - 2R_\mathrm{s0} \geq 0$ if $0 < R_\mathrm{s0} \leq \frac{R_\mathrm{i}}{2}$ or any $R_\ell \geq 0$ if $\frac{R_\mathrm{i}}{2} \leq R_\mathrm{s0} < R_\mathrm{i}$, the denominator of $R_{\mathrm{m}L_\mathrm{s}0}$ is > 0 and thus $R_{\mathrm{m}L_\mathrm{s}0} > 0$. But we still have to check whether $R_{\mathrm{m}L_\mathrm{s}0}$ stays within the (utmost) limits of R_m given by (3.20). Since $R_\mathrm{s}(R_{\mathrm{m}L_\mathrm{s}0}) = R_\mathrm{s0}$, (3.20) holds only if the following inequalities hold[3]

$$\begin{aligned} R_\ell - R_{\mathrm{m}L_\mathrm{s}0} &= (R_\ell + R_\mathrm{s0})\,\tfrac{R_\ell - R_\mathrm{i} + R_\mathrm{s0}}{R_\ell - R_\mathrm{i} + 2R_\mathrm{s0}} &> 0, \\ R_\mathrm{i} - R_{\mathrm{m}L_\mathrm{s}0} - R_\mathrm{s0} &= (R_\mathrm{i} - R_\mathrm{s0})\,\tfrac{R_\ell - R_\mathrm{i} + R_\mathrm{s0}}{R_\ell - R_\mathrm{i} + 2R_\mathrm{s0}} &> 0. \end{aligned}$$

Obviously both inequalities hold (under the preceding assumptions) only if $R_\ell > R_\mathrm{i} - R_\mathrm{s0}$. Since $0 \leq R_\mathrm{s0} \leq R_\mathrm{i}$ implies that $R_\mathrm{i} - R_\mathrm{s0} \geq R_\mathrm{i} - 2R_\mathrm{s0}$ and $R_\mathrm{i} - R_\mathrm{s0} \geq 0$, a valid $R_{\mathrm{m}L_\mathrm{s}0}$ is introduced for all $0 < R_\mathrm{s0} < R_\mathrm{i}$ and real (purely resistive) loads, thus $0 < R_{\mathrm{m}L_\mathrm{s}0} < R_\mathrm{mlim}$ (refer to Section 3.5.2.1). In case of a complex load exhibiting an inductive imaginary part a valid $R_{\mathrm{m}L_\mathrm{s}0}$ would additionally require $R_{\mathrm{m}L_\mathrm{s}0} > R_{\mathrm{m}L_{\ell\mathrm{p}}}$ to hold, which has to be checked separately for the given value of $L_{\ell\mathrm{p}}$.

Finally it should be noted that $R_{\mathrm{m}L_\mathrm{s}0} = R_\mathrm{mlim} = R_\mathrm{i} - R_\mathrm{s0}$ if $R_\ell = R_\mathrm{i} - R_\mathrm{s0}$.

---

[1] At a first glance, there seems to be another solution of $L_\mathrm{s} = 0$ at $R_\mathrm{m} = 0$ if $R_\mathrm{s0} = 0$. However, it's usually no valid solution because then $L_\mathrm{s} = 0$ and $R_\mathrm{s} = 0$, hence the matching network would just consist of $C_1 \to \infty$ in parallel to $L_\mathrm{2tot} = 0$. Each of those elements would act as a short, but they may compensate each other (in a parallel resonance) if the limit of $R_\mathrm{m} \to 0$ is considered and $R_\mathrm{i} = R_\ell$. But, as $R_\mathrm{i} = R_\ell$ would require no matching network at all and the indicated elements' values cannot be realised, the possible solution at $R_\mathrm{m} = 0$ is not considered further.

[2] For real loads or complex loads exhibiting a capacitive imaginary part, $R_\mathrm{m} = 0$ is no valid solution for $L_\mathrm{s} = 0$ if $R_\mathrm{s0} = 0$ because the matching network would then consist of a $C_1 \to \infty$ in parallel to a $C_2 \to \infty$ or $C_\mathrm{2tot} \to \infty$ (instead of $L_\mathrm{2tot} = 0$). Such a matching network would be an infinite capacitance in parallel to the load resistance R_ℓ, which would not match R_ℓ to R_i.

[3] Since a new limit is checked for, there are ">" in the inequalities instead of the "≥" in (3.20).

C.1.1.2 T network

For complex loads exhibiting an inductive imaginary part, the formula of the inductance L_p differs from that of complex loads exhibiting a capacitive imaginary part. In particular, the second square root is subtracted instead of added, introducing additional zeros of $\frac{1}{L_\mathrm{p}}$ which will be derived in the following section.

From (3.1), the definition of R_s, and the considerations regarding certain series-to-parallel transformed network elements' values in (A.18) we obtain

$$G_\mathrm{p}\left(\frac{1}{L_\mathrm{p}}=0\right)=\begin{cases}0 \text{ if } L_\mathrm{s}\to\infty\\ \frac{1}{R_\mathrm{s0}} \text{ if } L_\mathrm{s}=0 \text{ and } R_\mathrm{s0}>0\end{cases} \tag{C.3}$$

Putting this result in the reciprocal of (4.19) yields

$$0=\begin{cases}\omega\left(\sqrt{G_\mathrm{m}\left(G_\mathrm{i}-G_\mathrm{m}\right)}-\sqrt{G_\mathrm{m}\left(G_\ell-G_\mathrm{m}\right)}\right) & \text{if } L_\mathrm{s}\to\infty\\ \omega\left(\sqrt{\left(G_\mathrm{m}+\frac{1}{R_\mathrm{s0}}\right)\left(G_\mathrm{i}-G_\mathrm{m}-\frac{1}{R_\mathrm{s0}}\right)}-\sqrt{G_\mathrm{m}\left(G_\ell-G_\mathrm{m}\right)}\right) & \text{if } L_\mathrm{s}=0 \text{ and } R_\mathrm{s0}>0\end{cases}$$

In our frequency range of interest, the angular frequency ω stays finite. Thus $\frac{1}{L_\mathrm{p}}$ can only be zero if both square roots are equal. In particular, both square roots may be zero (similar to the capacitive case) or may have the same positive value.

Solving the former for G_m yields G_mlim as defined in (3.34) if $G_\ell = G_\mathrm{i}$. If $G_\ell \neq G_\mathrm{i}$, both square roots cannot be zero simultaneously[4,5]. However, if $L_\mathrm{s}=0$ there exists an additional solution as indicated in Section 3.5.3.1, Footnote ††.

---

[4]At a first glance, there seems to be another solution of $\frac{1}{L_\mathrm{p}}=0$ at $G_\mathrm{m}=0$. However, it's usually no valid solution because then $\frac{1}{L_\mathrm{p}}=0$ and:

- Either $L_\mathrm{s}\to\infty$ and thus $G_\mathrm{p}=0$, hence the matching network would just consist of $C_1=0$ in series to $L_\mathrm{2tot}\to\infty$. Each of those elements would act as an open circuit, but they may compensate each other (in a series resonance) if the limit of $G_\mathrm{m}\to 0$ is considered and $G_\mathrm{i}=G_\ell$. But $G_\mathrm{i}=G_\ell$ would require no matching network at all and the indicated elements' values cannot be realised.
- Or $L_\mathrm{s}=0$, $R_\mathrm{s0}>0$, and thus $G_\mathrm{p}=\frac{1}{R_\mathrm{s0}}$, hence the matching network would consist of finite and nonzero C_1 and G_p, but $L_\mathrm{2tot}\to\infty$, which would not match G_ℓ to G_i.

Thus the possible solution at $G_\mathrm{m}=0$ is not considered further.

[5]For real loads or complex loads exhibiting a capacitive imaginary part, $G_\mathrm{m}=0$ is no valid solution for $\frac{1}{L_\mathrm{p}}=0$ because then:

- Either $L_\mathrm{s}\to\infty$ and thus $G_\mathrm{p}=0$, hence the matching network would consist of a $C_1=0$ in series to a $C_2=0$ or $C_\mathrm{2tot}=0$ (instead of $L_\mathrm{2tot}\to\infty$). Such a matching network would be a zero capacitance in series to the load admittance G_ℓ, which would not match G_ℓ to G_i.
- Or $L_\mathrm{s}=0$, $R_\mathrm{s0}>0$, and thus $G_\mathrm{p}=\frac{1}{R_\mathrm{s0}}$, hence the matching network would consist of finite and nonzero C_1 and G_p, but $C_2=0$ or $C_\mathrm{2tot}=0$ (instead of $L_\mathrm{2tot}\to\infty$), which would not match G_ℓ to G_i.

Solving the latter in case of $L_s \to \infty$ requires $G_i = G_\ell$ to hold and yields all $0 \leq G_m \leq G_i = G_\ell$ (C_1 and L_{2tot} in series resonance), introducing no additional limits compared to (3.33).

Conversely, solving the latter in case of $L_s = 0$ requires

$$\sqrt{\left(G_m + \frac{1}{R_{s0}}\right)\left(G_i - G_m - \frac{1}{R_{s0}}\right)} = \sqrt{G_m\,(G_\ell - G_m)}$$

to be solved for G_m where $R_{s0} > 0$, yielding

$$G_{m1/L_{p0}} = \frac{1}{R_{s0}} \frac{G_i - \frac{1}{R_{s0}}}{G_\ell - G_i + 2\frac{1}{R_{s0}}}. \tag{C.4}$$

If $G_\ell = G_i - 2\frac{1}{R_{s0}}$, there is no $G_{m1/L_{p0}}$ which solves the equation unless $\frac{1}{R_{s0}} = G_i$ or $R_{s0} = R_i$. But, since then $G_\ell = -\frac{1}{R_{s0}}$, it would have to be ≤ 0 which would be out of the load's valid range.

Additionally, $G_{m1/L_{p0}}$ has to be > 0 and $< \mathrm{Min}\{G_\ell, G_{mlim}\}$ to introduce a new limit within the (utmost) valid range of G_m.

Compared to the π network, the T network introduces no limit for R_{s0} (refer to Section 3.5.3.1). Thus $0 < \frac{1}{R_{s0}} < G_i$ and $G_i \geq \frac{1}{R_{s0}}$ have to be considered — then the numerator of $G_{m1/L_{p0}}$ is positive or negative, respectively.

1. $0 < \frac{1}{R_{s0}} < G_i$ or $R_{s0} > R_i$, thus the numerator of $G_{m1/L_{p0}}$ is > 0

   If $G_\ell - G_i + 2\frac{1}{R_{s0}} < 0$, hence $0 \leq G_\ell < G_i - 2\frac{1}{R_{s0}}$ if $0 < \frac{1}{R_{s0}} < \frac{G_i}{2}$, the denominator of $G_{m1/L_{p0}}$ is < 0 and thus $G_{m1/L_{p0}} < 0$, introducing no additional limit of G_m.

   If $G_\ell - G_i + 2\frac{1}{R_{s0}} > 0$, hence $G_\ell > G_i - 2\frac{1}{R_{s0}} \geq 0$ if $0 < \frac{1}{R_{s0}} \leq \frac{G_i}{2}$ or any $G_\ell \geq 0$ if $\frac{G_i}{2} \leq \frac{1}{R_{s0}} < G_i$, the denominator of $G_{m1/L_{p0}}$ is > 0 and thus $G_{m1/L_{p0}} > 0$. But we still have to check whether $G_{m1/L_{p0}}$ stays within the (utmost) limits of G_m given by (3.33). Since $G_p(G_{m1/L_{p0}}) = \frac{1}{R_{s0}}$, (3.33) holds only if the following inequalities hold[6]

$$\begin{aligned} G_\ell - G_{m1/L_{p0}} &= (G_\ell + \tfrac{1}{R_{s0}})\,\frac{G_\ell - G_i + \frac{1}{R_{s0}}}{G_\ell - G_i + 2\frac{1}{R_{s0}}} > 0, \\ G_i - G_{m1/L_{p0}} - \frac{1}{R_{s0}} &= (G_i - \tfrac{1}{R_{s0}})\,\frac{G_\ell - G_i + \frac{1}{R_{s0}}}{G_\ell - G_i + 2\frac{1}{R_{s0}}} > 0. \end{aligned}$$

   Obviously both inequalities hold (under the preceding assumptions) only if $G_\ell > G_i - \frac{1}{R_{s0}}$. Since $0 < \frac{1}{R_{s0}} < G_i$ implies that $G_i - \frac{1}{R_{s0}} > G_i - 2\frac{1}{R_{s0}}$ and $G_i - \frac{1}{R_{s0}} > 0$, a valid $G_{m1/L_{p0}}$ is introduced for all $0 < \frac{1}{R_{s0}} < G_i$ or $R_{s0} > R_i$ and purely resistive loads, thus $0 < G_{m1/L_{p0}} < G_{mlim}$ (refer to Section 3.5.3.1). In case of a complex load exhibiting an inductive imaginary part $G_{m1/L_{p0}}$ would additionally require $G_{m1/L_{p0}} > G_{mL_{\ell s}}$ to hold, which has to be checked separately for the given value of $L_{\ell s}$.

[6] Since a new limit is checked for, there are ">" in the inequalities instead of the "≥" in (3.33).

2. $\frac{1}{R_{s0}} \geq G_i$ or $0 \leq R_{s0} \leq R_i$, thus the numerator of $G_{m1/L_{p0}}$ is ≤ 0

   In this case there exists no valid $G_{m1/L_{p0}}$ fulfilling (3.33), because the same differences as in case 1. occur, where both fractions are similar, but under the assumptions of case 2. the factor $G_\ell + \frac{1}{R_{s0}}$ is always > 0, whereas $G_i - \frac{1}{R_{s0}}$ is always ≤ 0. Hence, independently of the fraction's sign, one of both inequalities in (3.33) cannot apply. Therefore no new limit of G_m is introduced.

   Since variable air-core inductors consist of a low number of windings and the ferrite or iron powder cores of switchable inductors are designed for low losses, the assumption $R_{s0} \leq R_i$ usually applies if $R_i = 50\,\Omega$.

Finally it should be noted that besides the case of $L_s \to \infty$ and $G_\ell = G_i$ there may be another solution yielding $G_{m1/L_{p0}} = G_{mlim} = G_i - \frac{1}{R_{s0}}$ if $G_i \geq \frac{1}{R_{s0}}$, $G_\ell = G_i - \frac{1}{R_{s0}}$ and $L_s = 0$.

C.2 Exact analytical solutions for a constant Q central inductor

C.2.1 Example diagrams

C.2.1.1 Power gain's contour line Smith charts for L, π, and T networks

In the following diagrams, power gain's contour line Smith charts for different L, π, and T networks are shown. Their central inductor has a range of $0.1\,\mu H - 40\,\mu H$, a constant Q factor of 100, and the matching frequency is either 1.8 MHz, 7.35 MHz, or 30 MHz. The variable capacitances' ranges resemble different "typical" variable capacitors (a cheap 5 pF – 250 pF, a better 5 pF – 500 pF, and an expensive 25 pF – 4000 pF vacuum variable). The contour lines were calculated from the resulting matching networks of 100 x 100 equally spaced load reflection coefficients whose $\mathrm{Re}\{\underline{r}_\ell\}$, $\mathrm{Im}\{\underline{r}_\ell\} \in [-1, 1]$, where only those with $|\underline{r}_\ell| < 1$ were used.

In case of π and T networks, best and worst networks' power gain is shown.

In case of L networks, it is assumed that the network topology enables implementation of both "complementary" L networks (C_1 only or C_2 only), e. g. by using appropriate switches.

Additionally, the impact of a parasitic capacitance replacing one variable capacitance of a π or T network is considered (refer to Figure 4.21) — the resulting networks yield a more realistic description of "real world" L networks. Based on [3], the value of that parasitic capacitance was chosen to be equal to the minimum/maximum value of the remaining variable capacitance for L networks derived from π networks/T networks.

Since lossy L networks may theoretically exhibit more than one distinct solutions for a given load, it has to be noted that

- the pure L networks (without parasitic capacitances) and the L networks with a parasitic parallel capacitance derived from π networks yielded only a single valid solution throughout all complete Smith charts for the given network element ranges

- the L networks with a parasitic series capacitance derived from T networks yielded more than one solution within some region of the Smith charts for the given network element ranges, but the differences in power gain of best and worst solutions were low — for the chosen contour line values both diagrams were merely similar — thus only the best diagrams are shown.

To illustrate the latter — best and worst L networks' power gain differs by < 0.026 at 1.8 MHz, by < 0.054 at 7.35 MHz, and by < 0.0084 at 30 MHz for $5\,\text{pF} \leq C_{1,2} \leq 250\,\text{pF}$ with 250 pF parasitic series capacitance, by < 0.04 at 1.8 MHz, by < 0.017 at 7.35 MHz, and by < 0.0042 at 30 MHz for $5\,\text{pF} \leq C_{1,2} \leq 500\,\text{pF}$ with 500 pF parasitic series capacitance, or by < 0.0063 at 1.8 MHz, by < 0.0017 at 7.35 MHz, and by < 0.0005 at 30 MHz for $25\,\text{pF} \leq C_{1,2} \leq 4000\,\text{pF}$ with 4000 pF parasitic series capacitance.

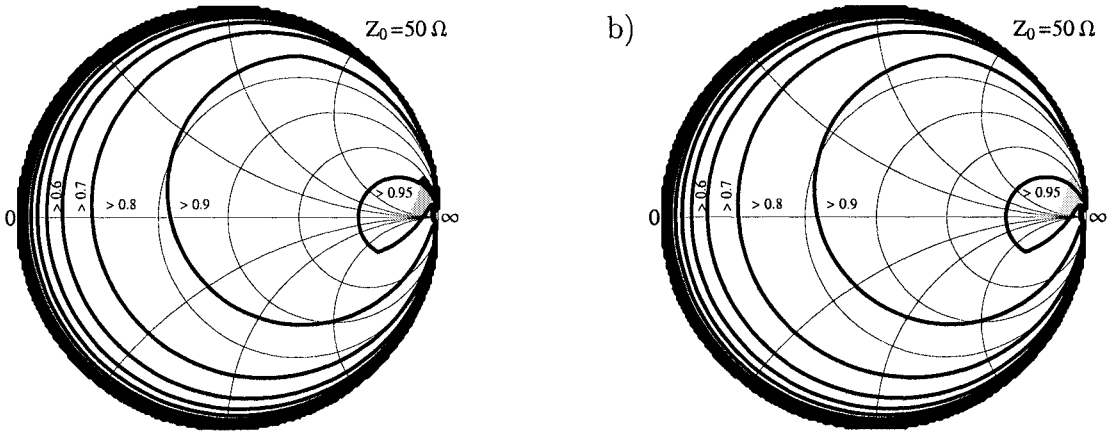

Figure C.1: a) Best and b) worst $g_{\text{loft,inma}}$ at 1.8 MHz, $R_\text{i} = 50\,\Omega$, $Q = 100$, $5\,\text{pF} \leq C_{1,2} \leq 500\,\text{pF}$, and $0.1\,\mu\text{H} \leq L_\text{s} \leq 40\,\mu\text{H}$, with 500 pF parasitics, undercompensation shaded in gray

Anyhow, a small difference can be seen in one of the examples given above. As depicted in Figure C.1, the > 0.98 contour line is visible for the best networks in Figure C.1 a) (above the right edge of the > 0.95 contour line), whereas there is no > 0.98 contour line at all for the worst networks in Figure C.1 b).

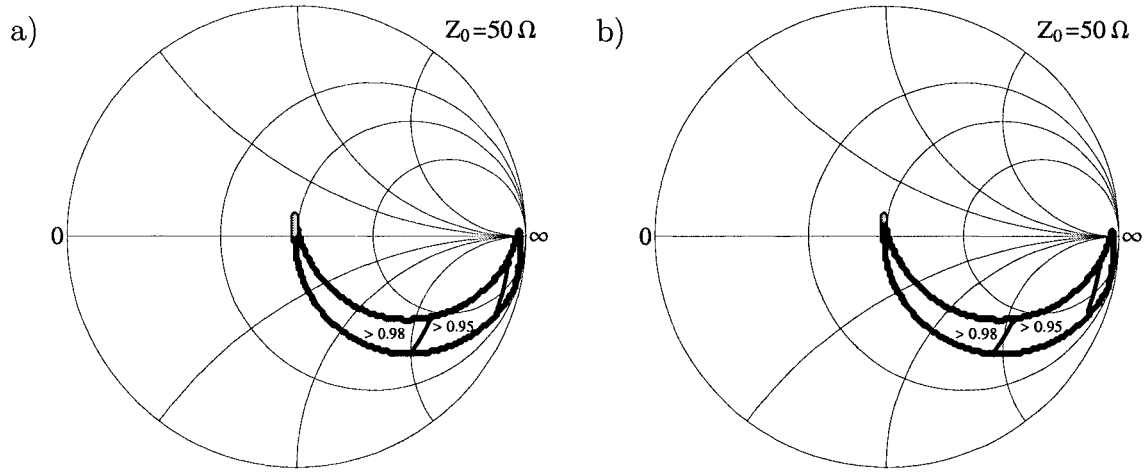

Figure C.2: a) Best and b) worst $g_{\pi,\mathrm{inma}}$ at 1.8 MHz, $R_\mathrm{i} = 50\,\Omega$, $Q = 100$, $5\,\mathrm{pF} \leq C_{1,2} \leq 250\,\mathrm{pF}$, and $0.1\,\mu\mathrm{H} \leq L_\mathrm{s} \leq 40\,\mu\mathrm{H}$, undercompensation shaded

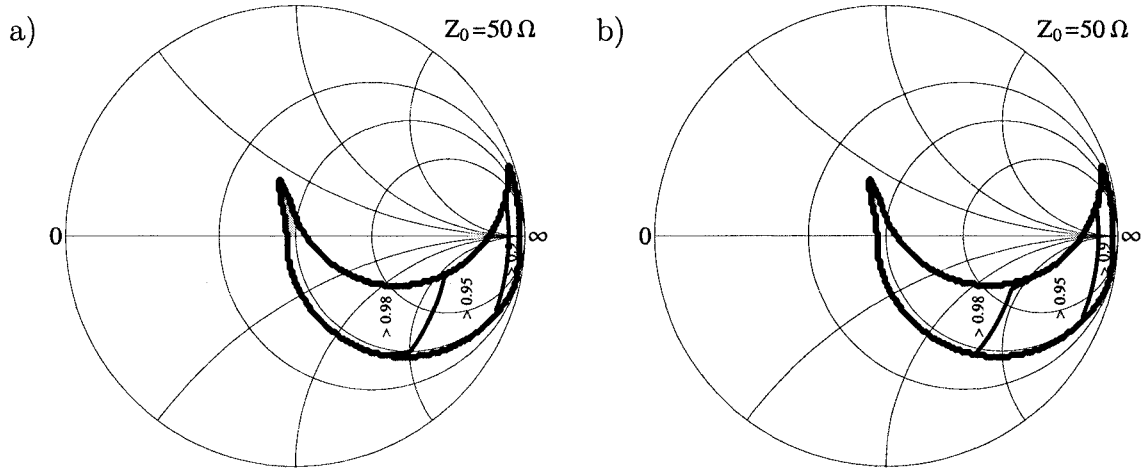

Figure C.3: a) Best and b) worst $g_{\pi,\mathrm{inma}}$ at 1.8 MHz, $R_\mathrm{i} = 50\,\Omega$, $Q = 100$, $5\,\mathrm{pF} \leq C_{1,2} \leq 500\,\mathrm{pF}$, and $0.1\,\mu\mathrm{H} \leq L_\mathrm{s} \leq 40\,\mu\mathrm{H}$, undercompensation shaded

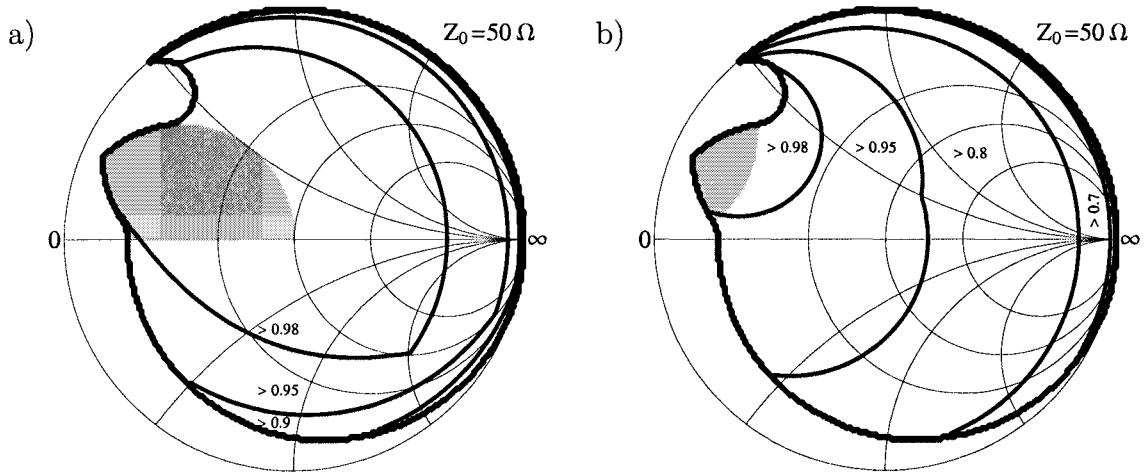

Figure C.4: a) Best and b) worst $g_{\pi,\mathrm{inma}}$ at 1.8 MHz, $R_\mathrm{i} = 50\,\Omega$, $Q = 100$, $25\,\mathrm{pF} \leq C_{1,2} \leq 4000\,\mathrm{pF}$, and $0.1\,\mu\mathrm{H} \leq L_\mathrm{s} \leq 40\,\mu\mathrm{H}$, undercomp. shaded

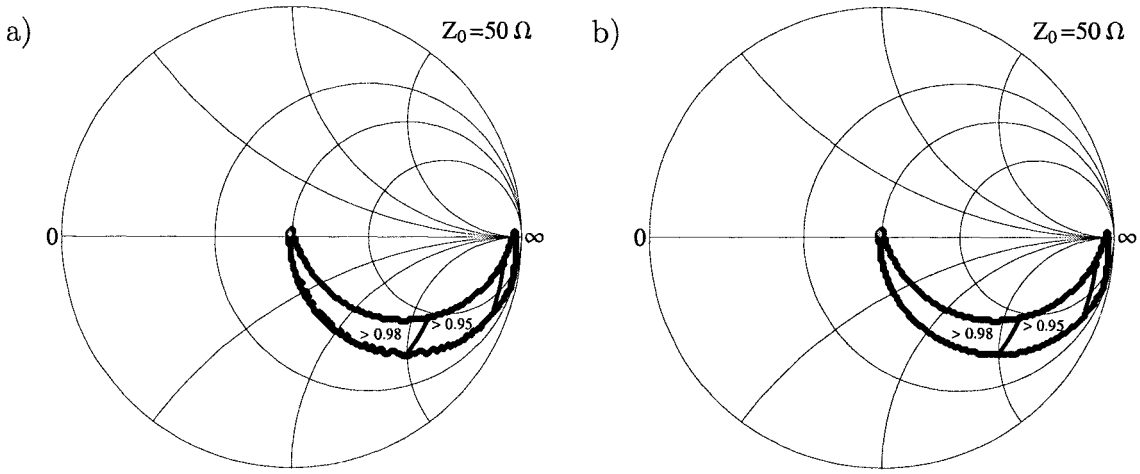

Figure C.5: $g_{\mathrm{lof}\pi,\mathrm{inma}}$ at 1.8 MHz, $R_\mathrm{i} = 50\,\Omega$, $Q = 100$, $5\,\mathrm{pF} \leq C_{1,2} \leq 250\,\mathrm{pF}$, and $0.1\,\mu\mathrm{H} \leq L_\mathrm{s} \leq 40\,\mu\mathrm{H}$, a) without, b) with 5 pF parasitics, uc. shaded

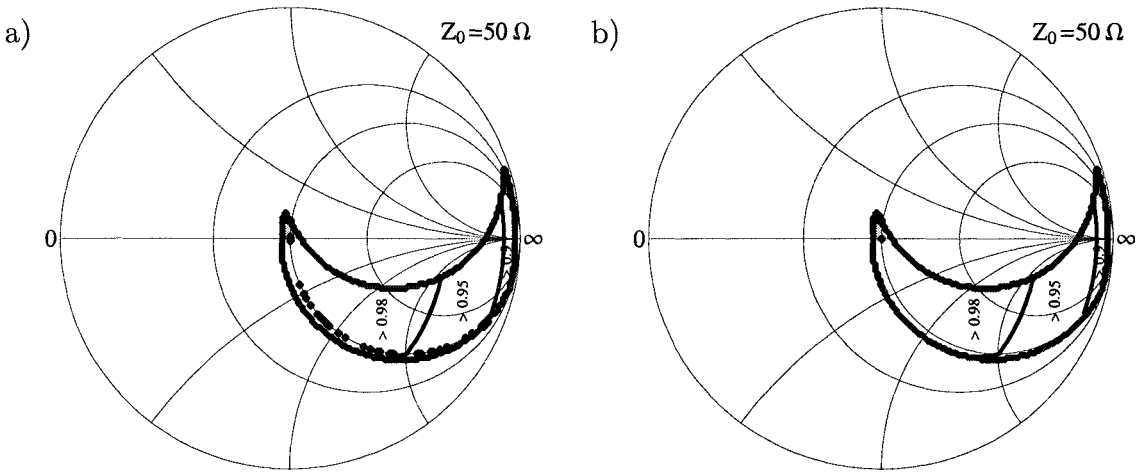

Figure C.6: $g_{\mathrm{lof}\pi,\mathrm{inma}}$ at 1.8 MHz, $R_\mathrm{i} = 50\,\Omega$, $Q = 100$, $5\,\mathrm{pF} \leq C_{1,2} \leq 500\,\mathrm{pF}$, and $0.1\,\mu\mathrm{H} \leq L_\mathrm{s} \leq 40\,\mu\mathrm{H}$, a) without, b) with 5 pF parasitics, uc. shaded

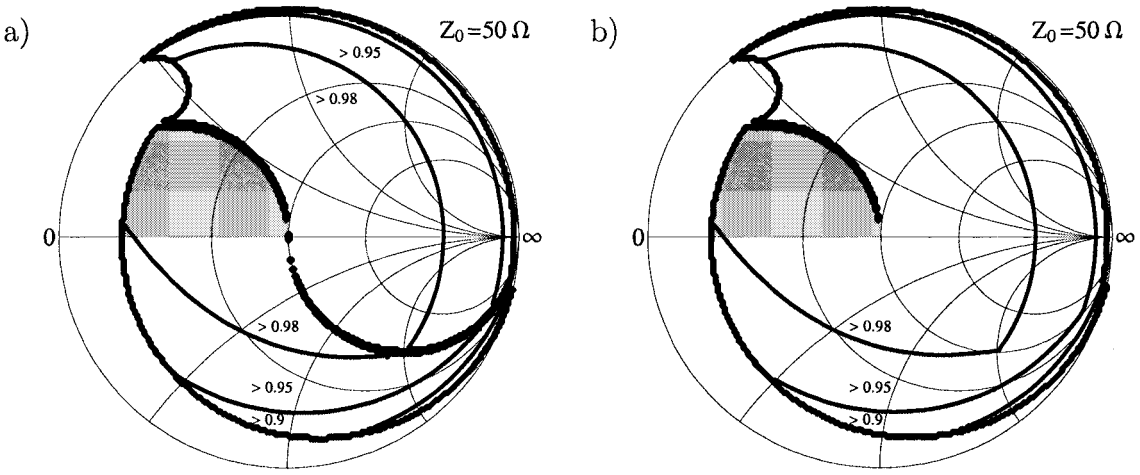

Figure C.7: $g_{\mathrm{lof}\pi,\mathrm{inma}}$ at 1.8 MHz, $R_\mathrm{i} = 50\,\Omega$, $Q = 100$, $25\,\mathrm{pF} \leq C_{1,2} \leq 4000\,\mathrm{pF}$, $0.1\,\mu\mathrm{H} \leq L_\mathrm{s} \leq 40\,\mu\mathrm{H}$, a) without, b) with 25 pF parasitics, uc. shaded

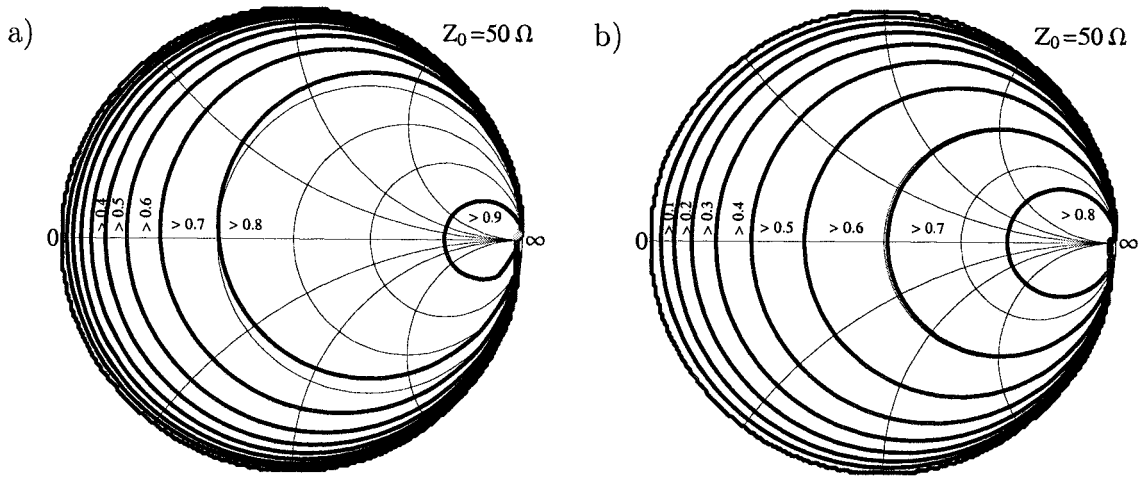

Figure C.8: a) Best and b) worst $g_{\mathrm{t,inma}}$ at 1.8 MHz, $R_{\mathrm{i}} = 50\,\Omega$, $Q = 100$, $5\,\mathrm{pF} \leq C_{1,2} \leq 250\,\mathrm{pF}$, and $0.1\,\mu\mathrm{H} \leq L_{\mathrm{s}} \leq 40\,\mu\mathrm{H}$, undercompensation shaded

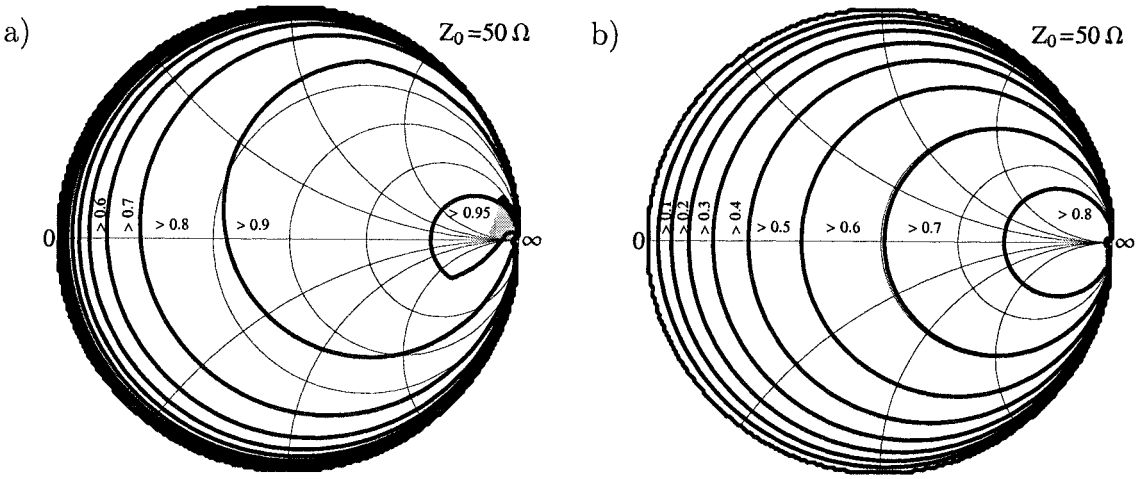

Figure C.9: a) Best and b) worst $g_{\mathrm{t,inma}}$ at 1.8 MHz, $R_{\mathrm{i}} = 50\,\Omega$, $Q = 100$, $5\,\mathrm{pF} \leq C_{1,2} \leq 500\,\mathrm{pF}$, and $0.1\,\mu\mathrm{H} \leq L_{\mathrm{s}} \leq 40\,\mu\mathrm{H}$, undercompensation shaded

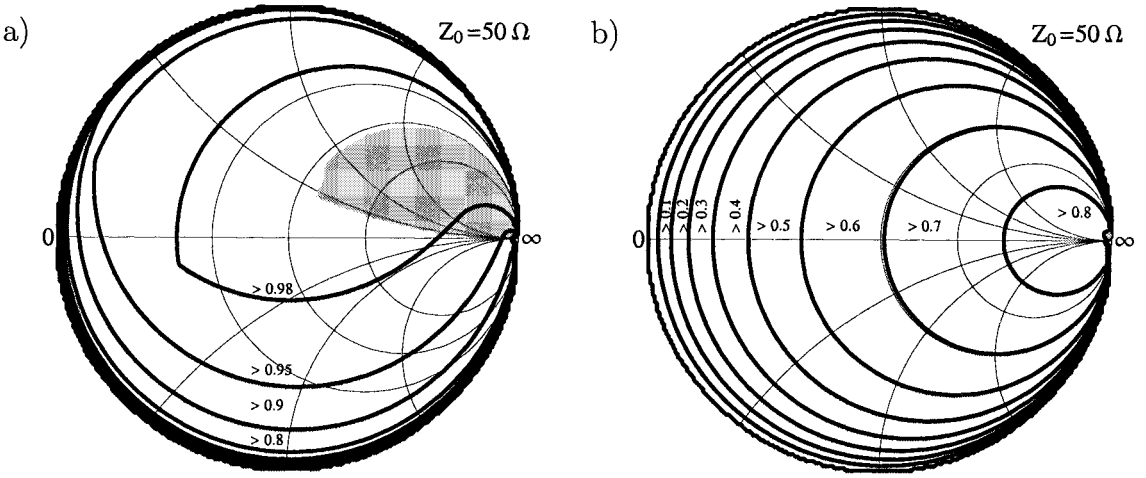

Figure C.10: a) Best and b) worst $g_{\mathrm{t,inma}}$ at 1.8 MHz, $R_{\mathrm{i}} = 50\,\Omega$, $Q = 100$, $25\,\mathrm{pF} \leq C_{1,2} \leq 4000\,\mathrm{pF}$, and $0.1\,\mu\mathrm{H} \leq L_{\mathrm{s}} \leq 40\,\mu\mathrm{H}$, undercomp. shaded

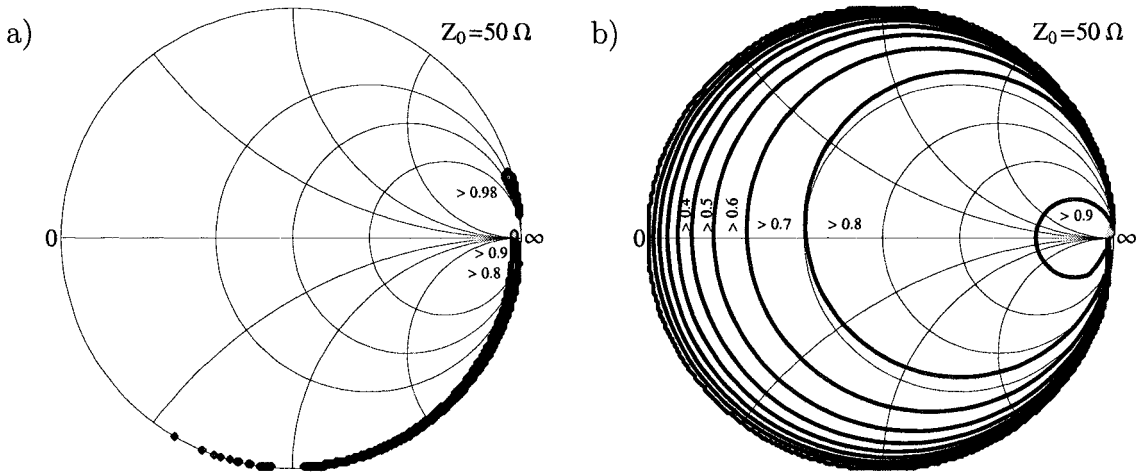

Figure C.11: $g_{\mathrm{loft,inma}}$ at 1.8 MHz, $R_\mathrm{i} = 50\,\Omega$, $Q = 100$, $5\,\mathrm{pF} \leq C_{1,2} \leq 250\,\mathrm{pF}$, and $0.1\,\mu\mathrm{H} \leq L_\mathrm{s} \leq 40\,\mu\mathrm{H}$, a) without, b) with 5 pF parasitics, uc. shaded

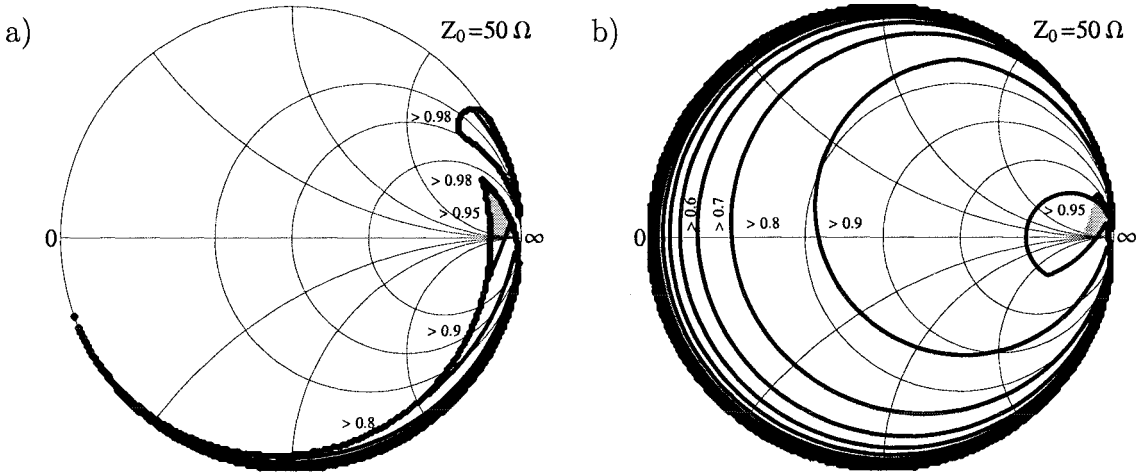

Figure C.12: $g_{\mathrm{loft,inma}}$ at 1.8 MHz, $R_\mathrm{i} = 50\,\Omega$, $Q = 100$, $5\,\mathrm{pF} \leq C_{1,2} \leq 500\,\mathrm{pF}$, and $0.1\,\mu\mathrm{H} \leq L_\mathrm{s} \leq 40\,\mu\mathrm{H}$, a) without, b) with 5 pF parasitics, uc. shaded

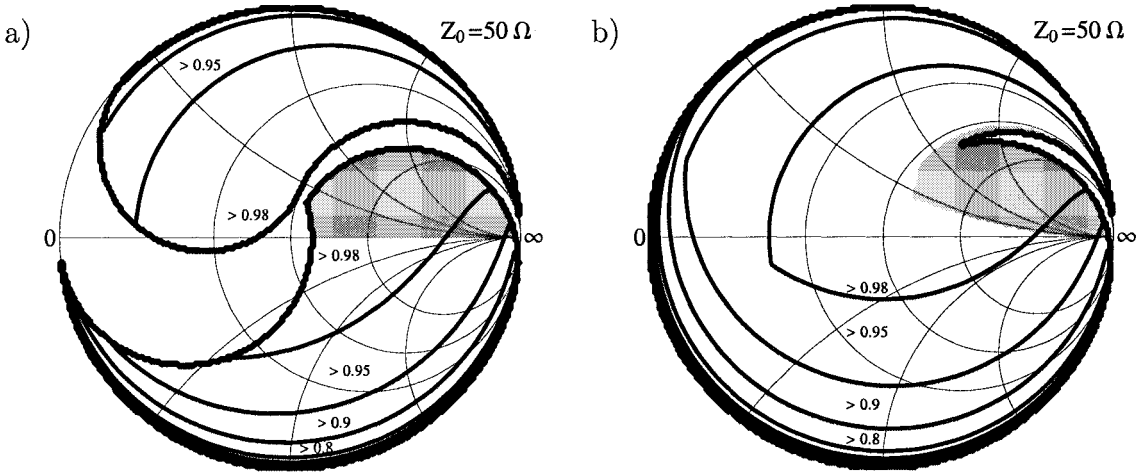

Figure C.13: $g_{\mathrm{loft,inma}}$ at 1.8 MHz, $R_\mathrm{i} = 50\,\Omega$, $Q = 100$, $25\,\mathrm{pF} \leq C_{1,2} \leq 4000\,\mathrm{pF}$, $0.1\,\mu\mathrm{H} \leq L_\mathrm{s} \leq 40\,\mu\mathrm{H}$, a) without, b) with 25 pF parasitics, uc. shaded

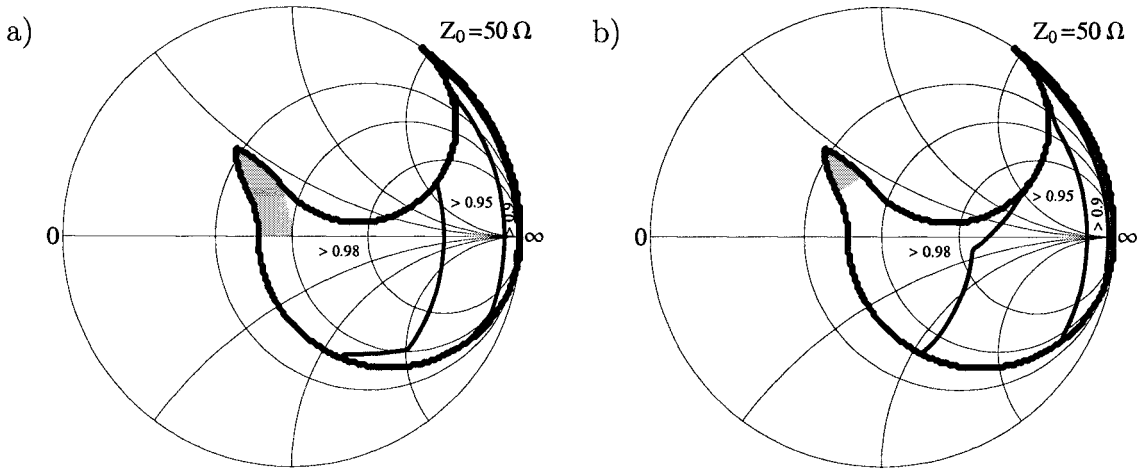

Figure C.14: a) Best and b) worst $g_{\pi,\mathrm{inma}}$ at 7.35 MHz, $R_\mathrm{i} = 50\,\Omega$, $Q = 100$, $5\,\mathrm{pF} \leq C_{1,2} \leq 250\,\mathrm{pF}$, and $0.1\,\mu\mathrm{H} \leq L_\mathrm{s} \leq 40\,\mu\mathrm{H}$, undercompensation shaded

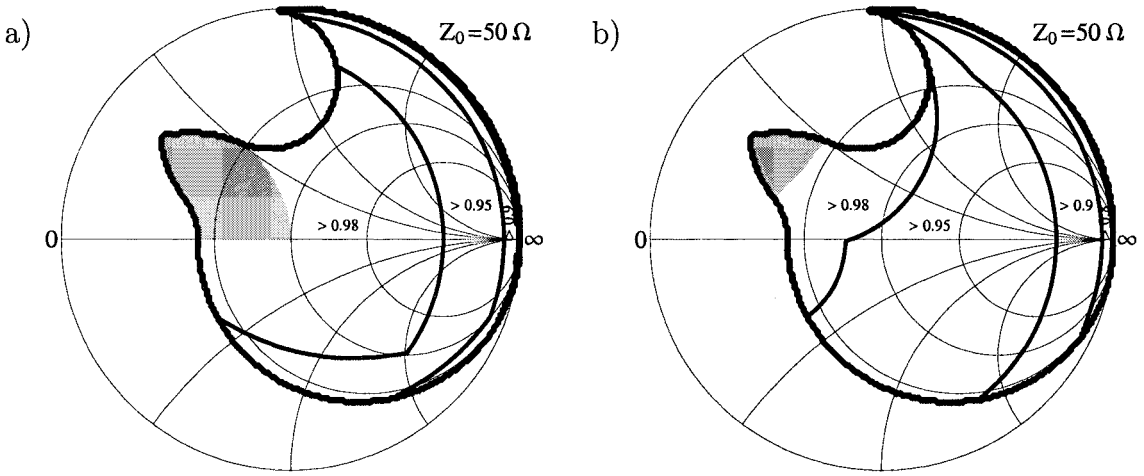

Figure C.15: a) Best and b) worst $g_{\pi,\mathrm{inma}}$ at 7.35 MHz, $R_\mathrm{i} = 50\,\Omega$, $Q = 100$, $5\,\mathrm{pF} \leq C_{1,2} \leq 500\,\mathrm{pF}$, and $0.1\,\mu\mathrm{H} \leq L_\mathrm{s} \leq 40\,\mu\mathrm{H}$, undercompensation shaded

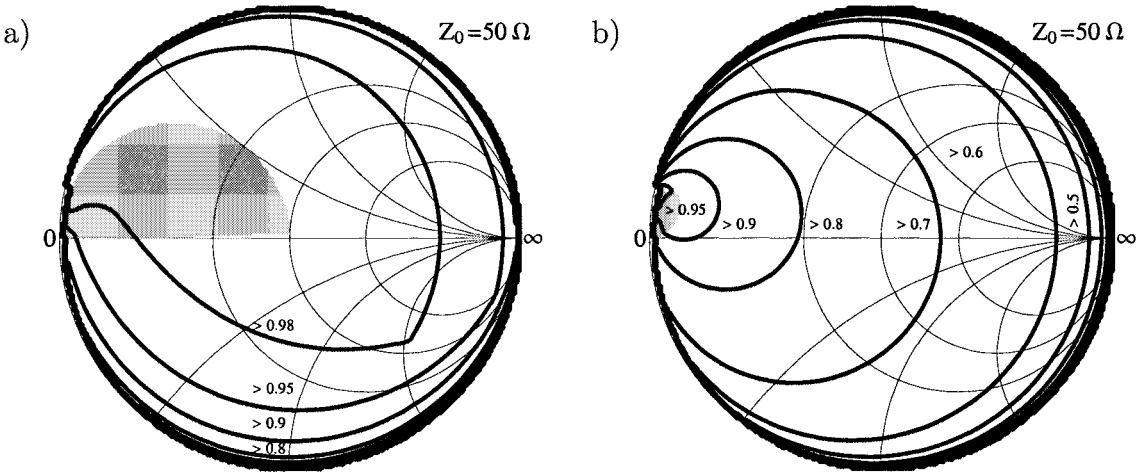

Figure C.16: a) Best and b) worst $g_{\pi,\mathrm{inma}}$ at 7.35 MHz, $R_\mathrm{i} = 50\,\Omega$, $Q = 100$, $25\,\mathrm{pF} \leq C_{1,2} \leq 4000\,\mathrm{pF}$, and $0.1\,\mu\mathrm{H} \leq L_\mathrm{s} \leq 40\,\mu\mathrm{H}$, undercomp. shaded

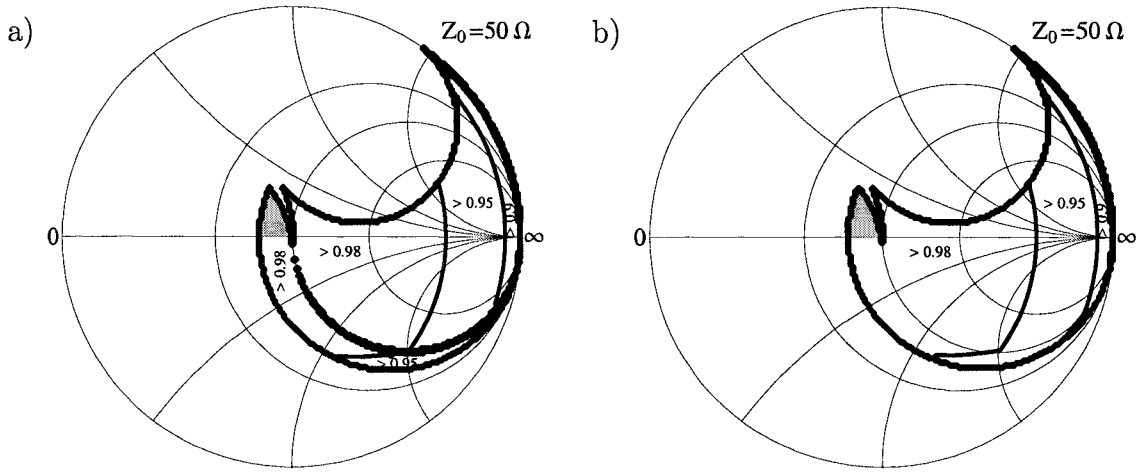

Figure C.17: $g_{\mathrm{lof}\pi,\mathrm{inma}}$ at 7.35 MHz, $R_\mathrm{i} = 50\,\Omega$, $Q = 100$, $5\,\mathrm{pF} \leq C_{1,2} \leq 250\,\mathrm{pF}$, and $0.1\,\mu\mathrm{H} \leq L_\mathrm{s} \leq 40\,\mu\mathrm{H}$, a) without, b) with 5 pF parasitics, uc. shaded

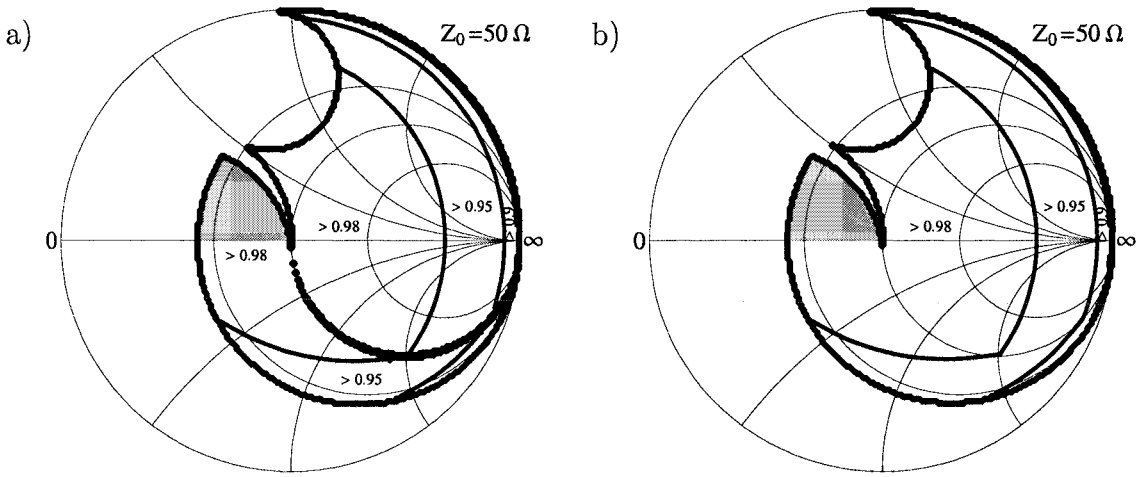

Figure C.18: $g_{\mathrm{lof}\pi,\mathrm{inma}}$ at 7.35 MHz, $R_\mathrm{i} = 50\,\Omega$, $Q = 100$, $5\,\mathrm{pF} \leq C_{1,2} \leq 500\,\mathrm{pF}$, and $0.1\,\mu\mathrm{H} \leq L_\mathrm{s} \leq 40\,\mu\mathrm{H}$, a) without, b) with 5 pF parasitics, uc. shaded

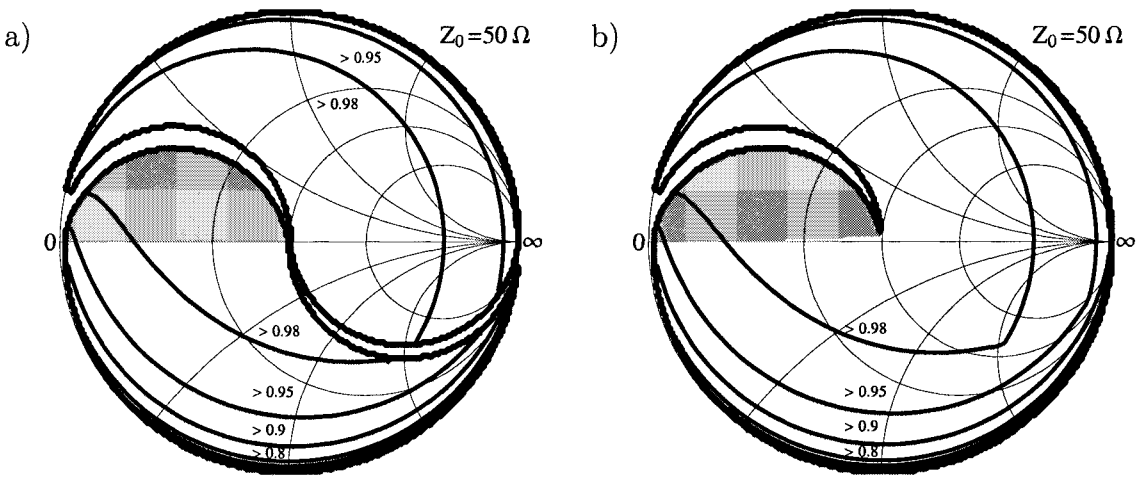

Figure C.19: $g_{\mathrm{lof}\pi,\mathrm{inma}}$ at 7.35 MHz, $R_\mathrm{i} = 50\,\Omega$, $Q = 100$, $25\,\mathrm{pF} \leq C_{1,2} \leq 4000\,\mathrm{pF}$, $0.1\,\mu\mathrm{H} \leq L_\mathrm{s} \leq 40\,\mu\mathrm{H}$, a) without, b) with 25 pF parasitics, uc. shaded

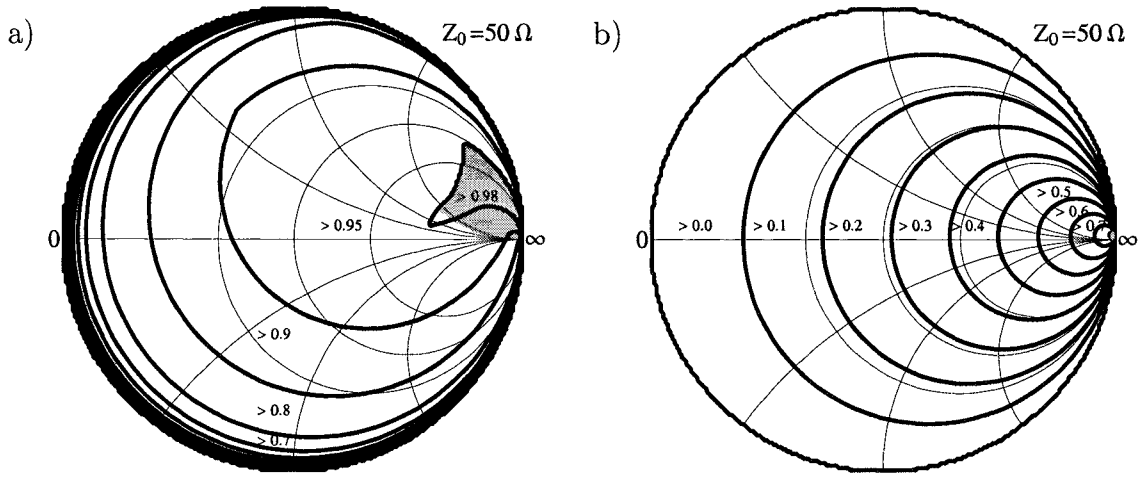

Figure C.20: a) Best and b) worst $g_{\mathrm{t,inma}}$ at 7.35 MHz, $R_{\mathrm{i}} = 50\,\Omega$, $Q = 100$, $5\,\mathrm{pF} \leq C_{1,2} \leq 250\,\mathrm{pF}$, and $0.1\,\mu\mathrm{H} \leq L_{\mathrm{s}} \leq 40\,\mu\mathrm{H}$, undercompensation shaded

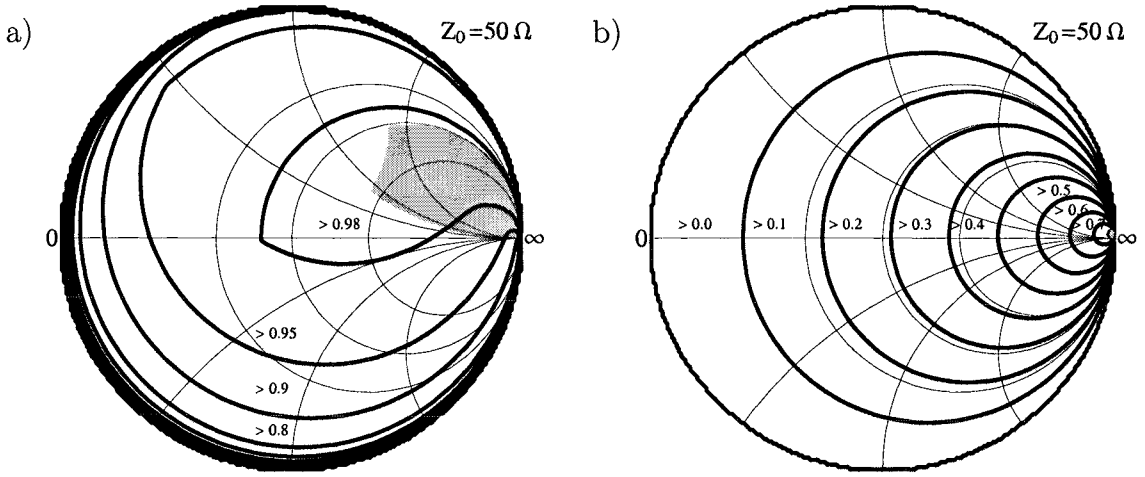

Figure C.21: a) Best and b) worst $g_{\mathrm{t,inma}}$ at 7.35 MHz, $R_{\mathrm{i}} = 50\,\Omega$, $Q = 100$, $5\,\mathrm{pF} \leq C_{1,2} \leq 500\,\mathrm{pF}$, and $0.1\,\mu\mathrm{H} \leq L_{\mathrm{s}} \leq 40\,\mu\mathrm{H}$, undercompensation shaded

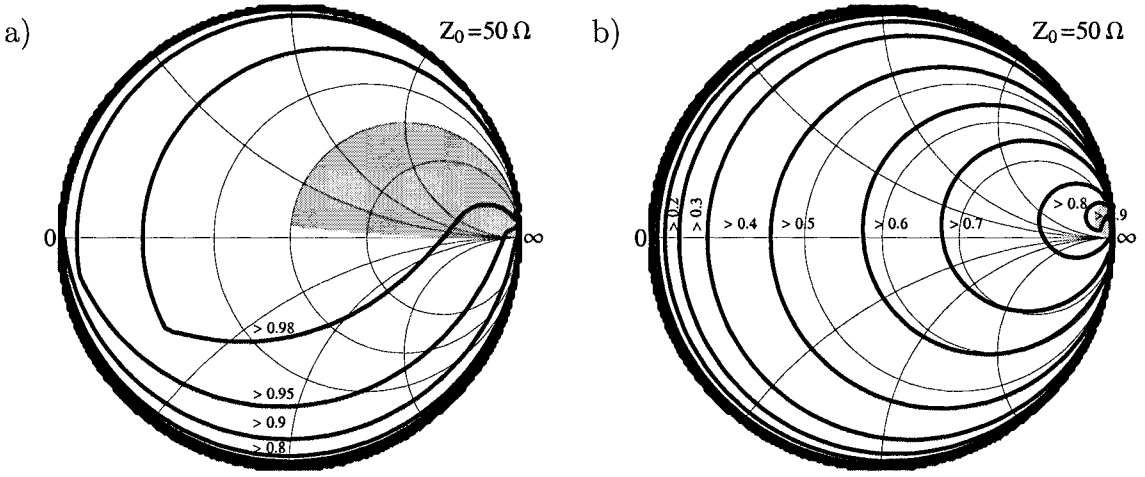

Figure C.22: a) Best and b) worst $g_{\mathrm{t,inma}}$ at 7.35 MHz, $R_{\mathrm{i}} = 50\,\Omega$, $Q = 100$, $25\,\mathrm{pF} \leq C_{1,2} \leq 4000\,\mathrm{pF}$, and $0.1\,\mu\mathrm{H} \leq L_{\mathrm{s}} \leq 40\,\mu\mathrm{H}$, undercomp. shaded

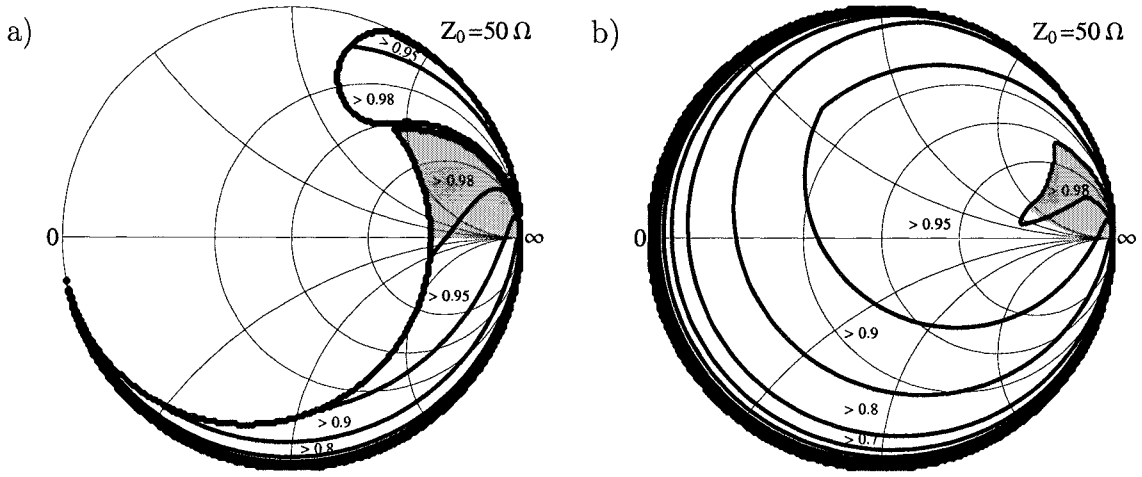

Figure C.23: $g_{\text{loft,inma}}$ at 7.35 MHz, $R_\text{i} = 50\,\Omega$, $Q = 100$, $5\,\text{pF} \leq C_{1,2} \leq 250\,\text{pF}$, and $0.1\,\mu\text{H} \leq L_\text{s} \leq 40\,\mu\text{H}$, a) without, b) with 5 pF parasitics, uc. shaded

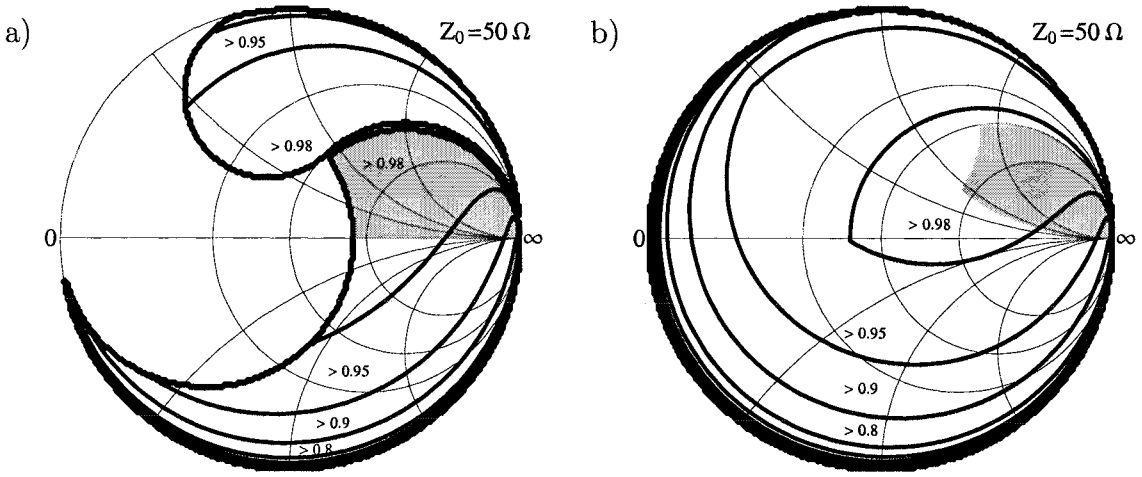

Figure C.24: $g_{\text{loft,inma}}$ at 7.35 MHz, $R_\text{i} = 50\,\Omega$, $Q = 100$, $5\,\text{pF} \leq C_{1,2} \leq 500\,\text{pF}$, and $0.1\,\mu\text{H} \leq L_\text{s} \leq 40\,\mu\text{H}$, a) without, b) with 5 pF parasitics, uc. shaded

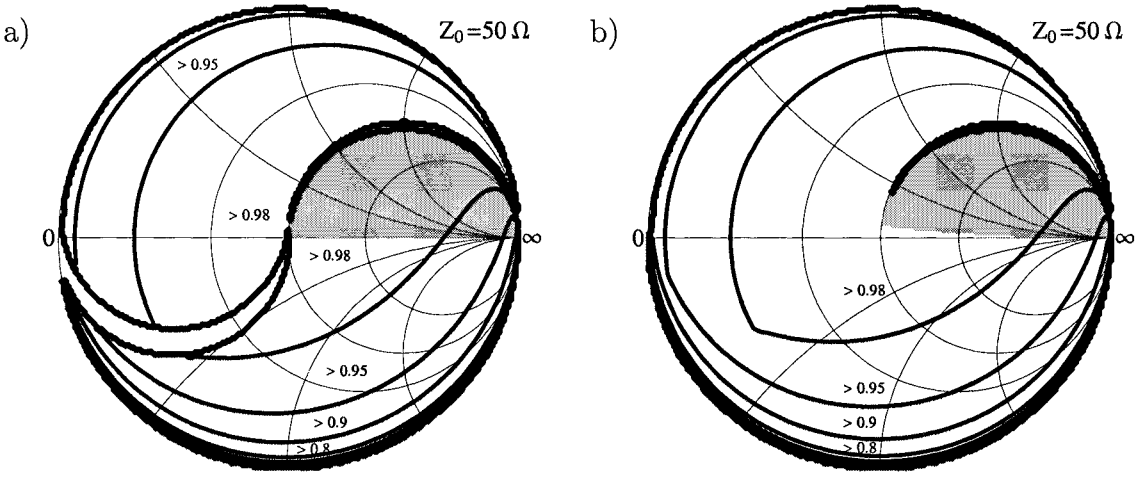

Figure C.25: $g_{\text{loft,inma}}$ at 7.35 MHz, $R_\text{i} = 50\,\Omega$, $Q = 100$, $25\,\text{pF} \leq C_{1,2} \leq 4000\,\text{pF}$, $0.1\,\mu\text{H} \leq L_\text{s} \leq 40\,\mu\text{H}$, a) without, b) with 25 pF parasitics, uc. shaded

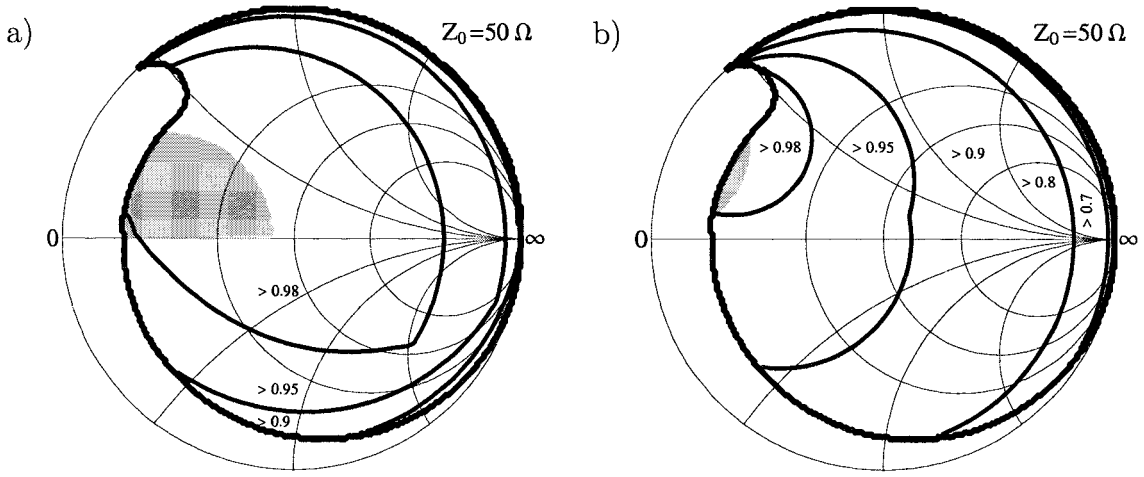

Figure C.26: a) Best and b) worst $g_{\pi,\mathrm{inma}}$ at 30 MHz, $R_\mathrm{i} = 50\,\Omega$, $Q = 100$, $5\,\mathrm{pF} \leq C_{1,2} \leq 250\,\mathrm{pF}$, and $0.1\,\mu\mathrm{H} \leq L_\mathrm{s} \leq 40\,\mu\mathrm{H}$, undercompensation shaded

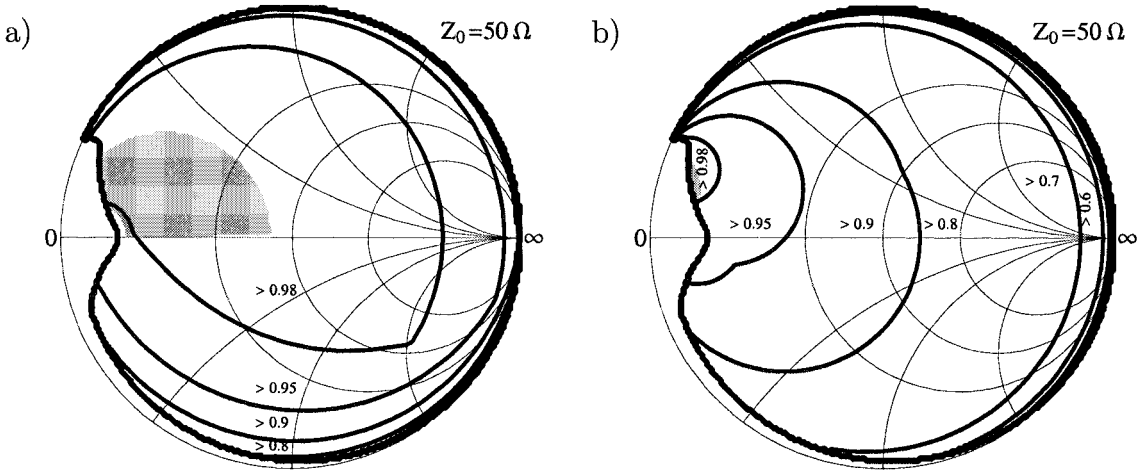

Figure C.27: a) Best and b) worst $g_{\pi,\mathrm{inma}}$ at 30 MHz, $R_\mathrm{i} = 50\,\Omega$, $Q = 100$, $5\,\mathrm{pF} \leq C_{1,2} \leq 500\,\mathrm{pF}$, and $0.1\,\mu\mathrm{H} \leq L_\mathrm{s} \leq 40\,\mu\mathrm{H}$, undercompensation shaded

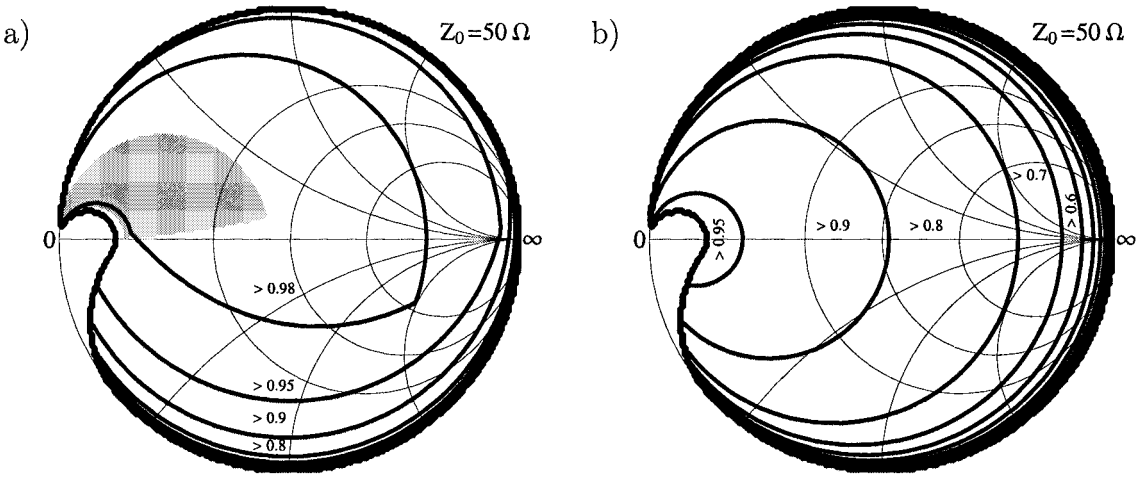

Figure C.28: a) Best and b) worst $g_{\pi,\mathrm{inma}}$ at 30 MHz, $R_\mathrm{i} = 50\,\Omega$, $Q = 100$, $25\,\mathrm{pF} \leq C_{1,2} \leq 4000\,\mathrm{pF}$, and $0.1\,\mu\mathrm{H} \leq L_\mathrm{s} \leq 40\,\mu\mathrm{H}$, undercomp. shaded

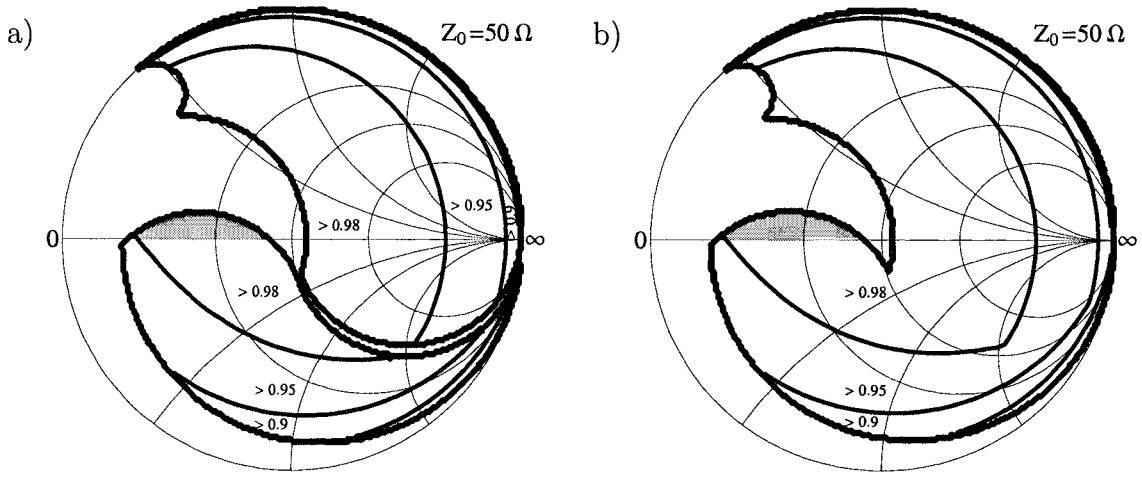

Figure C.29: $g_{\mathrm{lof}\pi,\mathrm{inma}}$ at 30 MHz, $R_\mathrm{i} = 50\,\Omega$, $Q = 100$, $5\,\mathrm{pF} \leq C_{1,2} \leq 250\,\mathrm{pF}$, and $0.1\,\mu\mathrm{H} \leq L_\mathrm{s} \leq 40\,\mu\mathrm{H}$, a) without, b) with 5 pF parasitics, uc. shaded

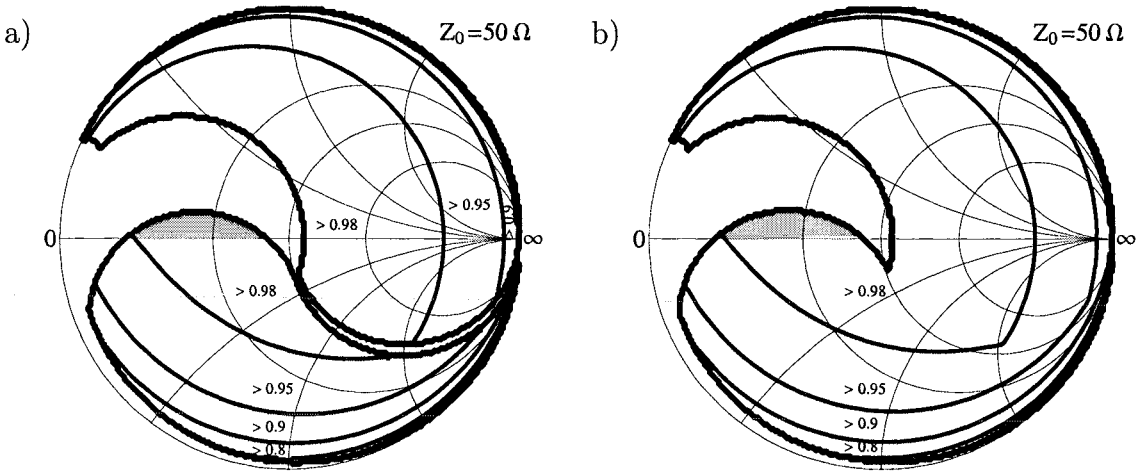

Figure C.30: $g_{\mathrm{lof}\pi,\mathrm{inma}}$ at 30 MHz, $R_\mathrm{i} = 50\,\Omega$, $Q = 100$, $5\,\mathrm{pF} \leq C_{1,2} \leq 500\,\mathrm{pF}$, and $0.1\,\mu\mathrm{H} \leq L_\mathrm{s} \leq 40\,\mu\mathrm{H}$, a) without, b) with 5 pF parasitics, uc. shaded

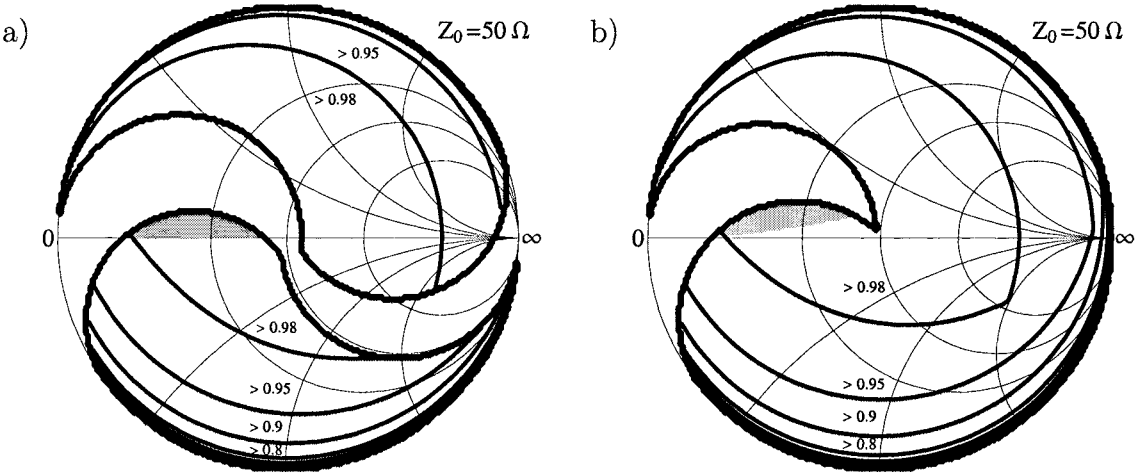

Figure C.31: $g_{\mathrm{lof}\pi,\mathrm{inma}}$ at 30 MHz, $R_\mathrm{i} = 50\,\Omega$, $Q = 100$, $25\,\mathrm{pF} \leq C_{1,2} \leq 4000\,\mathrm{pF}$, $0.1\,\mu\mathrm{H} \leq L_\mathrm{s} \leq 40\,\mu\mathrm{H}$, a) without, b) with 25 pF parasitics, uc. shaded

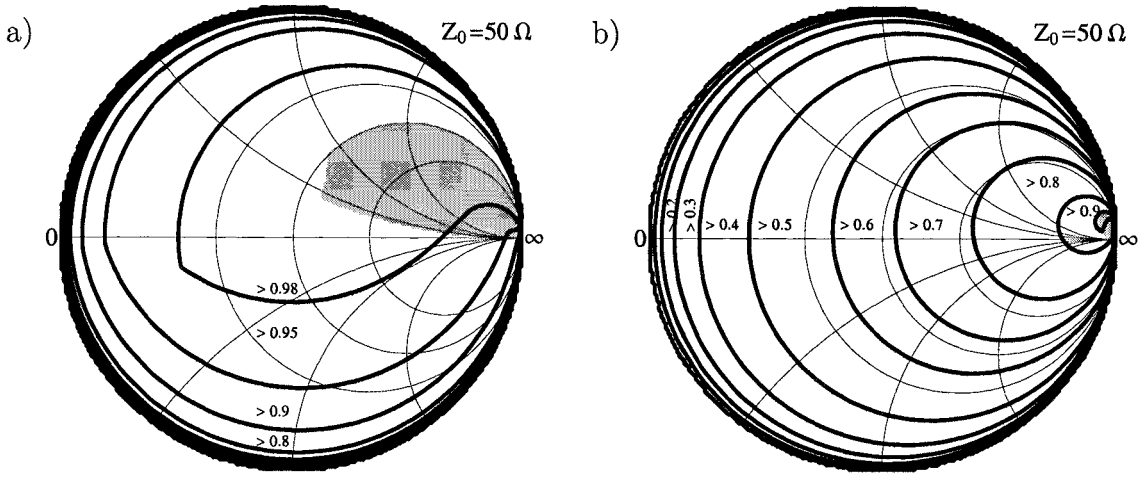

Figure C.32: a) Best and b) worst $g_{\mathrm{t,inma}}$ at 30 MHz, $R_\mathrm{i} = 50\,\Omega$, $Q = 100$, $5\,\mathrm{pF} \leq C_{1,2} \leq 250\,\mathrm{pF}$, and $0.1\,\mu\mathrm{H} \leq L_\mathrm{s} \leq 40\,\mu\mathrm{H}$, undercompensation shaded

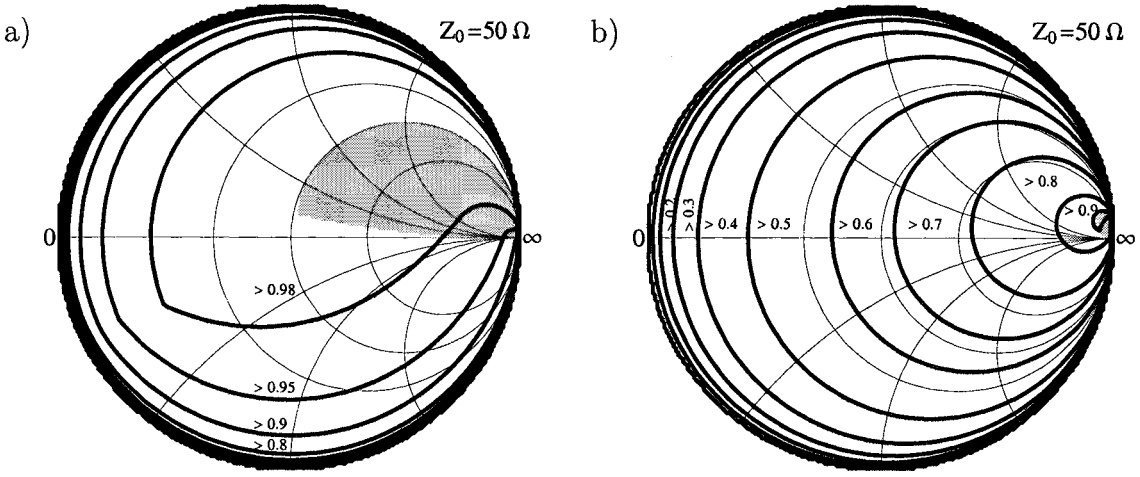

Figure C.33: a) Best and b) worst $g_{\mathrm{t,inma}}$ at 30 MHz, $R_\mathrm{i} = 50\,\Omega$, $Q = 100$, $5\,\mathrm{pF} \leq C_{1,2} \leq 500\,\mathrm{pF}$, and $0.1\,\mu\mathrm{H} \leq L_\mathrm{s} \leq 40\,\mu\mathrm{H}$, undercompensation shaded

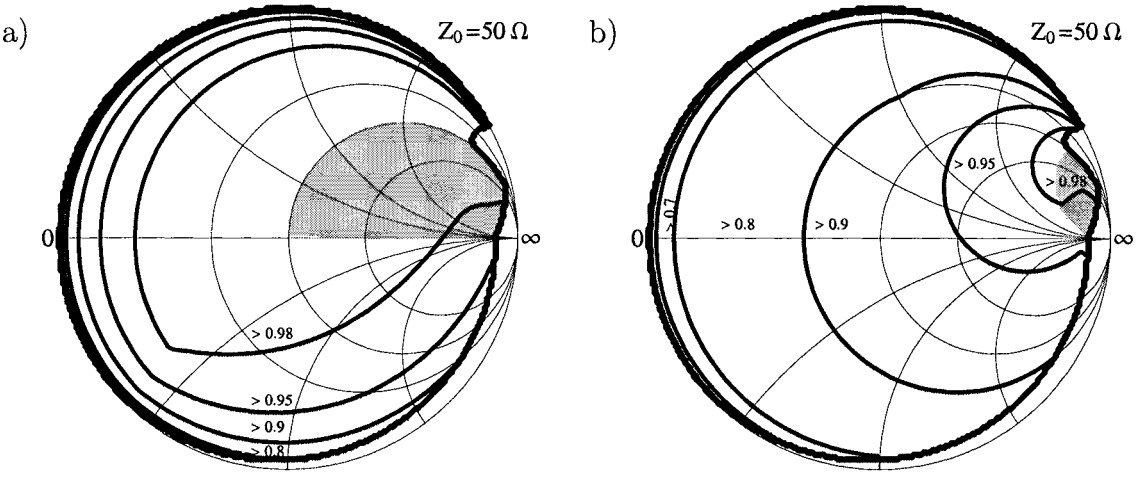

Figure C.34: a) Best and b) worst $g_{\mathrm{t,inma}}$ at 30 MHz, $R_\mathrm{i} = 50\,\Omega$, $Q = 100$, $25\,\mathrm{pF} \leq C_{1,2} \leq 4000\,\mathrm{pF}$, and $0.1\,\mu\mathrm{H} \leq L_\mathrm{s} \leq 40\,\mu\mathrm{H}$, undercomp. shaded

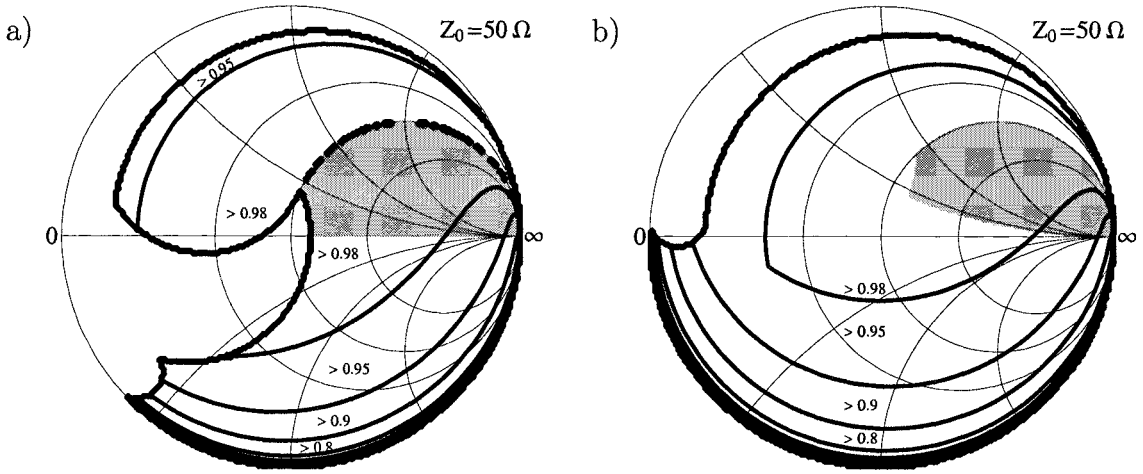

Figure C.35: $g_{\text{loft,inma}}$ at 30 MHz, $R_{\text{i}} = 50\,\Omega$, $Q = 100$, $5\,\text{pF} \leq C_{1,2} \leq 250\,\text{pF}$, and $0.1\,\mu\text{H} \leq L_{\text{s}} \leq 40\,\mu\text{H}$, a) without, b) with 5 pF parasitics, uc. shaded

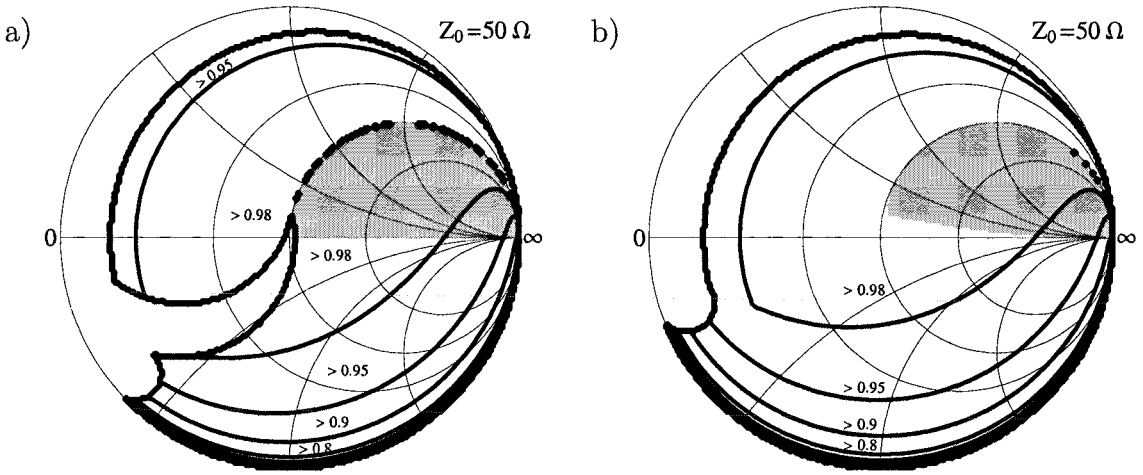

Figure C.36: $g_{\text{loft,inma}}$ at 30 MHz, $R_{\text{i}} = 50\,\Omega$, $Q = 100$, $5\,\text{pF} \leq C_{1,2} \leq 500\,\text{pF}$, and $0.1\,\mu\text{H} \leq L_{\text{s}} \leq 40\,\mu\text{H}$, a) without, b) with 5 pF parasitics, uc. shaded

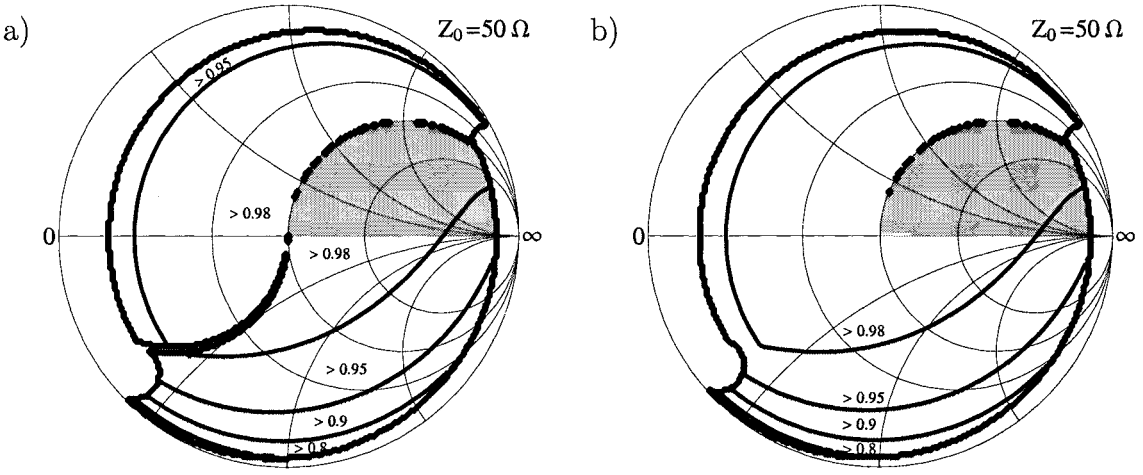

Figure C.37: $g_{\text{loft,inma}}$ at 30 MHz, $R_{\text{i}} = 50\,\Omega$, $Q = 100$, $25\,\text{pF} \leq C_{1,2} \leq 4000\,\text{pF}$, $0.1\,\mu\text{H} \leq L_{\text{s}} \leq 40\,\mu\text{H}$, a) without, b) with 25 pF parasitics, uc. shaded

Appendix D

Transmission Lines' and Total Losses in a Source, Line 1, Matching Network, Line 2, and Load System

D.1 Definitions/notations

From this chapter on, the following definitions/notations will be used:

Latin letters

a	Quadratic coefficient of $\underline{r}_{\ell\mathrm{opt}}$ in Appendix D.2
b	Linear coefficient of $\underline{r}_{\ell\mathrm{opt}}$ in Appendix D.2
c	Constant coefficient of $\underline{r}_{\ell\mathrm{opt}}$ in Appendix D.2
C_{iMBpmax}	Minimum (equivalent) parallel capacitance calculated from the limiting circle of the transformation spiral of $\underline{Y}_{\mathrm{iMB}}$ (π network)
C_{iMBpmin}	Minimum (equivalent) parallel capacitance calculated from the limiting circle of the transformation spiral of $\underline{Y}_{\mathrm{iMB}}$ (π network)
C_{iMBsmax}	Minimum (equivalent) series capacitance calculated from the limiting circle of the transformation spiral of $\underline{Z}_{\mathrm{iMB}}$ (T network)
C_{iMBsmin}	Minimum (equivalent) series capacitance calculated from the limiting circle of the transformation spiral of $\underline{Z}_{\mathrm{iMB}}$ (T network)
L_{iMBpmax}	Minimum (equivalent) parallel inductance calculated from the limiting circle of the transformation spiral of $\underline{Y}_{\mathrm{iMB}}$ (π network)
L_{iMBpmin}	Minimum (equivalent) parallel inductance calculated from the limiting circle of the transformation spiral of $\underline{Y}_{\mathrm{iMB}}$ (π network)
L_{iMBsmax}	Minimum (equivalent) series inductance calculated from the limiting circle of the transformation spiral of $\underline{Z}_{\mathrm{iMB}}$ (T network)
L_{iMBsmin}	Minimum (equivalent) series inductance calculated from the limiting circle of the transformation spiral of $\underline{Z}_{\mathrm{iMB}}$ (T network)
$\underline{r}_{1\mathrm{opt}}$	Input reflection coefficient of a transmission line with $X_0 \neq 0$ whose load is the optimum load impedance $\underline{Z}_{\ell\mathrm{opt}}$ (referred to $\underline{Z}_0$)
$\underline{r}_{\mathrm{iopt}}$	Optimum source reflection coefficient for a transmission line with $X_0 \neq 0$ whose load is the optimum load impedance $\underline{Z}_{\ell\mathrm{opt}}$ (referred to $\underline{Z}_0$)
$\underline{r}_{\ell\mathrm{opt}\pm}$	Reflection coefficient of the two solutions for optimum load impedance of a transmission line with $X_0 \neq 0$ distinguished by the sign in front of the square root (referred to $\underline{Z}_0$)
$\underline{Y}_{\mathrm{iMB}}$	Source admittance of a matchbox (π network)

$\underline{Z}_{1\mathrm{opt}}$	Input impedance of a transmission line with $X_0 \neq 0$ whose load is the optimum load impedance $\underline{Z}_{\ell\mathrm{opt}}$
$\underline{Z}_{\mathrm{iMB}}$	Source impedance of a matchbox (T network)
$\underline{Z}_{\ell\mathrm{opt}\pm}$	Two solutions for the optimum load impedance of a transmission line with $X_0 \neq 0$ distinguished by the by the sign in front of the square root

Greek letters

δ_{G}	$\operatorname{arsinh}\left(\frac{G'}{\omega C'}\right)$
δ_{R}	$\operatorname{arsinh}\left(\frac{R'}{\omega L'}\right)$

D.2 Losses and matching in a source, transmission line, and load system

To optimise g_{L} as described in Section 5.3, we have to solve

$$\begin{aligned} 0 \;=\; & \mathrm{j}R_0X_0\,\mathrm{e}^{-2\alpha l}\left(\mathrm{e}^{-2\alpha l}-\mathrm{e}^{-\mathrm{j}2\beta l}\right)\underline{r}_\ell^2 \\ & -\left(R_0^2\left(1-\mathrm{e}^{-4\alpha l}\right)+X_0^2\,\mathrm{e}^{-2\alpha l}\left(\mathrm{e}^{\mathrm{j}2\beta l}-\mathrm{e}^{-\mathrm{j}2\beta l}\right)\right)\underline{r}_\ell \\ & -\mathrm{j}R_0X_0\left(1-\mathrm{e}^{-2\alpha l}\,\mathrm{e}^{\mathrm{j}2\beta l}\right) \end{aligned}$$

or, slightly rearranged,

$$\begin{aligned} 0 \;=\; & \mathrm{j}R_0X_0\,\mathrm{e}^{-2\alpha l}\,\mathrm{e}^{-\mathrm{j}2\beta l}\left(1-\mathrm{e}^{-2\alpha l}\,\mathrm{e}^{\mathrm{j}2\beta l}\right)\underline{r}_\ell^2 \\ & +2\,\mathrm{e}^{-2\alpha l}\left(R_0^2\sinh(2\alpha l)+\mathrm{j}X_0^2\sin(2\beta l)\right)\underline{r}_\ell \\ & +\mathrm{j}R_0X_0\left(1-\mathrm{e}^{-2\alpha l}\,\mathrm{e}^{\mathrm{j}2\beta l}\right), \end{aligned}$$

involving two different cases:

1. $X_0 = 0$

   Then we have to solve

   $$0 = 2\,\mathrm{e}^{-2\alpha l}\,R_0^2\sinh(2\alpha l)\,\underline{r}_\ell.$$

   We assumed $l > 0$ and, according to [26c], $R_0 > 0$. Additionally, [26b] indicates that $\alpha \geq 0$.

   If $\alpha > 0$, the transmission line is either Heaviside's distortionless transmission line obtained for $\frac{R'}{\omega L'} = \frac{G'}{\omega C'} > 0$ and $\underline{Z}_0 = Z_{0\mathrm{II}}$ (where G' is the per-unit-length conductance and $L' = Z_{0\mathrm{II}}^2 C'$ the per-unit-length inductance of that line, defined in [26a]) or the approximation (2.5) is used. Then $\underline{r}_\ell = 0$ uniquely solves the equation, thus $\underline{Z}_\ell = Z_{0\mathrm{II}}$ yields the maximum g_{L}. If we terminate the line accordingly, its input resistance $\underline{Z}_1 = Z_{0\mathrm{II}}$, hence the source's impedance has to be $\underline{Z}_{\mathrm{i}} = Z_{0\mathrm{II}}$ to achieve maximum active input power. In particular, optimum source and load impedance is independent of (frequency and) line length.

   If $\alpha = 0$, the transmission line is lossless, hence $\frac{R'}{\omega L'} = \frac{G'}{\omega C'} = 0$. Then $g_{\mathrm{L}} = 1$ for any $\underline{Z}_\ell$. However, according to (2.20) only a choice of $\underline{Z}_\ell = \underline{Z}_0 = Z_{0\mathrm{II}}$

combined with $\underline{Z}_\mathrm{i} = Z_{0\mathrm{II}}$ yields a source impedance for maximum active power input which is independent of (frequency and) line length — thus no other choice is appropriate.

2. $X_0 \neq 0$

We assumed $l > 0$ and, according to [26c], $R_0 > 0$. Additionally, [26b] indicates that $\alpha \geq 0$, but in conjunction with [26c] we may conclude that $X_0 \neq 0$ is accompanied by $\alpha > 0$, hence we have to consider $\alpha > 0$ only.

Then all coefficients of $\underline{r}_\ell^2$, $\underline{r}_\ell$, and $\underline{r}_\ell^0 = 1$ in the equation to solve are $\neq 0$ except for $l \to \infty$ (another exception would be $l = 0$, but we assumed $l > 0$).

Solving for $\underline{r}_{\ell\mathrm{opt}\pm}$ if $l \in (0, \infty)$ yields two possible solutions,

$$\begin{aligned}\underline{r}_{\ell\mathrm{opt}\pm} &= -\frac{2\,\mathrm{e}^{-2\alpha l}\left(R_0^2\,\sinh(2\alpha l)+\mathrm{j}X_0^2\,\sin(2\beta l)\right)}{2\mathrm{j}R_0X_0\,\mathrm{e}^{-2\alpha l}\,\mathrm{e}^{-\mathrm{j}2\beta l}\,(1-\mathrm{e}^{-2\alpha l}\,\mathrm{e}^{\mathrm{j}2\beta l})} \\ &\quad \pm \frac{\sqrt{4\,\mathrm{e}^{-4\alpha l}\left(R_0^2\,\sinh(2\alpha l)+\mathrm{j}X_0^2\,\sin(2\beta l)\right)^2+4R_0^2X_0^2\,\mathrm{e}^{-2\alpha l}\,\mathrm{e}^{-\mathrm{j}2\beta l}\,(1-\mathrm{e}^{-2\alpha l}\,\mathrm{e}^{\mathrm{j}2\beta l})^2}}{2\mathrm{j}R_0X_0\,\mathrm{e}^{-2\alpha l}\,\mathrm{e}^{-\mathrm{j}2\beta l}\,(1-\mathrm{e}^{-2\alpha l}\,\mathrm{e}^{\mathrm{j}2\beta l})}.\end{aligned}$$

Prior to deciding which solution is valid we have to check the argument of the square root. It may be rewritten to

$$\begin{aligned}&4\,\mathrm{e}^{-4\alpha l}\left(R_0^2\,\sinh(2\alpha l)+\mathrm{j}X_0^2\,\sin(2\beta l)\right)^2+4R_0^2X_0^2\,\mathrm{e}^{-2\alpha l}\,\mathrm{e}^{-\mathrm{j}2\beta l}\,(1-\mathrm{e}^{-2\alpha l}\,\mathrm{e}^{\mathrm{j}2\beta l})^2 \\ &= 4\,\mathrm{e}^{-4\alpha l}\left(R_0^2\,(\cosh(2\alpha l)+1)+X_0^2\,(\cos(2\beta l)+1)\right) \\ &\quad \cdot\left(R_0^2\,(\cosh(2\alpha l)-1)+X_0^2\,(\cos(2\beta l)-1)\right) \\ &= 2\,\mathrm{e}^{-4\alpha l}\big(R_0^4\,(\cosh(4\alpha l)-1)+4R_0^2X_0^2\,(\cosh(2\alpha l)\,\cos(2\beta l)-1) \\ &\qquad +X_0^4\,(\cos(4\beta l)-1)\big) \\ &= 4\,\mathrm{e}^{-4\alpha l}\left(\left(R_0^2\cosh(2\alpha l)+X_0^2\cos(2\beta l)\right)^2-|\underline{Z}_0|^4\right).\end{aligned}$$

To determine its sign, we check the first rearrangement.

The factor $4\,\mathrm{e}^{-4\alpha l}$ is always > 0. The first term in parentheses is also always > 0 because $R_0^2\,(\cosh(2\alpha l)+1) \in [2\,R_0^2, \infty)$, $X_0^2\,(\cos(2\beta l)+1) \in [0, 2\,X_0^2]$, and $R_0 > 0$ holds (the latter according to [26c]).

The second term in parentheses equals zero if $l = 0$. To derive its values' range if $l > 0$ we compute its derivative with respect to l,

$$\frac{\mathrm{d}\left(R_0^2(\cosh(2\alpha l)-1)+X_0^2(\cos(2\beta l)-1)\right)}{\mathrm{d}l} = 2\,(\alpha R_0^2\,\sinh(2\alpha l)-\beta X_0^2\,\sin(2\beta l)).$$

The derivative equals zero if $l = 0$. Since we assumed $\alpha > 0$ and $\beta > 0$ (implied by $\omega > 0$)[1], $\sinh(2\alpha l) > 2\alpha l$ and $\sin(2\beta l) < 2\beta l$ holds if $l > 0$, thus

$$\frac{\mathrm{d}\left(R_0^2(\cosh(2\alpha l)-1)+X_0^2(\cos(2\beta l)-1)\right)}{\mathrm{d}l} > 4l\,(\alpha^2 R_0^2 - \beta^2 X_0^2) \geq 0.$$

The latter inequality applies because we obtain from [26b] and [26c] that

$$\alpha^2 R_0^2 - \beta^2 X_0^2$$
$$= \left(\frac{\omega L'}{\cosh(\delta_G)}\right)^2 \left(\left(\sinh\left(\tfrac{\delta_R+\delta_G}{2}\right)\cosh\left(\tfrac{\delta_R+\delta_G}{2}\right)\right)^2 - \left(\cosh\left(\tfrac{\delta_R-\delta_G}{2}\right)\sinh\left(\tfrac{\delta_R-\delta_G}{2}\right)\right)^2\right),$$

where $\delta_R = \operatorname{arsinh}\left(\frac{R'}{\omega L'}\right)$, $\delta_G = \operatorname{arsinh}\left(\frac{G'}{\omega C'}\right)$, $L', C' > 0$, and[2] $R', G' \geq 0$, or[2] $\delta_R, \delta_G \geq 0$, respectively. Hence $|\delta_R + \delta_G| \geq |\delta_R - \delta_G|$ holds, thus $\left|\sinh\left(\frac{\delta_R+\delta_G}{2}\right)\right| \geq \left|\sinh\left(\frac{\delta_R-\delta_G}{2}\right)\right|$, $\cosh\left(\frac{\delta_R+\delta_G}{2}\right) \geq \cosh\left(\frac{\delta_R-\delta_G}{2}\right)$ and $\alpha^2 R_0^2 - \beta^2 X_0^2 \geq 0$.

Summarising the preceding derivations, the second term in parentheses of the first rearrangement equals zero if $l = 0$ and increases with increasing l, hence it's always > 0 if $l > 0$.

Thus the argument of the square root in $\underline{r}_{\ell\mathrm{opt}\pm}$ stays > 0 if $l > 0$ — then the square root is always real.

Finally we have to check which of the possible solutions $\underline{r}_{\ell\mathrm{opt}\pm}$ is a valid solution. Since we consider passive loads, $\mathrm{Re}\{\underline{Z}_{\ell\mathrm{opt}\pm}\} \geq 0$ holds. Additionally, $|\underline{r}_{\ell\mathrm{opt}\pm}|$ is restricted according to [26f] or, even more accurately[3], to $|\underline{r}_{\ell\mathrm{opt}\pm}| \leq \frac{|Z_0|+|X_0|}{R_0} < 1 + \sqrt{2}$.

---

[1] Combining [26b] and [26c] yields $\alpha \geq 0$, $\beta > 0$, $R_0 > 0$ and $R_0 > |X_0|$ or $R_0^2 > X_0^2$, respectively. Additionally, as indicated above, $\alpha^2 R_0^2 - \beta^2 X_0^2 \geq 0$ holds, which is equivalent to $\alpha R_0 - \beta\,|X_0| \geq 0$.
Unlike R_0 and X_0, there is no common relation between α and β, which may be proved easily if we rewrite α, β (and R_0, X_0) using trigonometric functions (cos, sin, and arctan) instead of the hyperbolic functions (cosh, sinh, and arsinh) used by [26b]. By comparison of the two different descriptions we obtain $\operatorname{arsinh}\left(\frac{1}{x}\right) = \ln\left(\frac{\mathrm{e}^{\operatorname{arsinh}(x)}+1}{\mathrm{e}^{\operatorname{arsinh}(x)}-1}\right)$ for all (real) $x \geq 0$, which may alternatively be applied to derive the following relations between α and β from [26b].
Then we may conclude that $\alpha < \beta$ if $\frac{R'}{\omega L'} < \frac{1}{\frac{G'}{\omega C'}}$ or $\frac{G'}{\omega C'} < \frac{1}{\frac{R'}{\omega L'}}$, $\alpha = \beta$ if $\frac{R'}{\omega L'} = \frac{1}{\frac{G'}{\omega C'}}$ or $\frac{G'}{\omega C'} = \frac{1}{\frac{R'}{\omega L'}}$, and $\alpha > \beta$ if $\frac{R'}{\omega L'} > \frac{1}{\frac{G'}{\omega C'}}$ or $\frac{G'}{\omega C'} > \frac{1}{\frac{R'}{\omega L'}}$ ($R', G' \geq 0$, $L', C', \omega > 0$).
In particular, $\alpha < \beta$ if $R' > 0$ and $G' = 0$, $G' > 0$ and $R' = 0$, or $\frac{R'}{\omega L'}, \frac{G'}{\omega C'} < 1$. The latter holds for coaxial transmission lines in our frequency range of interest, where $\frac{R'}{\omega L'} \gg \frac{G'}{\omega C'}$ and $\frac{R'}{\omega L'}, \frac{G'}{\omega C'} \ll 1$.

[2] Due to assuming $\alpha > 0$, at least one of R' and G' or δ_R and δ_G, respectively, has to be > 0.

[3] [26f] derives $|\underline{r}|_{\max} \approx 1 + \sqrt{2}$ by considering the maximum phase angle of coaxial transmission lines' characteristic impedances. However, a more thorough investigation of passive impedances' reflection coefficients yields their locus in the complex reflection coefficient plane — they all lie within a circle of radius $\frac{|Z_0|}{R_0}$ and centre $-\mathrm{j}\,\frac{X_0}{R_0}$. The limiting circle describes the locus of purely imaginary impedances' reflection coefficients. According to (2.19) its centre is the reflection coefficient of the conjugate complex of the line's characteristic impedance. From [26c] we obtain $R_0 > 0$ and $R_0 > |X_0|$, hence the minimum magnitude of the reflection coefficient equals zero (matching), the maximum magnitude equals $\frac{|Z_0|+|X_0|}{R_0} < 1 + \sqrt{2}$. It's interesting to note that these relations hold for any "lines" involving transmission lines' differential equations.

The solution involving subtraction of the square root, $\underline{r}_{\ell\text{opt}-}$, violates both conditions. If we take into account that the square root in $\underline{r}_{\ell\text{opt}-}$ is always real for $l > 0$, we firstly obtain from (2.11)

$$\mathrm{Re}\{\underline{Z}_{\ell\text{opt}-}\} = -\frac{\sqrt{\left(R_0^2\cosh(2\alpha l)+X_0^2\cos(2\beta l)\right)^2-|\underline{Z}_0|^4}}{R_0\sinh(2\alpha l)+X_0\sin(2\beta l)},$$

which is always < 0 if $l > 0$ since $R_0\sinh(2\alpha l)+X_0\sin(2\beta l) \geq R_0\sinh(2\alpha l) - |X_0\sin(2\beta l)| > 2l(\alpha R_0 - \beta|X_0|) \geq 0$ if $l > 0$ (the latter inequality holds according to Footnote [1]). Secondly $|\underline{r}_{\ell\text{opt}-}| \to \infty$ for $l \to \infty$, since the denominator of both ratios in $\underline{r}_{\ell\text{opt}-}$ tends to zero, and both numerators to $-\infty$.

Conversely, the solution involving summing of the square root, $\underline{r}_{\ell\text{opt}+}$, yields

$$\mathrm{Re}\{\underline{Z}_{\ell\text{opt}+}\} = \frac{\sqrt{\left(R_0^2\cosh(2\alpha l)+X_0^2\cos(2\beta l)\right)^2-|\underline{Z}_0|^4}}{R_0\sinh(2\alpha l)+X_0\sin(2\beta l)},$$

which is always > 0 if $l > 0$. Additionally, $|\underline{r}_{\ell\text{opt}+}|$ tends to the proper limit for $l \to \infty$ because then $a\,\underline{r}_{\ell\text{opt}+}^2 + b\,\underline{r}_{\ell\text{opt}+} + c = 0$, where $a \to 0$, $b \to R_0^2$, and $c \to \mathrm{j}R_0X_0$. Since b is real and $b > 0$, application of l'Hospitale's rule gives $\lim\limits_{a\to 0}\frac{-b+\sqrt{b^2-4ac}}{2a} = \lim\limits_{a\to 0}\frac{-4c}{4\sqrt{b^2-4ac}} = -\frac{c}{b}$, thus $\underline{r}_{\ell\text{opt}+}$ is a valid solution[4].

Summarising the preceding considerations, we may conclude that

$$\underline{r}_{\ell\text{opt}} = \frac{\sqrt{\left(R_0^2\cosh(2\alpha l)+X_0^2\cos(2\beta l)\right)^2-|\underline{Z}_0|^4}-R_0^2\sinh(2\alpha l)-\mathrm{j}X_0^2\sin(2\beta l)}{\mathrm{j}R_0X_0\,\mathrm{e}^{-\mathrm{j}2\beta l}\left(1-\mathrm{e}^{-2\alpha l}\,\mathrm{e}^{\mathrm{j}2\beta l}\right)} \tag{D.1}$$

is the unique valid solution if $l \in (0, \infty)$.

Application of (2.11) and (2.12) yields the optimum load impedance,

$$\underline{Z}_{\ell\text{opt}} = \frac{\sqrt{\left(R_0^2\cosh(2\alpha l)+X_0^2\cos(2\beta l)\right)^2-|\underline{Z}_0|^4}-\mathrm{j}R_0X_0(\cosh(2\alpha l)-\cos(2\beta l))}{R_0\sinh(2\alpha l)+X_0\sin(2\beta l)}. \tag{D.2}$$

The transmission line's input impedance is given by (2.20), hence $\underline{r}_{1\text{opt}} = \underline{r}_{\ell\text{opt}}\,\mathrm{e}^{-2\alpha l}\,\mathrm{e}^{-\mathrm{j}2\beta l}$. If the line is terminated by the optimum load impedance indicated above, its input reflection coeffifient is $\underline{r}_{1\text{opt}} = \frac{R_0\,\underline{r}^*_{\ell\text{opt}}-\mathrm{j}X_0}{R_0-\mathrm{j}X_0\,\underline{r}^*_{\ell\text{opt}}}$. Then, according to (2.18), its input impedance is $\underline{Z}_{1\text{opt}} = \underline{Z}^*_{\ell\text{opt}}$ — if the transmission line is terminated by its optimum load impedance, its input impedance is the complex conjugate of the optimum load impedance!

From (2.23) we finally compute the optimum power gain,

$$g_{\text{Lopt}} = \frac{R_0^2\cosh(2\alpha l)+X_0^2\cos(2\beta l)-\sqrt{\left(R_0^2\cosh(2\alpha l)+X_0^2\cos(2\beta l)\right)^2-|\underline{Z}_0|^4}}{|\underline{Z}_0|^2}. \tag{D.3}$$

However, to achieve maximum active input power, the source impedance has to be equal to the complex conjugate of the line's input impedance, hence

[4] Application of l'Hospitale's rule requires $-b+\sqrt{b^2-4ac} \to 0$ for $a \to 0$, hence $b = |b|$ or $b \geq 0$ if b is real. Conversely, if $b \leq 0$, the proper limit would be achieved by the solution involving subtraction of the square root.

$\underline{Z}_{\mathrm{iopt}} = \underline{Z}^*_{\mathrm{lopt}} = \underline{Z}_{\ell\mathrm{opt}}$ or $\underline{r}_{\mathrm{iopt}} = \underline{r}_{\ell\mathrm{opt}}$. If the source impedance is chosen accordingly, the active input power is $P_{\mathrm{actlopt}} = P_{\mathrm{actmaxi}}$, thus $g_{\mathrm{T,Lopt}} = g_{\mathrm{Lopt}}$. Additionally, the line's output impedance is equal to the complex conjugate of its optimum load impedance because $\underline{r}_{\mathrm{iopt}}\,\mathrm{e}^{-2\alpha l}\,\mathrm{e}^{-\mathrm{j}2\beta l}$ in conjunction with $\underline{r}_{\mathrm{iopt}} = \underline{r}_{\ell\mathrm{opt}}$ describes an impedance of $\underline{Z}^*_{\ell\mathrm{opt}}$. Optimum active power input and transfer involves complex conjugate matching at the line's in- and output!

Comparison of the preceding optimum[5] derived for a complex characteristic impedance[6] where $X_0 \neq 0$ reveals a severe disadvantage compared to that of a real characteristic impedance where $X_0 = 0$ — the complex characteristic impedance's optimum load depends on **frequency and line length** — thus, depending on frequency and line length, different load and source impedances would have to be used.

To choose a useful length independent load impedance close to the optimised load, we consider its limits for $l \to 0$ and $l \to \infty$.

If $l = 0$, the equation to be solved for the optimum $\underline{r}_\ell$ changes to $0\,\underline{r}_\ell^2 + 0\,\underline{r}_\ell + 0 = 0$, hence any $\underline{r}_\ell$ or $\underline{Z}_\ell$ would involve optimum active power transfer — which holds since there is no line at all. To ensure maximum active input power, simply a source impedance of $\underline{Z}_{\mathrm{i}} = \underline{Z}^*_\ell$ is required.

Conversely, $\underline{r}_{\ell\mathrm{opt}}$ or $\underline{Z}_{\ell\mathrm{opt}}$ tend to particular limits for $l \to 0$, because they take into account the tiny, but nonzero line length, for which an optimum still exists.

If $\frac{X_0}{R_0} \neq -\frac{\alpha}{\beta}$ (more precisely, if $\frac{X_0}{R_0} > -\frac{\alpha}{\beta}$ according to Footnote [1]), we obtain

$$\begin{aligned}
\lim_{l\to 0} \underline{r}_{\ell\mathrm{opt}} &= \frac{\sqrt{|\underline{Z}_0|^2\left(\alpha^2 R_0^2 - \beta^2 X_0^2\right)} - \alpha R_0^2 - \mathrm{j}\beta X_0^2}{R_0 X_0\,(\beta + \mathrm{j}\alpha)} &&= \lim_{l\to 0} \underline{r}_{\mathrm{iopt}},\\
\lim_{l\to 0} \underline{Z}_{\ell\mathrm{opt}} &= \frac{\sqrt{|\underline{Z}_0|^2\left(\alpha^2 R_0^2 - \beta^2 X_0^2\right)}}{\alpha R_0 + \beta X_0} &&= \lim_{l\to 0} \underline{Z}_{\mathrm{iopt}},\\
\lim_{l\to 0} g_{\mathrm{Lopt}} &= 1 &&= \lim_{l\to 0} g_{\mathrm{T,Lopt}},
\end{aligned}$$

if $\frac{X_0}{R_0} = -\frac{\alpha}{\beta}$ (which requires $\frac{\alpha}{\beta} < 1$ because $\frac{|X_0|}{R_0} < 1$ according to Footnote [1]),

$$\begin{aligned}
\lim_{l\to 0} \underline{r}_{\ell\mathrm{opt}} &= 1 &&= \lim_{l\to 0} \underline{r}_{\mathrm{iopt}},\\
\mathrm{Re}\{\underline{Z}_{\ell\mathrm{opt}}\},\ \mathrm{Re}\{\underline{Z}_{\mathrm{iopt}}\} &\to \infty \quad \text{for} \quad l \to 0,
\end{aligned}$$

---

[5] Considering Footnote [1] of Section 5.3, we would suppose that g_{Lopt} decreases if l increases. To prove it, we compute $\frac{\mathrm{d}g_{\mathrm{Lopt}}}{\mathrm{d}l} = -2\,g_{\mathrm{Lopt}}\frac{\alpha R_0^2 \sinh(2\alpha l) - \beta X_0^2 \sin(2\beta l)}{\sqrt{\left(R_0^2\cosh(2\alpha l) + X_0^2\cos(2\beta l)\right)^2 - |\underline{Z}_0|^4}}$. Since $g_{\mathrm{Lopt}} > 0$ (line and load are entirely passive and $g_{\mathrm{Lopt}} \to 0$ only if $l \to \infty$) and $\alpha R_0^2 \sinh(2\alpha l) - \beta X_0^2 \sin(2\beta l) > 0$ if $l > 0$ (as indicated above), $\frac{\mathrm{d}g_{\mathrm{Lopt}}}{\mathrm{d}l} < 0$ if $l > 0$ (where $\frac{\mathrm{d}g_{\mathrm{Lopt}}}{\mathrm{d}l} \to 0$ for $l \to \infty$). However, $\left.\frac{\mathrm{d}g_{\mathrm{Lopt}}}{\mathrm{d}l}\right|_{l=0} = -2\sqrt{\frac{\alpha^2 R_0^2 - \beta^2 X_0^2}{|\underline{Z}_0|^2}}$ may equal zero if $\alpha^2 R_0^2 - \beta^2 X_0^2 = 0$, which (approximately) holds for coaxial transmission lines in our frequency range of interest

[6] It's interesting to note that the optimum reflection coefficient's limit for $X_0 \to 0$ is equal to the optimum reflection coefficient derived for $X_0 = 0$ and $\alpha > 0$.

$$\begin{aligned} &\mathrm{Im}\{\underline{Z}_{\ell\mathrm{opt}}\},\ \mathrm{Im}\{\underline{Z}_{\mathrm{iopt}}\} \ \to \infty \quad \text{for} \quad l \to 0, \\ &\lim_{l\to 0} g_{\mathrm{Lopt}} = \qquad 1 \qquad = \lim_{l\to 0} g_{\mathrm{T,\,Lopt}}. \end{aligned}$$

In particular, the latter applies if (2.4), hence $\underline{Z}_0 \approx Z_{0\mathrm{ll}}\,(1 - \mathrm{j}\,\frac{\alpha}{\beta})$, (approximately) describes the line's complex characteristic impedance. Then the limit of the optimum load impedance tends to an open circuit[7].

For $l \to \infty$ the equation to be solved for the optimum $\underline{r}_\ell$ changes to $0\,\underline{r}_\ell^2 + R_0^2\,\underline{r}_\ell + \mathrm{j}R_0X_0 = 0$. Since we already proved that $\underline{r}_{\ell\mathrm{opt}}$ tends to the proper solution, we obtain by solving for $\underline{r}_\ell$,

$$\lim_{l\to\infty} \underline{r}_{\ell\mathrm{opt}} = -\mathrm{j}\,\frac{X_0}{R_0} = \lim_{l\to\infty} \underline{r}_{\mathrm{iopt}},$$

which describes a

$$\lim_{l\to\infty} \underline{Z}_{\ell\mathrm{opt}} = \underline{Z}_0^* = \lim_{l\to\infty} \underline{Z}_{\mathrm{iopt}}$$

according to (2.19).

Since we assumed $\alpha > 0$, the optimum power gain becomes

$$\lim_{l\to\infty} g_{\mathrm{Lopt}} = \ 0 \ = \lim_{l\to\infty} g_{\mathrm{T,\,Lopt}}.$$

D.3 Losses and matching in a source, line 1, matching network, line 2, and load system

D.3.1 Lossy matching network

D.3.1.1 π network

To check the impact of source admittance transformation by the line on network design, in particular the necessity of extending the optimisation to complex source admittances, we have to consider the achieved susceptances if low loss coaxial cables are used.

If the source impedance equals the line's complex characteristic impedance, hence $\underline{Z}_0 \approx Z_{0\mathrm{ll}}\,(1 - \mathrm{j}\,\frac{\alpha}{\beta})$ according to (2.4), its (transformed) source admittance $\underline{\underline{Y}}_{\mathrm{iMB}}$ at matching frequency ω is equal to

$$\underline{\underline{Y}}_{\mathrm{iMB}} = \frac{1}{\underline{Z}_0} \approx \frac{1}{Z_{0\mathrm{ll}}\left(1 + \frac{\alpha^2}{\beta^2}\right)} + \mathrm{j}\omega\,\frac{\frac{\alpha}{\beta}}{\omega Z_{0\mathrm{ll}}\left(1 + \frac{\alpha^2}{\beta^2}\right)} \approx \frac{1}{Z_{0\mathrm{ll}}} + \mathrm{j}\omega\,\frac{\frac{\alpha}{\beta}}{\omega Z_{0\mathrm{ll}}} =: \frac{1}{R_{0\mathrm{p}}} + \mathrm{j}\omega C_{0\mathrm{p}},$$

which describes a conductance $\frac{1}{R_{0\mathrm{p}}} = \frac{1}{Z_{0\mathrm{ll}}}$ in parallel to a capacitance $C_{0\mathrm{p}} = \frac{\frac{\alpha}{\beta}}{\omega Z_{0\mathrm{ll}}}$.

[7] Although no active power may be transferred to an (ideal) open circuit, we have to keep in mind that optimisation required $l > 0$, hence at least tiny line lengths. Additionally $\underline{Z}_0 \approx Z_{0\mathrm{ll}}\,(1 - \mathrm{j}\,\frac{\alpha}{\beta})$ approximately describes the coaxial transmission line's complex characteristic impedance. Thus the optimum source and load impedances are close to, but not equal to an open circuit.

Conversely, if the source is designed for maximum active power input, its impedance equals the complex conjugate of the line's characteristic impedance, hence its admittance exhibits the same conductance, but in parallel to an inductance $\frac{Z_{0ll}\,(1+\frac{\alpha^2}{\beta^2})}{\omega\,\frac{\alpha}{\beta}} \approx \frac{Z_{0ll}}{\omega\,\frac{\alpha}{\beta}}$. However, it's further transformed by line 1 to $\underline{\widetilde{Y}}_{\mathrm{iMB}}$ at the matching network's input. The minimum/maximum real and imaginary part of the transformed source admittance may be derived by considering its limiting circle[8] of the transformation spiral in the complex reflection coefficient plane. We obtain

$$\begin{aligned}
\begin{matrix}\mathrm{Min}\\ \mathrm{Max}\end{matrix}\left\{\frac{1}{\mathrm{Re}\left\{\underline{\widetilde{Y}}_{\mathrm{iMB}}\right\}}\right\} &= Z_{0ll}\,\frac{1-\left(\frac{\alpha}{\beta}\right)^2}{1\pm\frac{2\,\frac{\alpha}{\beta}}{\sqrt{1+\left(\frac{\alpha}{\beta}\right)^2}}} \approx \frac{Z_{0ll}}{1\pm 2\,\frac{\alpha}{\beta}},\\
\widetilde{C}_{\mathrm{iMBpmin}} &= 0,\\
\widetilde{C}_{\mathrm{iMBpmax}} &= \frac{1}{\omega}\,\frac{\frac{\alpha}{\beta}}{Z_{0ll}}\,\frac{\frac{2}{\sqrt{1+\left(\frac{\alpha}{\beta}\right)^2}}+1}{1-\left(\frac{\alpha}{\beta}\right)^2} \approx \frac{3\,\frac{\alpha}{\beta}}{\omega Z_{0ll}},\\
\widetilde{L}_{\mathrm{iMBpmin}} &= \frac{Z_{0ll}\left(1-\left(\frac{\alpha}{\beta}\right)^2\right)}{\omega\,\frac{\alpha}{\beta}\left(\frac{2}{\sqrt{1+\left(\frac{\alpha}{\beta}\right)^2}}-1\right)} \approx \frac{Z_{0ll}}{\omega\,\frac{\alpha}{\beta}},\\
\widetilde{L}_{\mathrm{iMBpmax}} &\to \infty.
\end{aligned}$$

However, in our application coaxial cables with $\alpha \ll \beta$ are used, thus a generator of source impedance $Z_{0ll} \approx R_0$ is chosen which is further transformed by line 1 to $\underline{\widetilde{Y}}_{\mathrm{iMB}}$ at the matching network's input. The minimum/maximum real and imaginary part of the transformed source admittance may be derived in a similar manner by considering its limiting circle[9] of the transformation spiral in the complex reflection

[8]The limiting circle, the outer limit of the transformation spiral, is obtained if all $\mathrm{e}^{-2\alpha l_1}$ coefficients in the (transformed) reflection coefficient or its according admittance are replaced with 1. Doing so yields an outer limit of the transformed source admittance given by a circle of radius $\frac{1}{R_0}\,\frac{2\,\frac{|X_0|}{R_0}}{1-\left(\frac{X_0}{R_0}\right)^2}\,\frac{1}{\sqrt{1+\left(\frac{X_0}{R_0}\right)^2}}$ and centre $\frac{1}{R_0}\,\frac{1}{1-\left(\frac{X_0}{R_0}\right)^2}\left(1-\mathrm{j}\,\frac{X_0}{R_0}\right)$. (If $\frac{|X_0|}{R_0} > \frac{1}{\sqrt{3}} \approx 0.58$ the circle also encloses admittances exhibiting a negative real part — which indicates that in such a case involving high attenuation coefficients the transformation spiral stays far away from its limiting circle — source admittance, line, and hence transformed source admittance are entirely passive.)

[9]The limiting circle, the outer limit of the transformation spiral, is obtained if all $\mathrm{e}^{-2\alpha l_1}$ coefficients in the (transformed) reflection coefficient or its according admittance are replaced with 1. Doing so yields an outer limit of the transformed source admittance given by a circle of radius $\frac{1}{R_0}\,\frac{1}{2}\left(\frac{X_0}{R_0}\right)^2\sqrt{\frac{1+4\left(\frac{R_0}{X_0}\right)^2}{1+\left(\frac{X_0}{R_0}\right)^2}}$ and centre $\frac{1}{R_0}\,\frac{1+\frac{1}{2}\left(\frac{X_0}{R_0}\right)^2}{1+\left(\frac{X_0}{R_0}\right)^2}\left(1-\mathrm{j}\,\frac{X_0}{R_0}\right)$. (If $\frac{|X_0|}{R_0} > \frac{2}{\sqrt{3}}\sqrt{2\cos\left(\frac{1}{3}\arccos\left(-\frac{5}{32}\right)\right)-1} \approx 0.95$ the circle also encloses admittances exhibiting a negative real part — which indicates that in such a case involving high attenuation coefficients the transformation spiral stays far away from its limiting circle — source admittance, line, and hence transformed source admittance are entirely passive.)

coefficient plane. We obtain

$$\begin{aligned}
\underset{\text{Max}}{\text{Min}}\left\{\frac{1}{\text{Re}\{\underline{Y}_{\text{iMB}}\}}\right\} &= Z_{0\text{ll}}\,\frac{1+\left(\frac{\alpha}{\beta}\right)^2}{1+\frac{1}{2}\left(\frac{\alpha}{\beta}\right)^2 \pm \frac{\alpha}{\beta}\sqrt{1+\frac{1}{4}\left(\frac{\alpha}{\beta}\right)^2}\sqrt{1+\left(\frac{\alpha}{\beta}\right)^2}} \approx \frac{Z_{0\text{ll}}}{1\pm\frac{\alpha}{\beta}},\\
C_{\text{iMBpmin}} &= 0,\\
C_{\text{iMBpmax}} &= \frac{1}{\omega}\,\frac{\frac{\alpha}{\beta}}{Z_{0\text{ll}}}\,\frac{\sqrt{1+\frac{1}{4}\left(\frac{\alpha}{\beta}\right)^2}\sqrt{1+\left(\frac{\alpha}{\beta}\right)^2}+1+\frac{1}{2}\left(\frac{\alpha}{\beta}\right)^2}{1+\left(\frac{\alpha}{\beta}\right)^2} \approx \frac{2\,\frac{\alpha}{\beta}}{\omega\,Z_{0\text{ll}}},\\
L_{\text{iMBpmin}} &= \frac{Z_{0\text{ll}}\left(1+\left(\frac{\alpha}{\beta}\right)^2\right)}{\omega\,\frac{\alpha}{\beta}\left(\sqrt{1+\frac{1}{4}\left(\frac{\alpha}{\beta}\right)^2}\sqrt{1+\left(\frac{\alpha}{\beta}\right)^2}-1-\frac{1}{2}\left(\frac{\alpha}{\beta}\right)^2\right)} \approx \frac{8\,Z_{0\text{ll}}}{\omega\left(\frac{\alpha}{\beta}\right)^3},\\
L_{\text{iMBpmax}} &\to \infty.
\end{aligned}$$

D.3.1.2 T network

To check the impact of source impedance transformation by the line on network design, in particular the necessity of extending the optimisation to complex source impedances, we have to consider the achieved reactances if low loss coaxial cables are used.

If the source impedance equals the line's complex characteristic impedance, hence $\underline{Z}_0 \approx Z_{0\text{ll}}\,(1-\mathrm{j}\,\frac{\alpha}{\beta})$ according to (2.4), its (transformed) source impedance $\underline{\widetilde{Z}}_{\text{iMB}}$ at matching frequency ω is equal to

$$\underline{\widetilde{Z}}_{\text{iMB}} = \underline{Z}_0 \approx Z_{0\text{ll}} - \mathrm{j}Z_{0\text{ll}}\,\frac{\alpha}{\beta} = Z_{0\text{ll}} + \frac{1}{\mathrm{j}\,\omega\,\frac{1}{\omega Z_{0\text{ll}}\frac{\alpha}{\beta}}} =: \frac{1}{G_{0\text{s}}} + \frac{1}{\mathrm{j}\omega C_{0\text{s}}},$$

which describes a resistance $\frac{1}{G_{0\text{s}}} = Z_{0\text{ll}}$ in series to a capacitance $C_{0\text{s}} = \frac{1}{\omega Z_{0\text{ll}}\frac{\alpha}{\beta}}$.

Conversely, if the source is designed for maximum active power input, its impedance equals the complex conjugate of the line's characteristic impedance, hence it exhibits the same resistance, but in series to an inductance $\frac{1}{\omega}\,Z_{0\text{ll}}\,\frac{\alpha}{\beta}$. However, it's further transformed by line 1 to $\underline{\widetilde{Z}}_{\text{iMB}}$ at the matching network's input. The minimum/maximum real and imaginary part of the transformed source impedance may be derived by considering its limiting circle[10] of the transformation spiral in the

[10]The limiting circle, the outer limit of the transformation spiral, is obtained if all $\mathrm{e}^{-2\alpha l_1}$ coefficients in the (transformed) reflection coefficient or its according impedance are replaced with 1. Doing so yields an outer limit of the transformed source impedance given by a circle of radius $R_0\,\frac{2\,\frac{|X_0|}{R_0}}{1-\left(\frac{X_0}{R_0}\right)^2}\sqrt{1+\left(\frac{X_0}{R_0}\right)^2}$ and centre $R_0\,\frac{1+\left(\frac{X_0}{R_0}\right)^2}{1-\left(\frac{X_0}{R_0}\right)^2}\left(1+\mathrm{j}\,\frac{X_0}{R_0}\right)$. (If $\frac{|X_0|}{R_0} > \frac{1}{\sqrt{3}} \approx 0.58$ the circle also encloses impedances exhibiting a negative real part — which indicates that in such a case involving high attenuation coefficients the transformation spiral stays far away from its limiting circle — source impedance, line, and hence transformed source impedance are entirely passive.)

complex reflection coefficient plane. We obtain

$$\begin{aligned}
\underset{\text{Min}}{\overset{\text{Max}}{}}\left\{\text{Re}\left\{\underline{\widetilde{Z}}_{\text{iMB}}\right\}\right\} &= Z_{0\text{ll}}\frac{1+\left(\frac{\alpha}{\beta}\right)^2}{1-\left(\frac{\alpha}{\beta}\right)^2}\left(1\pm\frac{2\,\frac{\alpha}{\beta}}{\sqrt{1+\left(\frac{\alpha}{\beta}\right)^2}}\right)\approx Z_{0\text{ll}}\left(1\pm 2\,\frac{\alpha}{\beta}\right),\\
\widetilde{C}_{\text{iMBsmin}} &= \frac{1-\left(\frac{\alpha}{\beta}\right)^2}{\omega\,\frac{\alpha}{\beta}\,Z_{0\text{ll}}\left(1+\left(\frac{\alpha}{\beta}\right)^2\right)\left(\frac{2}{\sqrt{1+\left(\frac{\alpha}{\beta}\right)^2}}+1\right)}\approx\frac{1}{3\,\omega\,\frac{\alpha}{\beta}\,Z_{0\text{ll}}},\\
\widetilde{C}_{\text{iMBsmax}} &\to \infty,\\
\widetilde{L}_{\text{iMBsmin}} &= 0,\\
\widetilde{L}_{\text{iMBsmax}} &= \frac{1}{\omega}\,\frac{\alpha}{\beta}\,Z_{0\text{ll}}\,\frac{1+\left(\frac{\alpha}{\beta}\right)^2}{1-\left(\frac{\alpha}{\beta}\right)^2}\left(\frac{2}{\sqrt{1+\left(\frac{\alpha}{\beta}\right)^2}}-1\right)\approx\frac{1}{\omega}\,\frac{\alpha}{\beta}\,Z_{0\text{ll}}.
\end{aligned}$$

However, in our application coaxial cables with $\alpha \ll \beta$ are used, thus a generator of source impedance $Z_{0\text{ll}} \approx R_0$ is chosen which is further transformed by line 1 to $\underline{Z}_{\text{iMB}}$ at the matching network's input. The minimum/maximum real and imaginary part of the transformed source impedance may be derived in a similar manner by considering its limiting circle[11] of the transformation spiral in the complex reflection coefficient plane. We obtain

$$\begin{aligned}
\underset{\text{Min}}{\overset{\text{Max}}{}}\left\{\text{Re}\left\{\underline{Z}_{\text{iMB}}\right\}\right\} &= Z_{0\text{ll}}\left(1+\tfrac{1}{2}\left(\tfrac{\alpha}{\beta}\right)^2\pm\tfrac{\alpha}{\beta}\sqrt{1+\tfrac{1}{4}\left(\tfrac{\alpha}{\beta}\right)^2}\sqrt{1+\left(\tfrac{\alpha}{\beta}\right)^2}\right)\approx Z_{0\text{ll}}\left(1\pm\frac{\alpha}{\beta}\right),\\
C_{\text{iMBsmin}} &= \frac{1}{\omega\,\frac{\alpha}{\beta}\,Z_{0\text{ll}}\left(\sqrt{1+\frac{1}{4}\left(\frac{\alpha}{\beta}\right)^2}\sqrt{1+\left(\frac{\alpha}{\beta}\right)^2}+1+\frac{1}{2}\left(\frac{\alpha}{\beta}\right)^2\right)}\approx\frac{1}{2\,\omega\,\frac{\alpha}{\beta}\,Z_{0\text{ll}}},\\
C_{\text{iMBsmax}} &\to \infty,\\
L_{\text{iMBsmin}} &= 0,\\
L_{\text{iMBsmax}} &= \frac{1}{\omega}\,\frac{\alpha}{\beta}\,Z_{0\text{ll}}\left(\sqrt{1+\frac{1}{4}\left(\frac{\alpha}{\beta}\right)^2}\sqrt{1+\left(\frac{\alpha}{\beta}\right)^2}-1-\frac{1}{2}\left(\frac{\alpha}{\beta}\right)^2\right)\approx\frac{\left(\frac{\alpha}{\beta}\right)^3}{8\,\omega\,Z_{0\text{ll}}}.
\end{aligned}$$

[11]The limiting circle, the outer limit of the transformation spiral, is obtained if all $\mathrm{e}^{-2\alpha l_1}$ coefficients in the (transformed) reflection coefficient or its according impedance are replaced with 1. Doing so yields an outer limit of the transformed source impedance given by a circle of radius $R_0\,\frac{1}{2}\left(\frac{X_0}{R_0}\right)^2\sqrt{1+4\left(\frac{R_0}{X_0}\right)^2}\sqrt{1+\left(\frac{X_0}{R_0}\right)^2}$ and centre $R_0\left(1+\frac{1}{2}\left(\frac{X_0}{R_0}\right)^2\right)\left(1+\mathrm{j}\,\frac{X_0}{R_0}\right)$. (If $\frac{|X_0|}{R_0} > \frac{2}{\sqrt{3}}\sqrt{2\cos\left(\frac{1}{3}\arccos\left(-\frac{5}{32}\right)\right)-1} \approx 0.95$ the circle also encloses impedances exhibiting a negative real part — which indicates that in such a case involving high attenuation coefficients the transformation spiral stays far away from its limiting circle — source impedance, line, and hence transformed source impedance are entirely passive.)

Appendix E

Publications of This Work

1. R. J. Glöckner, J. K. Fidler, K. Busawon, "Exact Analytical Solutions for Lossy L, Pi and T Matching Networks", under preparation.

2. R. J. Glöckner, J. K. Fidler, K. Busawon, "Designing Lossy Pi and T Matching Networks for Optimum Power Gain", under preparation.

References

[1] M. J. Underhill and P. A. Lewis, Automatic Tuning of Antennae, The SERT Journal **8**, pp. 183-184 (1974)

[2] P. A. Lewis and M. J. Underhill, Quiet Tuning and Matching of Antennas for Radio-Silence Operation, IEE Proc. F **127**, pp. 361-367 (1980)

[3] M. J. Underhill, Wide Range Antenna Matching Networks, in *Radio Receivers and Associated Systems* (1981), no. 50 in IERE Conf. Proc., pp. 101-135

[4] P. Petrović, M. Mileusnić, and J. Todorović, Fast Antenna Tuners for High-Power HF Radio Systems, in *Proc. of the 1990 Bilkent Int. Conf. on New Trends in Comm., Control and Signal Processing* (Elsevier, Amsterdam, 1990), vol. 1, pp. 576-582

[5] Y. Sun and J. K. Fidler, High-Speed Automatic Antenna Tuning Units, in *Proceedings of the Ninth International Conference on Antennas and Propagation*, IEE Conference Publication **407**, pp. 218-222 (1995)

[6] M. Thompson and J. K. Fidler, Tuning the Pi-Network Using the Genetic Algorithm and Simulated Annealing, in *Proceedings of the 1997 European Conference on Circuit Theory and Design* (1997), vol. 2, pp. 949-954

[7] Y. Sun and W. K. Lau, Evolutionary Tuning Method for Automatic Impedance Matching in Communication Systems, in *1998 IEEE International Conference on Electronics, Circuits, and Systems* (1998), vol. 3, pp. 73-77

[8] Y. Sun and W. K. Lau, Antenna Impedance Matching Using Genetic Algorithms, in *Proceedings of the IEE National Conference on Antennas and Propagation*, IEE Conference Publication **461**, pp. 31-36 (1999)

[9a] F. E. Terman, *Radio Engineers' Handbook* (McGraw-Hill, New York, NY, 1943), pp. 77-82

[9b] F. E. Terman, *Radio Engineers' Handbook* (McGraw-Hill, New York, NY, 1943), pp. 84-85

[9c] F. E. Terman, *Radio Engineers' Handbook* (McGraw-Hill, New York, NY, 1943), pp. 210-214

[10] H. Norström, Experimental and Design Information for Calculating Impedance Matching Networks for Use in RF Sputtering and Plasma Chemistry, Vacuum **29**, pp. 341-350 (1979)

[11] W. B. Bruene, Pi-Network Calculator, Electronics, May 1945, pp. 140-146

[12] E. W. Pappenfus and K. L. Klippel, Pi Network Tank Circuits, CQ Amateur Radio, September 1950, pp. 27-32 and p. 69

[13] G. Grammer, Simplified Design of Impedance-Matching Networks, Part I-III, QST, March 1957, pp. 38-42, April 1957, pp. 32-35, and May 1957, pp. 29-34

[14] H. L. Gibson, An Improved Design Method for Pi and L Pi Network Couplers, Radio Communication, June 1969, pp. 390-392

[15] E. A. Wingfield, New and Improved Formulas for the Design of Pi and Pi-L Networks, QST, August 1983, pp. 23-29

[16] E. A. Wingfield, A Note on Pi-L Networks, QEX, December 1983, pp. 5-9

[17] Y. Sun and J. K. Fidler, Design of π Impedance Matching Networks, in *1994 IEEE International Symposium on Circuits and Systems* (1994), vol. 5, pp. 5-8

[18] Y. Sun and J. K. Fidler, Practical Considerations of Impedance Matching Network Design, in *Proceedings of the Sixth International Conference on HF Radio Systems and Techniques*, IEE Conference Publication **392**, pp. 229-233 (1994)

[19] Y. Sun and J. K. Fidler, Determination of the Impedance Matching Domain of Passive LC Ladder Networks: Theory and Implementation, Journal of the Franklin Institute B **333**, pp. 141-155 (1996)

[20] M. Thompson and J. K. Fidler, Pi-Network Design Software, in *Proceedings of the Third International Conference on Electronics, Circuits, and Systems* (1996), vol. 1, pp. 1-4

[21] M. Thompson and J. K. Fidler, Determination of the Impedance Matching Domain of Impedance Matching Networks, IEEE Trans. on Circuits and Systems **51**, pp. 2098-2106 (2004)

[22] G. S. Smith, Proximity Effect in Systems of Parallel Conductors, J. Appl. Phys. **43**, pp. 2196-2203 (1972)

[23] G. S. Smith, Radiation Efficiency of Electrically Small Multiturn Loop Antennas, IEEE Trans. on Ant. and Prop. **20**, pp. 656-657 (1972)

[24] R. G. Medhurst, H.F. Resistance and Self-Capacitance of Single-Layer Solenoids, The Wireless Eng. and Exp. Wireless **24**, pp. 35-43 (February 1947) and pp. 80-92 (March 1947)

[25] A. H. M. Arnold, The Resistance of Round-Wire Single-Layer Inductance Coils, Proceedings of the IEE, Part IV, **98**, pp. 94-100 (1951)

[26a] O. Zinke and H. Brunswig, *Lehrbuch der Hochfrequenztechnik*, 4th ed. (Springer, Berlin, 1990), vol. 1, p. 48

[26b] O. Zinke and H. Brunswig, *Lehrbuch der Hochfrequenztechnik*, 4th ed. (Springer, Berlin, 1990), vol. 1, pp. 52-53

[26c] O. Zinke and H. Brunswig, *Lehrbuch der Hochfrequenztechnik*, 4th ed. (Springer, Berlin, 1990), vol. 1, pp. 54-55 and p. 58

[26d] O. Zinke and H. Brunswig, *Lehrbuch der Hochfrequenztechnik*, 4th ed. (Springer, Berlin, 1990), vol. 1, p. 59

[26e] O. Zinke and H. Brunswig, *Lehrbuch der Hochfrequenztechnik*, 4th ed. (Springer, Berlin, 1990), vol. 1, p. 62

[26f] O. Zinke and H. Brunswig, *Lehrbuch der Hochfrequenztechnik*, 4th ed. (Springer, Berlin, 1990), vol. 1, pp. 90-92

[26g] O. Zinke and H. Brunswig, *Lehrbuch der Hochfrequenztechnik*, 4th ed. (Springer, Berlin, 1990), vol. 1, pp. 92-93

[26h] O. Zinke and H. Brunswig, *Lehrbuch der Hochfrequenztechnik*, 4th ed. (Springer, Berlin, 1990), vol. 1, pp. 142-143

[26i] O. Zinke and H. Brunswig, *Lehrbuch der Hochfrequenztechnik*, 4th ed. (Springer, Berlin, 1990), vol. 1, p. 182 and pp. 184-185

[27a] H. H. Meinke and F. W. Gundlach, *Taschenbuch der Hochfrequenztechnik*, 4th ed. (Springer, Berlin, 1986), vol. 1, p. C 37

[27b] H. H. Meinke and F. W. Gundlach, *Taschenbuch der Hochfrequenztechnik*, 4th ed. (Springer, Berlin, 1986), vol. 2, p. K 4

[27c] H. H. Meinke and F. W. Gundlach, *Taschenbuch der Hochfrequenztechnik*, 4th ed. (Springer, Berlin, 1986), vol. 3, p. R 3

[28] W. W. Macalpine, Computation of Impedance and Efficiency of Transmission Line with High Standing-Wave Ratio, Transactions of the AIEE, part I, **72**, pp. 334-339 (July 1953)

[29] W. W. Macalpine, Computation of Impedance and Efficiency of Transmission Line with High Standing-Wave Ratio, Electrical Communication **30**, pp. 238-246 (September 1953) (reprint of [28])

[30a] O. Zinke and H. Seither, *Widerstände, Kondensatoren, Spulen und ihre Werkstoffe*, 2nd ed. (Springer, Berlin, 1982), p. 235

[30b] O. Zinke and H. Seither, *Widerstände, Kondensatoren, Spulen und ihre Werkstoffe*, 2nd ed. (Springer, Berlin, 1982), pp. 254-257

[30c] O. Zinke and H. Seither, *Widerstände, Kondensatoren, Spulen und ihre Werkstoffe*, 2nd ed. (Springer, Berlin, 1982), pp. 257-260

[31] M. J. Underhill and P. A. Lewis, Quiet Tuning of Antennas, Electronics Letters **15**, pp. 37-38 (1979)

[32] P. A. Lewis and M. J. Underhill, Two Stage Tuning and Matching of HF Mobile Antennas, in *Proceedings of the Conference on Land Mobile Radio* (1979), no. 44 in IERE Conf. Proc., pp. 213-222

[33] D. L. Kincaid, An Automatic Antenna Tuner: The AT-11, QST, January 1996, pp. 35-39

[34a] H. H. Meinke and F. W. Gundlach, *Taschenbuch der Hochfrequenztechnik*, 3rd ed. (Springer, Berlin, 1968), pp. 8-13

[34b] H. H. Meinke and F. W. Gundlach, *Taschenbuch der Hochfrequenztechnik*, 3rd ed. (Springer, Berlin, 1968), pp. 27-29

[34c] H. H. Meinke and F. W. Gundlach, *Taschenbuch der Hochfrequenztechnik*, 3rd ed. (Springer, Berlin, 1968), p. 167

[35] E. Philippow, *Taschenbuch Elektrotechnik* (Verlag Technik, Berlin, 1969), vol. 3, pp. 388-389

[36] E. Böhmer, *Elemente der angewandten Elektronik*, 7th ed. (Vieweg, Braunschweig, 1990), pp. 72-73

[37] E. Böhmer, *Elemente der angewandten Elektronik*, 9th ed. (Vieweg, Braunschweig, 1994), pp. 64-65

[38] R. Feldtkeller, *Theorie der Spulen und Übertrager*, 4th ed. (Hirzel, Stuttgart, 1963), pp. 79-86

[39] S. Börner and W. Haist, Die Frequenzabhängigkeit des Scheinwiderstandes von einlagigen zylindrischen Luftspulen, Frequenz **19**, I. Teil pp. 169-175 and II. Teil pp. 191-200 (1965)

[40] W. Lorenz, Dimensionierung einlagiger Zylinderluftspulen mit optimaler Güte, Frequenz **24**, pp. 20-26 (1970)

[41a] F. W. Grover, *Inductance Calculations*, special reprint (Instrument Society of America, Research Triangle Park, NC, 1983), pp. 17-22

[41b] F. W. Grover, *Inductance Calculations*, special reprint (Instrument Society of America, Research Triangle Park, NC, 1983), pp. 143-148

[41c] F. W. Grover, *Inductance Calculations*, special reprint (Instrument Society of America, Research Triangle Park, NC, 1983), pp. 149-151

[41d] F. W. Grover, *Inductance Calculations*, special reprint (Instrument Society of America, Research Triangle Park, NC, 1983), pp. 163-164

[41e] F. W. Grover, *Inductance Calculations*, special reprint (Instrument Society of America, Research Triangle Park, NC, 1983), pp. 164-165

[41f] F. W. Grover, *Inductance Calculations*, special reprint (Instrument Society of America, Research Triangle Park, NC, 1983), p. 261

[42] A. Sommerfeld, Über das Wechselfeld und den Wechselstromwiderstand von Spulen und Rollen, Annalen der Physik, 4. series, **15**, pp. 673-708 (1904)

[43] A. Sommerfeld, Über den Wechselstromwiderstand der Spulen, Annalen der Physik, 4. series, **24**, pp. 609-634 (1907)

[44] G. Breit, Skin Effect in Solenoids, Nature (London), **110**, p. 668 (1922)

[45] S. Butterworth, Eddy-Current Losses in Cylindrical Conductors, with Special Applications to the Alternating Resistance of Short Coils, Phil. Trans. Roy. Soc. (London), series A, **222**, pp. 57-100 (1921)

[46] S. Butterworth, Note on the Alternating Current Resistance of Single Layer Coils, The Physical Review **23**, pp. 752-755 (1924)

[47] S. Butterworth, On the Alternating Current Resistance of Solenoidal Coils, Proc. Roy. Soc. (London) **107**, pp. 693-715 (1925)

[48] S. Butterworth, Effective Resistance of Inductance Coils at Radio Frequency — Part I-IV, Exp. Wireless and the Wireless Eng. **3**, pp. 203-210 (April 1926), pp. 309-316 (May 1926), pp. 417-424 (July 1926), and pp. 483-492 (August 1926)

[49] B. B. Austin, The Effective Resistance of Inductance Coils at Radio Frequency, The Wireless Eng. and Exp. Wireless **11**, pp. 12-16 (January 1934)

[50] S. Börner, *Die Beiträge von Wicklung und Ferrit-Ringkern zum Verlustwiderstand von einlagigen Spulen im MHz-Gebiet* (Ph.D. thesis at the University of Stuttgart, Stuttgart, 1967)

[51a] G. Janzen, *Kurze Antennen* (Franckh'sche Verlagshandlung, Stuttgart, 1986), pp. 76-80

[51b] G. Janzen, *Kurze Antennen* (Franckh'sche Verlagshandlung, Stuttgart, 1986), pp. 141-144

[52] W. B. Kuhn and N. M. Ibrahim, Approximate Analytical Modeling of Current Crowding Effects in Multi-Turn Spiral Inductors, in *2000 IEEE Radio Frequency Integrated Circuits (RFIC) Symposium Digest of Papers* (2000), pp. 271-274

[53] W. B. Kuhn and N. M. Ibrahim, Analysis of Current Current Crowding Effects in Multi-Turn Spiral Inductors, IEEE Trans. on Microwave Theory and Techniques **49**, no. 1, pp. 31-38 (2001)

[54] F. M. Rotella, V. Blaschke, and D. Howard, A Broad-Band Scalable Lumped-Element Inductor Model Using Analytic Expressions to Incorporate Skin Effect, Substrate Loss, and Proximity Effect, in *International Electron Devices Meeting 2002 Technical Digest* (2002), pp. 471-474

[55] P. L. Dowell, Effects of eddy currents in transformer windings, Proc. of the IEE **113**, no. 8, pp. 1387-1394 (1966)

[56] M. P. Perry, Multiple Layer Series Connected Winding Design for Minimum Losses, IEEE Trans. on Power Apparatus and Systems **98**, no. 1, pp. 116-123 (1979)

[57] J. P. Vandelac and P. Ziogas, A Novel Approach for Minimizing High Frequency Transformer Copper Losses, in *IEEE Power Electronics Specialists Conference Record* (1987), pp. 355-367

[58] A. M. Urling, V. A. Niemla, G. R. Skutt, and T. G. Wilson, Characterizing High-Frequency Effects in Transformer Windings — a Guide to Several Significant Articles, in *IEEE Applied Power Electronics Conference and Exposition* (1989), pp. 373-385

[59] C. R. Sullivan, Winding Loss Calculation with Multiple Windings, Arbitrary Waveforms, and Two-Dimensional Field Geometry, in *Conference Record of the 1999 IEEE Industry Applications Conference* (1999), vol. 3, pp. 2093-2099

[60] A. Massarini and M. K. Kazimierczuk, Modeling the Parasitic Capacitance of Inductors, in *16th Capacitor and Resistor Technology Symposium* (1996), pp. 78-85

[61] G. S. Smith, Efficiency of Electrically Small Antennas Combined with Matching Networks, IEEE Trans. on Ant. and Prop. **25**, pp. 369-373 (1977)

[62] B. D. H. Tellegen, A General Network Theorem, with Applications, Philips Journal of Research **7**, pp. 259-269 (1952)

[63] J. Millman and A. Grabel, *Microelectronics*, 2nd international edition (McGraw-Hill, New York, 1987), pp. 839-840

[64] K. Meyberg and P. Vachenauer, *Höhere Mathematik*, 1st revised reprint (Springer, Berlin, 1990), vol. 1, pp. 397-400

[65] K. Schmidt, Estimating T-Network Losses at 80 and 160 Meters, QEX, July 1996, pp. 16-20

[66] A. S. Griffith, Getting the Most Out of Your T-Network Antenna Tuner, QST, January 1995, pp. 44-47

[67] T. Preedy, Save Your Tuner for Two Pence, RadCom, May 2000, pp. 35-39

[68] D. DeMaw, B. Shriner, Matching the Transmitter to the Load, QST, February 1980, pp. 22-26

[69] T. H. Lee, *The Design of CMOS Radio-Frequency Integrated Circuits*, corrected reprint (Cambridge University Press, Cambridge, 1998), pp. 47-52

[70] M. Bekheit, S. Amari, and W. Menzel, Modeling and Optimization of Compact Microwave Bandpass Filters, IEEE Trans. on Microwave Theory and Techniques **56**, pp. 420-430 (February 2008)

[71] D. Wang and M. Yang, A Method of Passive Filter Design by Optimization, in *Proc. of the 36th Midwest Symposium on Circuits and Systems* (IEEE, Piscataway, NJ, 1993), vol. 1, pp. 617-620

[72a] M. H. W. Hoffmann, *Hochfrequenztechnik* (Springer, Berlin, 1997), p. 65

[72b] M. H. W. Hoffmann, *Hochfrequenztechnik* (Springer, Berlin, 1997), p. 155

[73] F. Landstorfer, *Hochfrequenztechnik I*, Section 3.5, lecture in winter term 1992/1993 at the University of Stuttgart, Stuttgart

[74a] *S-Parameter Techniques for Faster, More Accurate Network Design* (Hewlett-Packard Application Note 95-1, 1997), p. 58

[74b] *S-Parameter Techniques for Faster, More Accurate Network Design* (Hewlett-Packard Application Note 95-1, 1997), p. 59

[75] T. E. Shea, *Transmission Networks and Wave Filters*, reprint (D. van Nostrand, Princeton, NJ, 1958), pp. 52-55